Behaviour of Single and Double Row Bolted Shear Tab Connections and Weld Retrofits

By

Matthew Marosi

Faculty of Engineering

Department of Civil Engineering and Applied Mechanics

McGill University, Montreal

February 2011

A thesis submitted to McGill University in partial fulfillment of the requirements of the degree of Masters of Engineering

Behaviour of Single and Double Row Bolted Shear Tab Connections and Weld Retrofits

ABSTRACT

The use of shear tabs continues to be one of the most popular methods of connecting steel beams to columns or girders. The current design procedure for shear tab connections in the 2010 CISC Handbook of Steel Construction is based on research conducted in the late 1980s. Some of the tabulated design values in the Handbook are based partly on outdated resistance factors and clauses. The CISC design method is also limited in its applicability; it applies only for shear tabs having a single row of seven bolts or less. Consequently, an up to date design procedure applicable to single and double row bolted shear tab connections featuring up to ten bolts per row is proposed by the author for use in Canada.

In order to gain a better understanding of the behaviour of shear tab connections, sixteen full-scale tests were conducted using three different sized test beams. Connections varied in size from one row of three bolts to two rows of ten bolts. Six bolted connections and ten retrofit weld tests were conducted as there was a demand for information on retrofit welds from the consulting engineering community. Shear tab weld retrofits are often performed on construction sites when members are damaged or when detailing errors cause misalignments between bolts and holes. The tests on weld retrofits shear tab connections sought to determine whether they possessed sufficient ductility to accommodate the rotation demand and to establish the loads that these welded connections could withstand. The weld retrofit connections did reach the targeted rotations and did resist at least the same loads as their corresponding bolted connections were predicted to resist. The welded and bolted connections behaved differently in terms of the onsets of flexural and shear yielding. This behaviour was consistent for all test beam sizes for both single and double row tests. Weld retrofit connections tended to outperform their bolted counterparts in double row tests. The opposite was true in single row tests.

RÉSUMÉ

L'utilisation des plaques de cisaillement continue d'être l'une des méthodes les plus populaires pour connecter des poutres en acier aux colonnes ou aux poutres-maîtresses. La démarche de conception des assemblages avec plaques de cisaillement proposée par le *CISC (2010) Handbook of Steel Construction* est basée sur des recherches menées dans les années 1980. Le *Handbook* offer des tableaux de valeurs de capacité de connexion type basées en partie sur des facteurs de résistance et des clauses désuets. La méthode de conception du CISC (2010) est également limitée en application, car elle ne s'applique que sur les plaques de cisaillement ayant une seule rangée d'un maximum de sept boulons. En conséquence, une procédure de conception mise à jour, et applicable aux plaques de cisaillement avec une ou deux rangées boulonnés comportant jusqu'à dix boulons par rangée est proposé par l'auteur.

Afin de mieux comprendre le comportement des assemblages avec des plaques de cisaillement, seize essais en grandeur réelles ont été réalisées en utilisant des poutres de trois grandeurs différentes. Les configurations des assemblages ont été variées d'une plus petite rangée de trois boulons à une plus grande ayant deux rangées de dix boulons. Six assemblages boulonnés ont été testés. En plus, dix autres assemblages munis de soudures de réparation ont été éprouvés, pour répondre aux besoins exprimés par des bureaux de génie-conseil. Des soudures réparatoires sur des plaques de cisaillement sont souvent effectuées sur chantier au cas où les membrures sont endommagées, ou quand les trous à boulons de la plaque et ceux de la poutre ne s`alignent pas suite à des erreurs de détaillage ou de fabrication. Les essais sur les soudures réparatoires visent à déterminer si ces soudures possèdent une ductilité pour permettre une rotation suffisante au niveau des assemblages. Ils ont aussi été utilisés pour déterminer les charges maximales que ces assemblages soudés peuvent supporter. Les assemblages avec soudures de réparation ont atteint les rotations ciblées et ont au moins résisté aux mêmes charges pour lesquelles les assemblages boulonnés sont conçus. Les assemblages soudés et boulonnés ont montrés des comportements

différents vis-à-vis du commencement de plastification en flexion et en cisaillement. Ce même comportement est observé pour les poutres de toutes grandeurs, ainsi que dans les connexions avec rangées simples ou doubles. Parmi les assemblages avec rangées doubles, les assemblages ayant des soudures réparatoires avaient tendance à résister à plus de charge que les assemblages boulonnés. L'inverse est vrai quant aux assemblages ayant des rangées simples.

ACKNOWLEDGEMENTS

This project would not have been possible without the help of a great number of people, to whom I owe a debt of gratitude. I'd like to thank my advisor, Professor Colin Rogers for all of his hard work, valuable feedback, and dedication to this project and above all else, for his open-door policy, which allowed me to get back on track whenever I hit a roadblock. Professor Robert Tremblay of École Polytechnique de Montréal also provided valuable insight into the project and great ideas relevant to real-world applications. Dr. Bill Cook's expertise with the equipment in the structural lab was tremendously useful and much appreciated. Dr. Cook, along with the laboratory superintendent and technicians, Marek Przykorski, John Bartczak, Ron Sheppard, and Damon Kiperchuk were fantastic to work with and came up with some great ideas for the test setup during impromptu brainstorming sessions. Their willingness, not only to help me get the job done, but to teach me how to use the equipment properly will not soon be forgotten. Additional thanks for their help in the lab goes to Alireza Mirzaei, Anthony Caruso, Marco D'Aronco and Nisreen Balh. Groupe ADF Inc. generously provided us with the steel for almost the entire test setup and graciously took us on a tour of their fabrication plant. Denis D'Aronco, Martin Frappier, Émilie Leblanc, Chantal Tourigny and Michel Béland of DPHV were invaluable and extremely knowledgeable when it came to designing the test setups and coordinating the detailing, fabrication and delivery of the necessary pieces. Additionally, financial support was provided throughout the duration of the project by ADF, DPHV and NSERC, in effect making the research possible. Last of all, but certainly not least, I'd like to thank my family and friends for their support during the highs and lows of this undertaking. None of this would have been possible without them.

TABLE OF CONTENTS

ABSTRACT i

RÉSUMÉ ii

ACKNOWLEDGEMENTS iv

TABLE OF CONTENTS v

LIST OF FIGURES viii

LIST OF TABLES xi

1.0 CHAPTER 1: Introduction 1

1.1 Overview 1

1.2 Objectives 4

1.3 Scope 5

1.4 Outline 5

2.0 CHAPTER 2: Literature Review 7

2.1 Overview 7

2.2 Previous Research on Shear Tab Connections 7

2.2.1 North American Research 7

2.2.2 Australian Research 16

2.3 Detailed Current Design Procedures 17

2.3.1 Canadian Design Procedure (CISC Handbook, 10th edition) 17

2.3.2 American Design Procedure (AISC Handbook, 13th edition) 20

2.4 Industry Design Approach to Weld Retrofits 25

2.5 Summary 25

3.0 CHAPTER 3: Experimental Testing 27

3.1 Test Setup 27

3.1.1 Overview 27

3.1.2 Design and Fabrication of Stub Column Frame and End Frame 27
3.1.3 Design of Lateral Bracing System 31
3.2 Test Specimens 33
3.3 Design of Tested Connections 37
3.4 Test Setup and Instrumentation 40
3.4.1 Bolted Test Connections 40
3.4.2 Welded Test Connections 46
3.5 Test Procedure 49
3.5.1 Bolted Test Connections 49
3.5.2 Welded Test Connections 50
4.0 CHAPTER 4: Experimental Test Results and Analysis 51
4.1 Overview 51
4.2 Test Results and Observations 51
4.2.1 Single Row of 3 Bolts and Corresponding Weld Retrofits 52
4.2.2 Single Row of 6 Bolts and Corresponding Weld Retrofits 56
4.2.3 Single Row of 10 Bolts and Corresponding Weld Retrofit 60
4.2.4 Two Rows of 3 Bolts and Corresponding Weld Retrofits 63
4.2.5 Two Rows of 6 Bolts and Corresponding Weld Retrofits 66
4.2.6 Two Rows of 10 Bolts and Corresponding Weld Retrofit 73
4.3 Comparisons 76
4.3.1 Experimental Results and Predicted Values 76
4.3.2 Bolted Tests Compared to Weld Retrofits 78
4.3.3 Comparison of Beam Sizes 83
4.3.4 Comparison of Single and Double Row Tests 83
4.4 Coupon Testing 86
4.4.1 Test Methodology 86

4.4.2 Beam Webs and Flanges 87
4.4.3 Shear Tab Plates 89
4.4.4 Remarks on Material Properties 89
5.0 CHAPTER 5: Conclusions and Recommendations 92
5.1 Summary 92
5.2 Recommendations for Future Studies 94
6.0 CHAPTER 6: References 96
APPENDIX A: Test Setups and Instrumentation 99
APPENDIX B: Sample Calculations 120
APPENDIX C: Modified Method: Bolted Shear Tab Predictions 135
APPENDIX D: Test Result Photos and Selected Data 154

LIST OF FIGURES

Figure 1-1: Beam to Column Flange Shear Tab Connection (Rigid Support Condition) 1

Figure 1-2: Beam to Column Web Shear Tab Connection (Flexible Support Condition).... 2

Figure 1-3: Coped Beam to Girder Web Shear Tab Connection (Flexible Support Condition) 2

Figure 1-4: Single Plate Misfit on Construction Site (Photo Courtesy: DPHV)..... 3

Figure 1-5: Single Plate with Misaligned Holes on Construction Site (Photo Courtesy: DPHV)..... 3

Figure 1-6: Shear Tab Weld Retrofit on Construction Site 4

Figure 2-1: Eccentricities in a Single Plate Framing Connection..... 8

Figure 2-2: Proposed Shear-Rotation Loading Path (Astaneh et al., 1989)..... 11

Figure 2-3: Failure Modes Described by Astaneh et al. (1989) 13

Figure 2-4: Horizontal and Vertical Edge Distances of Conventional AISC Shear Tab Configuration 21

Figure 3-1: Test beam, shear tab and stub column 27

Figure 3-2: Elevation of Typical Test Frames 28

Figure 3-3: Plan View of Typical Test Frames 29

Figure 3-4: End Frame and End Actuator Shown with W310 Beam (Prior to running of test)..... 31

Figure 3-5: Lateral Bracing Arms Connected to Frames with Ball and Socket Joints 32

Figure 3-6: 3D Rendering of Test Frames with W610 Beam..... 33

Figure 3-7: Typical Weld Retrofits..... 35

Figure 3-8: Typical Setup and Instrumentation for a Bolted W310x60 Test Beam 42

Figure 3-9: Instrumentation at Connection for Test 1: W310x60 (Shear Tab Side) 43

Figure 3-10: Instrumentation at Connection for Test 1: W310x60 (Opposite Shear Tab Side) 43

Figure 3-11: Half Round, Plates and Rollers Shown Between Actuator Head and Test Beam 44

Figure 3-12: Hydraulic Jacks Used in Place of End Actuator for Test 15 45

Figure 3-13: Certified Welder Completing SMAW Weld Retrofit of Shear Tab to Beam Web 46

Figure 3-14: Welding Power Supply 47

Figure 3-15: Typical Setup and Instrumentation for a Welded W310x60 Test Beam 48

Figure 4-1: Test 1 after Failure - Pictured after Removal of Test Bolts 53

Figure 4-2: Test 3 after Failure - Full "C" Weld Retrofit Fracture and Deformation of Bolt Hole 54

Figure 4-3: Test 4 after Failure - Bolt Hole Deformations and Edge Distance Rupture 55

Figure 4-4: Comparison of Onset of Yielding Among Strain Gauges for Tests 1 and 3 55

Figure 4-5: Normalized Connection Shear vs. Beam End Rotation Relative to Column Face for Tests 1, 3 and 4 56

Figure 4-6: Test 7 after Failure - Shear/Bearing Deformations and Shear Tab Rupture (Bolts Removed) 57

Figure 4-7: Test 9 after Failure - Bolt Hole Deformations and Crack Propagation Along Line of Bolt Holes 58

Figure 4-8: Test 11 after Failure - Rupture Through Bolt Holes and Edge Distance 59

Figure 4-9: Connection Shear vs. Beam End Rotation for Tests 7, 9 and 11 60

Figure 4-10: Test 13 after Failure - Weld Fracture, Shear Tab Yielding and Rupture Along Bolt Line 61

Figure 4-11: Test 14 after Failure - Yielding and Shear Tab Rupture Along Line of Bolt Holes 62

Figure 4-12: Connection Shear Load Where Strain Gauges Reach Yield Strain (Test 14:Welded) 62

Figure 4-13: Connection Shear Load Where Strain Gauges Reach Yield Strain (Test 13:Bolted) 63

Figure 4-14: Test 8 after Failure - Yielding Along Bolt Line and Weld Fracture at Supporting Column Face 64

Figure 4-15: Full "C"-Shape (left, Test 10) and Partial "C"-Shape (right, Test 12) Retrofits after Failure 65

Figure 4-16: Connection Shear vs. Beam End Rotation Relative to Column Face for Tests 2, 5 and 6 66

Figure 4-17: Connection Shear vs. Beam End Rotation for Test 8 (Bolted) and Corresponding Photos 68

Figure 4-18: Photos A and B of Test 8 Corresponding to Figure 4-17 68

Figure 4-19: Photos C, D, E and F of Test 8 Corresponding to Figure 4-17....................... 69

Figure 4-20: Connection Shear vs. Beam End Rotation for Test 10 (Welded) and Corresponding Photos 70

Figure 4-21: Photos A, B and C of Test 10 Corresponding to Figure 4-20 70

Figure 4-22: Photos D, E, F and G of Test 10 Corresponding to Figure 4-20 71

Figure 4-23: Test 12 after Failure - Bolt Hole Deformations in Both Rows, Weld Fracture and Vertical Edge Distance Rupture 72

Figure 4-24: Connection Shear vs. Beam End Rotation Relative to Column Face for Tests 8, 10 and 12.. 72

Figure 4-25: Progression of Strain Gauge Yielding for Test 15 (Bolted) 74

Figure 4-26: Test 15 after Failure - Yielding of Beam (left) and Shear Tab Yielding Along Inner Row of Bolts (right)... 75

Figure 4-27: Test 16 after Failure - Yielding of Beam (left) and Yielding of Shear Tab Between Bolt Holes (right)... 75

Figure 4-28: Comparison of Partial "C" Weld Retrofit (Top) to Bolted Connections (Bottom) Shear Tab Deformations.. 82

Figure 4-29: Comparison of Two Row Weld Retrofit (Test 12) to One Row Weld Retrofit (Test 9) 85

Figure 4-30: Localization of Beam Web and Flange Coupons (Image courtesy: DPHV)... 86

Figure 4-31: Machined Coupon before Testing (top) and Two Coupons after Fracture (bottom).. 87

Figure 4-32: Typical Stress-Strain Response of a Beam Flange Tensile Test Coupon....... 88

Figure 4-33: Typical Stress-Strain Response of a Shear Tab Tensile Test Coupon 90

LIST OF TABLES

Table 3-1: Description of Shear Tab Test Specimens 36

Table 3-2: Factored Strengths Weld Groups Were Designed For 38

Table 3-3: Predicted Connection Resistances based on Nominal and Actual Material Properties 39

Table 3-4: Probable Ultimate Loads at Targeted Rotations 50

Table 4-1: Shear Tab Connection Tests - Summary of Results 52

Table 4-2: Experimental Results Compared to Predicted Values for Single Row Bolted Tests 79

Table 4-3: Experimental Results Compared to Predicted Values for Double Row Bolted Tests 80

Table 4-4: Experimental Results of Weld Retrofit Tests Compared to Predicted Resistance of Corresponding Bolted Connection Tests 84

Table 4-5: Summary of Beam Flange Tensile Coupon Tests 88

Table 4-6: Summary of Beam Web Tensile Coupon Tests 89

Table 4-7: Summary of Shear Tab Plate Tensile Coupon Tests 90

1.0 CHAPTER 1: Introduction

1.1 Overview

Single plate shear tabs, having a relatively simple design approach and being relatively inexpensive, are one of the most common types of connections used to connect steel beams to their supporting members. They are known by many names such as fin plates, cleat plates, single plates, and shear tabs and will be referred to as shear tabs in this document. In these types of connections the plate is typically fillet welded, on one or both sides, to the supporting column or girder, and subsequently bolted to the web of the supported beam as depicted in Figures 1-1 through 1-3

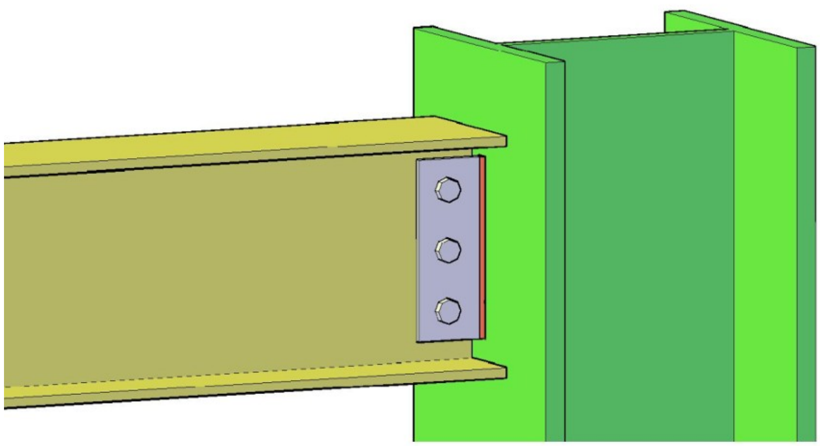

Figure 1-1: Beam to Column Flange Shear Tab Connection (Rigid Support Condition)

Support conditions are classified as rigid when the shear tab is restrained from following the rotation of the supported member, as is the case in Figure 1-1, where the strong axis of the column is aligned with the plate. Conversely, support conditions are considered flexible when the supporting column or girder still have some stiffness and will restrain the rotation of the shear tab, but to a lesser extent, as is the case in Figure 1-2 and Figure 1-3.

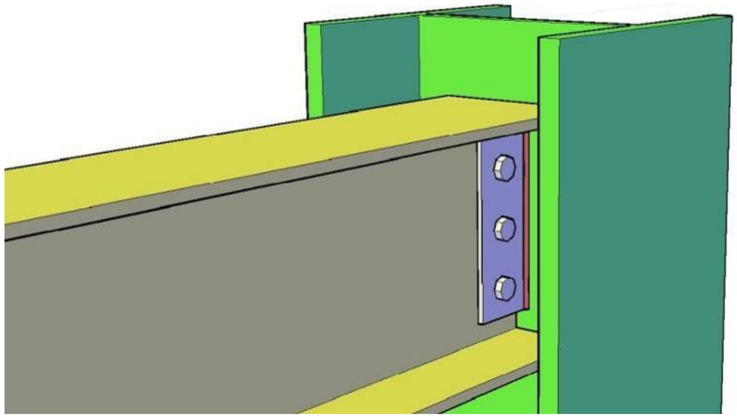

Figure 1-2: Beam to Column Web Shear Tab Connection (Flexible Support Condition)

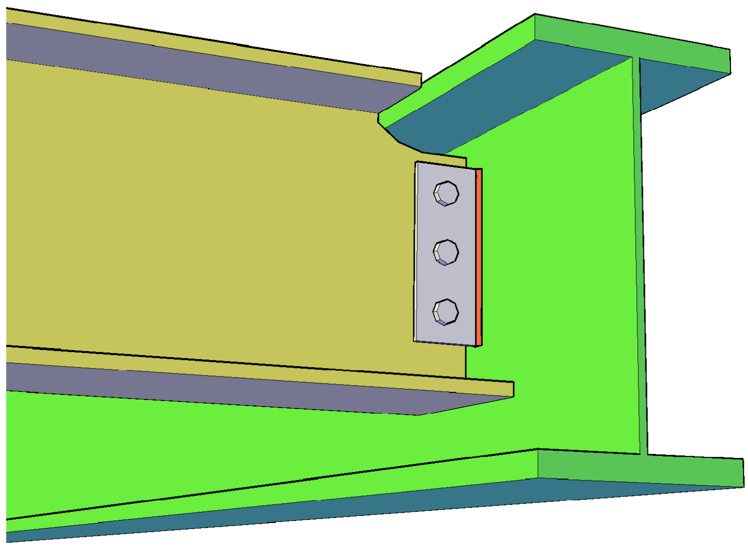

Figure 1-3: Coped Beam to Girder Web Shear Tab Connection (Flexible Support Condition)

Despite the simplicity of this type of connection, bolt holes in the beam web and plate may not always line up properly on the construction site. This could be a result of fabrication error, erection error, a beam or shear tab being damaged on site, or a design error on the part of an engineer or detailer. Shear plates may have been welded on upside-down, backwards, or at the wrong height; bolt holes may not have been drilled in the shear plate or in the beam; and dimensions and spacings of holes may have been detailed erroneously as shown in Figures 1-4 and 1-5.

Figure 1-4: Single Plate Misfit on Construction Site (Photo Courtesy: DPHV)

Figure 1-5: Single Plate with Misaligned Holes on Construction Site (Photo Courtesy: DPHV)

Consequently, weld retrofits are often used on construction sites to connect the beam to the supporting member when the bolts do not fit into place as depicted in Figure 1-6.

Additionally, it should be noted that historically most shear tabs were detailed with a single row of bolts; as such, a large extent of the research conducted to arrive at design procedures for these types of connections was based on laboratory tests performed on shear tabs with one row of bolts. In current design practice it has become common to provide shear tabs with multiple rows of bolts due to the expected higher beam reactions and/or the presence of axial forces in the beam. The design procedures in the CISC Handbook (2010) for shear tab beam connections are based on the work of

Figure 1-6: Shear Tab Weld Retrofit on Construction Site

Astaneh et al. (1989) and do not contain guidelines for shear tab connections with multiple rows of bolts. The majority of past shear tab tests were carried out on connections having between two and nine bolts in a single row with shear capacities seldom exceeding 1100 kN. Single plate connections with rows of 10 bolts, for example, have not been previously tested in the laboratory. For this reason the current shear tab design tables in the Canadian Institute of Steel Construction Handbook (CISC, 2010) apply only for connections with two to seven bolts. The American Institute of Steel Construction (AISC, 2005) does offer an extended shear tab design method for multiple rows of bolts however it has not been verified by means of testing for a full range of beam sizes as documented herein.

1.2 Objectives

The research being undertaken aims to make design recommendations for single plate shear tab connections with one and two rows of bolts and for larger single plate connections that have not been tested before. The experimental program being undertaken looks to build upon this past research and will include experimental tests featuring shear tabs with up to two rows of ten bolts, capable of resisting shear forces upwards of 3000 kN. The research also seeks to compare predicted capacities based on current design methods of the AISC (2005) and CISC (2010) with new experimental results. Additionally, various weld retrofit connections, where the holes have been drilled in the plate but where no bolts are present and the plate is welded to the supported beam on site, will be examined in the laboratory in order to determine whether or not they possess the necessary strength and ductility for their intended application.

1.3 Scope

A series of sixteen full-scale shear tab connections were tested in the laboratory. Six tests were carried out on W310 beams. Six tests were conducted on W610 beams, and lastly four tests were carried out on W920 beams. For each beam size, both single and double row bolted connections as well as weld retrofit connections were performed. Rows of three bolts were used in the W310 tests, rows of six bolts were used in the W610 tests and rows of ten bolts were used in the W920 tests. The support conditions in the experiments were considered rigid as the beam framed into the strong axis of a stub column which restrained rotation. Rotations were imposed on the connection by a beam end actuator. Measurements were taken to determine the strain, deflections, rotations, strength and how much inelastic rotation could be accomodated for each connection and observations were made to better understand the behaviour of the connections. Comparisons were made between predicted and experimental results in order to recommend a design approach that can account for multiple row bolted shear tab connections.

1.4 Outline

The findings will be presented as follows:

Chapter 2 contains a summary of the findings of past shear tab research and a detailed description of design procedures used in practice today in the United States and Canada.

Chapter 3 describes the test setup, instrumentation, test configurations and procedures used in the connection experiments.

Chapter 4 examines the results of the connection experiments and compares measured resistances with the predicted values based on the current AISC Specification (2005a) and CSA-S16 Standard (CSA, 2009). It also lists and explains the material properties of the specimens tested and provides information regarding coupon tests of the steel beams and plates.

Chapter 5 presents conclusions and recommendations for future studies in this area of research.

2.0 CHAPTER 2: Literature Review

2.1 Overview

Chapter 2 contains a review of previous research conducted in the area of single plate shear tabs and presents the current American Institute of Steel Construction (AISC) and Canadian Institute of Steel Construction (CISC) design methods in detail.

2.2 Previous Research on Shear Tab Connections

Past research is presented subsequently by location and from earliest to most recent.

2.2.1 North American Research

Tests were conducted at the University of British Columbia by Lipson (1968), in which single shear tabs were welded to supporting beams and bolted to the supported beam web. The connections tested had a single row of between 2 and 6 A325 bolts. The test specimens were subjected to either pure bending moments, where the beams were spliced together in the middle at the point of zero shear, or to a combination of bending moment and shear, where the beam was supported by a column on one side and a frame at the other. Lipson's investigations sought to determine the behaviour of the connections under working loads, to find the maximum rotational capacities of the connections, to determine an appropriate and consistent factor of safety for the ultimate load, and lastly to find out whether the connections were in fact flexible. The failure modes in the tests were classified as weld rupture, bolt tear-out or plate yielding. Lipson's investigation showed that it was feasible to use these welded-bolted type connections. Lipson also showed that the centre of rotation of the shear tab connection was located close to the centroid of the bolt group.

Caccavale (1975) followed up on the work of Lipson by conducting finite element analyses on models of Lipson's connection tests and performing a series of single bolt, single shear tests. Caccavale validated the 1968 test specimen findings from the

University of British Columbia. Caccavale also commented on the deformations that occurred during testing, noting that the bolts themselves did not deform, but rather the plate material surrounding them did.

Additional research by Richard et al. (1980) consisted of the evaluation of end moments in single plate framing connections. As single plate connections do not, in fact, work as perfect pins, there will be some eccentricity, e_b, between the point of zero moment and the centroid of the bolt group and also, e_w, between the point of zero moment and the weld connecting the shear tab to the column and as a result, an end moment may be present as shown in Figure 2-1. Various approaches exist when it comes to defining this eccentricity as will be evidenced later in this Chapter.

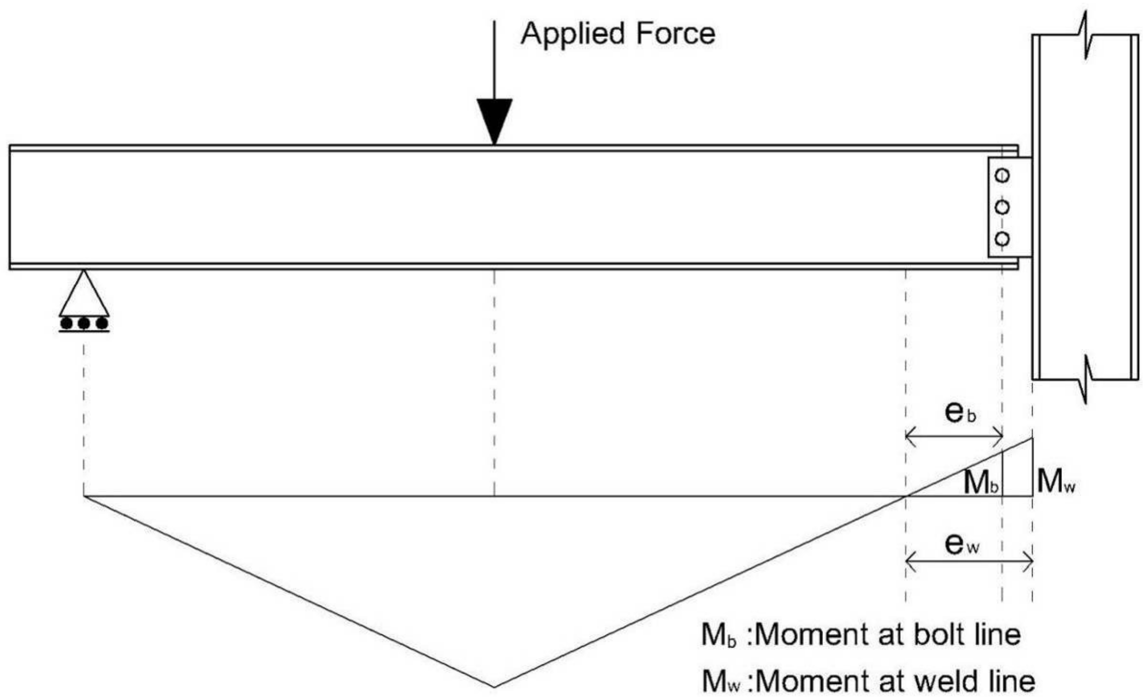

Figure 2-1: Eccentricities in a Single Plate Framing Connection

The beam-line method was used in conjunction with finite element models by Richard et al. (1980) to determine end moments. The beam line itself, represented graphically, would intersect the beam's simple span end rotation along the x-axis and the beam fixed end moment along the y-axis. When superimposed over the moment-rotation curve of the connection, the point of intersection of the curve and the beam line yields the end moment and end rotation of the beam. Building upon the finite element modeling of Caccavale (1975), and by running single-bolt single-shear tests and observing the deformation characteristics, Richard et al. (1980) were able to calculate bolt eccentricities based on beam lines and connection properties and verified their findings with a series of five stub beam single-row shear tab tests. The connections tested had single rows of three, five, and seven bolts. Richard et al. developed a design procedure and calculated bolt eccentricity based on the number of bolts, the size of the bolts, the span to depth ratio, *L/d*, and the section modulus of the beam. Young and Disque (1981) developed tabular design aids, expanding upon the work of Richard et al. (1980).

Ricles (1980) conducted eight full-scale tests in conjunction with finite element modeling to study double row bolted shear connections. Effects of end and edge distances of the plates were examined, as was the impact of slotted and standard holes. The research went on to show that the AISC Specification (1978) at the time did not predict block shear failures accurately in double-row bolted connections and that the factors of safety based on the AISC Specification were sometimes inadequate. Block shear failures occurred in Ricles' tests when they were not expected to, based on the Specification. Ricles proposed an equation to calculate the block shear failure resistance of bolted connections. Additionally, Ricles points out that vertical stress concentrations were generally higher at the location of the row of bolts closest to the supporting column in double-row connections.

Richard et al. (1982) carried out further tests on shear tabs connected with A307 bolts; they examined the effects of horizontal short slotted and standard holes, finding that short slotted holes lessened the moment at the connection.

Hormby et al. (1984), expanded further on shear tab research by extending experimental testing to Grade-50 steel beams. An equation was proposed to modify the eccentricity of the connection based on the stronger steel beams. Off-axis bolt groups, where the centroid of the bolt group does not coincide with the neutral axis of the beam, were also studied.

Stiemer et al. (1986) investigated the ultimate strength of single plate connections with flexible support conditions, where the supported beam framed into a supporting girder web. Also, skewed connections were tested, where the supported beam framed into the supporting girder at an angle other than 90°.

Astaneh and his collaborators at the University of California, Berkeley, published a series of findings on shear connections between 1989 and 1993. Astaneh (1989) studied the demand and supply of ductility in steel shear connections. Shear force, bending moment, and rotation interactions were examined. Astaneh proposed a modified beam line concept to better predict end moments and end rotations. It was also concluded that when measuring shear strength, one must apply both shear and rotation simultaneously as this is representative of realistic conditions. Likewise, moment-rotation curves should be obtained under these same realistic conditions with appropriate shear forces, moments and rotations applied. Additionally, a shear-rotation curve was proposed that simple connections based on a plastic design method should be able to meet.

Astaneh et al. (1989) proposed a new design procedure for single plate shear connections with a single row of between two and seven bolts. Prior to conducting five full-scale tests on connections with three, five and seven bolts, a tri-linear shear-rotation loading path was proposed. The first segment of the loading path represents the elastic phase. The second segment occurs as the beam yields in bending at mid-span and begins to soften, causing slightly larger rotations while taking on less shear force. The last segment begins as the beam reaches its plastic moment capacity. At this point the shear vs. rotation slope decreases further as the beam is subjected to strain hardening.

As shown in Figure 2-2, the yield moment, M_y, obtained by dividing the ultimate moment, $M_{u,}$ by the shape factor Z/S, was targeted at 0.02 radians and the plastic moment, $M_{p,}$ was targeted at 0.03 radians, at which point the single plate was to reach its yield strength. Z and S are the plastic and elastic section moduli respectively. Lastly, Astaneh et al. (1989) assumed the ultimate rotation to be 0.1 radians at a beam shear force value of $(F_u/F_y)M_p$. After the full-scale experiments which applied the aforementioned shear forces and rotations had been completed, a new empirical formula was developed to calculate the eccentricities of the bolt line and of the weld line to the vertical reaction load. The terms M_y and M_p in Figure 2-2 are to show when yielding occurs and when a plastic hinge is formed at the mid-span of the beam. At the 0.03 radian rotation point, the plastic hinge has formed at the beam mid-span and the single plate will begin yielding.

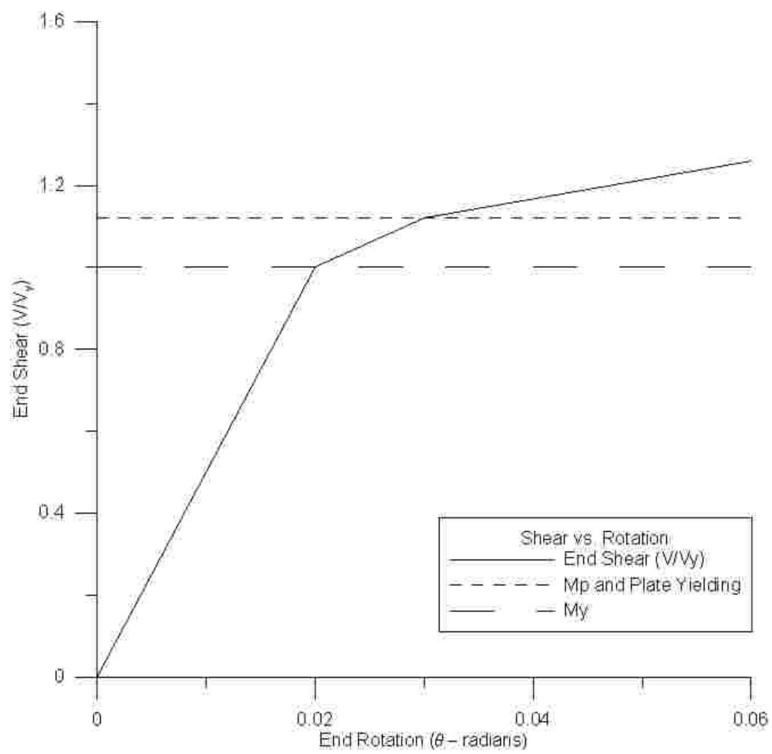

Figure 2-2: Proposed Shear-Rotation Loading Path (Astaneh et al., 1989)

Astaneh et al. (1989) recommended the following equations when determining weld and bolt eccentricities for design purposes:

For rigid support conditions,

Weld line to inflection point = $e_w = (n - 1)$, in. [Eq. 2.1]

Bolt line to inflection point = $e_b = (n - 1) - a$, in. [Eq. 2.2]

For flexible support conditions,

Weld line to inflection point = $e_w = (n - 1) \geq a$, in. [Eq. 2.3]

Bolt line to inflection point = $e_b = [(n - 1) - a] \geq a$, in. [Eq. 2.4]

where n corresponds to the number of bolts and a corresponds to the distance between the weld line and bolt line for single row connections. It was also found that rotational ductility decreased as the number of bolts in the connection was increased. The design procedure proposed by Astaneh et al. (1989) makes recommendations for bolt spacing, edge distances, material grade, thickness of single plates, aspect ratio of single plates, and bolt strength based on the experimental findings.

Astaneh et al. (1993), after conducting single-plate connection tests with single rows of three, five, seven, and nine bolts, presented a new design procedure addressing six limit states of strength for the connection. The limit states of concern were plate yielding, bearing failure around bolt holes, fracture along the net section of the plate, fracture along the edge distance of the plate, as well as bolt and weld fracture. Sketches of these failure modes are shown in Figure 2-3.

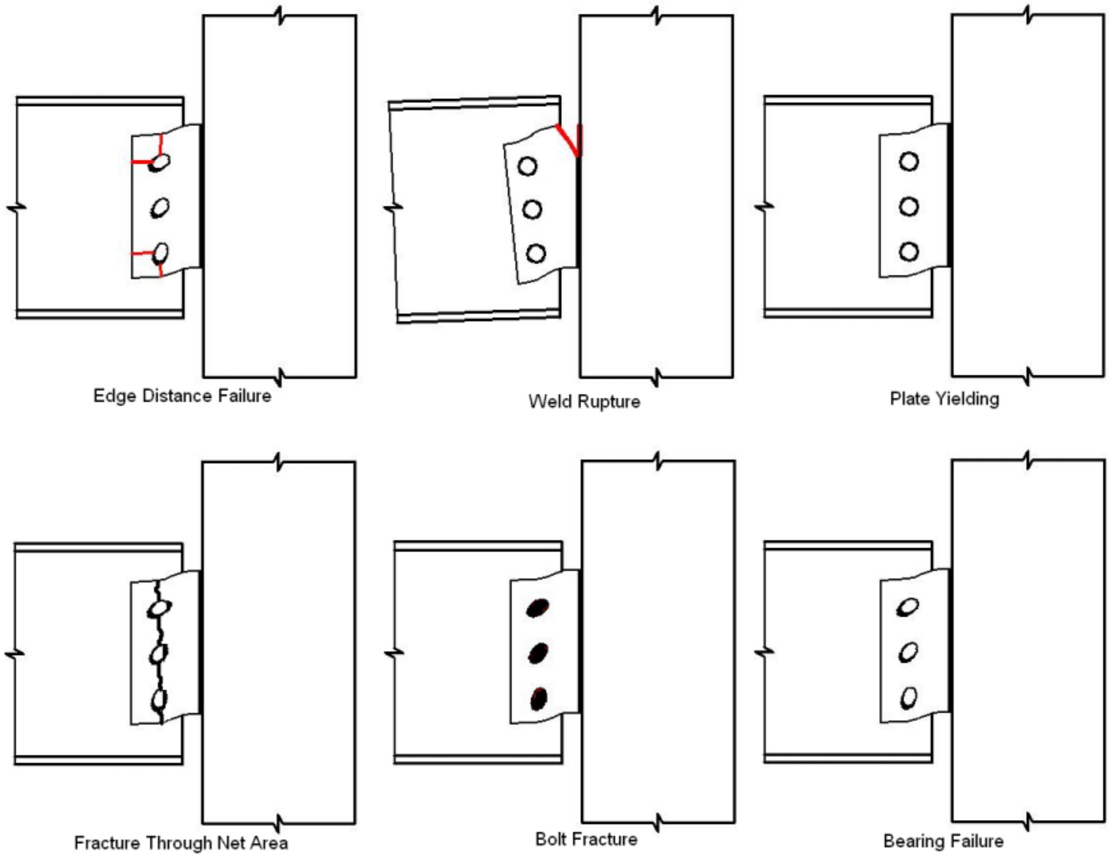

Figure 2-3: Failure Modes Described by Astaneh et al. (1989)

This procedure was geared towards the reduction of rotational stiffness by exploiting bearing deformations and shear yielding in the plate to reduce the end moments present. The design procedure sought to obtain ductile modes of failure, such as plate yielding and bearing of the bolt holes, prior to the remaining brittle modes of failure (Figure 2-3). It should also be noted that the previous equations to calculate connection eccentricity provided by Astaneh et al. (1989) were modified to incorporate absolute value operators to better approximate the eccentricities as follows:

For rigid support conditions,

Weld line to inflection point = $e_w = (n - 1)$, in. [Eq. 2.5]

Bolt line to inflection point = $e_b = |n - 1 - a|$, in. [Eq. 2.6]

For flexible support conditions,

Weld line to inflection point = $e_w = n$, in. [Eq. 2.7]

Bolt line to inflection point = $e_b = |n - 1 - a| \geq a$, in. [Eq. 2.8]

Astaneh et al. (2002) published findings regarding shear tab connections under gravity loads, as well as under combined gravity and cyclic lateral loads with concrete slabs present. The research again presented evidence showing that the design method allowed sufficient rotation to take place while maintaining the necessary shear strength, and allowed for ductile failure modes to precede brittle ones.

Sherman and Ghorbanpoor (2002) conducted a research program comprising of 31 full-scale tests with the goal of developing a design procedure for extended shear tabs. Extended shear tabs are generally welded to the web of a column or girder and extend beyond the flanges of the supporting member to avoid having to cope the flanges of the supported beam. The first phase examined three and five bolt extended shear plate connections and later tests focused on larger six and eight bolt connections. The tests involved shear tabs with single rows of bolts. The researchers established new formulas to calculate eccentricities in the connections. AISC design criteria for single plates were modified and Sherman and Ghorbanpoor presented a design procedure to the AISC for stiffened extended shear tabs.

Ashakul (2004) studied single plate shear connections using the finite element analysis program, ABAQUS (2000), and investigated the effects of plate thickness, plate material, position of bolt group with respect to the beam neutral axis, and the distance between the weld line and bolt line. Ashakul (2004) noted that the distance between weld and bolt lines did not have an effect on the shear rupture strength of the bolt group. He also modeled double row, single plate bolted connections and noted that force redistribution in these scenarios causes the bolts in the outer row to take more of the forces and fracture prior to the inner row, especially when Grade 50 plates thicker than ½’’ were used. The research comments on the shear stress distribution in the plate during strain hardening and proposes a method to calculate the shear yielding strength of the plate. Ashakul (2004) suggests further study is needed and that plate shear rupture and ductility of thicker Grade 50 steel plates should be investigated. Ashakul (2004) had performed FE analyses on plates with thicknesses up to ¾'', noting that the plate thickness had an effect on how much force would be transmitted to each row of bolts in shear tab connections with two rows of bolts.

Research by Creech (2005) sought to investigate the specified design method of the AISC's LRFD Manual (2003) and address its conservative nature. Creech conducted a comparison of numerous design methods with experimental data and sought to improve the current design procedure for single plate connections with both rigid and flexible support conditions. Ten full-scale tests were conducted, subjecting connections to both shear and rotation, up to a beam end rotation of 0.03 radians at the ultimate loading level. Connections having single rows of bolts with both standard and slotted holes were examined, as were connections with and without slab restraints, having two, three, and seven bolts.

On the subject of calculating bolt eccentricities, for single row shear tab connections, Creech concluded that it should be done for two and three bolt connections, but that beyond three bolt connections the magnitude of connection eccentricity was insignificant and calculating the connection's direct shear strength was sufficient.

With regards to rotational behaviour, Creech pointed out that the rotational neutral axis does not, in fact, coincide with the centroid of the bolt group, and is dependent on support conditions and restraints. Creech also asserts that the hierarchy of failure modes should be maintained from the ductile to the more brittle, as suggested by Astaneh et al. (1993), and that lower grade steel should be used for single plates. The thickness of these plates should meet the AISC (2003) design recommendations.

In a research program conducted by Baldwin Metzger (2006) eight full-scale shear tab tests were conducted with single plate connections designed according to the

2005 LRFD AISC approach. Four of the connections were designed according to the conventional method and the remaining four according to the extended method of the AISC (2005), which will be presented in Section 2.3.2. Tests applied a combined shear and rotation on the beam, in an effort to reach a 0.03 radian rotation at failure. The tests involved single rows of three, four, five, and seven bolts, as well as double rows of three and five bolts.

Baldwin Metzger's experimental results showed that the AISC (2005) design procedure will conservatively predict the ultimate strengths of both the current and extended configurations. She also concludes that the bolt group action factor of 0.8 used by the AISC (2005) should not be considered and that the most accurate method of predicting the bolt group strength was to take the distance between the bolt line and weld line of the single plate as the eccentricity.

On the topic of future research, Baldwin Metzger suggested tests be performed to determine the maximum allowable plate thicknesses for Grade-50 steel based on the diameter of connection bolts, as a number of her tests showed little or no elongation of bolt holes even as measured plate stresses exceeded 60 ksi.

2.2.2 Australian Research

Pham and Mansell (1982) conducted five tests on single plate connections with two rows of two, three, and five connection bolts to develop a better understanding of their behaviour and to verify earlier tabulated design values set forth by Hogan and Firkins (1978) from computational models. Pham and Mansell found large margins of safety and high reserves of strength above the tabulated values, but also noted that more desirable failure modes and serviceability criteria may be reached sooner.

Patrick et al. (1986) ran an experimental program to determine the shear capacity of single plate connections under conditions that would be expected in an actual structure, where rotations would be implemented by lowering one beam end as increasing load was applied in steps. The researchers sought to understand the rotational stiffness of the connections, the interaction between connection components, the interaction between shear and bending moment and through which mechanisms the connection was able to deform to provide ductility.

The researchers commented on the behaviour of the connection's centre of rotation, which was found to move from above the centroid of the bolt group to the centroid of the bolt group as the shear force was increased. On the subject of shear-moment interaction, the researchers showed that bending moment increased as the far end of the test beam was lowered to simulate rotation while the load was temporarily being held constant, and the bending moment decreased as additional shear force was added during a load step. With regards to component interaction, it was noted that as the single plate began deforming during tests, there was a redistribution of forces and the bolt group was relieved of some of the load. Patrick et al. (1986) also point out that local deformation of the web of the beam and single plate caused by the bolts in bearing made an important contribution to the ductility of the connection.

2.3 Detailed Current Design Procedures

2.3.1 Canadian Design Procedure (CISC Handbook, 10th edition)

The design procedure for single plates, bolted to the supported member with a single line of bolts and welded to the supporting member, in the CISC Handbook (2010) is based on the recommendations of Astaneh et al. (1989). It presents factored design values in tabular form (Table 3-41, CISC, 2010) for single plate connections with one row of two to seven bolts, having either rigid or flexible support conditions. Values in the table are based on the following assumptions:

- The distance from the weld line to the bolt line is 75mm.
- The distance between bolts is 80mm.
- The edge distance is 35mm.

- The shear tab plate is of Grade 300W Steel.
- Bolts are of Grade A325 and A325M.
- Bolt holes are considered punched (i.e. d_b + 4mm).
- Threads of bolts are assumed to be intercepted by the shear plane.

The methodology of the design is based on the early eccentricity equations, Eq. 2.1 and Eq. 2.2, developed by Astaneh et al. (1989). The eccentricity of the vertical reaction from the bolt line is first calculated. The bolt group coefficient can then be obtained from Table 3-14: *Eccentric Loads on Bolt Groups* (CISC, 2010). This bolt group coefficient, *C*, is based on the instantaneous centre of rotation method. Once the bolt group coefficient is known, the strength of the bolt group can be determined as follows:

$$V_{r\ BOLT} = (0.6\ \phi_b n m A_b)\ [\text{ x 0.7 if threads intercepted}] \qquad \text{[Eq. 2.9]}$$

$$V_{r\ CONN} = (C \times V_{r\ BOLT}) \qquad \text{[Eq. 2.10]}$$

where *n* refers to the number of bolts, *m* refers to the number of shear planes, A_b refers to the cross-sectional area of the bolt, and ϕ_b is the bolt resistance factor. It is important to note that all of the tabulated design values in Table 3-41 in the current Handbook (CISC, 2010) were calculated using $\phi_b = 0.67$, which has since been changed to $\phi_b = 0.80$ in the CSA S16 Standard (2009). This results in the tabulated values being even more conservative.

The plate thickness was determined based on the following requirements:

$$t_p \geq V_{r\ CONN} / (0.50\phi L_n F_u) \qquad \text{[Eq. 2.11]}$$

$$t_p \geq V_{r\ BOLT} / (3\phi_{br} d F_u) \qquad \text{[Eq. 2.12]}$$

$$t_p \geq 6\text{ mm} \qquad \text{[Eq. 2.13]}$$

$$t_p \leq (d/2) + 2\text{ mm} \qquad \text{[Eq. 2.14]}$$

where L_n refers to the length of the plate minus the diameters of bolt holes, F_u refers to the ultimate tensile strength of the plate material, ϕ_{br} is the bolt bearing resistance factor and is 0.67, ϕ from Eq. 2.11 is 0.90, and d is the bolt diameter.

Eq. 2.11 comes from Cl. 13.4.4 of the CSA S16 Standard (1994) which has since been removed and is no longer present in the latest edition, but still forms part of the basis of the tabulated values in the CISC Handbook (2010). It is described as the factored shear resistance, in this case through the net section of the shear tab. and is applicable when connecting elements are loaded primarily in shear. It is deemed somewhat conservative in the CSA S16 Standard (1994) when compared to elements in shear with regards to the block tear out failure mode. Eq. 2.12 provides for a check of the bearing capacity of the plate. Eq 2.13 denotes the minimum recommended plate thickness to be used. Eq. 2.14 is based on the recommendations of Astaneh et al. (1989); the plate thickness should not exceed half of the bolt diameter plus $^{1}/_{16}$''. These two equations aim to allow minor bolt hole deformation to occur to enhance the connection's ductility and rotational flexibility. It should also be noted that the use of high-strength steel (50 ksi / 350 MPa) for the plates was not recommended (Astaneh et al., 1989) for these same reasons. In addition to these checks, resistance to tension and block shear failure should be also checked according to Cl. 13.11 (CSA, 1994), where the lesser of Eqs. 2.15 and 2.16 controls.

$$T_r + V_r = \phi A_{nt} F_u + 0.60\ \phi A_{gv} F_y \qquad \text{[Eq. 2.15]}$$

$$T_r + V_r = \phi A_{nt} F_u + 0.60\ \phi A_{nv} F_u \qquad \text{[Eq. 2.16]}$$

In the preceding equations, A_{nt} is the net cross-sectional area of the plate in tension, A_{nv} is the net cross-sectional area in shear, and A_{gv} is the gross cross-sectional area in shear. Cl. 13.11 has since been changed in the more recent CSA S16 Standard (2009), but the tabulated values still remain unchanged in the CISC Handbook (2010). The new method of calculating block shear failure is:

$$T_r = \phi_u [U_t A_n F_u + 0.60\ A_{gv}(F_y + F_u)/2] \qquad \text{[Eq. 2.17]}$$

where U_t, is an efficiency factor and ϕ_u = 0.75.

The selection of the weld size in the tabulated design values refers to the recommendation of Astaneh et al. (1989) that the fillet weld size connecting the shear tab to the supporting member be ¾ the thickness of the plate.

For connections having more than seven bolts or multiple rows of bolts, there are no explicit instructions for design. In Tables 3-14 through 3-20, *Eccentric Loads on Bolt Groups* (CISC, 2010), bolt group coefficients for use with up to four rows of twelve bolts can be found.

2.3.2 American Design Procedure (AISC Handbook, 13th edition)

The AISC Handbook (2005) presents two design approaches for single plate connections based on the configuration of the connection; conventional configuration and extended configuration. The simpler conventional configuration approach applies when the following conditions are met:

- There is one row of bolts.
- There are between two and twelve bolts in the connection.
- The distance from the bolt line to the weld line, *a* (Figure 2-4), is less than or equal to 3 ½ inches.
- Either standard or short-slotted holes are used in the connection.
- The horizontal edge distance, L_{eh} (shown in Figure 2-4) for both the plate and beam web must be greater than or equal to twice the bolt diameter.
- The vertical edge distance, L_{ev}, must respect the values given in Table J3.4, *Minimum Edge Distance from Center of Standard Hole to Edge of Connected Part*, of the AISC Specification (2005a).

- Either the web of the beam or the plate must have a thickness not exceeding half of the bolt diameter + $^{1}/_{16}$''.

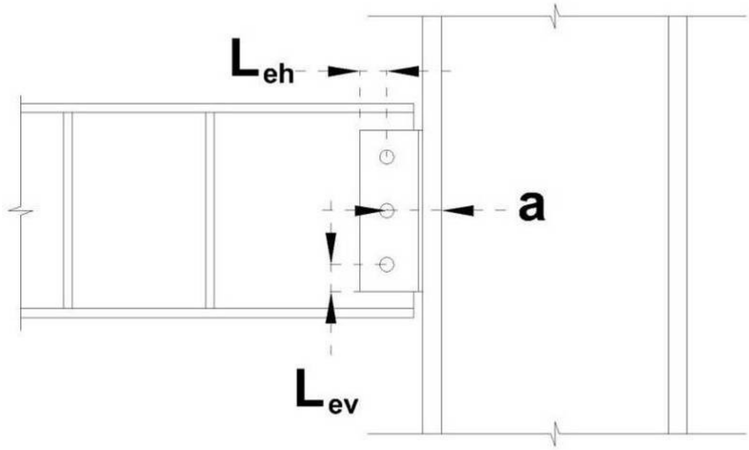

Figure 2-4: Horizontal and Vertical Edge Distances of Conventional AISC Shear Tab Configuration

If these conditions are met, the designer would then check the connection for block shear rupture, bolt bearing, bolt shear, shear yielding of the plate and shear rupture of the plate. Eccentricities may be ignored altogether for connections having short slotted holes and up to twelve bolts. Eccentricities may also be ignored for connections having standard holes and nine or fewer bolts. Connections with ten to twelve bolts and standard holes should be assumed to have an eccentricity of:

$$e_b = n - 4 \qquad \text{[Eq. 2.18]}$$

and the calculated eccentricity coefficient, *C*, from Table 7.7 (AISC, 2005) should be multiplied by 1.25 when determining the strength of the eccentrically loaded bolt group. The basis for this particular 1.25 factor is not described in the design procedure (AISC, 2005), however,using values from Table 7.7 (AISC, 2005), it does render the effective number of bolts almost equal to the actual number of bolts present. This suggests that while the eccentricities may not be ignored entirely for these cases, as they may be for the cases having nine or fewer bolts, the reduction in bolt group strength is assumed to be relatively small.

Shear yielding of the plate, shear rupture of the plate, and block shear rupture of the plate are determined as shown in Eqs. 2.19, 2.20 and 2.21, respectively:

$$\phi R = 0.6\phi F_y A_{gv} \quad \text{[Eq. 2.19]}$$

$$\phi R = 0.6\phi F_u A_{nv} \quad \text{[Eq. 2.20]}$$

$$\phi R = \phi F_u A_{nt} U_{bs} + min(0.6\phi F_u A_{nv}, 0.6\phi F_y A_{gv}) \quad \text{[Eq. 2.21]}$$

where U_{bs} is a reduction coefficient based on the stress distribution, F_y is yield strength, F_u is ultimate strength, A_{nt} is the net area of the plate in tension, A_{nv} is the net area in shear, A_{gv} is the gross area in shear, and ϕ is taken as 0.75.

Bolt bearing resistance may be determined as:

$$\phi R = 2.4\phi F_u t d_b \quad \text{[Eq. 2.22]}$$

where t is the thickness of the plate or beam web and F_u is the ultimate strength of the plate or beam web.

The AISC Handbook (2005) presents the available strengths of bolts, welds and single plates in tabular form, in Tables 10-9a and 10-9b, for both Grade 36 and Grade 50 plates, with threads intercepted or threads excluded from the shear plane, with standard or short-slotted holes and with A325, A490 or F1852 grade bolts. The values from these tables take several limit states into consideration; shear yielding of the plate, bolt shear, bolt bearing on the plate, block shear rupture of the plate and weld shear capacity. The tabulated values are based on a distance between the support and the bolt line of 3'' and may be considered conservative if the actual distance between the bolt line and support is between 2-1/2'' and 3''. Weld sizes used were 5/8 times the single plate thickness being used. The tables have the added benefit of providing information for different bolt sizes and for arrangements having two and twelve bolts in a single row.

When single plate connections do not meet the requirements of the conventional configuration, the extended configuration method may be used. The extended configuration method:

- Does not restrict the number of bolts allowed in the connection.
- Allows multiple rows of bolts to be used.
- Does not limit the distance, *a*, from the bolt line to the weld line.
- Requires edge distance restrictions from Table J3.4 (AISC, 2005a) to be met.
- Requires hole properties to respect Section J3.2 (AISC, 2005a) requirements.

As in the conventional configuration, the bearing and shear strength of the bolt group must be determined. The eccentricity of the bolt group is considered to be equal to *a*, the distance from the support to the centroid of the bolt group. The maximum allowable thickness of the plate is calculated as:

$$t_{max} = 6M_{max} / F_y d^2 \qquad \text{[Eq. 2.23]}$$

$$M_{max} = 1.25 F_v A_b C' \qquad \text{[Eq. 2.24]}$$

where F_v is the shear strength of an individual bolt, F_y is specified plate yield stress, d is the depth of the plate, A_b is the cross-sectional area of one bolt, C' is the coefficient for the eccentric bolt group with the instantaneous centre of rotation at the centroid of the bolt group (Tables 7.7-7.14, AISC, 2005). Since this limit on the thickness of the plate serves to ensure ductility in the connection, the check is done using the nominal resistances and not the factored ones.

Again, as with the conventional method, the designer must check the plate for shear yielding, shear rupture, and block shear rupture using Eqs. 2.19, 2.20 and 2.21.

The flexural yielding strength of the plate, ϕM, must also be checked based on a critical stress, F_{cr} , as follows:

$$M = F_{cr}Z \qquad \text{[Eq. 2.25]}$$

$$F_{cr} = (F_y^2 - 3f_v^2)^{1/2} \qquad \text{[Eq. 2.26]}$$

$$f_v = V / t_pL \qquad \text{[Eq. 2.27]}$$

$$V = F_y / ((a/Z)^2 + 3(1/t_pL)^2)^{1/2} \qquad \text{[Eq. 2.28]}$$

where Z is the plastic section modulus of the plate, and L, t_p, and F_y are the length, thickness, and yielding strength of the plate respectively.

Additionally, plate buckling should be checked for. The available buckling stress can be calculated as:

$$F_{cr} = F_yQ \qquad \text{[Eq. 2.29]}$$

where Q is a full reduction factor for slender compression elements, based on the dimensions and yield stress of the single plate. Q decreases as slenderness, λ, of the plate increases. The equations are based upon the classical plate buckling equation and are adopted for the worst case scenario where a shear tab is attached to a beam with coped top and bottom flanges. The terms are defined as follows in Equations 2.30 through 2.33:

$$\lambda = [(h_o(F_y)^{1/2}) \; / \; [10t_w(475 + 280(h_o/c)^2)^{1/2}] \qquad \text{[Eq. 2.30]}$$

$$Q = 1 \qquad \text{when } \lambda \leq 0.7 \qquad \text{[Eq. 2.31]}$$

$$Q = (1.34 - 0.486\lambda) \qquad \text{when } 0.7 < \lambda \leq 1.41 \qquad \text{[Eq. 2.32]}$$

$$Q = (1.30 / \lambda^2) \qquad \text{when } \lambda > 1.41 \qquad \text{[Eq. 2.33]}$$

where c is defined as the length of plate parallel to the compressive force, h_o is the depth of the plate, t_w is the thickness of the plate, and F_y is the yield stress of the plate.

2.4 Industry Design Approach to Weld Retrofits

As mentioned previously, when connections do not fit together properly on a construction site, weld retrofits are often used. These retrofits can be as simple as a vertical weld along the height of the shear tab, or it may be in the shape of a partial-*C* or *L* weld around the shear tab. In both cases it is assumed that the capacity of the weld group may be calculated using the tables in the CISC Handbook (2010) for eccentric loads on weld groups. The tabulated values are based on the instantaneous centre of rotation method. The tables present coefficients based on the dimensions and orientation of the welds, which allow the designer to determine the weld size required to resist a given eccentric load.

2.5 Summary

A brief review of past research in the area of single plate shear tab connections has been presented. It was shown that the Canadian design approach in use today is largely based on the work of Astaneh et al. (1989) and that the tabulated design values in the CISC Handbook (2010) are based partly on outdated resistance factors and clauses from CSA S16 (1994). The design methodologies of both the CISC and AISC were outlined and the various design checks that must be completed are presented. The design procedures of the AISC Handbook (2005) are based on more recent research and the extended configuration design method allows designers to consider a wider variety of connections with less restrictions. Finally, a brief explanation of the commonly used design process for weld retrofits is given.

The research being undertaken aims to prove or explain the extent of the applicability of recent design methods to double row, bolted shear tab connections as well as larger single row bolted connections than have not been tested in the past. Additionally, it will shed light on the properties and behaviour of weld retrofits at their ultimate limit state as there seems to be a demand for this in the industry and a lack of research in this area in the past.

3.0 CHAPTER 3: Experimental Testing

3.1 Test Setup

3.1.1 Overview

Chapter 3 presents the design and setup of the test frames in the structural laboratory. The test specimens will also be presented and listed in tabular form in order to outline the grade, thickness and size of plates and beams tested, the number, grade and type of fasteners used in each connection, as well as the grade and size of the welds used. The instrumentation used to collect data will be explained in detail and photos of typical instrument setups will be presented to further clarify the descriptions. Once the test setups and connection details have been made clear, the testing protocols and procedure, including how the applied load and beam rotation were controlled during testing, will be explained.

3.1.2 Design and Fabrication of Stub Column Frame and End Frame

The explanation of the test frame designs will be divided into two sections, with the first covering the stub column frame and end frame, and the second covering the lateral bracing frames. The typical test frames are depicted in Figures 3-1, 3-2 and 3-3.

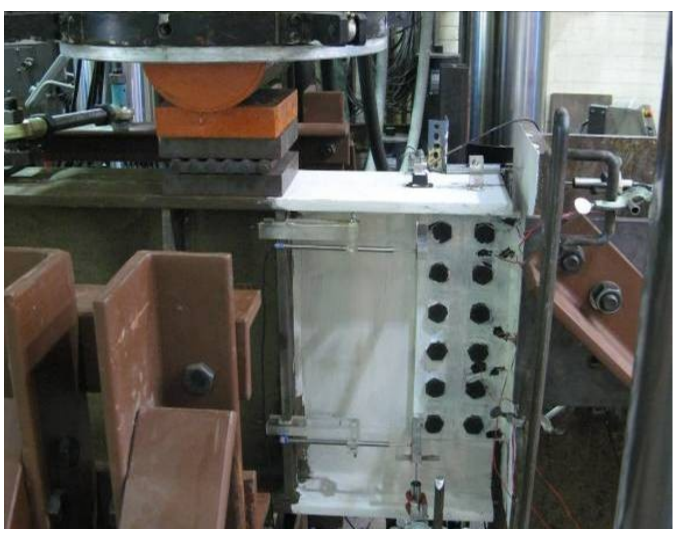

Figure 3-1: Test beam, shear tab and stub column

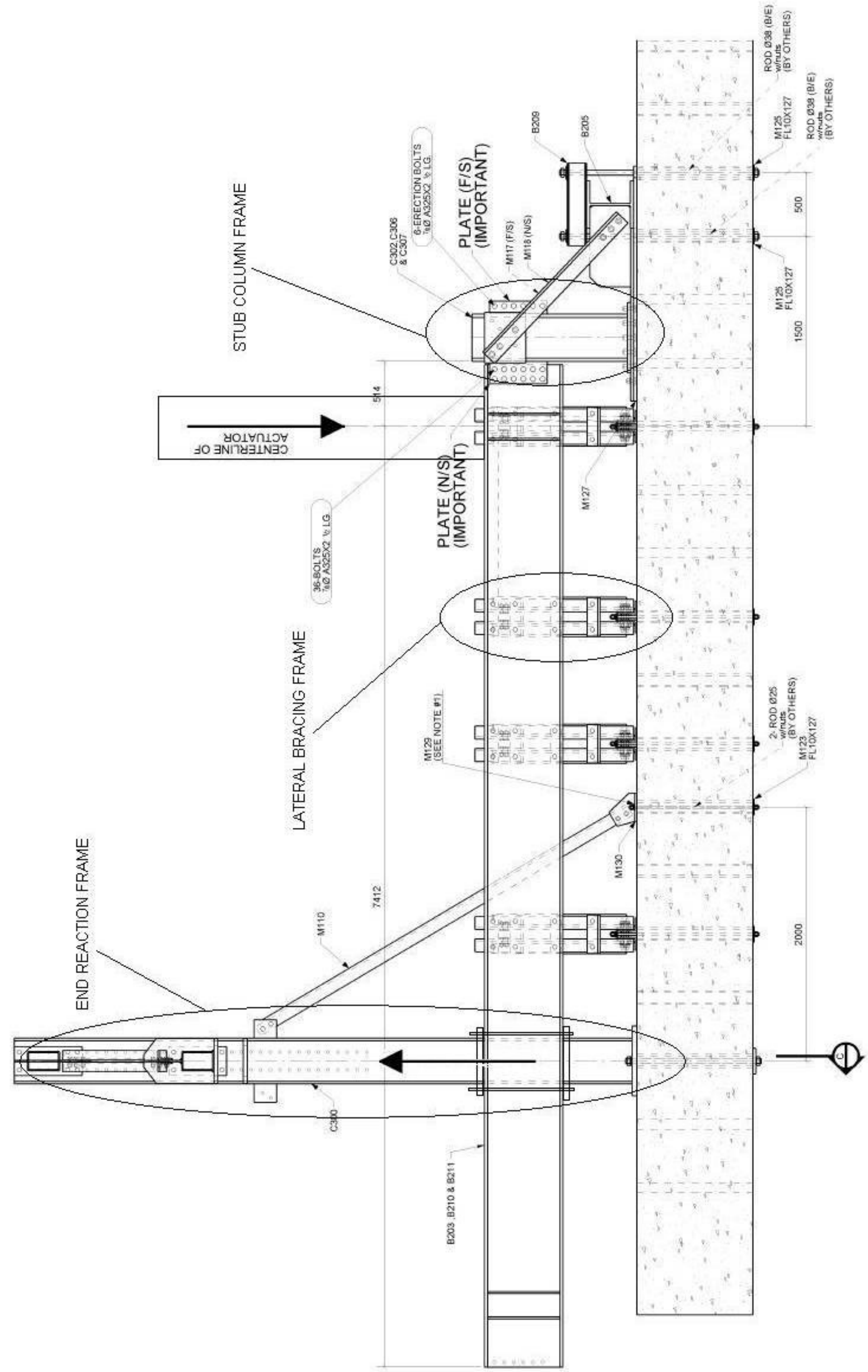

Figure 3-2: Elevation of Typical Test Frames

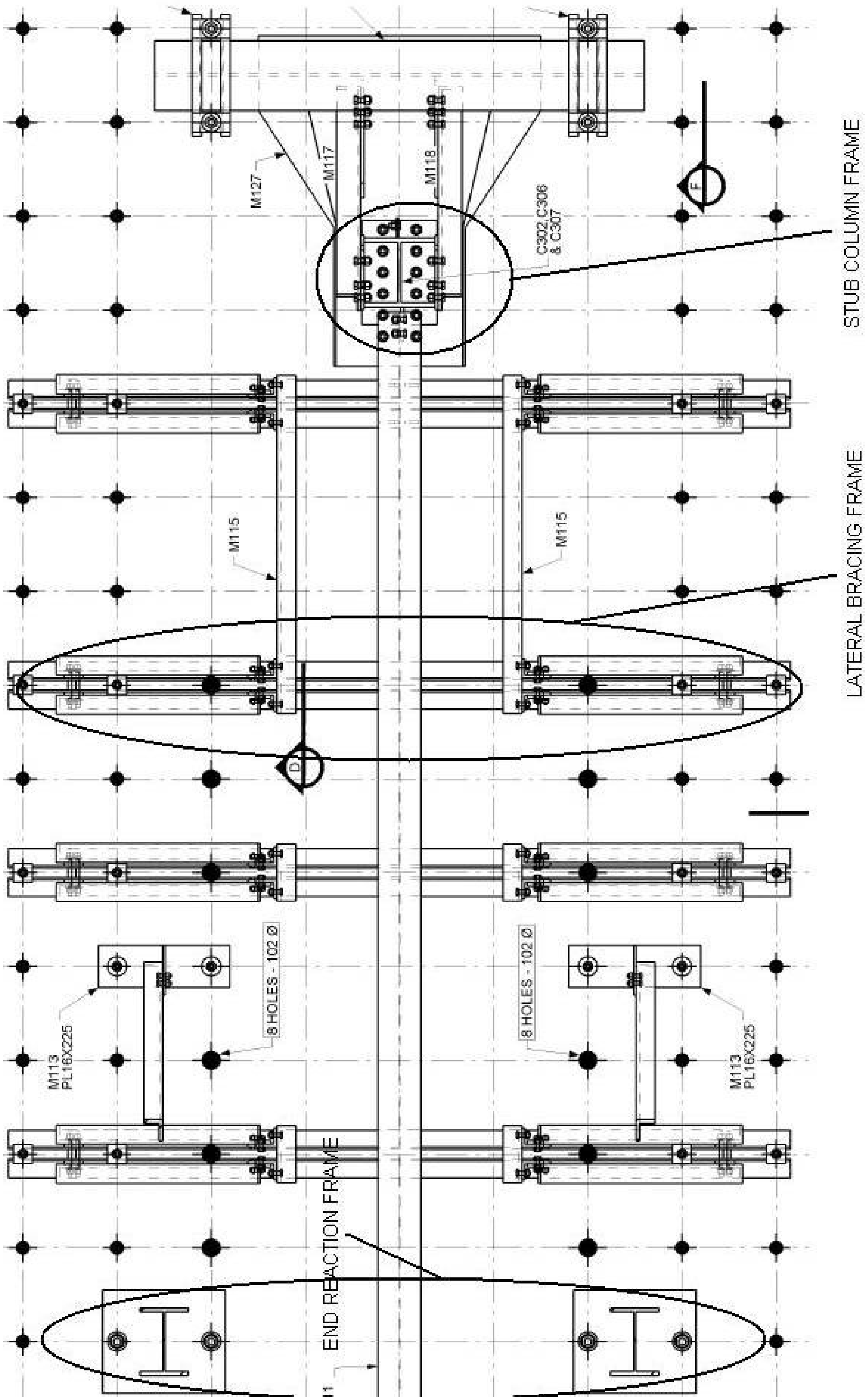

Figure 3-3: Plan View of Typical Test Frames

The single plates were shop welded to the stub column, which ultimately carried the reaction of the beam through the shear tab connection. Welding procedures are outlined in detail in Section 3.2. The shear tab beam-to- stub column connection was located close to the 12 MN hydraulic actuator that was used to load the test beam. In order to minimize rotation of the column, it was braced by two L127x127x19 inclined angles, which were attached to a W360x196 beam that had been pre-tensioned to the strong floor. The layout was limited due to the positioning of anchor holes, represented by black circles in Figure 3-2, through the concrete strong floor in the structures laboratory. A shear tab plate was welded to both sides of each column, such that each column could be used for two tests.

The end frame consisted of a truss with HSS-member chords that could be lowered or raised between two W-section columns to accommodate different sized members and obtain the travel needed from the actuator. The end actuator was suspended from this truss. The actuator was operated in tension, taking the vertical reaction while lowering the beam end to simulate rotation while force was applied by the larger 12 MN actuator closest to the connection being tested. The capacity of the actuator operating in tension was 269 kN. The frame was braced by angles on either side anchored through the concrete strong floor of the lab. The columns themselves were also anchored through the concrete strong floor. Figure 3-3 shows the end frame with the actuator attached prior to the first test. Note that the end of the beam was blocked by wood at this point. That was not part of the setup and was used to maintain the beam in the correct position until all of the hydraulic systems were brought online.

Figure 3-4: End Frame and End Actuator Shown with W310 Beam (Prior to running of test)

3.1.3 Design of Lateral Bracing System

The lateral bracing frames were designed to provide lateral stability over the entire length of the beam. They were positioned at spacings well under L_u, the maximum unbraced length that can be considered before the moment resistance of the beam is decreased to account for lateral torsional buckling. As with the rest of the framing, these braces were anchored through the concrete strong floor with tensioned threaded rods. Along the beam, at the locations of the lateral braces, plates were clamped to the compression flange. These plates were equipped with a high-strength bolt, which acted as a pivot point in the middle of the plate. A plate that was free to rotate about this bolt, itself equipped with two bolts at opposite ends, was then added to the setup. The two bolts on this plate fit perfectly into end-rod ball and socket joints.

Ball and socket joints connected rods from the lateral support frames to the bolts on the pivot plates. This allowed the beam to rotate and move freely in the vertical plane but prevented any lateral displacements from occurring by subjecting one of the rods to tension and the other to compression at all times. The design of this lateral bracing system was inspired by research conducted by Yarimci et al. (1967). Figure 3-4 shows the ball and socket assembly with the aforementioned threaded rods which take the lateral forces out to the support frames. Lastly, the test frames are depicted in Figure 3-5. The lateral bracing rods are not shown.

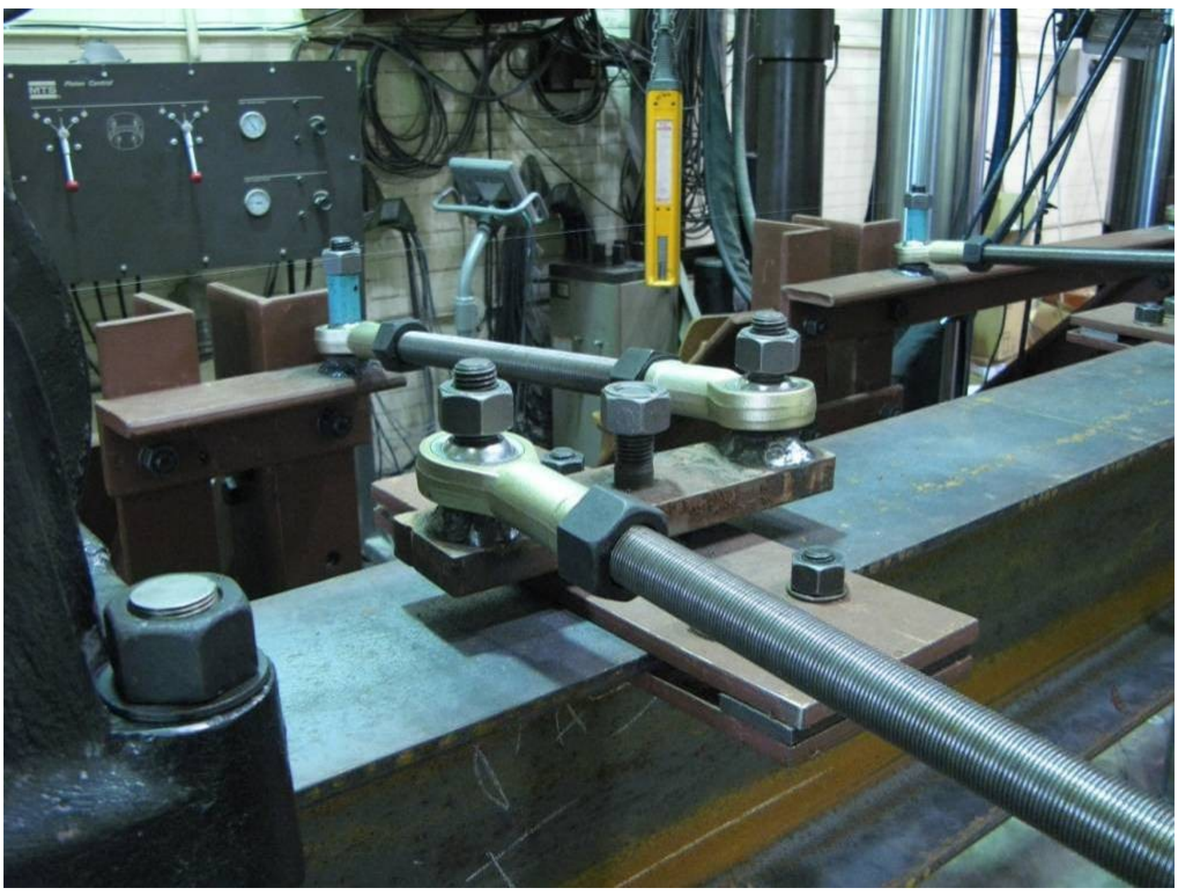

Figure 3-5: Lateral Bracing Arms Connected to Frames with Ball and Socket Joints

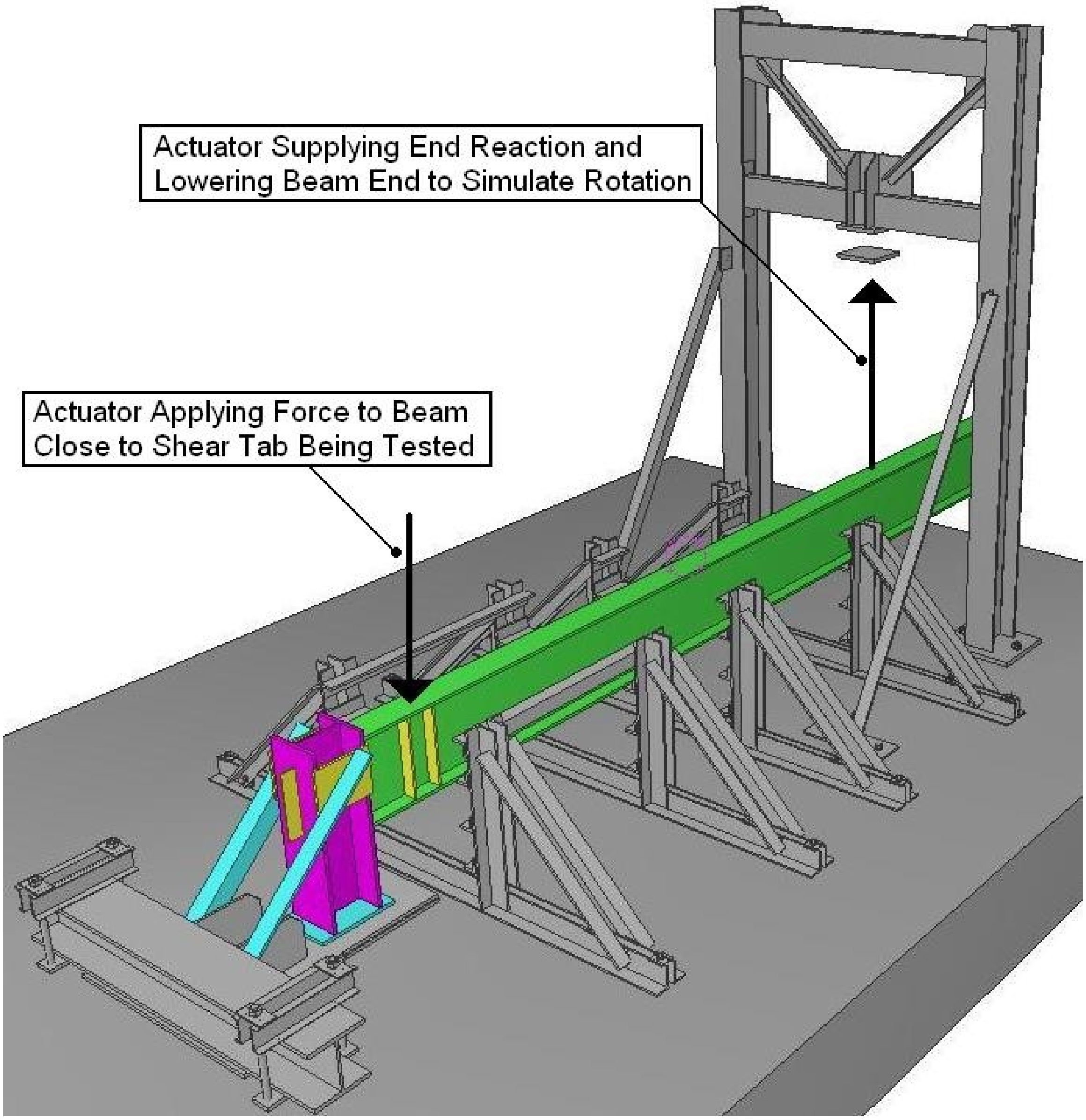

Figure 3-6: 3D Rendering of Test Frames with W610 Beam

3.2 Test Specimens

Sixteen full-scale tests were conducted in the structures laboratory; Table 3-1 presents the connection configuration, shear tab size, number and size of bolts, number of bolt rows, fillet weld retrofit shape and size if applicable and beam that were used in each of the tests. The welding of the shear tabs to the supporting stub columns was performed in the shop used flux-cored wire and gas shielding. A semi-automatic wire-fed machine was used for this flux-cored arc welding (FCAW) process. Tubular flux-cored wire was fed from a spool to the welding gun and a line of 100% CO_2 shielding gas also fed into the welding gun. The designation of the welding wire used was 1/16'' diameter E71T where E stands for electrode, 7 refers to minimum tensile strength times 10^4 (70 ksi electrode in this case), 1 refers to the positions this electrode can be welded in ("1" refers to all positions) and T denotes the tubular nature of the welding wire. These welds generally offer consistent and reliable results as they are performed in a controlled environment with dual-shielding because of the use of both the flux-core and the carbon dioxide shielding gas. Additionally, they are compliant with the AWS A5.20 'D' (2005) designation requirements of the American Welding Society.

Typical weld retrofit shapes are depicted in Figure 3-6. To further clarify the weld retrofit designations referred to in Table 3-1, full "C" weld retrofits are done around the entire perimeter of the shear tab to the test beam. Partial "C" weld retrofits are done around the perimeter of the shear tab but exclude the area from the centreline of the innermost row of bolt holes to the end of the test beam. Lastly, "L" shape weld retrofits extend around the perimeter of the shear tab from the bottom at the centreline of the row of bolt holes closest to the column, completely along the vertical face of the shear tab, and a distance two times the fillet weld size along the top face of the shear tab. The "L" shape was used because the area between the top flange and the top of the shear tab was initially thought to be too confining for the welder to work in. This was not the case and as a result, "C" shape welds were used in the majority of tests.

Detailed sketches of each test setup and corresponding weld retrofit are provided in Appendix A. Further details regarding weld retrofit design and layout are given in subsequent sections of this Chapter, particularly in Section 3.4.2.

Shear tab connections that lay within the scope of current design procedures in the CISC Handbook of Steel Construction (2010), as well as connections frequently used in the steel construction industry but falling outside of the scope of current Canadian design procedures, were selected for experimental testing. For many connections used

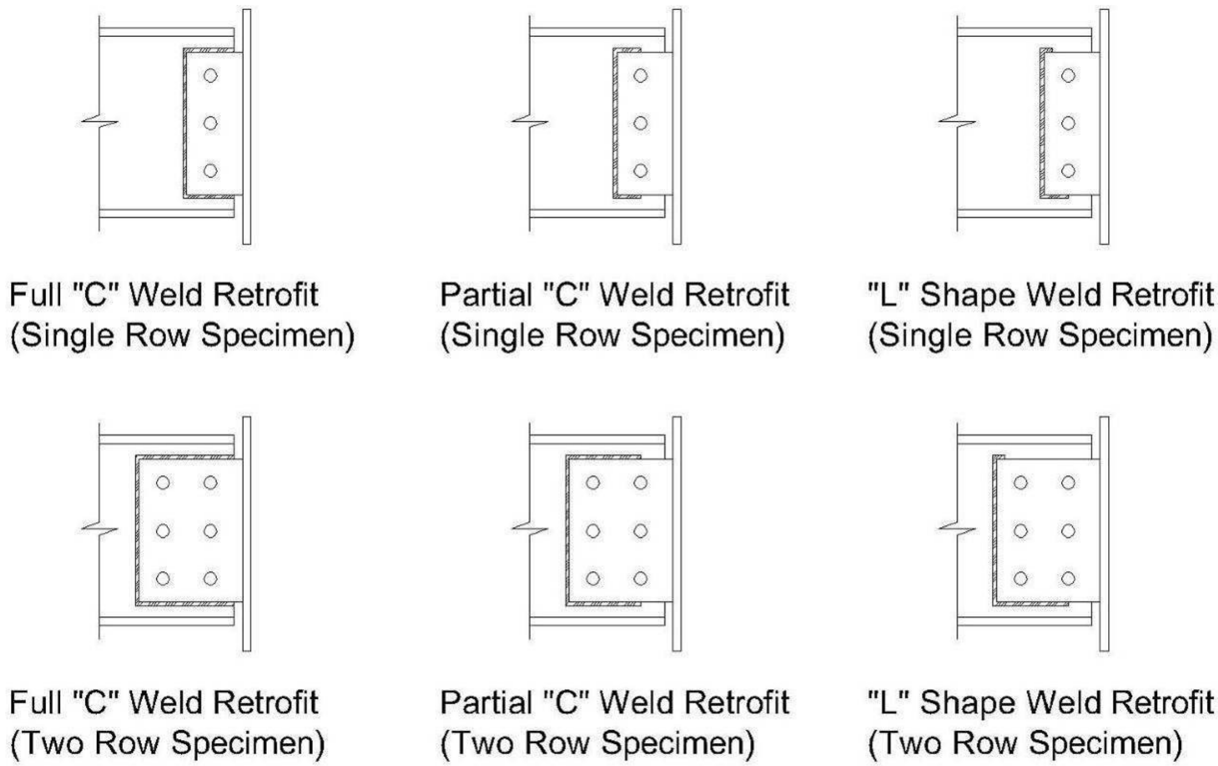

Figure 3-7: Typical Weld Retrofits

in the steel construction industry, there is little or no available test data to refer to for design considerations. To this end, both single and double row connections were considered. The single row tests using three and six bolts in a row could be compared to recommended design values in the Handbook (CISC, 2010) and the experimental results obtained from larger test connections, both double row tests and tests exceeding the current number of bolts allowed in single row connections, could be used to recommend design procedures for these cases and serve as a basis for further research to come. In terms of the grade of steel used for the shear tabs, Grade A572-GR50 (50 ksi) steel was selected since most of the past research focused on the use of 36 ksi steel and questions remained about the ability of these higher strength plates to deform and accommodate rotation effectively. With regards to the selection of test beams, in the first iteration of test specimen selections, lighter beams of equal depth had been selected but were then replaced by heavier ones listed in Table 3-1. It was determined

Table 3-1: Properties of Shear Tab Test Specimens

Test	Type	Test Beam	Rows of Bolt Holes	Bolts per row	Shear Tab Thickness	Weld Retrofit Shape	Retrofit Fillet Weld Size (D)	Shear Tab to Column Weld Size (both sides) (D)
1	Bolted	W310x60	1	3 x 3/4'' A325	6 mm	N/A	N/A	6 mm
2	Bolted	W310x60	2	3 x 3/4'' A325	10 mm	N/A	N/A	6 mm
3	Welded	W310x60	1	N/A	6 mm	Full "C"	3/16"	6 mm
4	Welded	W310x60	1	N/A	6 mm	Partial "C"	1/4"	6 mm
5	Welded	W310x60	2	N/A	10 mm	Full "C"	1/4"	6 mm
6	Welded	W310x60	2	N/A	10 mm	Partial "C"	5/16"	6 mm
7	Bolted	W610x140	1	6 x 7/8'' A325	8 mm	N/A	N/A	6 mm
8	Bolted	W610x140	2	6 x 7/8'' A325	16 mm	N/A	N/A	10 mm
9	Welded	W610x140	1	N/A	8 mm	Partial "C"	5/16"	6 mm
10	Welded	W610x140	2	N/A	16 mm	"L"-shape	7/16"	10 mm
11	Welded	W610x140	1	N/A	8 mm	Partial "C"	5/16"	6 mm
12	Welded	W610x140	2	N/A	16 mm	"L"-shape	9/16"	10 mm
13	Bolted	W920x223	1	10 x 1'' A325	10 mm	N/A	N/A	6 mm
14	Welded	W920x223	1	N/A	10 mm	Partial "C"	5/16"	6 mm
15	Bolted	W920x223	2	10 x 1'' A325	22 mm	N/A	N/A	14 mm
16	Welded	W920x223	2	N/A	22 mm	Partial "C"	5/8"	14 mm

Notes: -Bolt threads were always excluded from the shear plane.
-Test beams were Grade A992 Steel
-Test shear tabs were Grade A572-GR50 Steel
-Horizontal and vertical edge distances were all 1.5''.
-Centre-to-centre spacing of all bolt holes was 3''.
-Centre-to-centre spacing of all bolt holes was 3''.
-Retrofit weld specifications and layouts may be found in Appendix A.
-Grade E70 electrodes were used for all welds.

that the lighter beams themselves would fail either in bending or shear prior to the connection reaching the predicted shear strength. As it was the intent of the research to examine the behaviour and deformations of the single plate shear tabs as they failed, it was necessary to select these heavier beams in order to avoid inelastic deformations in the test beams prior to the shear tab failing. The W920x150 beams could not be replaced by heavier beams however, as they had been purchased prior to the start of the research project. The determination of the predicted shear tab failure loads is described in Section 3.3.

3.3 Design of Tested Connections

The design methodology for both the bolted and welded connections will be explained in this section. For the bolted connections, the preliminary design checks were carried out using the conventional and extended shear tab design procedures of the AISC Steel Construction Manual (2005) and of the CISC Handbook (2010) to determine predicted capacities, where applicable, for single and double row shear tab tests having rows of three, six, and ten bolts. Some of these design approaches were not applicable to certain cases. For example, the CISC Handbook (2010) method does not apply to single row connections having more than 7 bolts, or having multiple rows of bolts. Also, the AISC Conventional approach (2005) does not apply to connections when multiple rows of bolts are present. The constraints and steps of each design approach are presented in detail in Chapter 2. Because coupon testing could only be carried out after the shear tab tests due to equipment availability, overstrength values of $1.1F_y$ and $1.1F_u$ were initially assumed as probable yielding and ultimate strengths of the shear tabs when checking to ensure that the shear tabs would fail prior to inelastic deformations taking place in the test beams.

A modified AISC shear tab design method was also developed to account for the strength of the bolt group. Kulak et al. (1987) showed that the average strength of A325 bolts in shear was 62% of the ultimate tensile strength, whereas the strength in the AISC Specification (2005a) is 50% of the ultimate tensile strength. As such, $0.62F_u$ was used in the modified procedure. Another difference, when using the modified AISC method, was that when determining the maximum plate thickness, the 1.25 factor used to remove the 20% reduction in shear strength of bolts to account for end-loaded bolt groups was omitted. This is done because $0.62F_u$ is already 1.24 times $0.5F_u$. Having looked at each of the applicable design methods for each of the bolted shear tab test scenarios, the predicted failure modes and the predicted loads at which they would occur were noted. Detailed calculations and step by step checks are presented for each of the aforementioned approaches in Appendix B. A summary of the predicted shear tab capacities and failure modes for each of the bolted specimens is given in Table 3-3. It lists both the initial predicted values based on the nominal properties using the minimum specified yield and ultimate strengths as well as the predicted values based on actual material properties obtained from coupon tests conducted upon completion of the connection tests. For the loading and rotation protocols described in Section 3.5, it should be noted that values of $1.1F_y$ and $1.1F_u$ were used rather than the specified minimum yield and ultimate strengths.

For the welded connections, design engineers at DPHV Structural Consultants were approached to determine what types of weld retrofits were being used in practice on construction sites. Some examples of these include “C” and “L”-shaped welds as are depicted in Figure 3-6. From there, Tables 8.4 through 8.11 (AISC, 2005) and Tables 3-26 through 3-33 (CISC, 2010), providing the capacity of welds subjected to eccentric loads were used to design the retrofit welds and match the predicted factored strength of equivalent bolted connections. The predicted resistances of the bolt groups were set equal to the predicted resistances of the weld groups. The factored strengths for which the weld groups were designed are listed in Table 3-2. Knowing the configuration of the weld group, appropriate fillet weld sizes were then chosen. The tables used are based on the instantaneous centre of rotation method, which requires the designer to assume an eccentricity between the centroid of the weld group and the line of force being applied. The eccentricities used in calculating these weld group capacities were taken as the distance from the face of the stub column to the centroid of the weld group. The resistance of an eccentrically loaded weld group will be a function of the size of weld used, the strength of electrode used, the geometry of the weld group and its position with respect to the applied force.

Table 3-2: Factored Strengths Weld Groups Were Designed For

Test Beam	Rows of Bolt Holes	Factored Strengths Weld Groups Designed to Resist (kN)
W310x60	1 x 3 bolts	213
W310x60	2 x 3 bolts	320
W610x140	1 x 6 bolts	503
W610x140	2 x 6 bolts	1006
W920x150	1 x 10 bolts	945
W920x150	2 x 10 bolts	2206

Table 3-3: Predicted Connection Resistances based on Nominal and Actual Material Properties

	Unfactored Predicted Resistance Based on Nominal Material Properties (kN)	Predicted Failure Mode	Unfactored Predicted Resistance Based on Measured Material Properties (kN)	Predicted Failure Mode
Test 1: 1Rx3Bolt				
AISC Conventional	285	SR	297	SR
AISC Extended	257	PF	263	BG
CISC Handbook*	237	SR	247	SR
Modified Method	257	PF	297	SR
Test 2: 2Rx3Bolt				
AISC Extended	397	BG	397	BG
Modified Method	405	PF	424	PF
Test 7: 1Rx6Bolt				
AISC Conventional**	676	SR	737	SR
AISC Extended	676	SR	737	SR
CISC Handbook*	564	SR	576	BG
Modified Method	676	SR	737	SR
Test 8: 2Rx6Bolt				
AISC Extended	1333	SR	1433	BG
Modified Method	1333	SR	1476	PF
Test 13: 1Rx10Bolt				
AISC Conventional**	1323	SR	1531	SR
AISC Extended	1323	SR	1531	SR
Modified Method	1323	SR	1531	SR
Test 15: 2Rx10Bolt				
AISC Extended	2887	BSR	3515	BSR
Modified Method	2887	BSR	3515	BSR

*The CISC Method forces a specific failure mode by choosing the plate thickness. For comparison purposes, the design checks were performed with the plate thicknesses being used in the tests, rather than choosing the plate thickness.

**Connection did not respect edge distance requirement for AISC Conventional Design Method but did respect CISC edge distance requirements.

Minimum specified Fy and Fu were used for *nominal* predictions.

Failure Modes
SR = Shear Rupture through net area of plate
BG = Shear failure of bolt group
PF = Plate flexure with von Mises shear reduction
BSR = Block Shear Rupture

3.4 Test Setup and Instrumentation

3.4.1 Bolted Test Connections

The first step prior to each test was to bolt the stub column to its base plate and secure the angle braces to the floor beam. The test beam was then lowered into place using an overhead crane. One or two bolts were inserted through the shear tab and beam web. The beam was subsequently leveled and centred and the bolts were snug tightened, securing the beam in place. The remaining bolts were then installed followed by setup of the lateral bracing system. This consisted of clamping plates to the beam flanges and positioning the threaded-rods with ball and socket joints onto the bolts that served as pivot points. All bolts in the test setup were snug tight and not pretensioned.

The instrumentation was then installed as shown in Figure 3-7, for a typical W310x60 beam. Linear variable differential transducers (LVDTs) were used to measure vertical and horizontal displacements throughout the testing process. Vertical displacements of the beam directly under the bolt group at the connection end, shear tab, stub column, and bottom bolt were all measured with +/- 15mm stroke LVDTs.

Each actuator, also being equipped with LVDTs, provided vertical displacements at those locations. For the smaller 269kN capacity end actuator, string potentiometers were used to provide additional measurements of vertical and horizontal displacements. To determine whether the beam was twisting out-of-plane, +/-25 mm stroke LVDTs were placed against the top and bottom flanges, as indicated in Figure 3-7. Horizontal displacements at the centreline of the top and bottom bolt holes were taken with separate pairs of +/-25mm stroke LVDTs in order to find the rotation of the bolt group and shear tab. Similarly, another pair of +/- 15mm stroke LVDTs measured horizontal displacements from the top and bottom beam flanges against the stub column, again in order to be able to calculate the rotation of the beam relative to the stub column. One last +/- 15mm LVDT measured the horizontal displacement at the top of the stub column at a known height above the ground.

For redundancy, inclinometers were used on the bottom beam flange directly below the centreline of the 12MN actuator, as well as on the top flange of the test beam at a distance of 150mm from the end of the test beam.

Strain gauges were used on the shear tab as depicted in Figure 3-7. A rosette strain gauge was typically used near the centre of the shear tab, however, after having a few malfunctions over the first series of tests, the rosette strain gauges were phased out and replaced by single strain gauges positioned at 45° to measure shear strain. The strain gauge configuration was not identical in each test and all of the strain gauge layouts are shown in Appendix A.

As a means of observing yielding patterns and deformations, both the beam web and shear tab were painted with a lime / water whitewash. Figures 3-8 and 3-9 provide close-up views of the whitewashed beam and shear tab and the instrumentation in the immediate vicinity of the connection on both sides of the beam. It should be noted that for each test, rollers and a half-round rocker were placed directly under the 12 MN actuator, to accommodate the rotation and overcome friction where the load was applied. They are shown in Figure 3-10.

Test setups and instrumentation for the bolted W610x140 and W920x223 beams were quite similar in principle and are shown in Appendix A. The only bolted shear tab test setup that differed considerably was Test 15, in which the connection consisted of two rows of ten 1'' bolts. The tensile capacity of the end actuator was insufficient to carry the anticipated reaction at the tip of the beam. Two 60 kip (≈ 267 kN) capacity hydraulic jacks, having a stroke of 250 mm were used at the far end in this case and are shown in Figure 3-11.

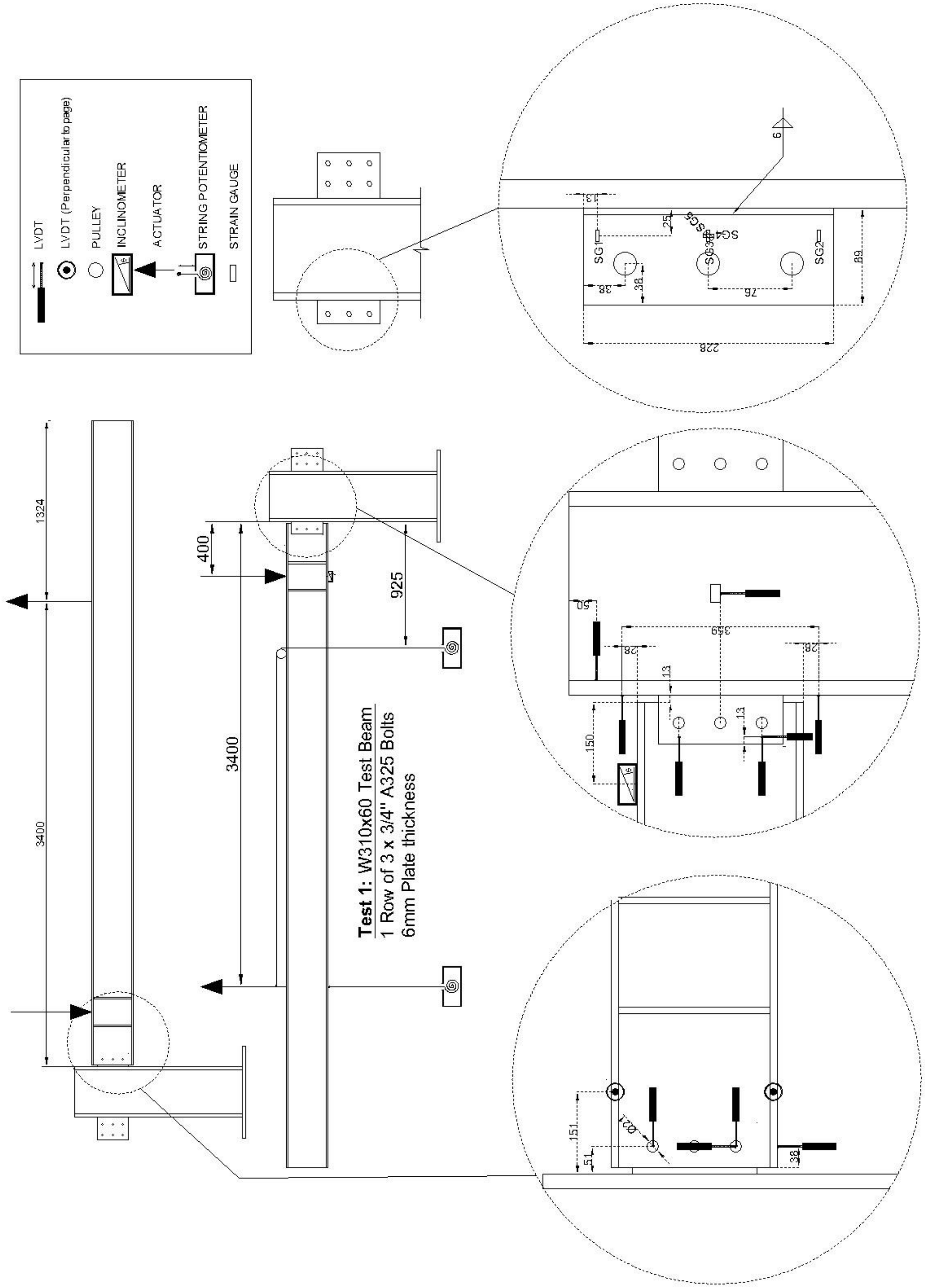

Figure 3-8: Typical Setup and Instrumentation for a Bolted W310x60 Test Beam

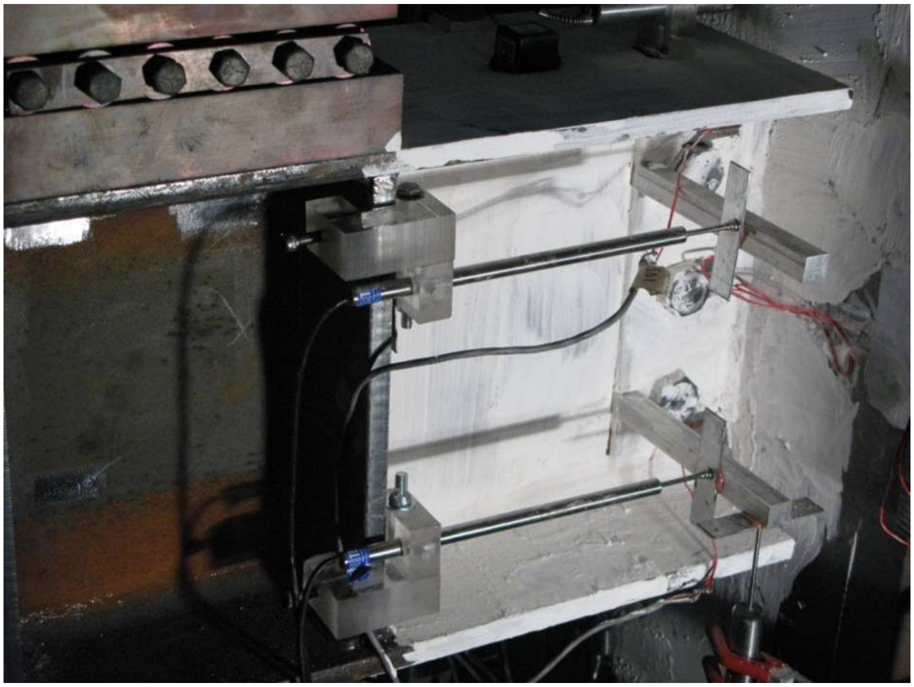

Figure 3-9: Instrumentation at Connection for Test 1: W310x60 (Shear Tab Side)

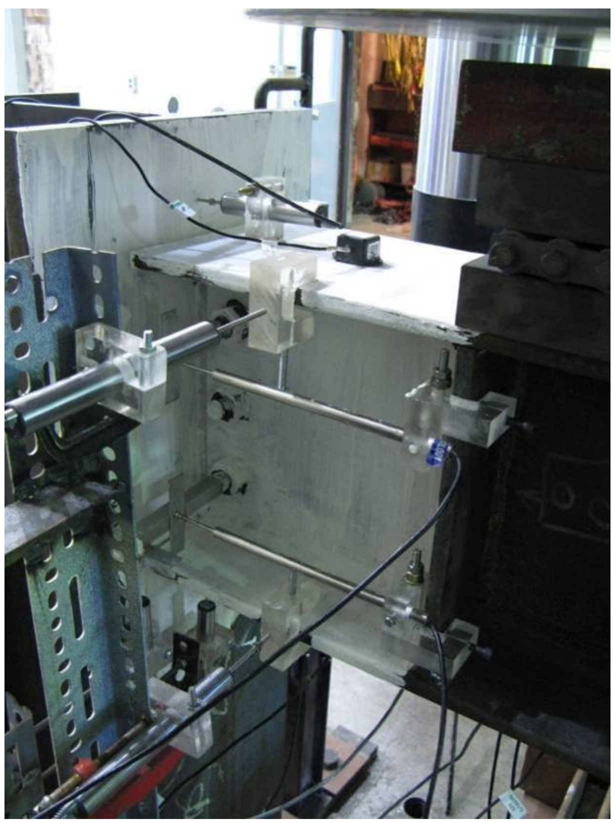

Figure 3-10: Instrumentation at Connection for Test 1: W310x60 (Opposite Shear Tab Side)

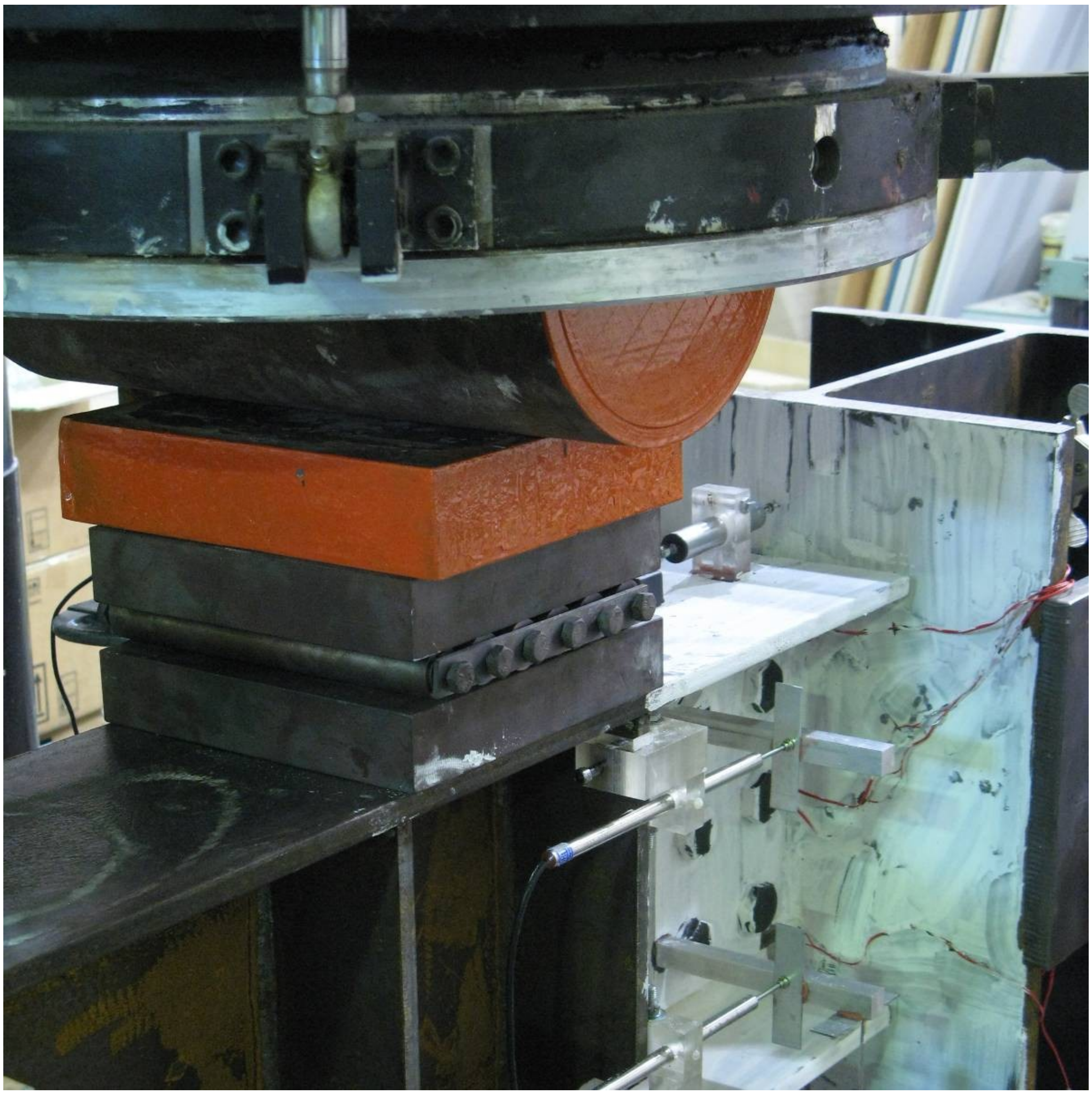

Figure 3-11: Half Round, Plates and Rollers Shown Between Actuator Head and Test Beam

Figure 3-12: Hydraulic Jacks Used in Place of End Actuator for Test 15

The hydraulic jacks supported a spreader beam which was a built-up section of channels and plates. Threaded rods were used to attach the top flange of the beam to the spreader beam. On the concrete strong floor, 75 mm thick plates and 150 mm diameter rollers were used to ensure the supports were not restrained, but rather free to move horizontally as the end of the test beam was lowered. A hand pump was used to control the vertical displacement of the jacks. Load cells with 100 kip (≈ 445 kN) were installed under the jacks to record the end reaction.

3.4.2 Welded Test Connections

The setup for the weld retrofit shear tab connections was almost identical to the bolted shear tab connection setup with the exception that once the erection bolts were in place and the beam had been centred and leveled, a certified welder welded the shear tab to the beam web on site in the structures laboratory as shown in Figure 3-12.

Figure 3-13: Certified Welder Completing SMAW Weld Retrofit of Shear Tab to Beam Web

Shielded metal arc welding (SMAW) was used for these field welds. This type of welding makes use of electrode sticks coated in flux. Electric current is provided from a power source, shown in the foreground of Figure 3-13, and creates an arc between the electrode and metal to be welded. The flux surrounding the electrode releases gases which shield the area from unwanted contaminants. In the structures laboratory, 1/8'' E7018-1 MR Performance Plus electrodes having a minimum tensile strength of 70 ksi were used. This particular procedure was chosen in order to replicate typical field weld conditions.

Figure 3-14: Welding Power Supply

The erection bolts were then removed and the instrumentation was added. The instrumentation was similar to that used in the bolted connection tests. The main difference was that there were no measurements taken to determine displacements of bolts, as there were no bolts present in these tests. A typical welded test setup for a W310x60 test beam is provided in Figure 3-14.

Again, the only weld retrofit connection test setup that differed significantly from that shown in Figure 3-14 was Test 16, having two rows of ten bolt holes. The end actuator did not have the capacity in tension to provide the end reaction, and hydraulic jacks were used as in Test 15.

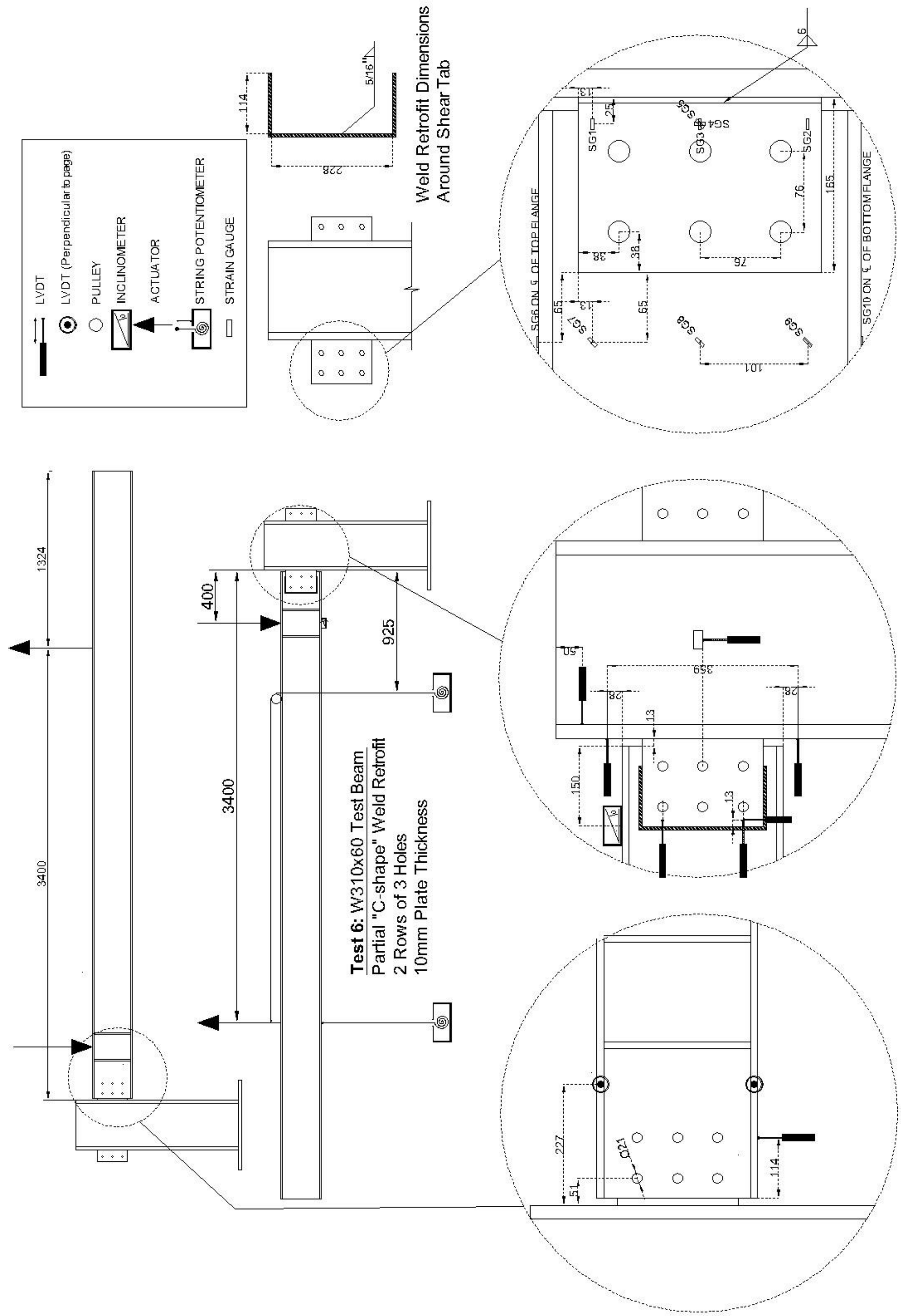

Figure 3-15: Typical Setup and Instrumentation for a Welded W310x60 Test Beam

3.5 Test Procedure

3.5.1 Bolted Test Connections

All of the tests were conducted using both of the actuators in displacement control, with the exception of Test 15 and Test 16 as described in Section 3.4.1, where hydraulic jacks were used instead of the end actuator. Stub column to beam rotations of 0.02 radians for W310 test beams and 0.015 radians for W610 and W920 test beams were targeted to be reached at the probable ultimate resistance of the shear tab, using values of ϕ =1.0, and 1.1F_y and 1.1F_u since coupon testing only took place afterwards. The rotations chosen may seem excessive considering most beams would fail in bending before these shear forces are reached, however, in buildings where there are column setbacks and/or transfer beams, these shear forces may be reached and the connections must still be able to rotate sufficiently. Additionally, in some cases blast loads must be considered. If an explosion were to occur, it would be desirable for the connection to deform and accommodate rotation at the beam support. Note that this relative rotation being described between the supporting column and the beam can differ slightly from the absolute end rotation should the stub column tilt forward under loading. The lowest probable ultimate resistance for each shear tab test was chosen from among the different applicable design procedures. The targeted probable ultimate resistances at these rotations are provided in Table 3-4. The design procedures that were used for specific tests are shown in Table 3-3. A smaller rotation was targeted for the W610 and W920 beams as they were deeper and more restrained from rotating than the W310 beams. Astaneh et al. (1989) had proposed a loading path where the end rotation would reach 0.02 radians as the test beam yielded in bending and 0.03 radians as the plastic moment of the test beam was attained. Because heavier beams with higher yield strengths were used for this new series of experiments in order to ensure failure of the shear tabs and not the test beams, the loading path suggested by Astaneh et al. (1989) was not considered to be appropriate in this case. It will be shown, however, in Chapter 4, that there was a great deal of rotational ductility available in these shear tab connections.

By using real-time measurements from the LVDTs on the top and bottom flange against the stub column face, and having measured the distance between the two LVDTs, the relative rotation of the beam-to-column joint was calculated continuously throughout the testing process. As the shear tab began to soften due to yielding, the rate of vertical displacement at the end actuator could be slowed down to keep the target ratio of connection shear and beam rotation. The experiments were paused several times throughout to make adjustments to the rates of travel of both actuators. On average, at the beginning of tests, the large 12MN actuator ran at 0.08 mm/min and the end actuator was adjusted accordingly to reach the targeted ratio. Once yielding started to occur, the ratio was maintained and the displacement rates of both actuators were increased in multiples of 1.5 to 2 at a time to speed up the process, generally peaking at about 1mm/min for the 12MN actuator.

Table 3-4: Probable Ultimate Loads at Targeted Rotations

Test Beam	Rows of Bolt Holes	Probable Ultimate Load (kN)*
W310x60	1 x 3 bolts	283
W310x60	2 x 3 bolts	424
W610x140	1 x 6 bolts	738
W610x140	2 x 6 bolts	1455
W920x150	1 x 10 bolts	1386
W920x150	2 x 10 bolts	3208

* Based on probable ultimate and yield strengths of 1.1 F_u and 1.1 F_y.

3.5.2 Welded Test Connections

The loading procedure was very similar for the welded test connections as they had been designed using the same factored resistance as the bolted connections. Having already conducted the bolted shear tab tests for each beam size before moving onto the weld retrofit connections for that beam size facilitated matters, as the targeted rotation at the predicted probable resistance of the connection was the same for the weld retrofit counterparts to each bolted test.

4.0 CHAPTER 4: Experimental Test Results and Analysis

4.1 Overview

Chapter 4 will present the experimental test results from the sixteen full-scale connection tests as well as from coupon tests conducted to determine material properties. Comparisons will be made between predicted connection resistances using different methods and the resistances measured in the laboratory. The general behaviour of each test connection, in addition to modes of failure and onset of yielding will be reported on. The effectiveness of weld retrofits when compared to their bolted counterparts will be addressed. The impact of beam size, number of rows of holes, and type of connection, be it bolted or welded, will be presented. Recommendations will be given to improve the current shear tab design method of the CISC Handbook of Steel Construction (2010).

4.2 Test Results and Observations

A summary of the maximum connection shear force reached, the maximum beam end rotation relative to the supporting column and the maximum vertical deflection of the beam relative to the supporting column at the test connection end is provided in Table 4-1 for all sixteen connection tests. All sixteen connection tests exceeded the unfactored predicted resistances using minimum specified yield stress and minimum specified ultimate stress values. Similarly, fourteen of the sixteen connection tests exceeded predicted connection resistances using measured material strengths that were determined from coupon testing. A discussion of the test-to-predicted results is presented in Section 4.3. Comments regarding the amounts of rotation attained in each test are presented in Sections 4.2.1 through 4.2.6. Additional photos and graphs documenting the progression of the failure of each test connection are given in Appendix D.

Table 4-5: Shear Tab Connection Tests - Summary of Results

	Maximum Connection Shear (kN)	Maximum Beam End Rotation Relative to Column Face (rads)	Maximum Vertical Deflection of Beam End Relative to Column (mm)
Single Row - W310 Test Beam			
Test 1	363	0.061	25.7
Test 3	357	0.063	20.3
Test 4	386	0.054	29.4
Double Row - W310 Test Beam			
Test 2	513	0.050	17.3
Test 5	620	0.059	27.1
Test 6	666	0.044	28.6
Single Row - W610 Test Beam			
Test 7	961	0.033	21.7
Test 9	849	0.034	26.0
Test 11	854	0.035	25.7
Double Row - W610 Test Beam			
Test 8	1734	0.033	31.6
Test 10	1850	0.034	29.5
Test 12	1771	0.038	26.7
Single Row - W920 Test Beam			
Test 13	1762	0.027	25.7
Test 14	1546	0.026	21.0
Double Row - W920 Test Beam			
Test 15	3489	0.021	14.2
Test 16	3330	0.016	12.1

4.2.1 Single Row of 3 Bolts and Corresponding Weld Retrofits

The single row connections featuring a W310x60 test beam with three bolt holes (bolted and and welded configurations) exceeded the targeted beam end rotation relative to the supporting column face. With regards to the weld retrofit tests, both the rotations and loads resisted were comparable to those of the bolted connection. The behaviour of all three tests is presented in Figure 4-5 where normalized connection shear ($V_{measured}$ / $V_{ultimate}$) is plotted against rotation relative to the column face. In the bolted test, bearing deformations were observed around bolt holes, pictured in Figure 4-1 after the test bolts had been removed, and significant shear deformations occurred in the shear tab between the row of bolts and the weld at the supporting stub-column face. Additionally, a weld fracture, approximately 40 mm in length between the shear tab and stub-column face near the top of the shear tab, occurred after yielding of the shear tab near the end of the test. Strain gauges indicate that shear yielding of the plate occurred prior to flexural yielding in the bolted connection configuration. The opposite was true for the weld retrofit connections. A graph which plots the connection shear against the beam end rotation relative to the column face shows the onset of yielding for Tests 1 and 3 in Figure 4-4 to demonstrate this point. The crosshairs on each graph represent the point during testing at which the indicated strain gauge reached its yield strain. Strain gauges SG1 and SG2 were placed horizontally at the top and bottom of every shear tab, while the remaining gauges were placed at 45° and served to determine when that particular region of the shear tab reached its shear yielding strain. Note that both flexural and shear yielding occurs sooner into the test for the welded connection configuration than for the bolted connection configuration.

Figure 4-1: Test 1 after Failure - Pictured after Removal of Test Bolts

This may be a result of the larger eccentricity to the centroid of the weld group when compared to the centroid of the bolt group. Finite element studies could be used to shed more light on this phenomenon. In the weld retrofit connection tests, flexural yielding of the shear tab occurred, followed by shear yielding and ovalization of the bolt holes. Shear deformations also took place between the row of bolt holes and the column face. The horizontal section of weld at the top and bottom of the full “C”-shape retrofit weld fractured up to the centreline of the row of bolts, as shown in Figure 4-2.

Figure 4-2: Test 3 after Failure - Full "C" Weld Retrofit Fracture and Deformation of Bolt Hole

Conversely, the partial “C”-shape weld retrofit did not fracture, but the shear tab itself was beginning to fracture along the vertical edge distance as shown in Figure 4-3. It should also be noted that the partial “C”-shape retrofit allowed the bolt holes to deform to a greater degree than the full “C”-shape retrofit, the latter of which extended around the entire perimeter of the shear tab. The resulting connection resistances did

Figure 4-3: Test 4 after Failure - Bolt Hole Deformations and Edge Distance Rupture

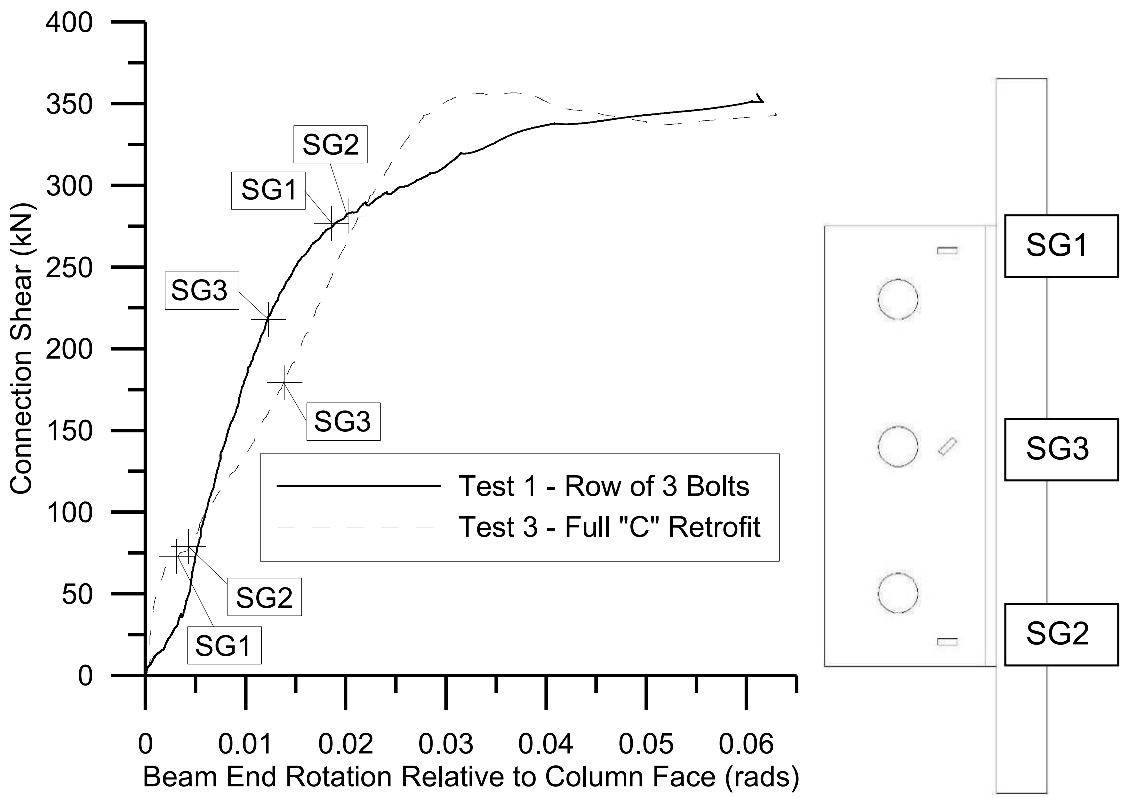

Figure 4-4: Comparison of Onset of Yielding Among Strain Gauges for Tests 1 and 3

not differ a great deal between the tests and the levels of rotation attained were quite similar when comparing the two weld retrofit configurations to the bolted test as shown in Figure 4-5.

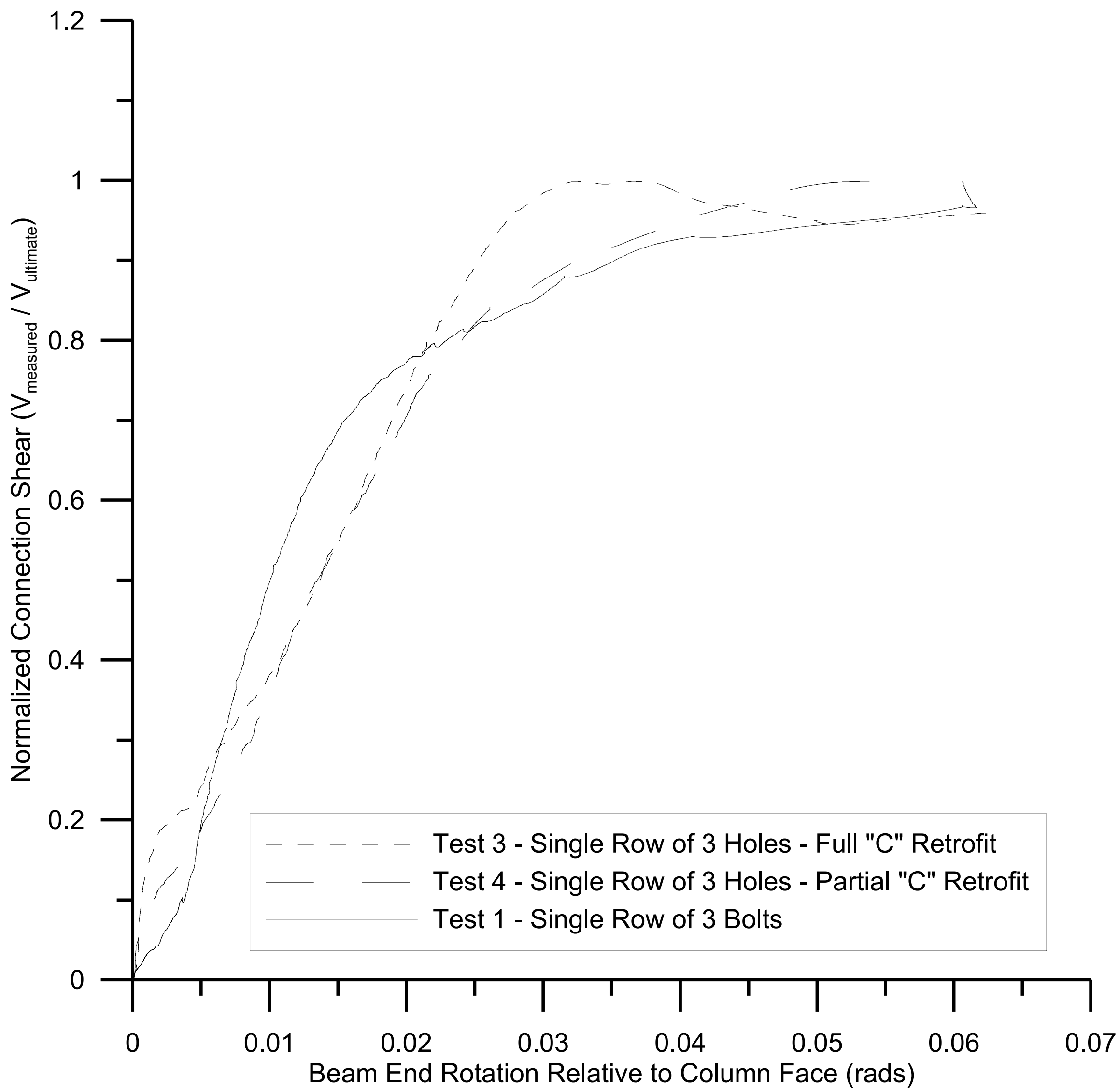

Figure 4-5: Normalized Connection Shear vs. Beam End Rotation Relative to Column Face for Tests 1, 3 and 4

The reason the loads stop increasing but do not begin decreasing, in Figure 4-5, is because tests were stopped due to the limited travel of the end actuator.

4.2.2 Single Row of 6 Bolts and Corresponding Weld Retrofits

The single row shear tab connections featuring W610x140 test beams with six bolt holes (bolted and welded configurations) performed satisfactorily. The connections were able to meet the targeted rotations at the beam end relative to the column face. The weld retrofit connections did not match the ultimate capacity of the bolted connection, falling short by just over 100kN both times, as shown in Figure 4-9. Both the bolted and weld retrofit connections, however, did surpass the predicted connection capacities based on AISC (2005) and CISC (2010) design procedures. The test-vs-predicted results will be expanded upon in Section 4.3.

The bolted connection test resulted in shear yielding along the line of bolt holes accompanied by bearing deformations around the bolt holes and eventually shear fracture through the net area of the plate as pictured in Figure 4-6. Strain gauges SG1 and SG2, placed horizontally at the top and bottom of the shear tab, indicated that flexural yielding of the shear tab took place shortly after all of the remaining strain gauges had yielded in shear.

Figure 4-6: Test 7 after Failure - Shear/Bearing Deformations and Shear Tab Rupture (Bolts Removed)

The partial "C"-shape weld retrofit failed in a similar manner to the bolted test with the exception of the bearing deformations around the holes. Bolt holes deformed significantly and shear fractures propagated from hole to hole just prior to the reduction in load-carrying capacity as depicted in Figure 4-7.

Figure 4-7: Test 9 after Failure - Bolt Hole Deformations and Crack Propagation Along Line of Bolt Holes

The use of full “C” shape weld retrofits was abandoned for the remainder of test beam sizes after the single row tests on the W310x60 beams since the extra leg of weld fractured, effectively rendering the retrofit into a partial “C” shape without losing any overall resistance or rotational capacity. Consequently, the “L”-shape weld retrofit was used for Test 11; it allowed the shear tab to deform more along its top horizontal length due to the fact that it was not as restrained by the weld along that length. This is made evident in Figure 4-8. The onsets of flexural and shear yielding occurred simultaneously in the welded test configurations according to the strain gauges and ovalization occurred in the holes again, starting with the top holes getting wider horizontally and the bottom holes being compressed together horizontally. After deforming to the point where the bolt holes essentially closed up, cracks began to propagate from each hole to the next leading to another shear fracture through the net section of the shear tab. With each crack that formed, the load carrying capacity of the connection began to decrease. An edge distance fracture also occurred after the ultimate load had been attained; it ran from the bottom bolt hole to the edge of the shear tab where the retrofit weld ended, as shown in Figure 4-8 in the picture on the right hand side.

Figure 4-8: Test 11 after Failure - Rupture Through Bolt Holes and Edge Distance

As was the case with the single row tests on the W310x60 beams, the type of weld retrofit configuration did not influence the overall connection behaviour. The loading paths taken in the two weld retrofit cases are almost identical, as can be seen in Figure 4-9. The single row tests with W610x140 beams differed from the single row tests using W310x60 beams in terms of ultimate failure mode. The shear fractures that were observed through the net section of the shear tab in the W610x140 single row tests were not seen in the W310x60 single row tests. This may be due to the fact that loading was stopped in the W310 tests when the actuator ran out of displacement. The same cracks would likely have appeared had additional rotations been applied.

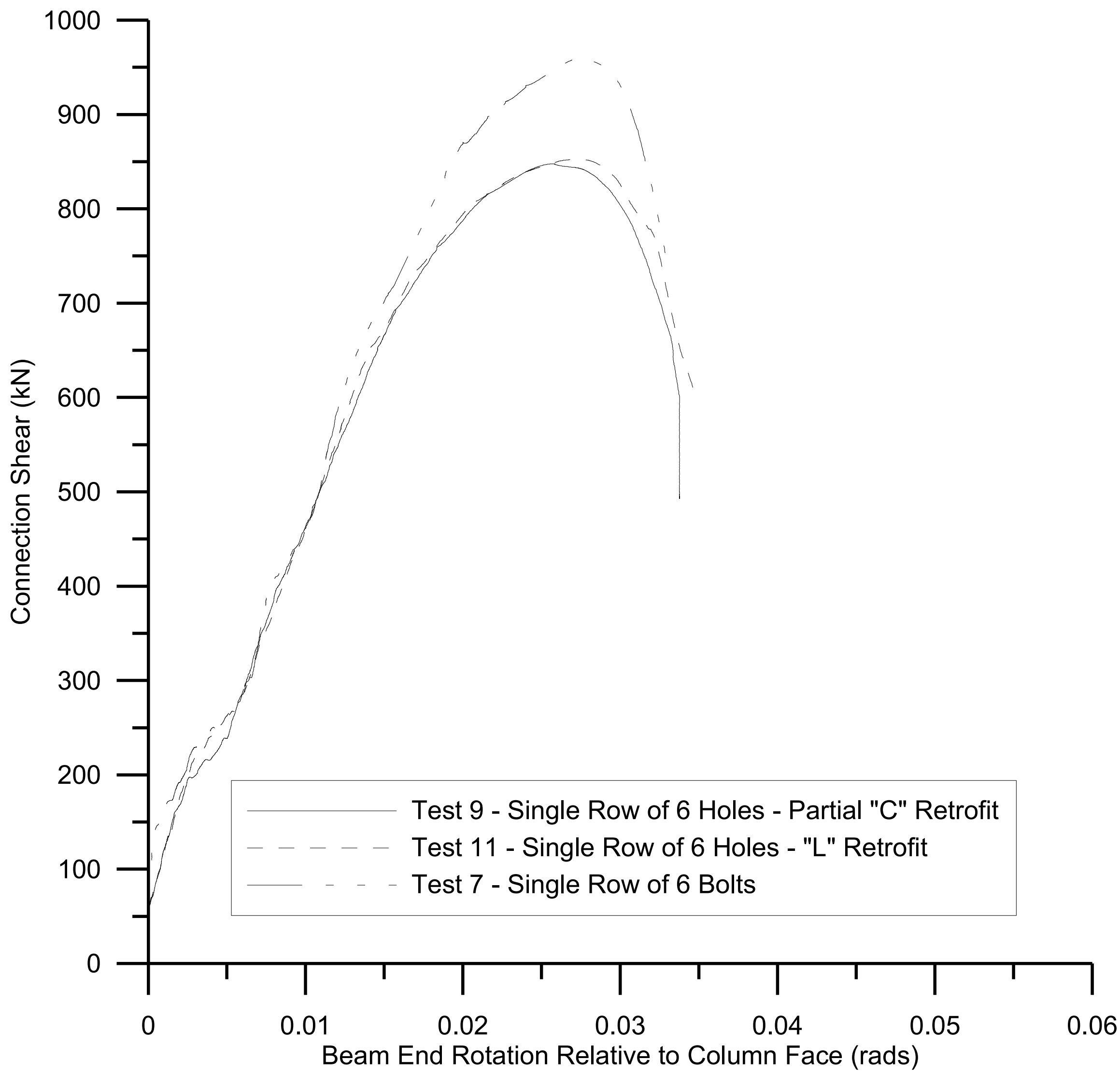

Figure 4-9: Connection Shear vs. Beam End Rotation for Tests 7, 9 and 11

4.2.3 Single Row of 10 Bolts and Corresponding Weld Retrofit

The largest of the single row shear tab tests, using the W920x223 test beams and having ten 1'' bolt holes (both bolted and welded configurations) performed adequately. Both the bolted and welded test reached the targeted beam end rotations as well as the predicted ultimate connection shear loads. The weld retrofit test, however, resisted just over 200 kN less than the bolted connection test as can be seen when comparing Figures 4-12 and 4-13. This lower resistance was not a result of the weld size since the retrofit welds themselves did not fail.

The bolted test is shown after failure in Figure 4-10. Yielding is made evident by the whitewash that has flaked off. Flexural and shear yielding were recorded early on in the test and then bearing deformations occurred around the bolt holes and a shear fracture eventually took place through the shear tab between some of the bolt holes. A weld fracture between the column face and shear tab occurred at the top of the shear tab and measured approximately 160 mm in length upon completion of the experiment. The weld retrofit test is pictured after failure in Figure 4-11. Shear fracture had begun taking place through the net area of the shear tab along the line of bolt holes. Figures 4-12 and 4-13 plot connection shear against beam end rotation relative to the stub column face for the weld retrofit configuration and bolted configuration respectively.

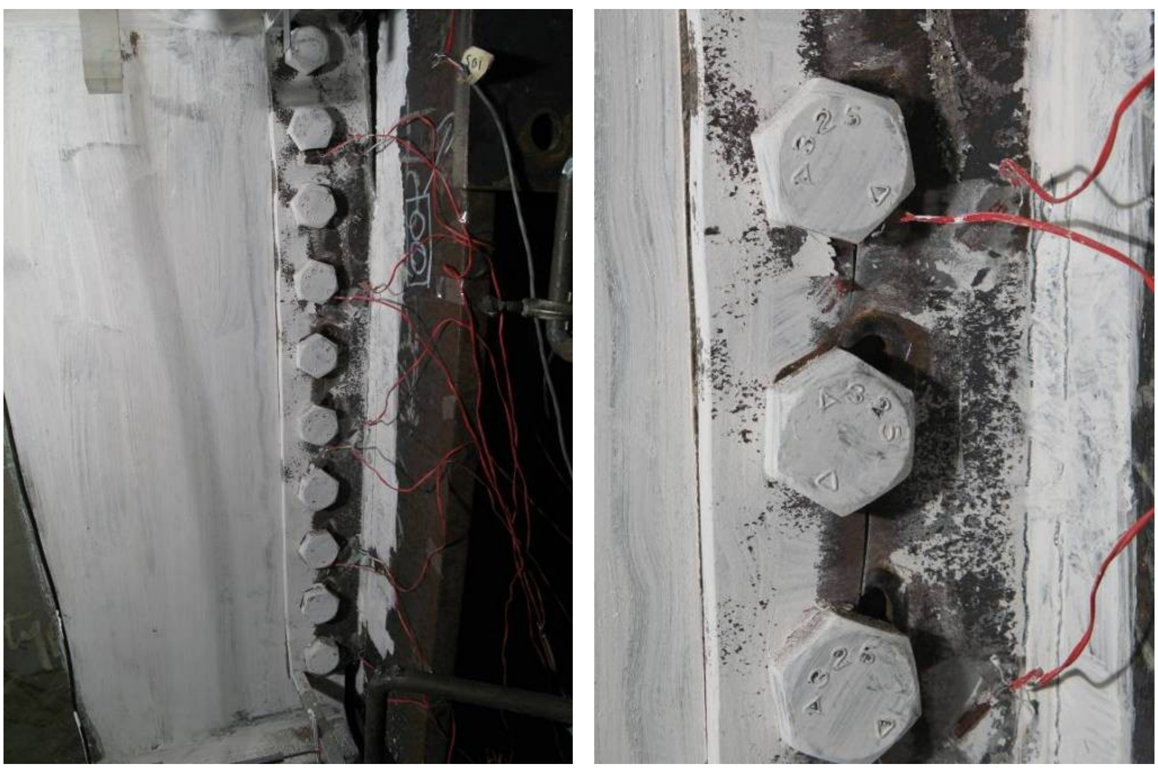

Figure 4-10: Test 13 after Failure - Weld Fracture, Shear Tab Yielding and Rupture Along Bolt Line

Figure 4-11: Test 14 after Failure - Yielding and Shear Tab Rupture Along Line of Bolt Holes

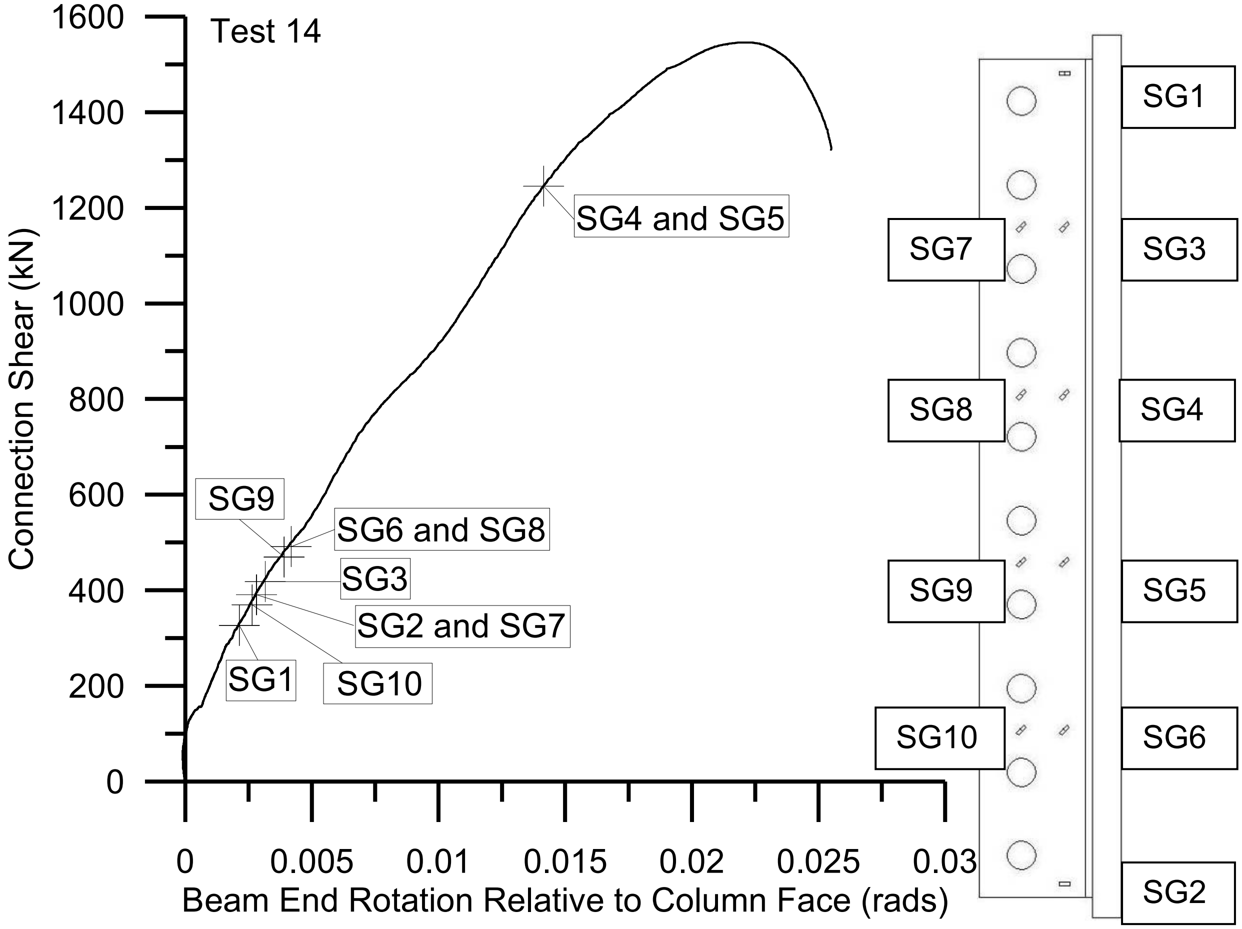

Figure 4-12: Connection Shear Load Where Strain Gauges Reach Yield Strain (Test 14:Welded)

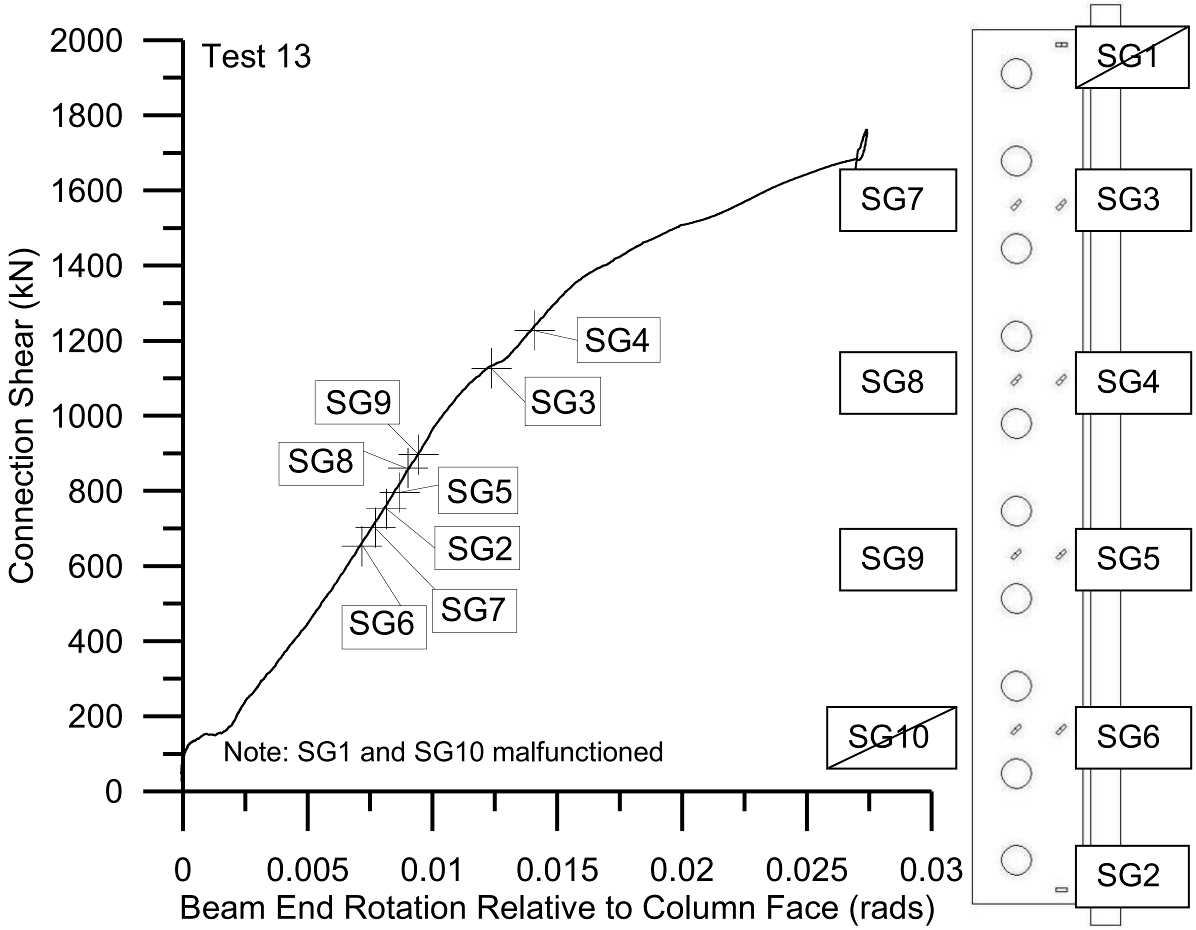

Figure 4-13: Connection Shear Load Where Strain Gauges Reach Yield Strain (Test 13:Bolted)

Note that yielding occurred earlier on in the weld retrofit test relative to the bolted connection test, and that although both tests met the targeted rotation and surpassed the predicted connection resistance, the bolted connection withstood 1762 kN, whereas the partial “C”-shape weld retrofit withstood 1546 kN. This may be as a result of the load path taken due to the retrofit welds. Shear deformations are restricted by the weld retrofits and stress concentrations are thus created where the horizontal legs of the weld retrofits end. Investigation with finite element software may provide insight into this behaviour.

4.2.4 Two Rows of 3 Bolts and Corresponding Weld Retrofits

The bolted and weld retrofit connections using W310x60 test beams and two rows of three bolts were able to attain the target rotation at the predicted probable ultimate loads. These double row tests, however, did not reach the same levels of rotation as the single row tests using the same test beam size. This may be due to an increased resistance to rotation from the increased length in the shear tabs. The connections withstood higher forces than were anticipated based on the predictions; this will be elaborated upon in Section 4.3. The shear tab in the bolted test configuration yielded along the inner row of bolts. There were minor deformations in the bolt holes in the innermost row but the bolts remained undamaged as in all of the previous bolted tests. A weld fracture measuring close to 85 mm developed at the column face and can be seen in Figure 4-14, with and without test bolts in place.

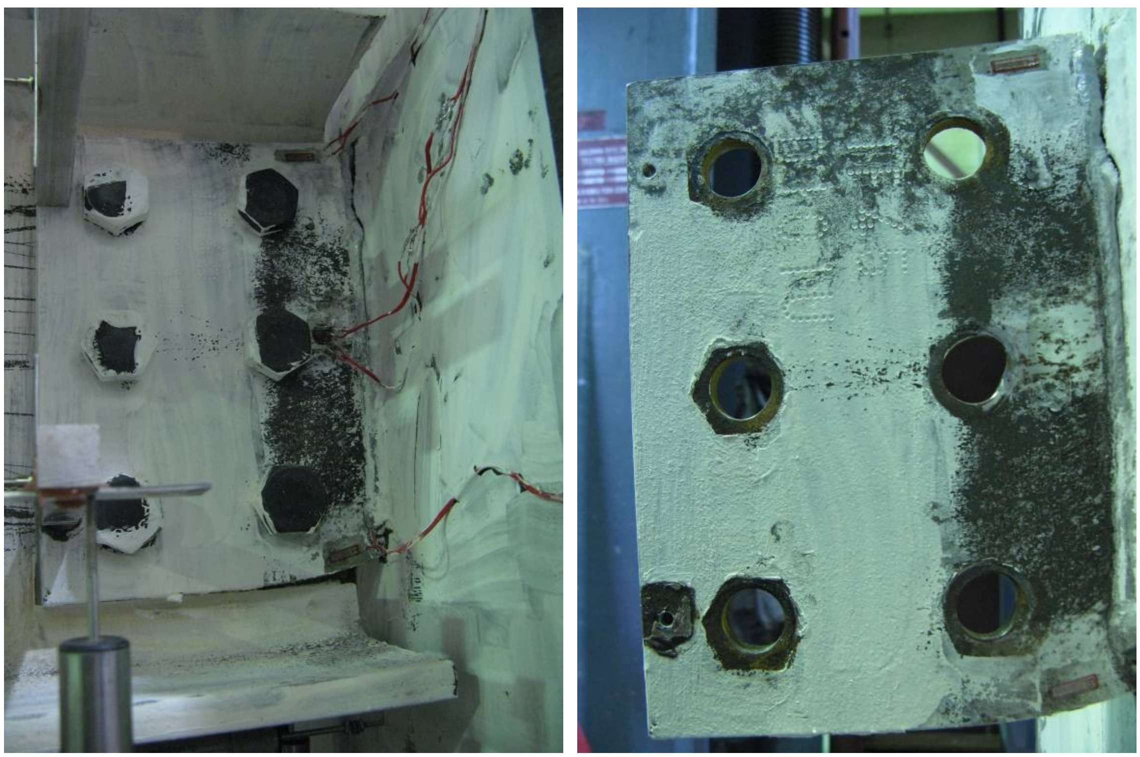

Figure 4-14: Test 8 after Failure - Yielding Along Bolt Line and Weld Fracture at Supporting Column Face

The first of the two weld retrofits was a full “C”-shape weld around the perimeter of the shear tab where it made contact with the web of the beam, as shown previously in Figure 3-6. After the shear tab had undergone flexural and shear yielding, the onsets of which had occurred simultaneously according to strain gauge readings, the weld retrofit fractured along the top and bottom horizontal legs up to the centreline of the inner row of bolts, as pictured in Figure 4-15. This phenomenon was also observed when the single row full “C’-shape weld retrofit failed in Test 3. The majority of deformations that took place in these double row weld retrofit connections occurred between the supporting column face and the area just beyond the inner row of bolt holes; see Figure 4-15 (left). When compared to the partial “C”-shape weld retrofit in Figure 4-15 (right), it becomes apparent that the bolt holes were not as deformed in the full “C”-shape weld retrofit test and no vertical edge distance failure was observed in this case. In both cases, the onset of flexural and shear yielding through the line of bolt holes occurred simultaneously, whereas in bolted tests some shear yielding occurred prior to flexural yielding. In the case of the full “C”-shape retrofit, the horizontal leg welds fractured next, followed by the vertical weld at the column face. In the case of the partial “C”-shape weld retrofit connection, the vertical weld near the top of the column face fractured first, followed in turn by the shear tab vertical edge distance fracture at the bottom of the shear tab from the centreline of the bolt hole after the resisted load had begun to decrease.

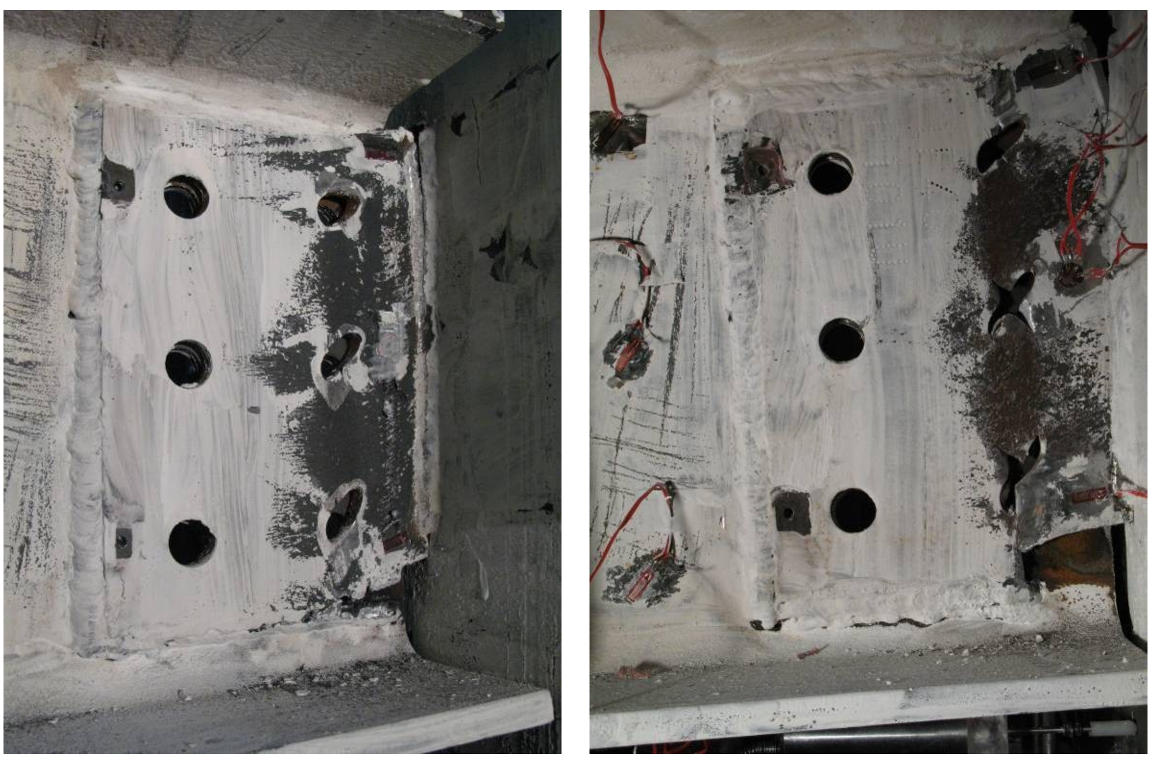

Figure 4-15: Full "C"-Shape (left, Test 10) and Partial "C"-Shape (right, Test 12) Retrofits after Failure

Both of the weld retrofits withstood connection forces over 100 kN higher than the bolted test specimen while maintaining comparable beam end rotations relative to the column face. The connection shear resisted is plotted against rotation relative to the column face in Figure 4-16 for comparison purposes. The lower shear resistance of the bolted configuration may be a result of additional bearing stresses caused by the bolts along the net section of the shear tab. Another plausible explanation is that the welded configuration tests were able to deform to a much larger extent due to the absence of bolts. Consequently, the forces seem to have been redistributed in a manner which plastically deformed a larger portion of the shear tab, rather than causing a brittle fracture of the vertical weld at the supporting column face earlier on in the test, as was observed in the case of the bolted configuration.

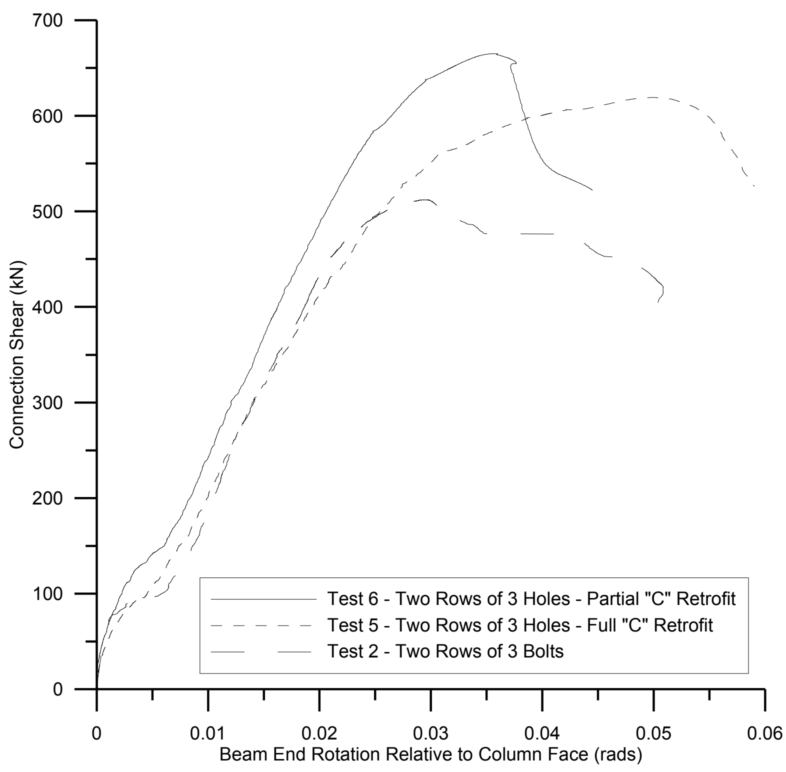

Figure 4-16: Connection Shear vs. Beam End Rotation Relative to Column Face for Tests 2, 5 and 6

4.2.5 Two Rows of 6 Bolts and Corresponding Weld Retrofits

The bolted and weld retrofit connection tests using W610x140 test beams and two rows of six bolt holes showed that the targeted rotations could be attained using the configurations in Tests 8, 10 and 12. In fact, these double row connections were able to reach the same level of rotation as the tests using a single row of six bolt holes. Both the partial “C”-shape weld retrofit and the “L”-shape weld retrofit resisted higher loads at the connection than the bolted configuration did. Again, this may be a result of the bearing stress caused by the bolts or may be a result of the manner in which the shear tabs were able to deform, allowing plastic deformations to occur over a larger portion of the tab. In order to compare the behaviour of each of the three two row tests, the connection shear is plotted against the rotation of the beam end relative to the column in Figure 4-24.

The graphs and corresponding photos provided in Figures 4-17 through 4-22 aim to show the progression of the failure modes of Tests 8 and 10. Additional photos present the progression of failures for other shear tab tests in Appendix D. Both configurations began to yield relatively early on into the test along the innermost row of bolt holes. The partial “C”-shape weld retrofit used in Test 10 caused the area around the second row of bolt holes, furthest from the supporting column face, to deform to a greater extent than the bolted configuration did. In the bolted configuration connection test, shear yielding began taking place along the inner row of bolts, closest to the supporting stub column, followed by flexural yielding and some additional shear yielding in the middle of the shear tab through the outer row of bolts. In both of the weld retrofit connection tests, shear yielding along the inner row of bolts and flexural yielding began taking place at the same time according to strain gauge readings. Ultimately, shear fractures propagated vertically between the inner row of bolt holes, closest to the supporting column, in tests using the bolted configuration and using the partial “C”-shape weld retrofit configuration, but were absent in the test using the “L”-shape weld retrofit configuration shown in Figure 4-23. The “L”-shape weld retrofit, however, was subject to a vertical edge distance fracture from the bottom of the shear tab to the bottom bolt in the inner row of bolt holes. This fracture occurred after the ultimate load had been reached at the connection and may be a result of the weld restricting shear

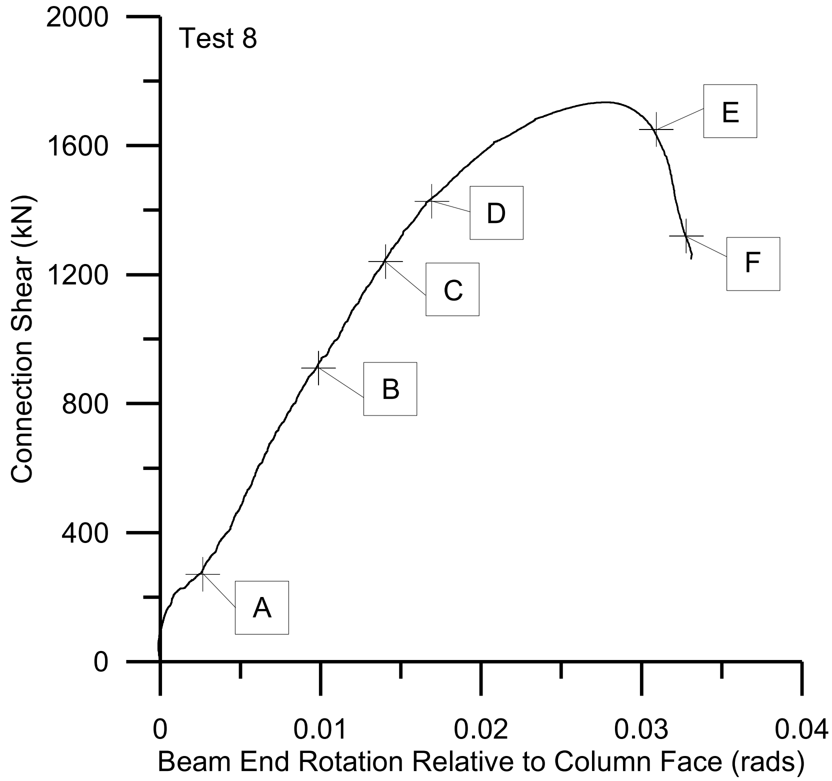

Figure 4-17: Connection Shear vs. Beam End Rotation for Test 8 (Bolted) and Corresponding Photos

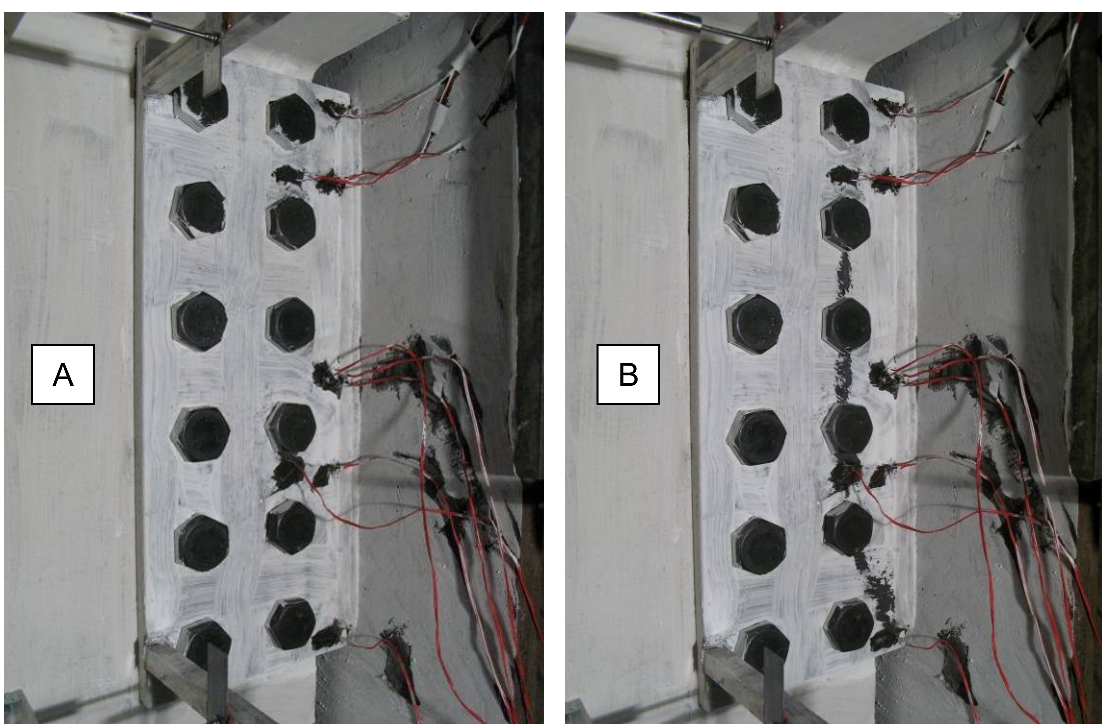

Figure 4-18: Photos A and B of Test 8 Corresponding to Figure 4-17

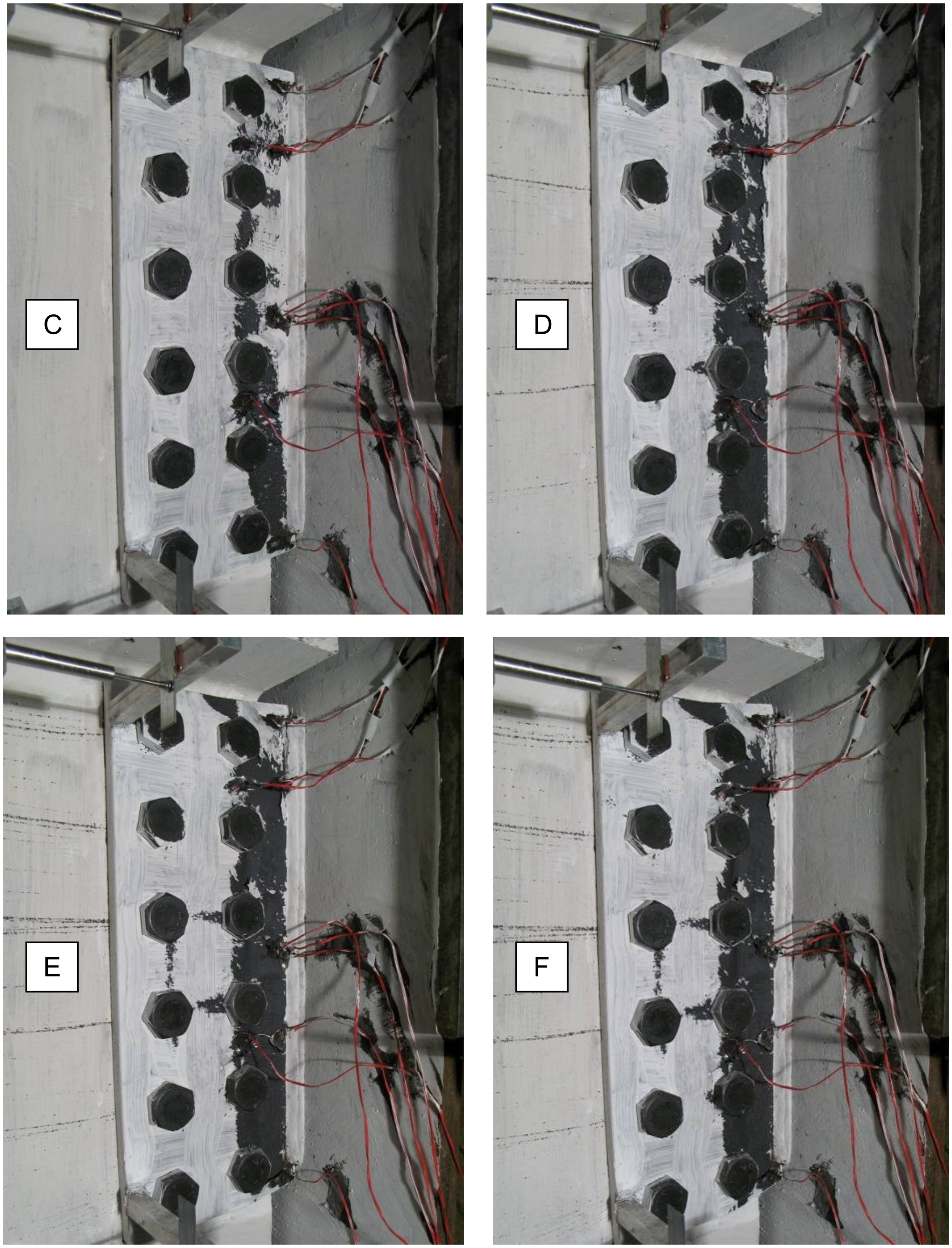

Figure 4-19: Photos C, D, E and F of Test 8 Corresponding to Figure 4-17

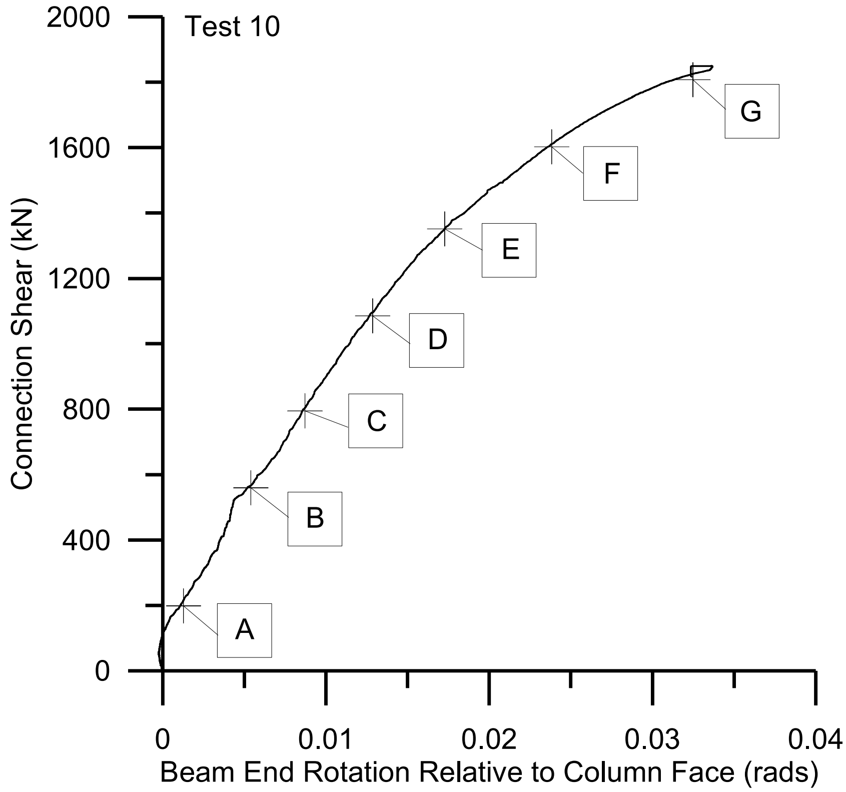

Figure 4-20: Connection Shear vs. Beam End Rotation for Test 10 (Welded) and Corresponding Photos

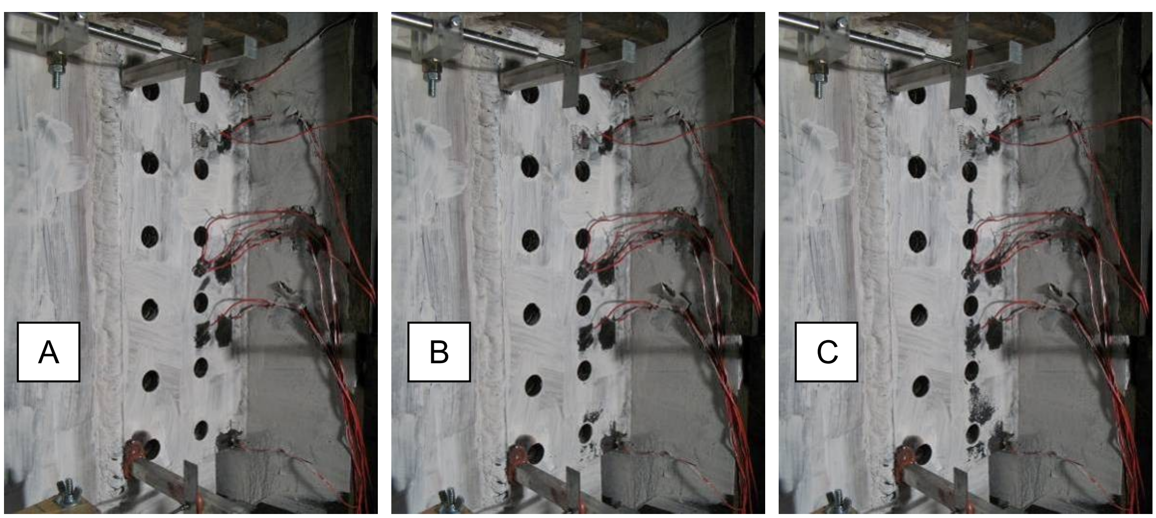

Figure 4-21: Photos A, B and C of Test 10 Corresponding to Figure 4-20

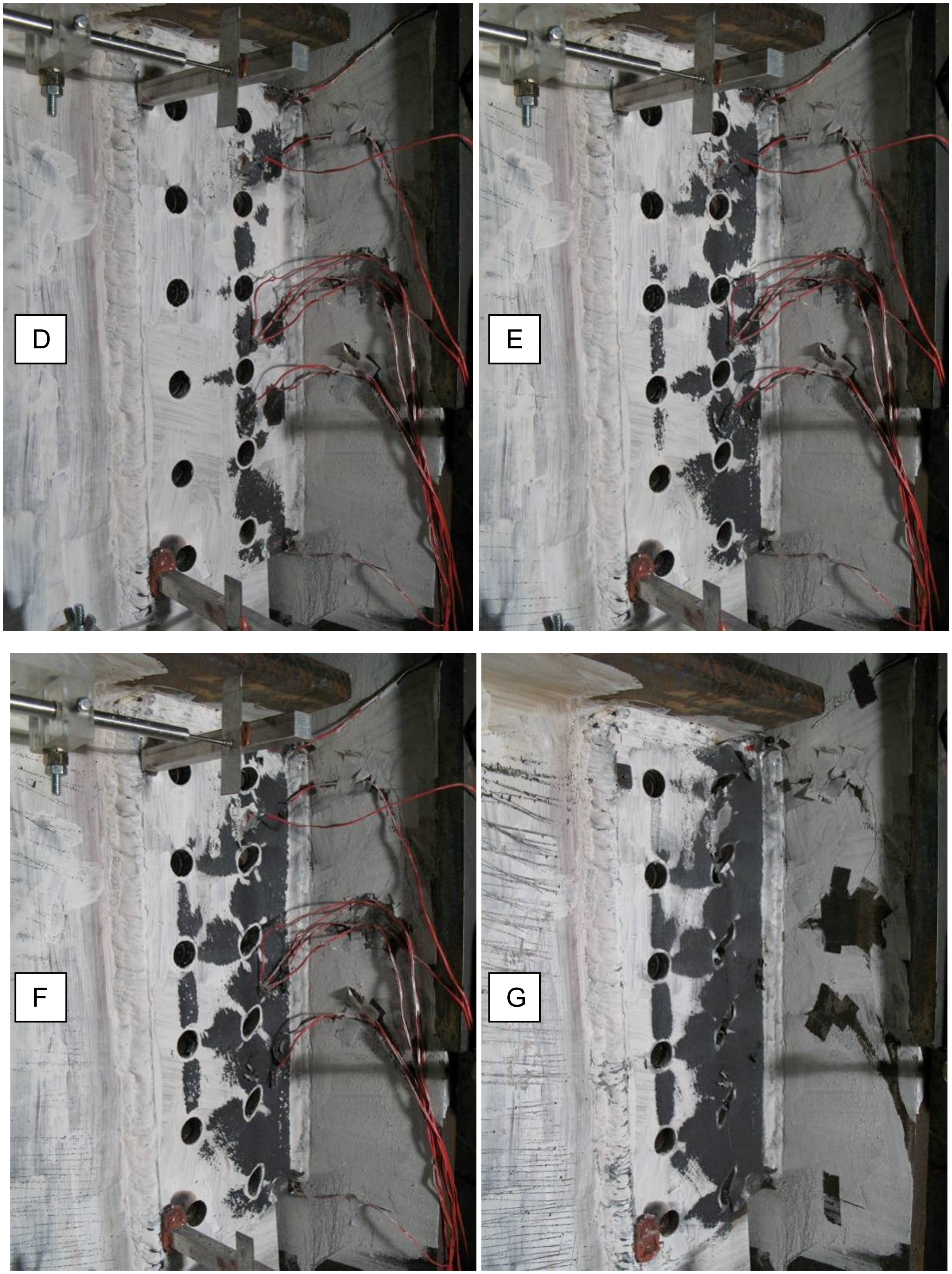

Figure 4-22: Photos D, E, F and G of Test 10 Corresponding to Figure 4-20

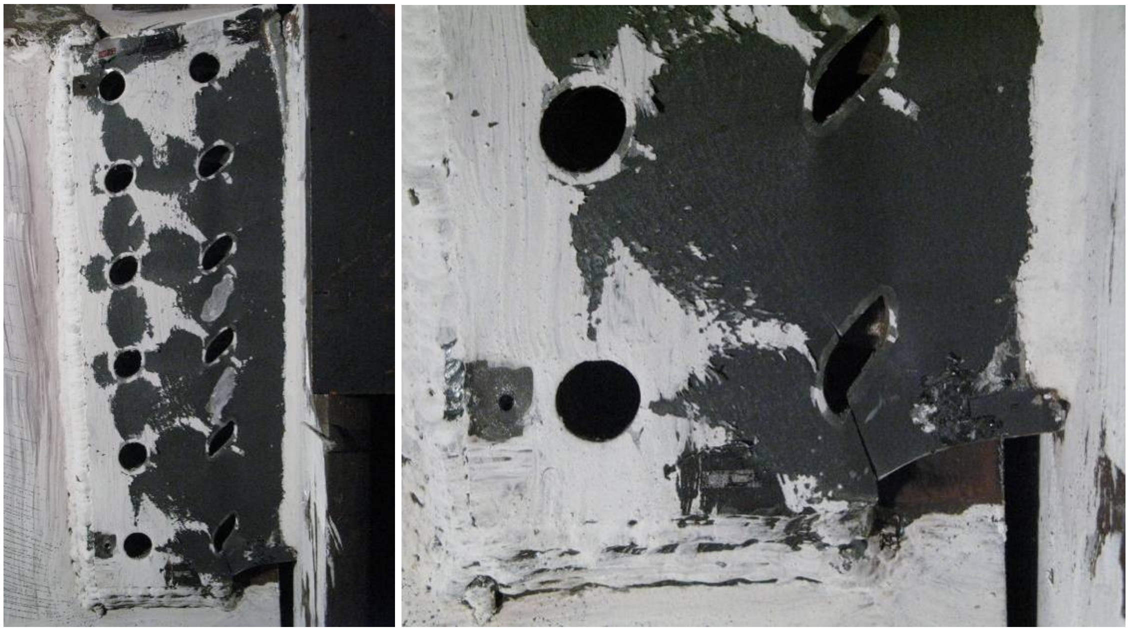

Figure 4-23: Test 12 after Failure - Bolt Hole Deformations in Both Rows, Weld Fracture and Vertical Edge Distance Rupture

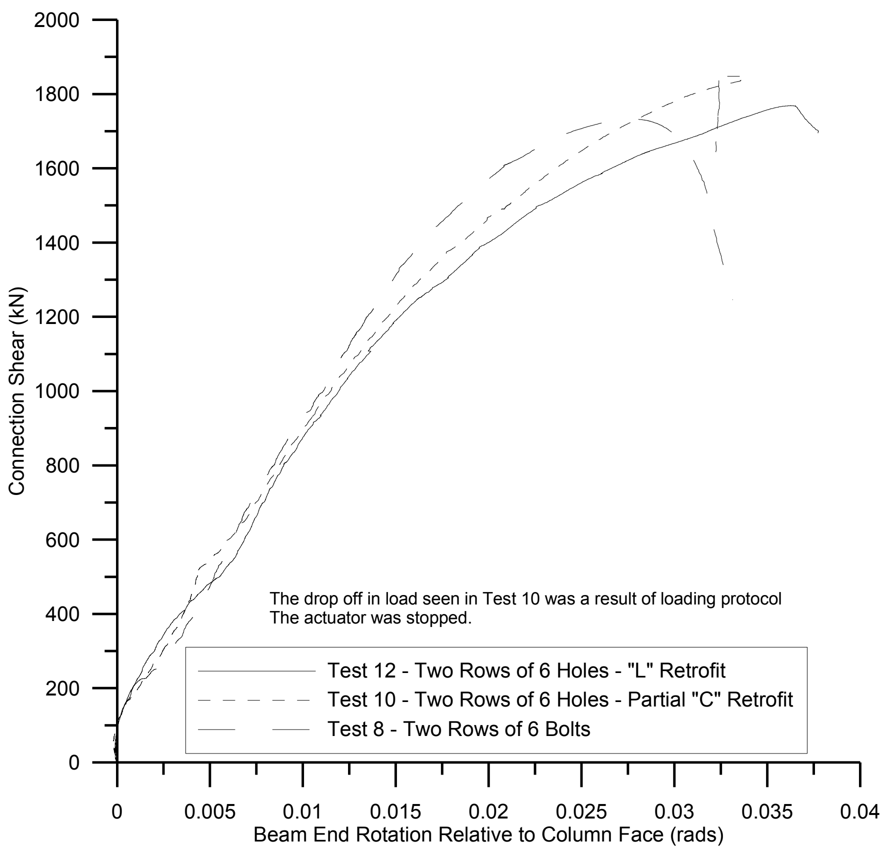

Figure 4-24: Connection Shear vs. Beam End Rotation Relative to Column Face for Tests 8, 10 and 12

deformations in the area and causing a concentration of stress to build up at the end of the horizontal leg of the weld.

4.2.6 Two Rows of 10 Bolts and Corresponding Weld Retrofit

The largest of the shear tab connection tests presented a few difficulties as a test of this magnitude and scale had never been performed before. The biggest problem was the yielding of the test beam, a W920x223 section. Plastic deformations were clearly noticeable in the top and bottom flanges of the test beam and the shear deformations in the beam web were evidenced by the flaking of the whitewash solution that was painted on prior to testing. These phenomena may be observed in Figure 4-26 and 4-27. As a result of this, the test had to be stopped before the connection itself had reached its ultimate load-carrying capacity. Nevertheless, the bolted connection did resist 99% of the predicted load based on the actual material strength of the shear tab and 121% of the predicted load based on the minimum specified material strengths of the shear tab. The partial "C"-shape weld retrofit test had to be stopped at a load corresponding to 95% of the predicted connection strength based on actual measured material strengths of the shear tab and 115% of the predicted connection strength based on minimum specified material strengths of the shear tab. It should also be noted that the predicted failure mode was a block shear rupture. While there was evidence of yielding along the inner row of bolts, block shear rupture did not appear imminent at the time the bolted test was stopped. Had the test beam not yielded, it is very probable that the connection could have continued taking on load. In fact, strain gauges SG1 and SG2, placed horizontally at the top and bottom of the shear tab in every test, as shown in Figure 4-25 only registered strains around 50% of ε_{yield} for the bolted test configuration. For a clearer picture of the progression of yielding among the strain gauges in the bolted test, see Figure 4-25. Note that shear yielding occurs first at the bottom of the shear tab and progresses to the top. While the weld retrofit configuration test did yield to a greater extent than the bolted one, the deformations seen around bolt holes in Figure 4-27 were minimal when compared to the double row weld retrofit tests featuring three or six bolt holes per row.

Concerning the ability of these connections to accommodate enough rotation, both test configurations reached beam end rotations relative to the column face in excess of the targeted 0.015 radians at probable ultimate load. The rotation could also have proceeded further, had it not been for the opposite end of the beam running out of room and making contact with the concrete strong floor. The double row tests were unable to match the levels of beam end rotation relative to the stub column face that were attained by the corresponding single row tests conducted with the W920x223 test beams.

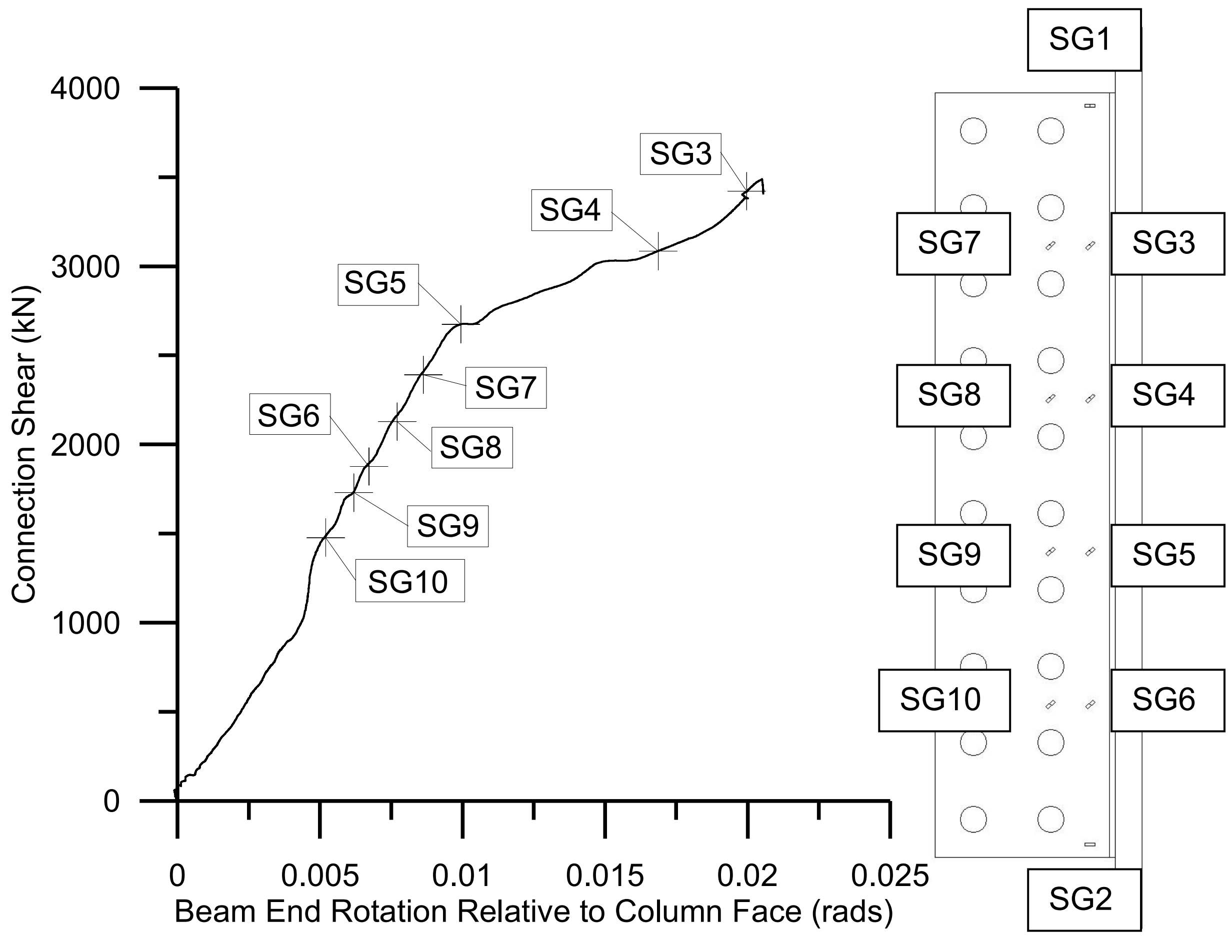

Figure 4-25: Progression of Strain Gauge Yielding for Test 15 (Bolted)

Figure 4-26: Test 15 after Failure - Yielding of Beam (left) and Shear Tab Yielding Along Inner Row of Bolts (right)

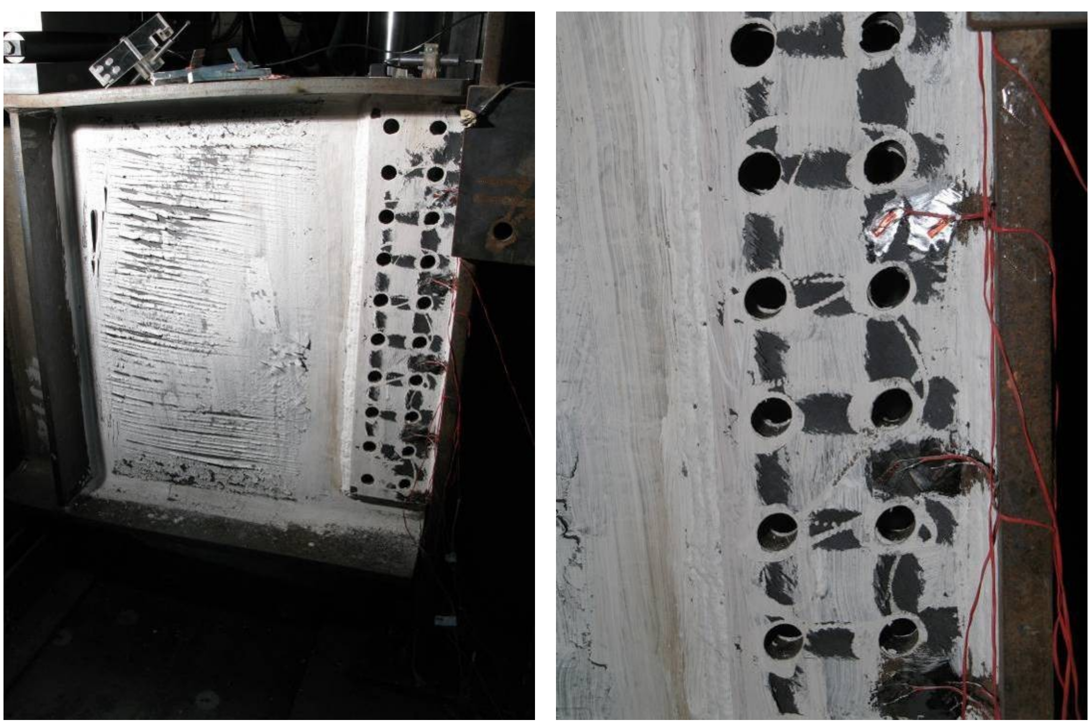

Figure 4-27: Test 16 after Failure - Yielding of Beam (left) and Yielding of Shear Tab Between Bolt Holes (right)

4.3 Comparisons

4.3.1 Experimental Results and Predicted Values

The experimental single and double-row bolted test connection results are summarized in Tables 4-2 and 4-3 and compared to the predicted resistances described previously in Chapter 3. In these tables, the term 'nominal properties' indicates that the values have not been factored and no material overstrength values have been used. These nominal values are in essence what the design procedures would yield without applying resistance factors. The term 'measured properties' indicates that the values used in the predictions are based on material properties determined through coupon testing. Detailed descriptions of the design procedures are presented in Sections 2.3 and 3.3.

Upon inspection of the experimental results, it becomes clear that the predictions based on the current CISC (2010) design approach are quite conservative. The CISC (2010) design approach predicted results are not only the most conservative in all cases, but also the least applicable in terms of types of connection configurations they can be used for. The approach is not applicable for single row connections having more than seven bolts, nor is it applicable for connections having multiple rows of bolts. Add to this the fact that the CISC (2010) design approach uses outdated resistance factors in design tables featured in the CISC Handbook (2010) making the results more conservative than the results of this comparison indicates (outdated resistance factors were not used in these predictions since they are unfactored predictions), and it becomes clear that the approach requires an update. Conversely, based on nominal properties, the AISC (2005) conventional method came closest to the experimental results for the test featuring a single row of three bolts, and provided the same predictions as the AISC (2005) extended method and modified method for the remaining tests since the shear rupture mode governed in each case. This can be explained since shear fracture of the bolt group was deemed an undesirable failure mode due to its brittle nature and was purposely avoided when initially designing and detailing the shear tab configurations. Since calculation of the shear strength of the bolt group is one of the major differences between the AISC (2005) conventional and extended methods, the predictions from these two design methods were often identical because a failure mode common to both approaches, shear fracture of the shear tab, governed the design on several occasions. Likewise, the proposed modified method often resulted in identical predictions, as it also differed in predicting the shear strength of the bolt group against shear fracture, a failure mode which was purposely avoided. On the subject of bolt group shear strength, the proposed increase in bolt shear strength in the modified method from 0.50Fu to 0.62Fu, based on the work of Kulak et al. (1987) appears to be warranted, as bolts did not show signs of damage or deformation throughout testing. The shear failure of bolt groups predicted in Tables 4-2 and 4-3 did not occur, again reinforcing the validity of the proposed change in bolt strength.

With regards to test configurations having two rows of bolts, the AISC (2005) extended method and the proposed modified method differed in their predictions of connection strength, with the exception of Test 16, featuring two rows of ten bolts where both methods predicted the same failure mode and resistance based on nominal and actual material properties. In the two tests where the predictions differed, they differed as a result of the calculation of the shear strength of the bolt group. For Test 2, featuring two rows of three bolts, the extended AISC (2005) method predicted a shear fracture of the bolt group as the ultimate failure mode using both nominal and actual properties. For Test 8, using actual properties, the extended AISC (2005) method again predicts shear fracture of the bolt group to occur. Conversely, the proposed modified method, due to the use of a higher predicted bolt shear strength, predicts a combination of flexural and shear yielding to be the controlling failure mode for Tests 2 and 8. When looking back on the results of these tests, the bolts were not deformed and remained undamaged after testing, whereas the shear tabs had undergone both flexural and shear yielding. Looking at a photo of Test 8 after failure in Figure 4-19, a shear fracture through the net section of the shear tab was visible, but when seen in conjunction with Figure 4-17, it becomes evident that the ultimate load had already been reached and the connection shear load was decreasing before the shear fracture through the inner line of bolts occurred.

The proposed modified method, when looking at predictions based on actual material properties, offered the most accurate prediction or shared the most accurate prediction with other design approaches in all six bolted tests in terms of experimentally tested connection strength versus predicted connection strength. It is the recommendation of the author that this method be considered as an alternative to the current CISC (2010) design approach for bolted shear tab connections for both single and double row connections featuring up to ten bolts per row.

4.3.2 Bolted Tests Compared to Weld Retrofits

All of the weld retrofit shear tab configurations performed satisfactorily, to the extent that they resisted at least the predicted loads based on actual material properties that their corresponding bolted connections were designed to take, with the exception of Test 16 where the test needed to be stopped prematurely due to yielding of the test beam. It is extremely likely the connection would have been able to resist the predicted load had the W920x223 test beam not failed in bending. Also, all of the weld retrofit configurations were able to attain the desired level of rotation at the beam end relative to the stub column face. The fact that the weld retrofit configurations had *empty* bolt holes that were able to deform significantly contributed to the overall ductility of the connections.

A common trend observed in all tests was that strain gauges SG1 and SG2, positioned horizontally at the top and bottom of each shear tab, would always yield earlier on in weld retrofit test connections relative to the corresponding bolted test connections. This phenomenon may be due to retrofit welds constraining shear deformations. Additionally, when present, strain gauges along the innermost line of bolt holes closest to the stub column, typically yielded prior to those located between the

Table 4-2: Experimental Results Compared to Predicted Values for Single Row Bolted Tests

	Measured Resistance (kN)	Predicted Resistance Based on **Nominal** Properties (kN)	Measured/ Predicted	Predicted Failure Mode	Predicted Resistance Based on **Measured** Properties (kN)	Measured/ Predicted	Predicted Failure Mode
Test 1: 1Rx3Bolt	363	Observed Failure Mode: Combination SR and PF					
AISC Conventional		285	**1.28**	SR	297	**1.22**	SR
AISC Extended		257	**1.41**	PF	263	**1.38**	BG
CISC Handbook*		237	**1.53**	SR	247	**1.47**	SR
Modified Method		257	**1.41**	PF	297	**1.22**	SR
Test 7: 1Rx6Bolt	961	Observed Failure Mode: Combination SR and PF					
AISC Conventional**		676	**1.42**	SR	737	**1.30**	SR
AISC Extended		676	**1.42**	SR	737	**1.30**	SR
CISC Handbook*		564	**1.71**	SR	576	**1.67**	BG
Modified Method		676	**1.42**	SR	737	**1.30**	SR
Test 13: 1Rx10Bolt	1762	Observed Failure Mode: Combination SR and PF					
AISC Conventional**		1323	**1.33**	SR	1531	**1.15**	SR
AISC Extended		1323	**1.33**	SR	1531	**1.15**	SR
Modified Method		1323	**1.33**	SR	1531	**1.15**	SR

*The CISC Method forces a specific failure mode by choosing the plate thickness. For comparison purposes, the design checks were performed with the plate thicknesses being used in the tests, rather than choosing the plate thickness.

**Connection did not respect edge distance requirement for AISC Conventional Design Method.

****Nominal* refers to minimum specified material strength for shear tabs and test beams.

*****Measured* refers to yield stresses and ultimate stresses obtained via coupon testing for shear tab and test beam material.

*****All resistance factors were taken as 1.0

Failure Modes

SR = Shear Rupture through net area of plate

PF = Plate flexure with von Mises shear reduction

BG = Shear failure of bolt group

BSR = Block Shear Rupture

Table 4-3: Experimental Results Compared to Predicted Values for Double Row Bolted Tests

	Measured Resistance (kN)	Predicted Resistance Based on **Nominal** Properties (kN)	Measured/ Predicted	Predicted Failure Mode	Predicted Resistance Based on **Measured** Properties (kN)	Measured/ Predicted	Predicted Failure Mode
Test 2: 2Rx3Bolt	513	Observed Failure Mode: Combination SR and PF					
AISC Extended		397	**1.29**	BG	397	**1.29**	BG
Modified Method		405	**1.27**	PF	424	**1.21**	PF
Test 8: 2Rx6Bolt	1735	Observed Failure Mode: Combination SR and PF					
AISC Extended		1334	**1.30**	SR	1433	**1.21**	BG
Modified Method		1334	**1.30**	SR	1476	**1.18**	PF
Test 15: 2Rx10Bolt	3489	Observed Failure Mode: Beam Yielded in Shear and Bending Prematurely					
AISC Extended		2887	**1.21**	BSR	3515	**0.99**	BSR
Modified Method		2887	**1.21**	BSR	3515	**0.99**	BSR

*The CISC Method forces a specific failure mode by choosing the plate thickness. For comparison purposes, the design checks were performed with the plate thicknesses being used in the tests, rather than choosing the plate thickness.

**Connection did not respect edge distance requirement for AISC Conventional Design Method.

***_Nominal_ refers to minimum specified material strength for shear tabs and test beams.

****_Measured_ refers to yield stresses and ultimate stresses obtained via coupon testing for shear tab and test beam material.

*****All resistance factors were taken as 1.0.

Failure Modes

SR = Shear Rupture through net area of plate

BG = Shear failure of bolt group

PF = Plate flexure with von Mises shear reduction

BSR = Block Shear Rupture

row of bolt holes and the supporting column. According to the strain gauges, in each bolted connected test, some shear yielding occurred in the shear tab prior to flexural yielding. This was not always the case in weld retrofit connections, where flexural yielding of the shear tab would either occur prior to or at the same time as shear yielding.

The fact that the strain gauges indicated these regions of the shear tab were indicating yielding early on during testing, when looking at the ultimate loads reached, suggests that there must have been an effective redistribution of forces throughout the experiment which allowed for a great deal of deformation to take place in the shear tab prior to the ultimate failure in both welded and bolted connection tests. Strain gauges generally indicated the onset of yielding between 20% and 30% of the ultimate connection shear load for weld retrofit connection tests and between 30% and 50% of the ultimate connection shear load for bolted connection tests.

Another trend worthy of note when analyzing the progression of yielding indicated by strain gauges throughout testing was that the strain gauges in weld retrofit tests had a tendency to indicate yielding at a lower connection shear load than the strain gauges in the bolted tests having the same configuration.

An additional phenomenon that was observed in several of the weld retrofit configurations with partial “C”-shape and “L-shape configurations but not in the majority of bolted connection tests was the occurrence of vertical edge distance failures between the bottom bolt hole in the innermost row and the bottom of the shear tab at the point where the bottom horizontal leg of the weld ended. This only occurred after the connection had reached its peak load. The edge distance fractures are thought to be caused by a higher strain concentration at the end of the horizontal leg of the weld retrofit. The bolted test connections were able to deform more evenly across the horizontal length of the shear tab and as a result, these vertical edge distance fractures were not observed in the bolted test configurations. The bottom of a bolted connection and partial “C”-shape connection are shown in Figure 4-28 to demonstrate this point. It should also be noted that while the vertical edge distance fractures were only observed in weld retrofit connections, shear fractures between bolt holes were seen in both bolted and weld retrofit connections.

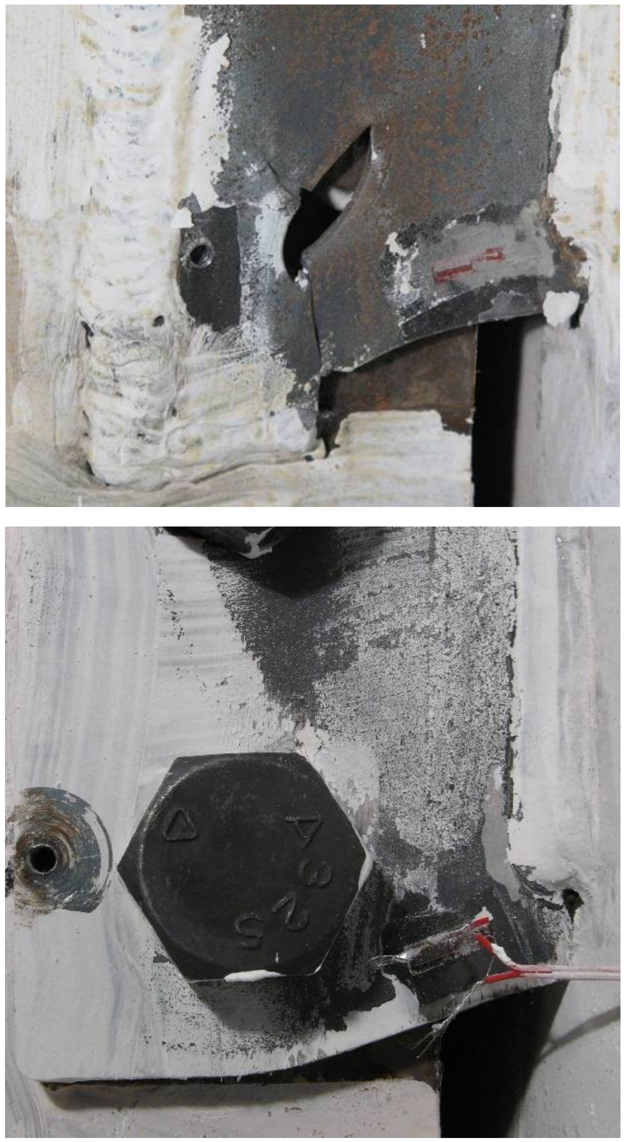

Figure 4-28: Comparison of Partial "C" Weld Retrofit (Top) to Bolted Connections (Bottom) Shear Tab Deformations

Ratios of weld retrofit connection resistances to predicted connection resistances based on corresponding bolted configurations are shown in Table 4-4. Recall that each weld retrofit was designed using the instantaneous centre of rotation method to resist the same factored load as its corresponding bolted connection. The table shows that all weld retrofit connections reached at least the connection strength predicted for their corresponding bolted connections based on both nominal and actual properties except for Test 16 where the test beam yielded prematurely. Further commentary on trends in Table 4-4 is presented in Sections 4.3.3 and 4.3.4.

4.3.3 Comparison of Beam Sizes

A pattern emerges when examining the ratios of test-to-predicted results for different beam sizes. The smaller the test beam size was, the more conservative the predicted connection strength was. This pattern applies to both single and double row connections and to both bolted and welded connections. In Table 4-4, for example, the test-to-predicted ratios for weld retrofit configurations decrease as the test beam sizes increase.

In terms of the progression of flexural yielding and shear yielding in the shear tabs, beam size seemed to have little effect. Strain gauge readings show that the greatest influencing factor in this respect was whether the connection was bolted or welded. Bolted connections experienced shear yielding before flexural yielding for all three test beam sizes. Weld retrofit connection tests all experienced flexural yielding before or at the same time as shear yielding regardless of test beam size. The bolted connection tests were less restricted from rotation than the weld retrofit connections initially since the bolts were snug tight and some slipping occurred as rotation and load were applied to the connection.

4.3.4 Comparison of Single and Double Row Tests

Both single and double row test connections demonstrated the ability to accommodate the targeted beam end rotations relative to the supporting stub column suggesting that all of the connections were sufficiently ductile to fail in a safe manner and avoid a sudden catastrophic collapse without warning. The connection configurations with two rows of bolts or bolt holes, however, did not reach the same

Table 4-4: Experimental Results of Weld Retrofit Tests Compared to Predicted Resistance of Corresponding Bolted Tests

	Connection Shear Resisted by Weld Retrofit Configuration (kN)	*Lowest **Nominal** Predicted Resistance of Corresponding Bolted Connection Test (kN)	Resisted by Weld Retrofit Shear Tab / ***Nominal** Predicted Resistance for Bolted Shear Tab	**Lowest Predicted Resistance of Corresponding Bolted Connection Test Based on **Measured** Properties (kN)	Resisted by Weld Retrofit Shear Tab / **Predicted Resistance Based on **Measured** Properties for Bolted Shear Tab
Single Row of 3 Holes					
Test 3 - Full "C"	357	257	**1.39**	263	**1.36**
Test 4 - Partial "C"	386	257	**1.50**	263	**1.47**
Two Rows of 3 Holes					
Test 5 - Full "C"	620	397	**1.56**	397	**1.56**
Test 6 - Partial "C"	666	397	**1.68**	397	**1.68**
Single Row of 6 Holes					
Test 9 - Partial "C"	849	676	**1.26**	737	**1.15**
Test 11 - "L" Shape	854	676	**1.26**	737	**1.16**
Two Rows of 6 Holes					
Test 10 - Partial "C"	1850	1334	**1.39**	1433	**1.29**
Test 12 - "L" Shape	1771	1334	**1.33**	1433	**1.24**
Single Row of 10 Holes					
Test 14 - Partial "C"	1546	1323	**1.17**	1531	**1.01**
Two Rows of 10 Holes					
***Test 16 - Partial "C"	3330	2887	**1.15**	3515	**0.95*** **

*Using minimum tensile and ultimate strengths

**Using measured material strengths from coupon testing results.

***Test was stopped prematurely due to yielding of test beam.

****Weld retrofit connections were designed to resist the same factored loads as corresponding bolted connections.

This table compares loads resisted by weld retrofit connections to the *predicted* resistances of their bolted counterparts regardless of failure mode.

No weld retrofit weld groups failed, nor did any bolt groups fail in shear.

levels of rotation as their single row counterparts with the exception of the tests conducted using W610x140 test beams.

A noticeable trend in Table 4-4 is that the ratios of tested weld retrofit connection strength to predicted resistances for corresponding bolt groups were higher for double row weld retrofit tests than they were for single row tests. This may be a result of additional plastic deformations throughout larger regions of the shear tab when compared to single row weld retrofit tests that had a tendency to fracture in shear along the inner row of bolt holes after yielding. The two row welded tests yielded along the inner row of bolt holes initially and then plastic deformations progressed to the second row of bolts instead of progressing directly to a fracture. This comparison between a double row weld retrofit and a single row weld retrofit is illustrated in Figure 4-29 by Tests 12 and 9.

Figure 4-29: Comparison of Two Row Weld Retrofit (Test 12) to One Row Weld Retrofit (Test 9)

4.4 Coupon Testing

4.4.1 Test Methodology

In order to obtain accurate material strengths for all test beams, coupons were cut from the test beams as shown in Figure 4-30 to test the properties of both the flanges and web of each beam. Additional coupons were cut from each of the plates used as shear tabs. The coupons were then machined in accordance with the tensile test procedures of the ASTM A370 Standard (ASTM, 1995) as depicted in Figure 4-31.

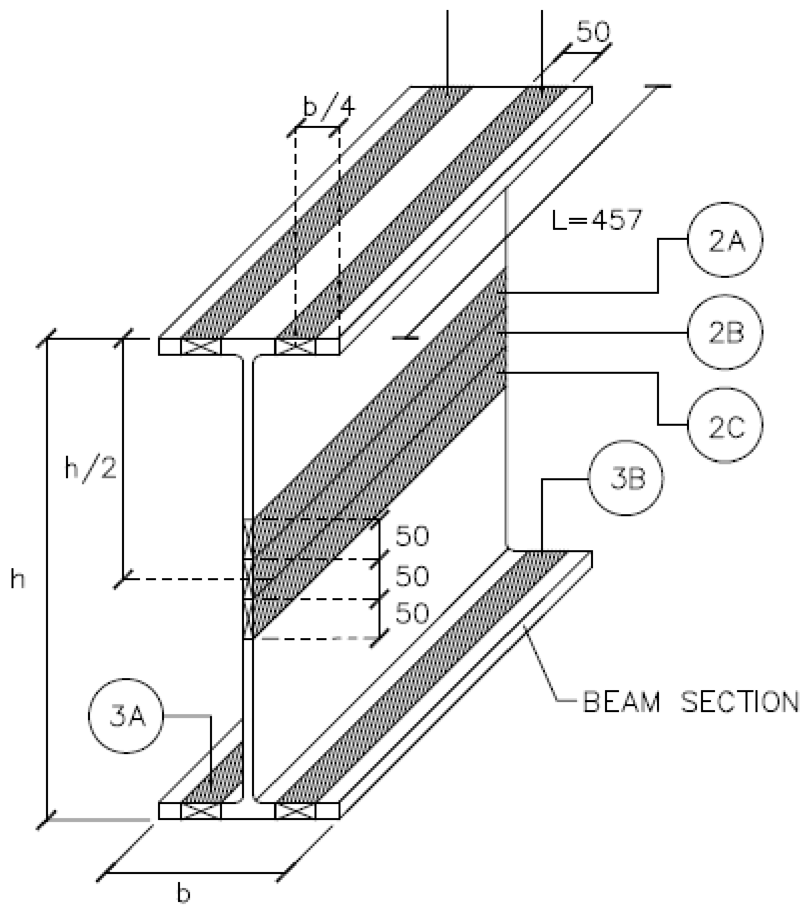

Figure 4-30: Localization of Beam Web and Flange Coupons (Image courtesy: DPHV)

The tests were carried out using a 1000 kN hydraulic actuator with tension grips and an LVDT in the actuator head. Cross head rates of 0.0026 mm/s and 0.026 mm/s were used for the elastic and post-elastic regions respectively. Each individual test coupon was measured with a micrometer prior to testing. Gauge lengths (8’’) were marked on the coupons such that the overall ductility could be measured. For an additional level of precision, an extensometer was attached along the 200 mm gauge length of each specimen to measure elongation. When recording the yield stress and ultimate tensile stress of each specimen, both dynamic and static values were taken. To obtain the static values, the tests were paused at several points during loading for one minute while the displacement was held constant. Each time a test was paused, the load would drop off; the average decrease in load was noted and later used in the calculation of the static yield stress and static ultimate tensile stress. Moduli of elasticity were determined using strain gauges.

Figure 4-31: Machined Coupon before Testing (top) and Two Coupons after Fracture (bottom)

4.4.2 Beam Webs and Flanges

Averages of three web coupon tests and three flange coupon tests were taken for each test beam. Results were plotted and both yield stress and ultimate tensile stress were recorded. Figure 4-32 shows a typical graph of a beam flange result. Summaries of the material properties of the beam flanges and webs are given in Tables 4-5 and 4-6 respectively. The material for all test beams was ASTM A992 Grade 50 steel.

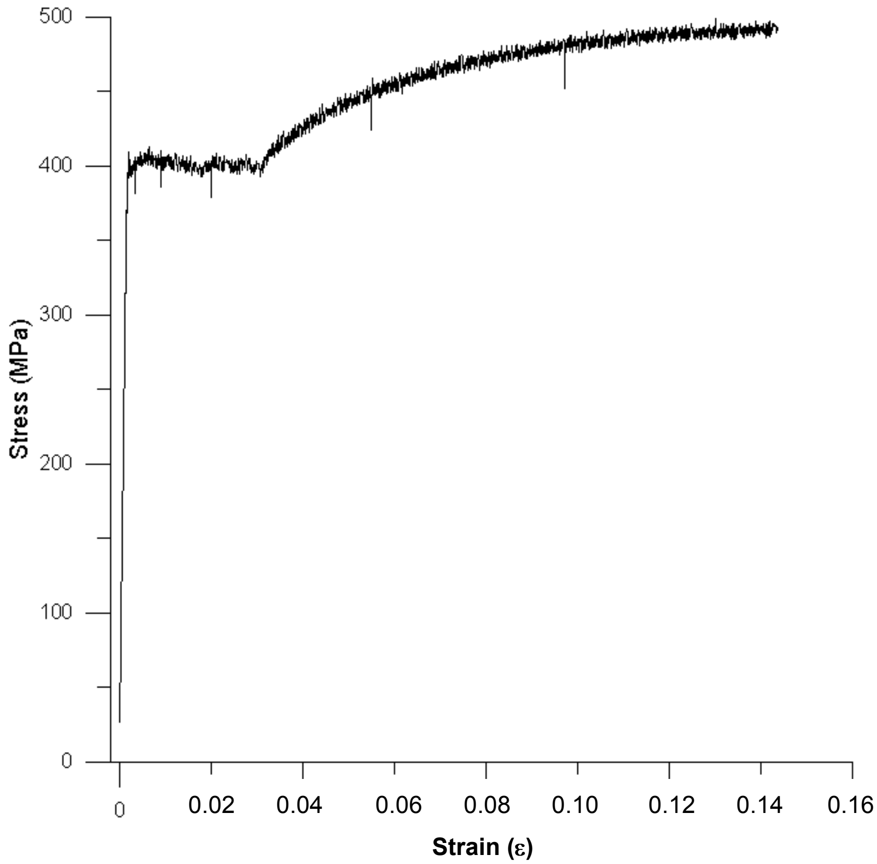

Figure 4-32: Typical Stress-Strain Response of a Beam Flange Tensile Test Coupon

Table 4-6: Summary of Beam Flange Tensile Coupon Tests

		Beam 1	**Beam 2**	**Beam 3**	**Beam 4**	**Beam 5**
Beam Flanges	**$F_{uSTATIC}$ (MPa)**	478	551	487	490	497
	$F_{ySTATIC}$ (MPa)	356	388	380	374	362
	%Elongation	28	28	29	31	27
	E (GPa)	204	206	206	217	205
	F_u/F_y	1.34	1.42	1.28	1.31	1.37
	R_y	1.03	1.13	1.10	1.08	1.05
	R_T	1.07	1.23	1.09	1.09	1.11
	Beam Used in Tests #:	1, 2, 3, 4, 5 and 6	7 and 8	11 and 12	9 and 10	13, 14, 15 and 16

Table 4-7: Summary of Beam Web Tensile Coupon Tests

		Beam 1	Beam 2	Beam 3	Beam 4	Beam 5
Beam Web	$F_{uSTATIC}$ (MPa)	485	570	527	523	518
	$F_{ySTATIC}$ (MPa)	380	434	440	433	408
	%Elongation	26	23	28	24	27
	E (GPa)	206	207	215	215	203
	F_u/F_y	1.28	1.31	1.20	1.21	1.27
	R_y	1.10	1.26	1.28	1.26	1.18
	R_T	1.08	1.27	1.18	1.17	1.16
	Beam Used in Tests #:	1, 2, 3, 4, 5 and 6	7 and 8	11 and 12	9 and 10	13, 14, 15 and 16

4.4.3 Shear Tab Plates

Similarly, averages of the results of three shear tab plate coupons were taken for each shear tab thickness. Yield and ultimate tensile stresses were determined for these specimens. A typical stress vs. strain graph for a shear tab coupon test (from the Plate 9 specimen) is shown in Figure 4-33 and a summary of the material properties obtained from the shear tab coupon tests is provided in Table 4-7. Plates used to fabricate shear tabs were made of ASTM A572 - Grade 50 steel.

It should be noted that the stress did drop back down and the coupon did eventually rupture. This is not represented graphically because this particular plot is based on extensometer readings and the extensometer reached its maximum stroke prior to the ultimate failure of the coupon. The actuator LVDT measured the extension of the coupons beyond the range of the extensometer however the more accurate extensometer readings were used, especially in the elastic range in order to determine the modulus of elasticity of each specimen.

4.4.4 Remarks on Material Properties

Both the shear tab coupons and the test beam coupons exhibited very similar stress vs. strain behaviour. While the magnitudes of the tensile yield and tensile ultimate stresses did differ considerably from one specimen to the next, they all exhibited a readily distinguishable elastic region, a yield plateau, a gradual increase in stress due to strain hardening, and ultimately necking and rupture. All specimens exceeded their minimum yielding stress and minimum ultimate stress ratings.

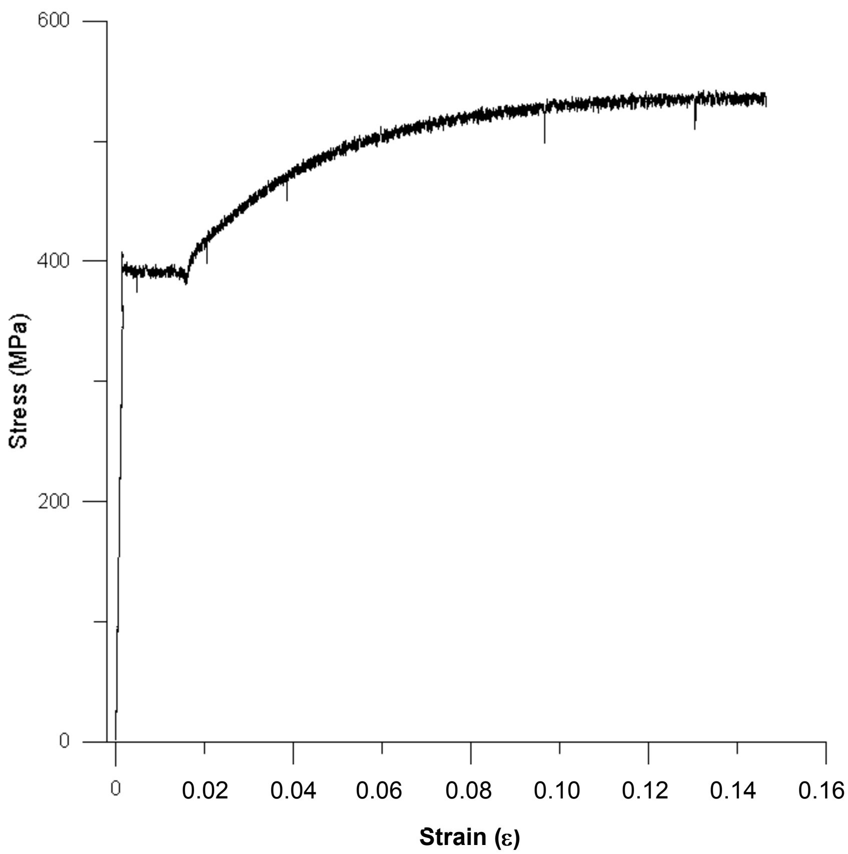

Figure 4-33: Typical Stress-Strain Response of a Shear Tab Tensile Test Coupon

Table 4-8: Summary of Shear Tab Plate Tensile Coupon Tests

	Plate 6	Plate 7	Plate 8	Plate 9	Plate 10
$F_{uSTATIC}$ (MPa)	472	494	508	524	548
$F_{ySTATIC}$ (MPa)	406	371	365	373	388
%Elongation	25	26	25	26	26
E (GPa)	198	202	206	207	211
F_u/F_y	1.16	1.33	1.39	1.40	1.41
R_Y	1.18	1.08	1.06	1.08	1.13
R_T	1.05	1.10	1.13	1.17	1.22
Plate Used as Shear Tab in Tests #:	1, 3 and 4	7, 9 and 11	2, 5, 6, 13 and 14	8, 10 and 12	15 and 16

The use of 50 ksi (345 MPa) steel as a material for shear tabs was shown to be acceptable as extensive deformations occurred during testing and the shear tabs possessed enough ductility to meet targeted rotations. Desirable bolt hole deformations were observed in plates up to 22 mm thick.

5.0 CHAPTER 5: Conclusions and Recommendations

5.1 Summary

In an effort to better understand the behaviour of single and double row bolted shear tab connections, six full-scale bolted connection tests were carried out on three test beam sizes. One single and one double row bolted test was carried out on each test beam size, featuring rows of three, six, and ten bolts. Such tests had never been carried out on shear tabs with ten bolts. Ten additional full-scale weld retrofit tests without bolts were conducted to investigate the rotational capacity and shear resistance of these types of connections which are commonly used when members do not align properly on site during the construction process.

Predicted resistances of the connections were made based on design procedures from the AISC (2005) Steel Construction Manual and the CISC (2010) Handbook of Steel Construction. The current shear tab design procedure in the CISC (2010) Handbook was found to be outdated in the sense that it uses clauses and resistance factors in its design tables that have been updated over the past two decades. Additionally, it is limited in its application and does not address the design of multi-row shear tab connections or single row connections having more than seven bolts. For the connection tests that the CISC (2010) design method was applicable for, it was found to give the most conservative predictions.

Consequently, a new shear tab design method was proposed for use in Canada; it is applicable to connections featuring up to two rows of ten bolts. The new method incorporates many of the design checks from the AISC (2005) extended shear tab design approach and uses higher shear strength values when determining the resistance of the bolt group to shear fracture. The proposed modified method proved to be the most accurate in predicting ultimate connection shear force and failure mode. It should be noted, however, that the connections tested were designed and detailed purposely not to fail by shear fracture of the bolt group since other more ductile failure modes were desirable.

In Tests 2 and 8, the AISC (2010) extended shear tab design method did predict shear fracture of the bolt group as the failure mode, whereas the proposed modified method predicted a combined flexural and shear yielding of the shear tab. That latter of the two proved to be right in both cases and the bolts remained undamaged after testing, suggesting that the modification to the shear strength of bolts in the proposed modified design procedure was warranted.

With regards to the behaviour of weld retrofits, it was found through experimental testing that these connections possessed sufficient ductility to meet rotational demands at the beam end. Also, through the use of the instantaneous centre of rotation method, the weld retrofit connections were designed to resist the same loads as had been predicted for their corresponding bolted tests. For example, a single row shear tab having three bolt holes and a field weld around a portion of the perimeter of the shear tab was designed to withstand the same loads as a conventionally connected single row shear tab featuring three bolts. The weld retrofit connections were able to resist the loads predicted for their bolted counterparts and in some cases these connections resisted higher loads than their bolted counterparts. The accuracy of the instantaneous centre of rotation weld group design method cannot be commented upon, as none of the weld groups failed.

Regarding the use of 50 ksi (345 MPa) steel as a shear tab material; it was shown that this grade of steel exhibited sufficient ductility to meet rotational demands. Extensive deformations were seen in shear tabs throughout testing, especially in the vicinities of the bolt holes.

The progression of shear and flexural yielding in the shear tab were found to differ when connections were bolted as opposed to welded. The shear tabs in all of the bolted connections underwent shear yielding prior to flexural yielding. All of the weld retrofit connections underwent flexural yielding before or at the same time as shear yielding. This was likely caused by the restraint of the weld group on the deformation of the shear tab. This behaviour was consistent for both single and double row connections as well as for all three test beam sizes.

With regards to beam size, predicted-to-experimental ratios were generally most conservative for the smallest beam size, the W310x60 sections, and became less and less conservative as beam size increased.

Concerning the behaviour of the single row shear tab tests as opposed to the double row shear tab tests, the beam end rotations relative to the supporting column face were generally larger in the single row tests.

Additionally, in double row tests, the weld retrofit connections tended to outperform the bolted connections in terms of maximum load resisted. This may be due to the fact that a larger area of the shear tab was subjected to plastic deformations in the welded tests as opposed to the bolted test where deformations were much more concentrated in the row of bolt holes closest to the supporting stub column which led to fractures occurring along that line of bolt holes before other parts of the shear tab saw significant plastic deformations.

5.2 Recommendations for Future Studies

Uncertainty still remains about why single row bolted connection tests generally withstood higher connection loads than their welded counterparts, whereas double row bolted connections generally did not resist loads as high as the weld retrofit specimens. An investigation into the stress concentrations and distributions that each connection configuration was subjected to using finite element analyses may provide a better understanding of this behaviour. If the effect of bearing stress from the bolts could be incorporated into a finite element model as well, it could shed additional light on the development of shear fractures through bolted connections as opposed to the shear fractures seen through weld retrofit connections where bolt holes underwent more significant deformations prior to fracture. In addition to this, the vertical edge distance fractures that occurred only in weld retrofit tests and not in bolted tests could likely be better understood through finite element analyses.

Investigations into the effect of slab restraints on multi-row connections may prove useful in improving design procedures and determining how the ability of the connection to accommodate rotation would be affected.

As mentioned in Chapter 1, this research focused specifically on rigid support conditions where test beams framed into the strong axis of the supporting columns. Future tests on flexible support conditions could broaden or restrict the applicability of the findings of this research to specific support conditions.

6.0 CHAPTER 6: References

ABAQUS [2000], *ABAQUS/Standard User's Manual Vol. I-III*, Hibbitt, Karlsson and Sorenson, Inc. Pawtucket, RI.

AISC [1978], *Specification for the Design, Fabrication and Erection of Structural Steel for Buildings*. American Institute of Steel Construction. New York.

AISC [2003], *Steel Construction Manual: Load and Resistance Factor Design, 3rd Edition*. American Institute of Steel Construction. Chicago.

AISC [2005], *Steel Construction Manual: 13th Edition*. American Institute of Steel Construction. Chicago, IL.

AISC [2005a], Specification for Structural Steel Buildings. American Institute of Steel Construction. Chicago, IL.

Ashakul, A. [2004], "Finite Element Analysis of Single Plate Shear Connections", Ph.D Dissertation, Virginia Polytechnic Institute and State University. Blacksburg.

Astaneh, A. [1989], "Demand and Supply of Ductility in Steel Shear Connections", Journal of Constructional Steel Research, 14, pp. 1-19.

Astaneh, A., Call, S.M., and McMullin, K.M. [1989], "Design of Single Plate Shear Connections", American Institute of Steel Construction Engineering Journal, Volume 26, 1st Quarter, pp. 21-32.

Astaneh, A., McMullin, K.M., and Call, S.M. [1993], "Behaviour and Design of Steel Single Plate Shear Connections", Journal of Structural Engineering, ASCE, Volume 119, No. 8, pp. 2421-2440.

Astaneh, A., Liu, J., and McMullin, K.M., [2002], "Behaviour and Design of Single Plate Shear Connections", Journal of Constructional Steel Research, Volume 58, pp. 1121-1141.

ASTM [2009], *ASTM A370-09 Standard Test Methods and Definitions for Mechanical Testing of Steel Products*. Volume 01.03. American Society for Testing and Materials. Philadelphia, PA.

AWS [2005], *AWS A5.20:2005 Specification for Carbon Steel Electrodes for Flux Cored Arc Welding.* American Welding Society. Miami, FL.

Baldwin Metzger, K. A. [2006], "Experimental Verification of a New Single Plate Shear Connection Design Model", M.Sc. Thesis, Virginia Polytechnic Institute and State University. Blacksburg, VA.

Caccavale, S.E. [1975], "Ductility of Single Plate Framing Connections", M.Sc. Thesis, University of Arizona. Tucson, AZ.

CISC [2000], *Handbook of Steel Construction, 7th Edition*. Canadian Institute of Steel Construction. Toronto, ON.

CISC [2006], *Handbook of Steel Construction, 9th Edition*. Canadian Institute of Steel Construction. Toronto, ON.

CISC [2010], *Handbook of Steel Construction, 10th Edition*. Canadian Institute of Steel Construction. Toronto, ON.

Creech, D.D. [2005], "Behavior of Single Plate Shear Connections with Rigid and Flexible Supports", M. Sc. Thesis, North Carolina State University. Raleigh.

CSA [1994], *CSA Standard S16-94 Design of Steel Structures*. Canadian Standards Association. Mississauga, ON.

CSA [2009], *CSA Standard S16-09 Design of Steel Structures*. Canadian Standards Association. Mississauga, ON.

Hogan, T.J. and Firkins, A. [1978], "Standardized Structural Connections – Part A: Details and Design Capacities", Australian Institute of Steel Construction.

Hormby, D.E., Richard, R.M., and Kriegh, J.D. [1984], "Single Plate Framing Connections with Grade-50 Steel and Composite Construction", American Institute of Steel Construction Engineering Journal, Volume 21, 3rd Quarter, pp. 125-138.

Kulak, G.L., Fisher, J.W., and Struik, J.H.A. [1987], *Guide to Design Criteria for Bolted and Riveted Joints*. American Institute of Steel Construction. Chicago, IL

Lipson, S.L. [1968], "Single-Angle and Single-Plate Beam Framing Connections". Proceedings of *Canadian Structural Engineering Conference*. pp. 141-162. Toronto, ON.

Patrick, M., Thomas, I.R., and Bennetts, I.D. [1986], "Testing of the Web Side Plate Connection", Australian Welding Research, AWRA Report P6-1-87.

Pham, L. and Mansell, D.S. [1982], "Testing of Standardized Connections", Australian Welding Research, AWRA Report P6-22-81.

Richard, R.M., Gillett, P.E., Kriegh, J.D., and Lewis, B.A. [1980], "The Analysis and Design of Single Plate Framing Connections", American Institute of Steel Construction Engineering Journal, Volume 17, 2nd Quarter, pp. 38-52.

Richard, R.M., Kriegh, J.D., and Hormby, D.E. [1982], "Design of Single Plate Framing Connections with A307 Bolts", American Institute of Steel Construction Engineering Journal, Volume 19, 4th Quarter, pp. 209-213.

Ricles, J.M. [1980], “The Behaviour and Analysis of Double Row Bolted Shear Web Connections”, M.Sc. Thesis, University of Texis. Austin, TX.

Sherman, D.R. and Ghorbanpoor, A. [2002], “Design of Extended Shear Tabs”, American Institute of Steel Construction Final Report, University of Wisconson, Milwaukee, WI.

Stiemer, S.F., Wong, H.H., and Ho, A. [1986], “Ultimate Capacity of Single Plate Connectors”, Proceedings of *The Pacific Structural Steel Conference*: *August 4-8, 1986*. Auckland.

Yarimci, E., Yura, J.A., and Lu, L.W. [1967], “Techniques for Testing Structures Permitted to Sway”, Experimental Mechanics, Volume 7, Number 8, pp. 321-331.

Young, N.W. and Disque, R.O. [1981], “Design Aids for Single Plate Framing Connections”, Engineering Journal, American Institute of Steel Construction, Volume 18, 4^{th} Quarter, pp. 129-148.

APPENDIX A: Test Setups and Instrumentation

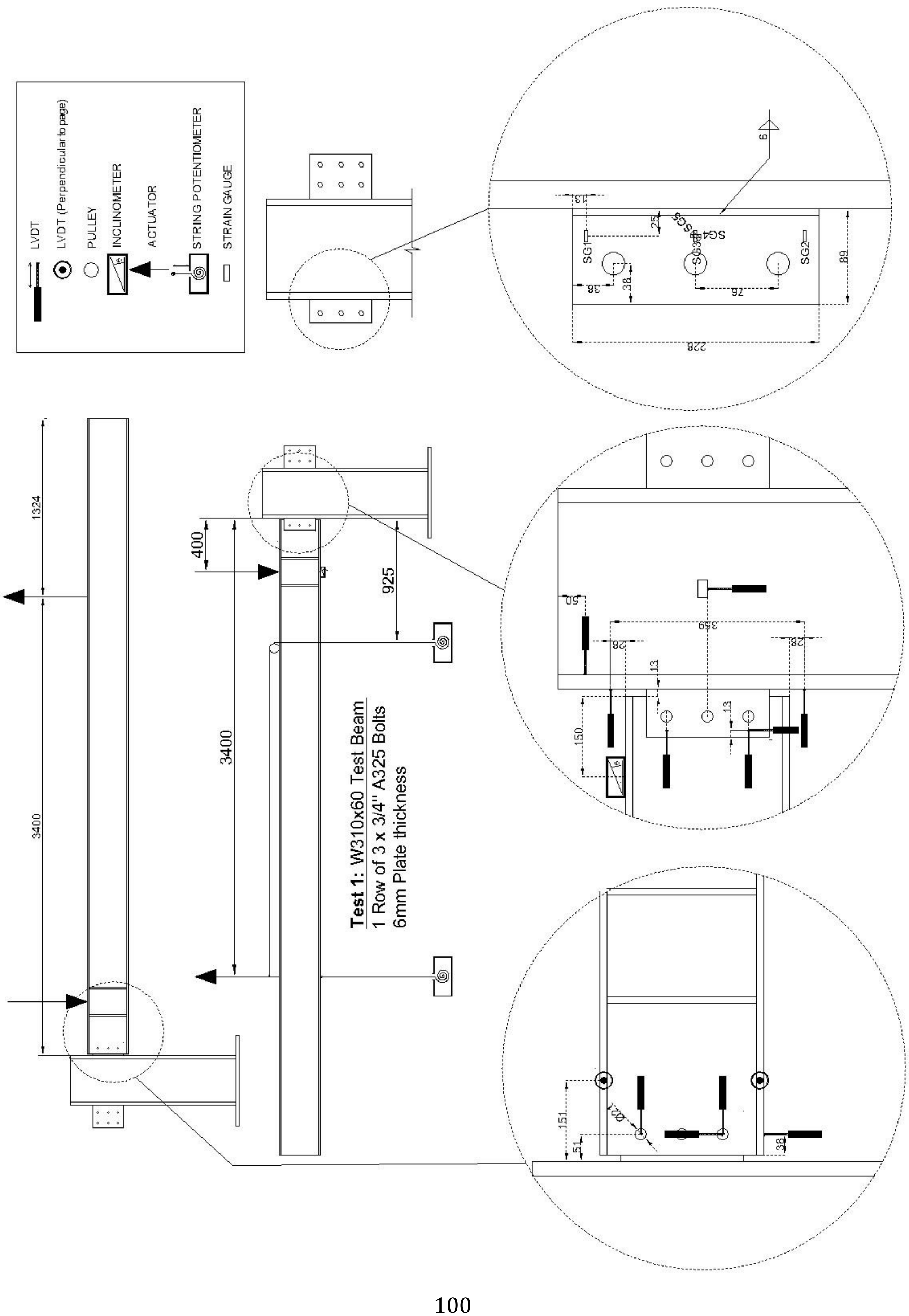

LVDT
LVDT (Perpendicular to page)
PULLEY
INCLINOMETER
ACTUATOR
STRING POTENTIOMETER
STRAIN GAUGE
Test 1: W310x60 Test Beam
1 Row of 3 x 3/4" A325 Bolts
6mm Plate thickness
1324
3400
400
925
3400
228
89
76
38
38
25
13
6
SG1
SG2
SG3
SG4
SG5
359
28
28
50
13
13
150
151
51
38

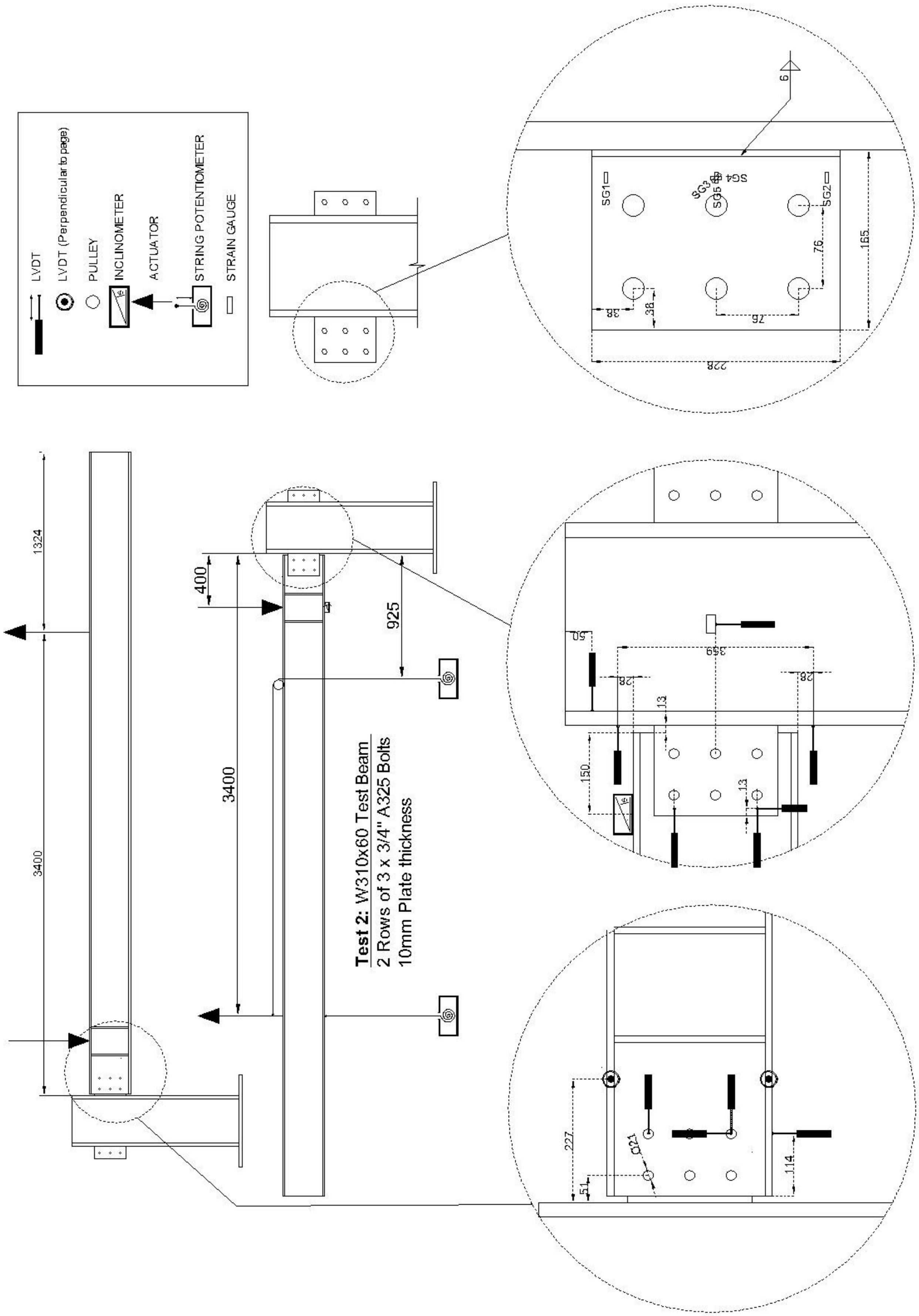
LVDT
LVDT (Perpendicular to page)
PULLEY
INCLINOMETER
ACTUATOR
STRING POTENTIOMETER
STRAIN GAUGE
1324
3400
400
925
3400
Test 2: W310x60 Test Beam
2 Rows of 3 x 3/4" A325 Bolts
10mm Plate thickness
SG1
SG2
SG3
SG4
SG5
6
76
165
38
38
76
228
50
359
28
28
13
150
13
227
Ø21
51
114

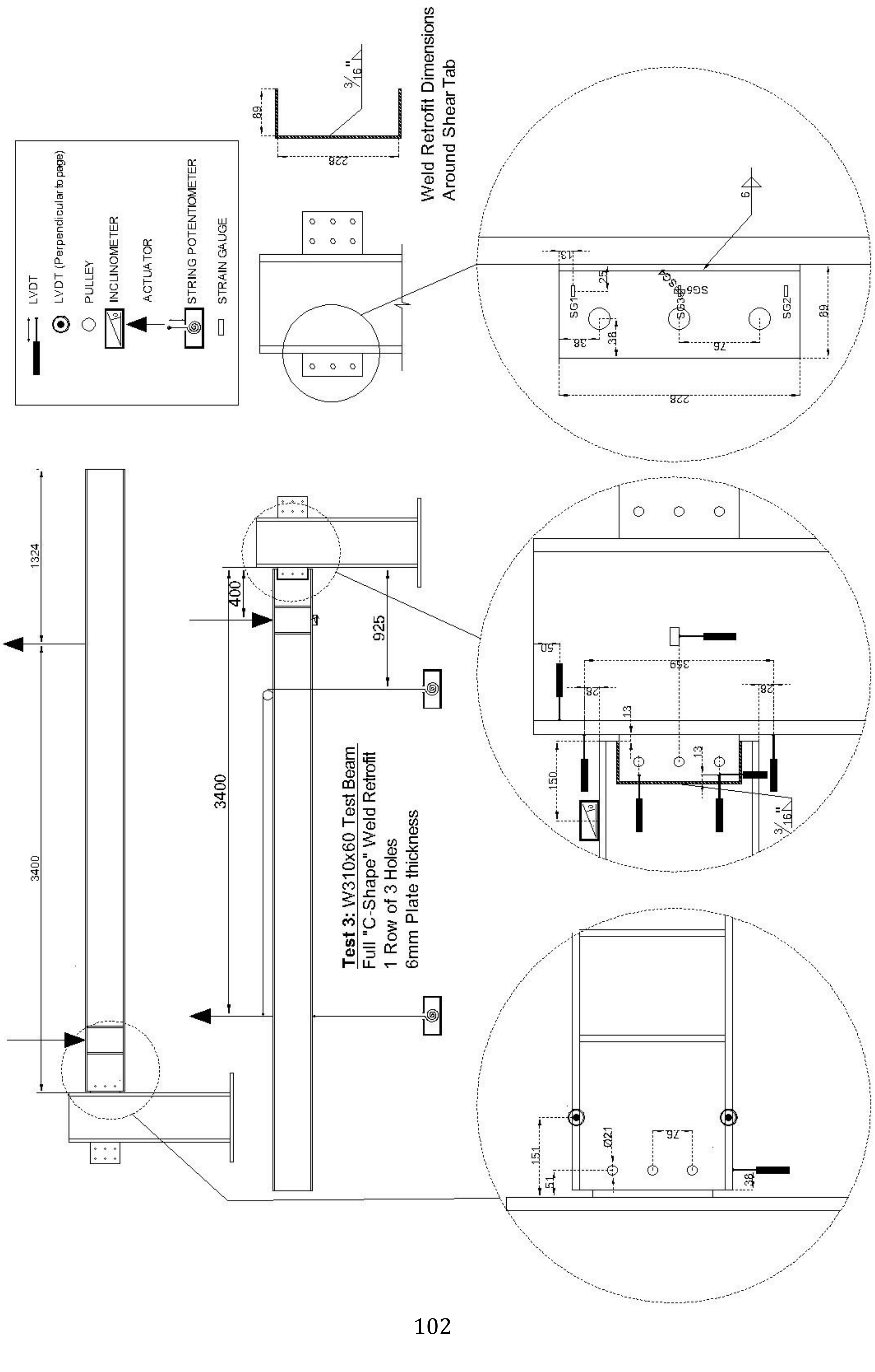
LVDT
LVDT (Perpendicular to page)
PULLEY
INCLINOMETER
ACTUATOR
STRING POTENTIOMETER
STRAIN GAUGE
Weld Retrofit Dimensions
Around Shear Tab
Test 3: W310x60 Test Beam
Full "C-Shape" Weld Retrofit
1 Row of 3 Holes
6mm Plate thickness
1324
3400
400
925
SG1
SG2
SG3
SG4
SG5
228
89
76
38
25
13
150
369
28
50
151
51
Ø21

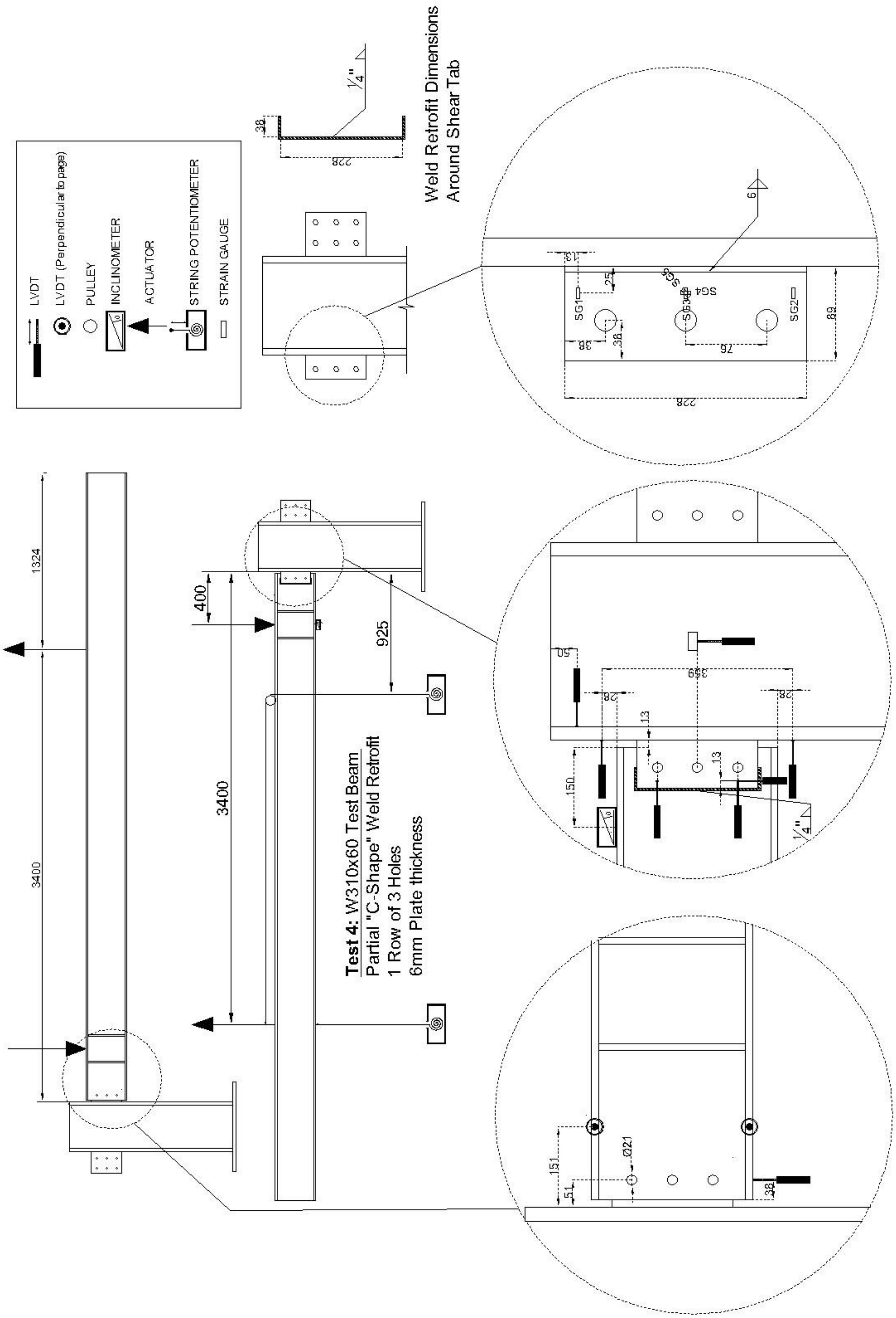
LVDT
LVDT (Perpendicular to page)
PULLEY
INCLINOMETER
ACTUATOR
STRING POTENTIOMETER
STRAIN GAUGE
Weld Retrofit Dimensions
Around Shear Tab
Test 4: W310x60 Test Beam
Partial "C-Shape" Weld Retrofit
1 Row of 3 Holes
6mm Plate thickness
1324
3400
400
925
3400
228
38
1/4"
SG1
SG2
SG3
SG4
SG5
6
25
13
76
89
359
28
50
150
151
51
Ø21

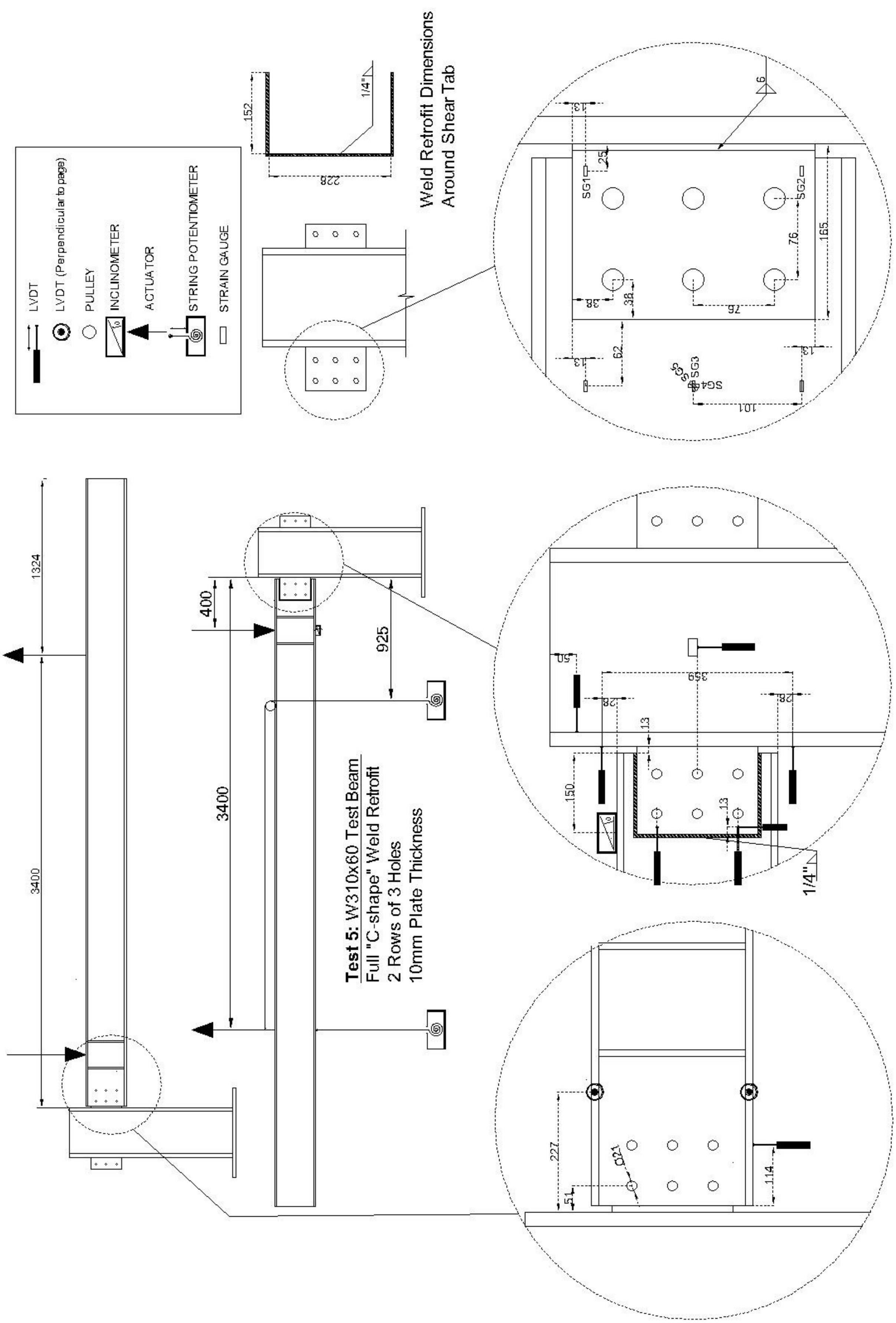

LVDT
LVDT (Perpendicular to page)
PULLEY
INCLINOMETER
ACTUATOR
STRING POTENTIOMETER
STRAIN GAUGE
Weld Retrofit Dimensions
Around Shear Tab
Test 5: W310x60 Test Beam
Full "C-shape" Weld Retrofit
2 Rows of 3 Holes
10mm Plate Thickness
1324
3400
3400
400
925
152
228
1/4"

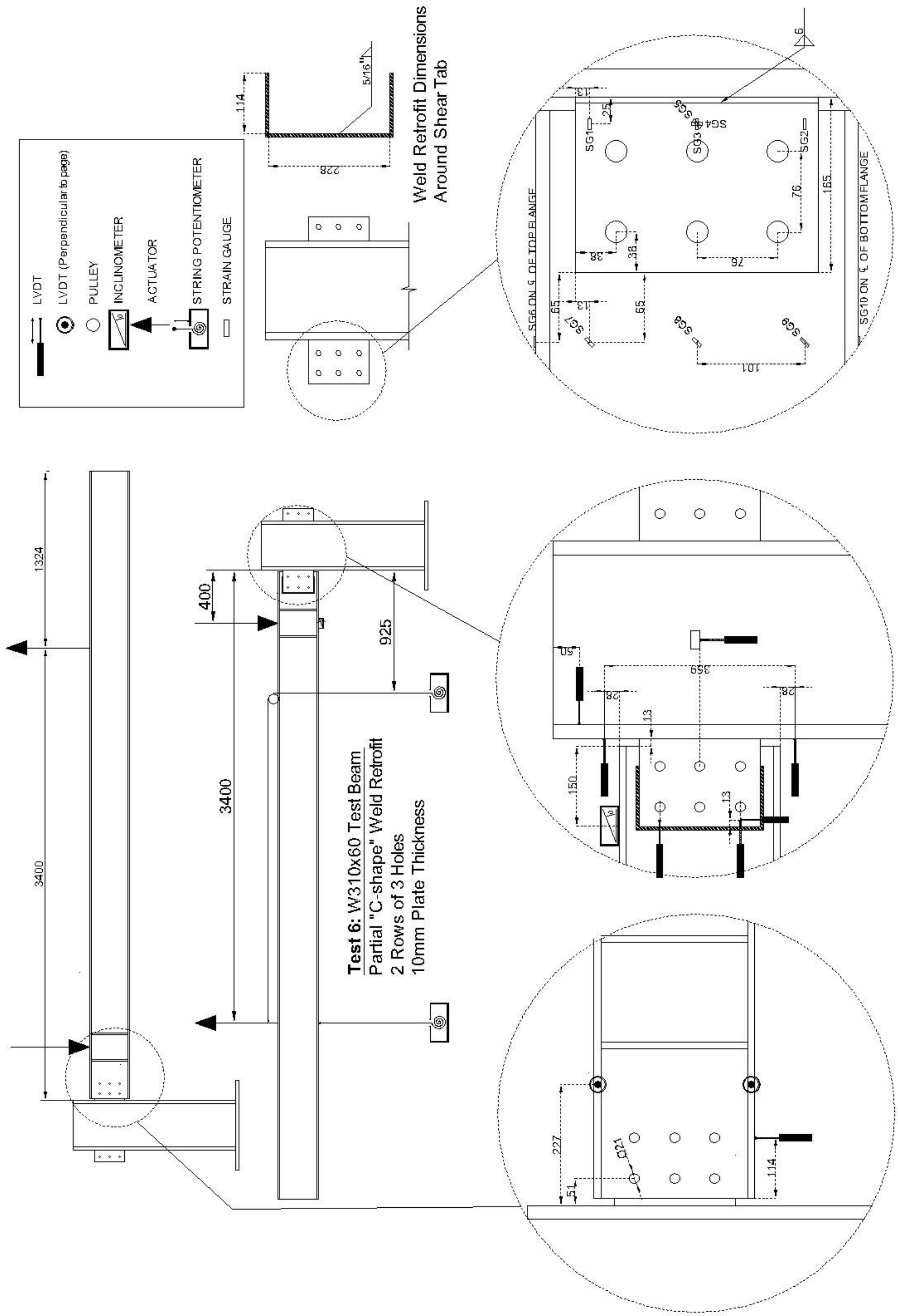

LVDT
LVDT (Perpendicular to page)
PULLEY
INCLINOMETER
ACTUATOR
STRING POTENTIOMETER
STRAIN GAUGE
Weld Retrofit Dimensions
Around Shear Tab
Test 6: W310x60 Test Beam
Partial "C-shape" Weld Retrofit
2 Rows of 3 Holes
10mm Plate Thickness
SG6 ON ℄ OF TOP FLANGE
SG10 ON ℄ OF BOTTOM FLANGE

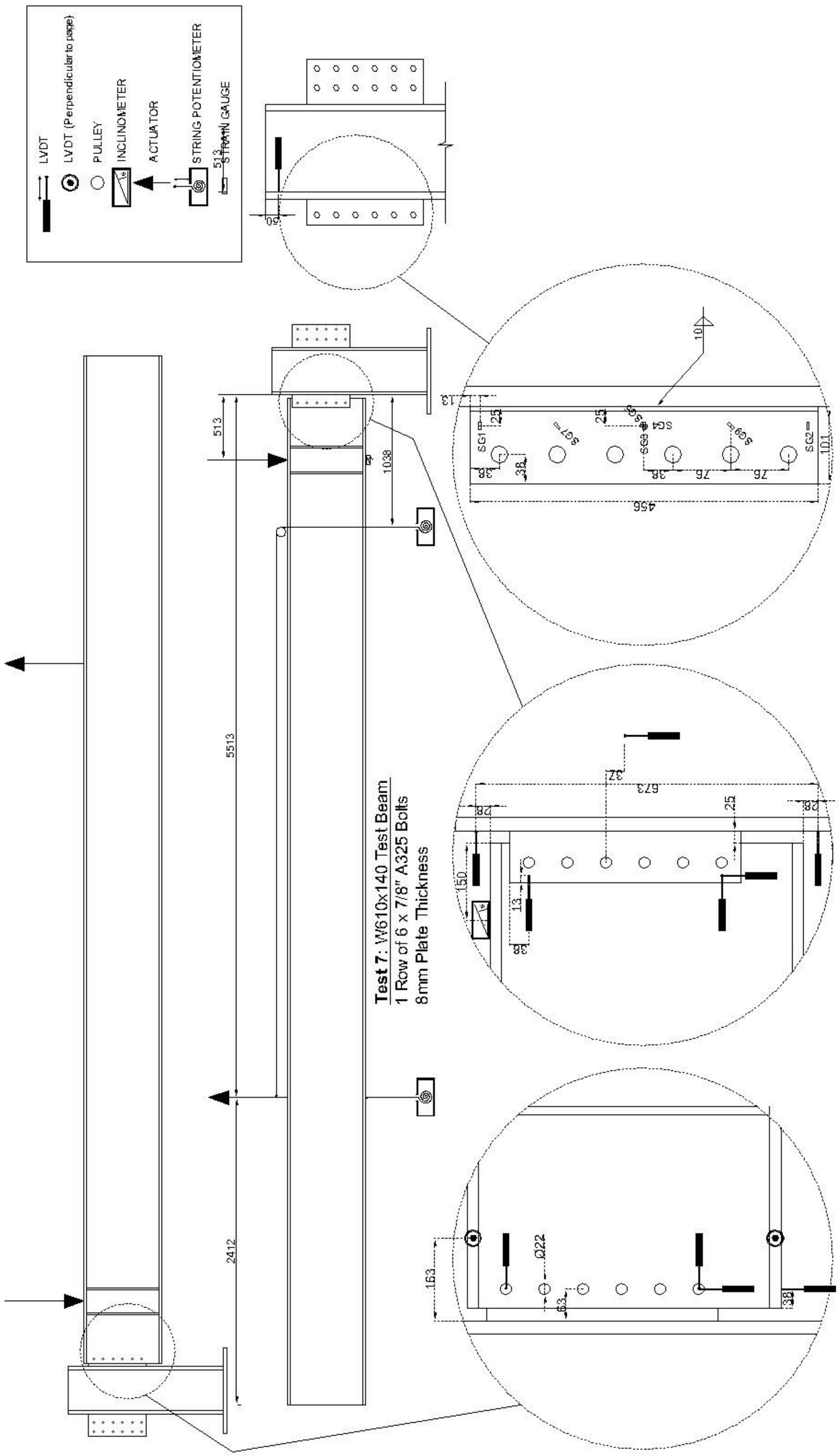
LVDT
LVDT (Perpendicular to page)
PULLEY
INCLINOMETER
ACTUATOR
STRING POTENTIOMETER
STRAIN GAUGE
Test 7: W610x140 Test Beam
1 Row of 6 x 7/8" A325 Bolts
8mm Plate Thickness
513
5513
2412
1038
456
673
163
Ø22

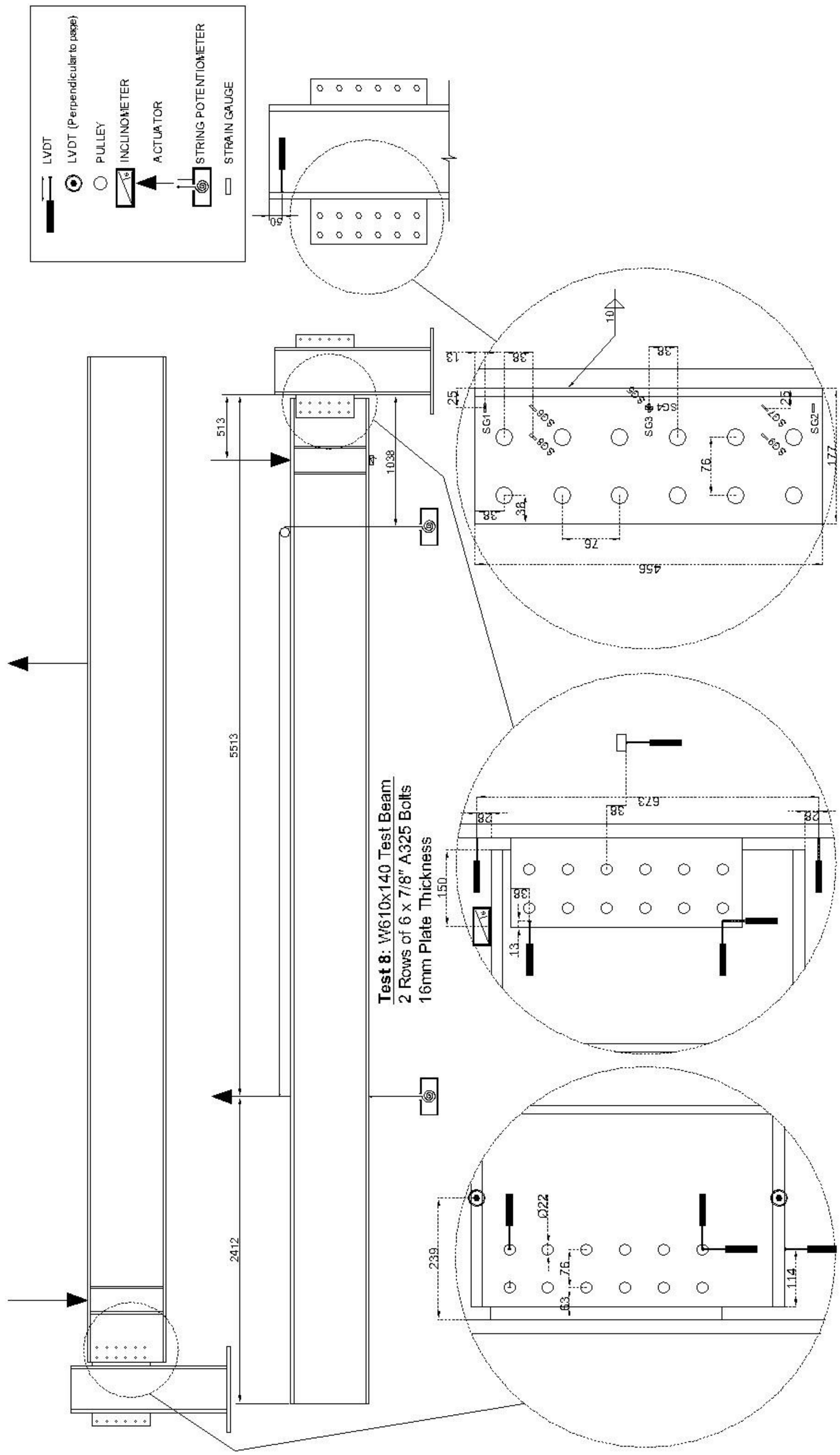
LVDT
LVDT (Perpendicular to page)
PULLEY
INCLINOMETER
ACTUATOR
STRING POTENTIOMETER
STRAIN GAUGE
Test 8: W610x140 Test Beam
2 Rows of 6 x 7/8" A325 Bolts
16mm Plate Thickness
513
1038
5513
2412
673
456
177
239
114
Ø22

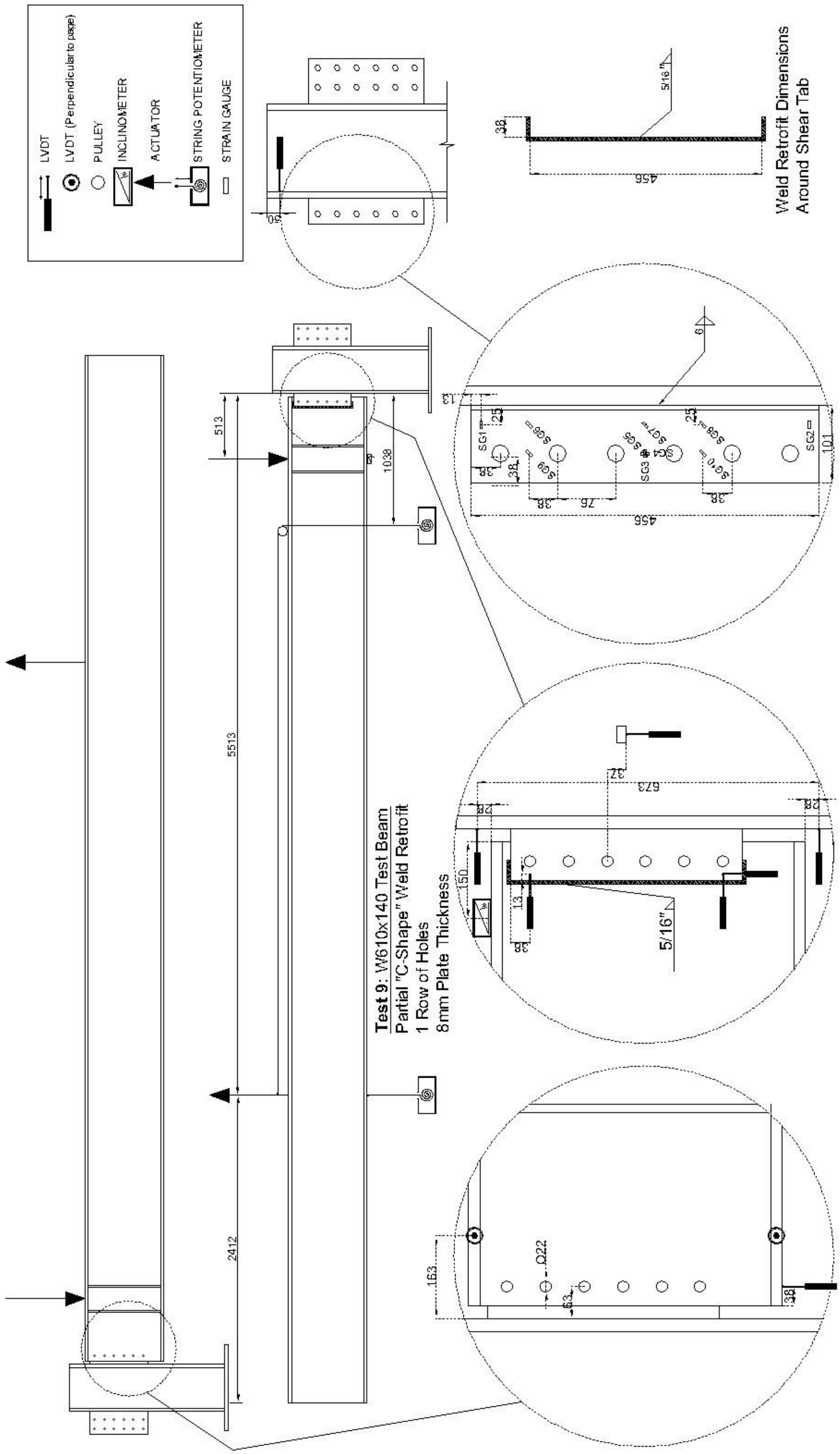

LVDT
LVDT (Perpendicular to page)
PULLEY
INCLINOMETER
ACTUATOR
STRING POTENTIOMETER
STRAIN GAUGE
Test 9: W610x140 Test Beam
Partial "C-Shape" Weld Retrofit
1 Row of Holes
8mm Plate Thickness
Weld Retrofit Dimensions
Around Shear Tab
5513
513
2412
1038
456
673
5/16"

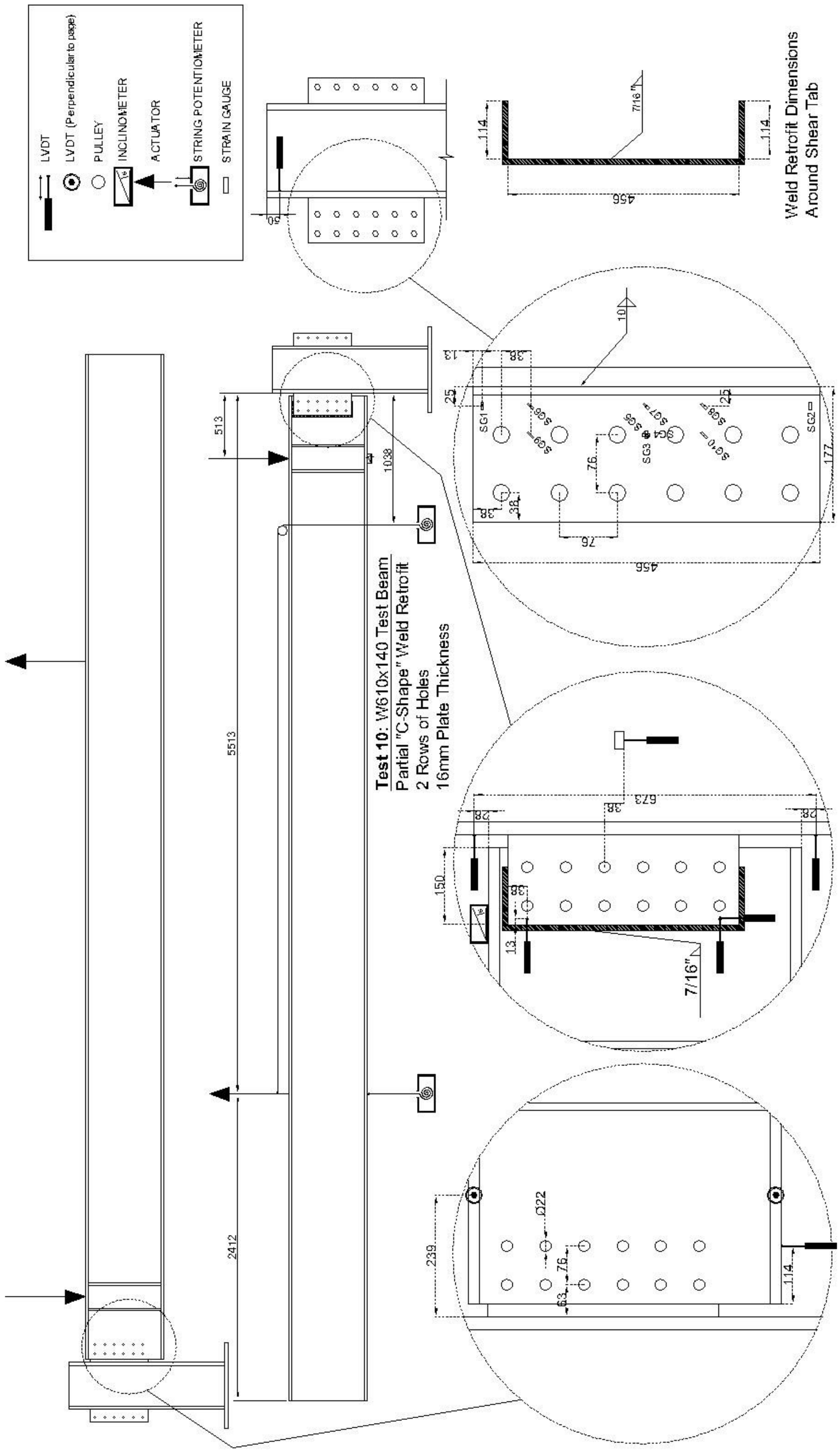
LVDT
LVDT (Perpendicular to page)
PULLEY
INCLINOMETER
ACTUATOR
STRING POTENTIOMETER
STRAIN GAUGE
Test 10: W610x140 Test Beam
Partial "C-Shape" Weld Retrofit
2 Rows of Holes
16mm Plate Thickness
Weld Retrofit Dimensions
Around Shear Tab
513
5513
2412
1038
456
114
7/16"
7/16"
673
150
239
Ø22
76
63
177
SG1
SG2
SG3
SG4
SG5
SG6
SG7
SG8
SG9
SG10

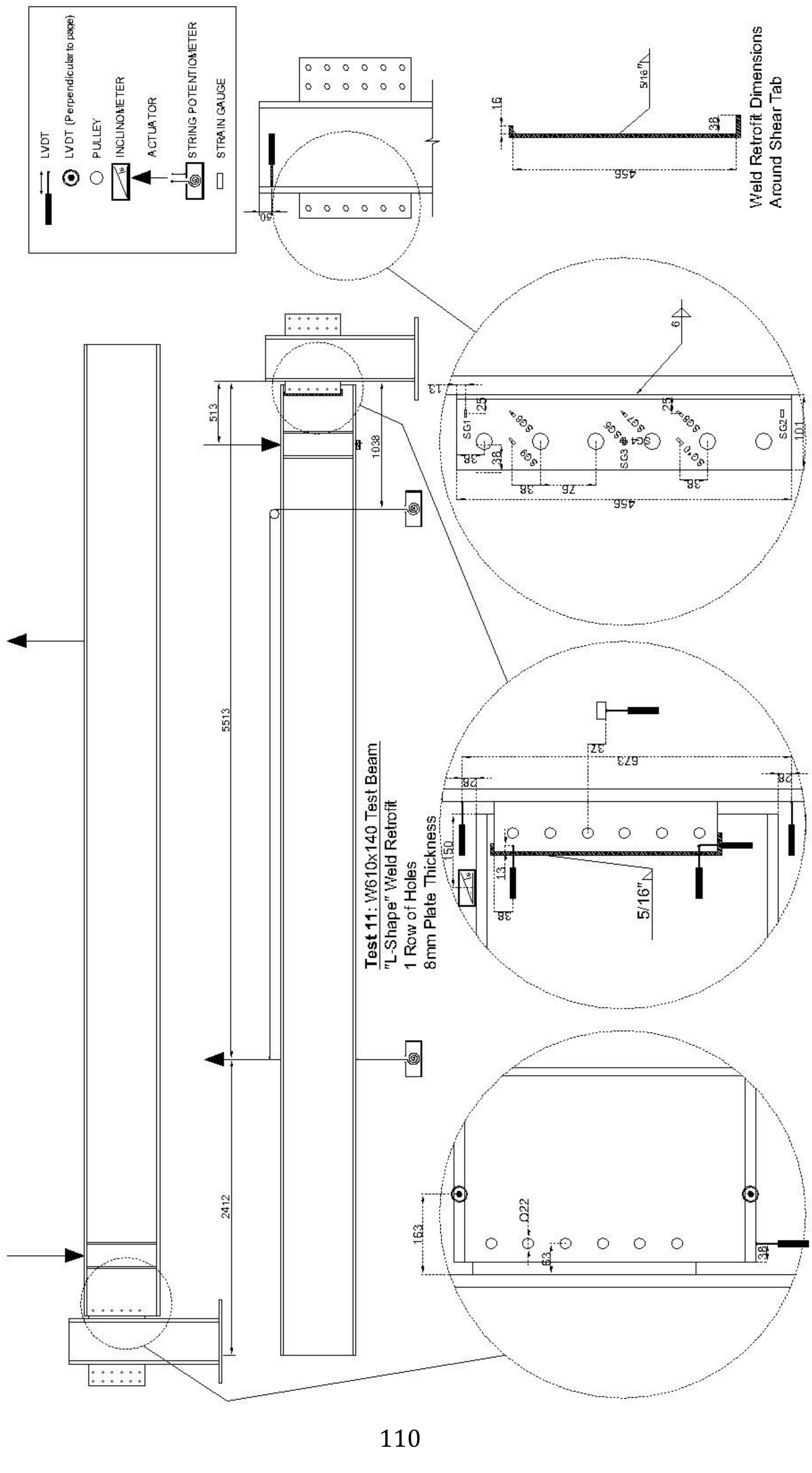
LVDT
LVDT (Perpendicular to page)
PULLEY
INCLINOMETER
ACTUATOR
STRING POTENTIOMETER
STRAIN GAUGE
Weld Retrofit Dimensions
Around Shear Tab
Test 11: W610x140 Test Beam
"L-Shape" Weld Retrofit
1 Row of Holes
8mm Plate Thickness
5513
2412
513
1038
456
673
5/16"

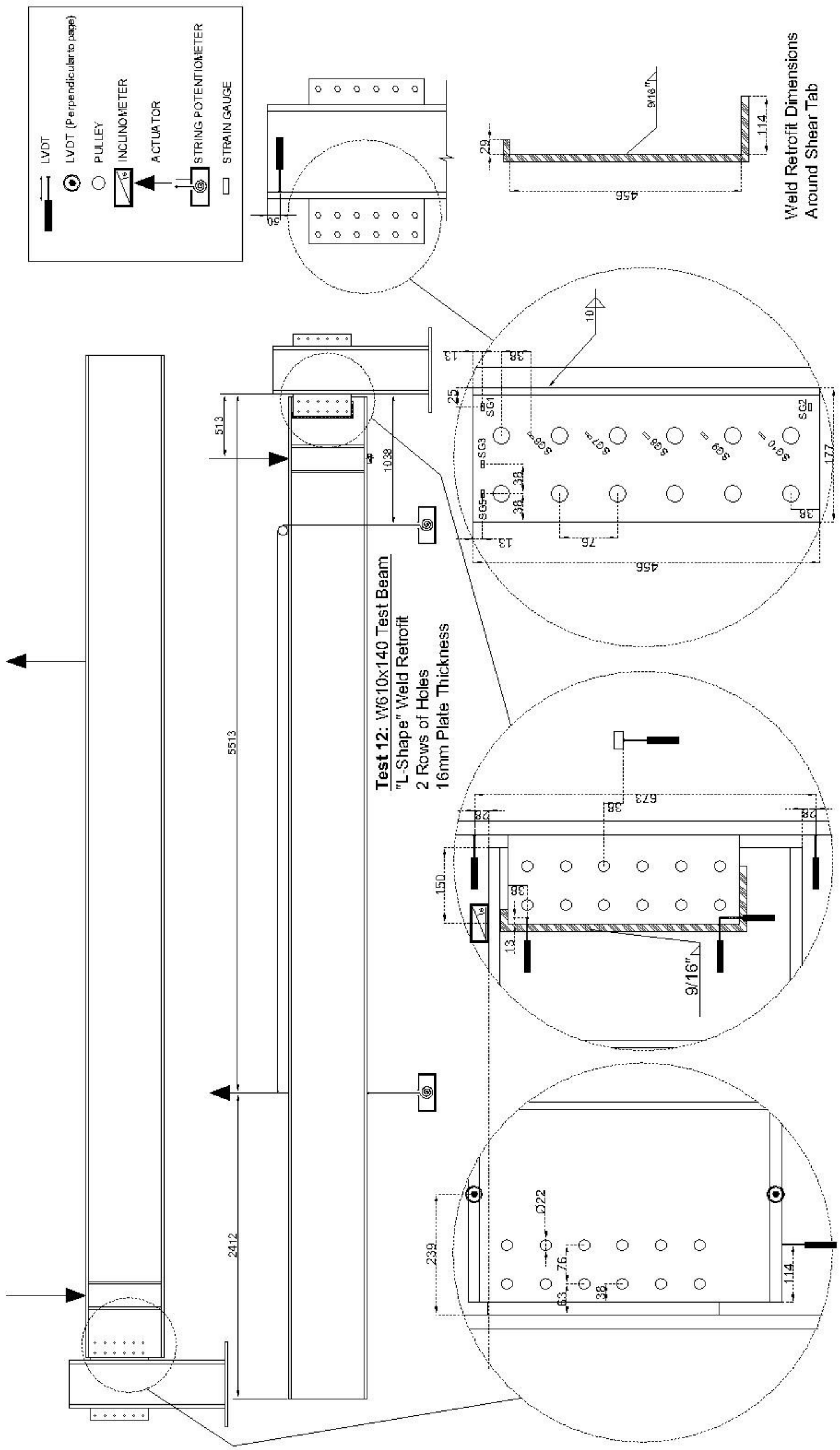

LVDT
LVDT (Perpendicular to page)
PULLEY
INCLINOMETER
ACTUATOR
STRING POTENTIOMETER
STRAIN GAUGE
Weld Retrofit Dimensions
Around Shear Tab
Test 12: W610x140 Test Beam
"L-Shape" Weld Retrofit
2 Rows of Holes
16mm Plate Thickness
9/16"
Ø22

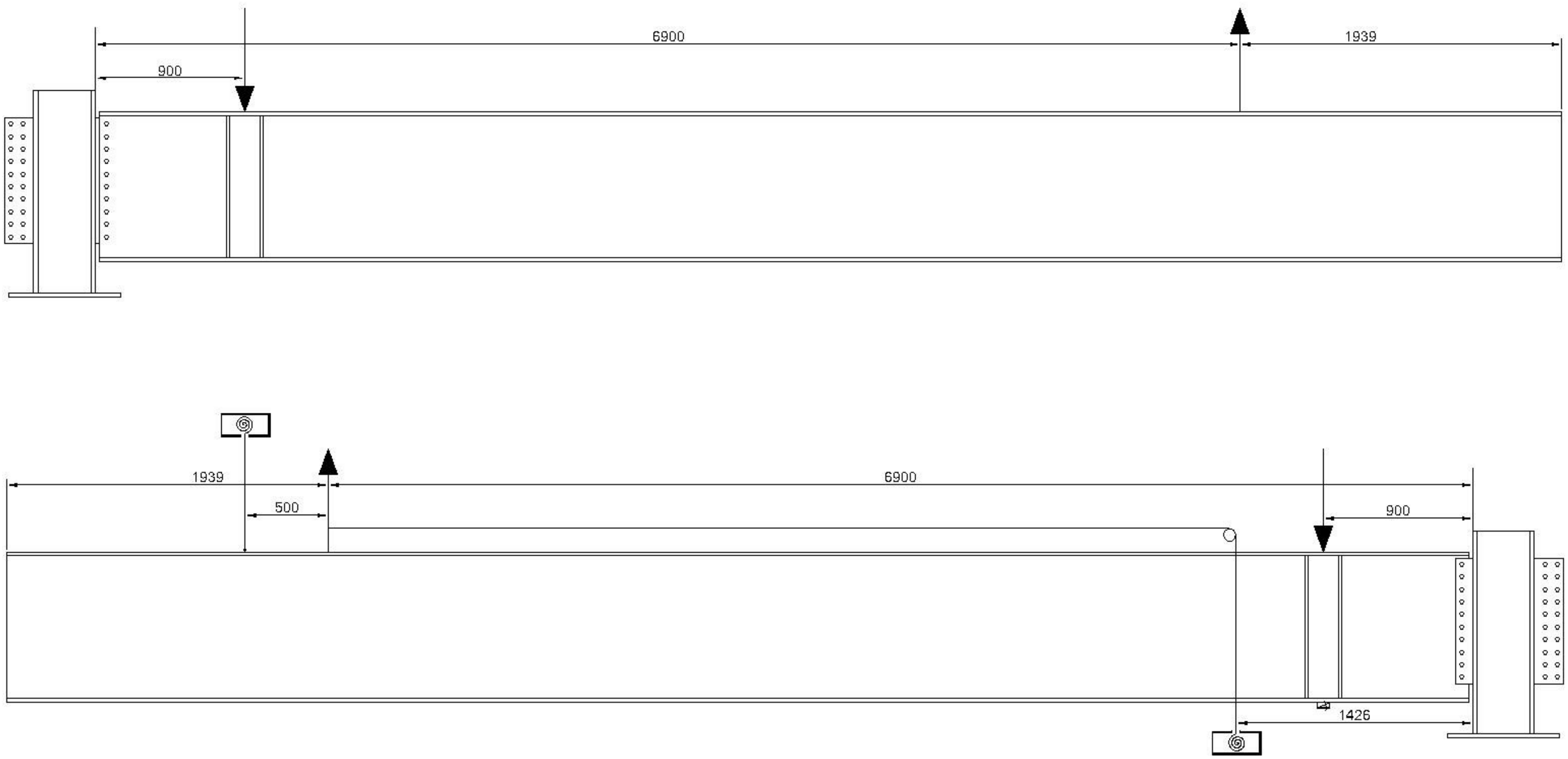

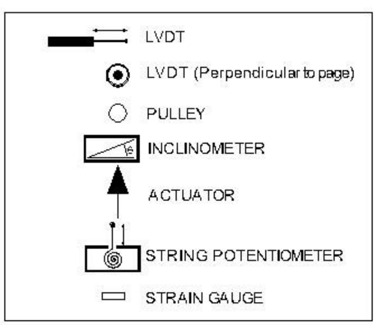

Test 13: W920x223 Test Beam
1 Row of 10 x 1" A325 Bolts
10mm Plate Thickness

Test 13: Drawing 1 of 2

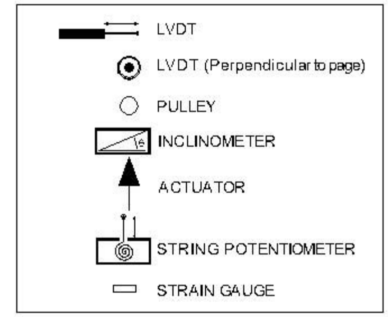

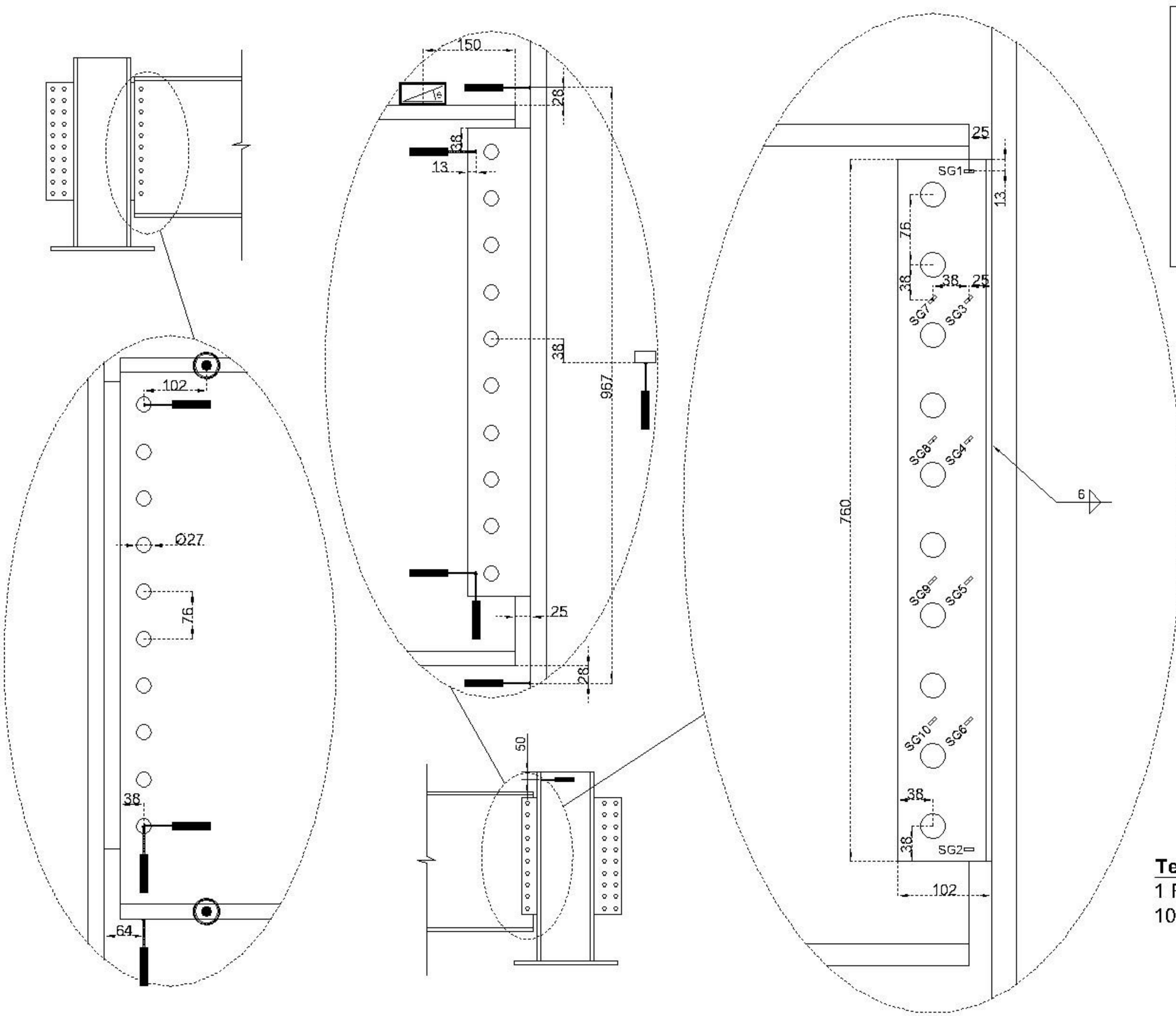

Test 13: W920x223 Test Beam
1 Row of 10 x 1" A325 Bolts
10mm Plate Thickness

Test 13: Drawing 2 of 2

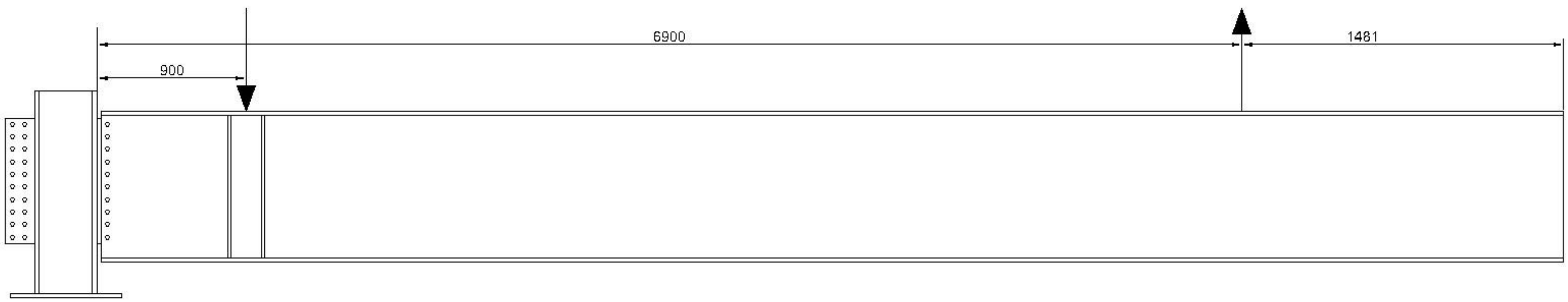

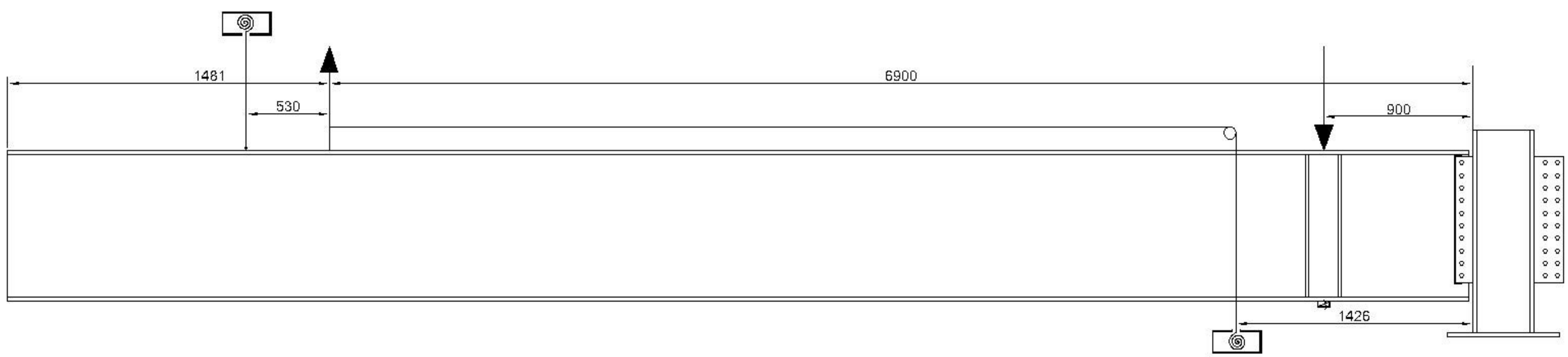

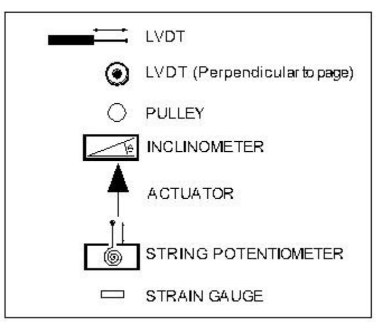

Test 14: W920x223 Test Beam
Partial "C-Shape" Weld Retrofit
1 Row of Holes
10mm Plate Thickness

Test 14: Drawing 1 of 2

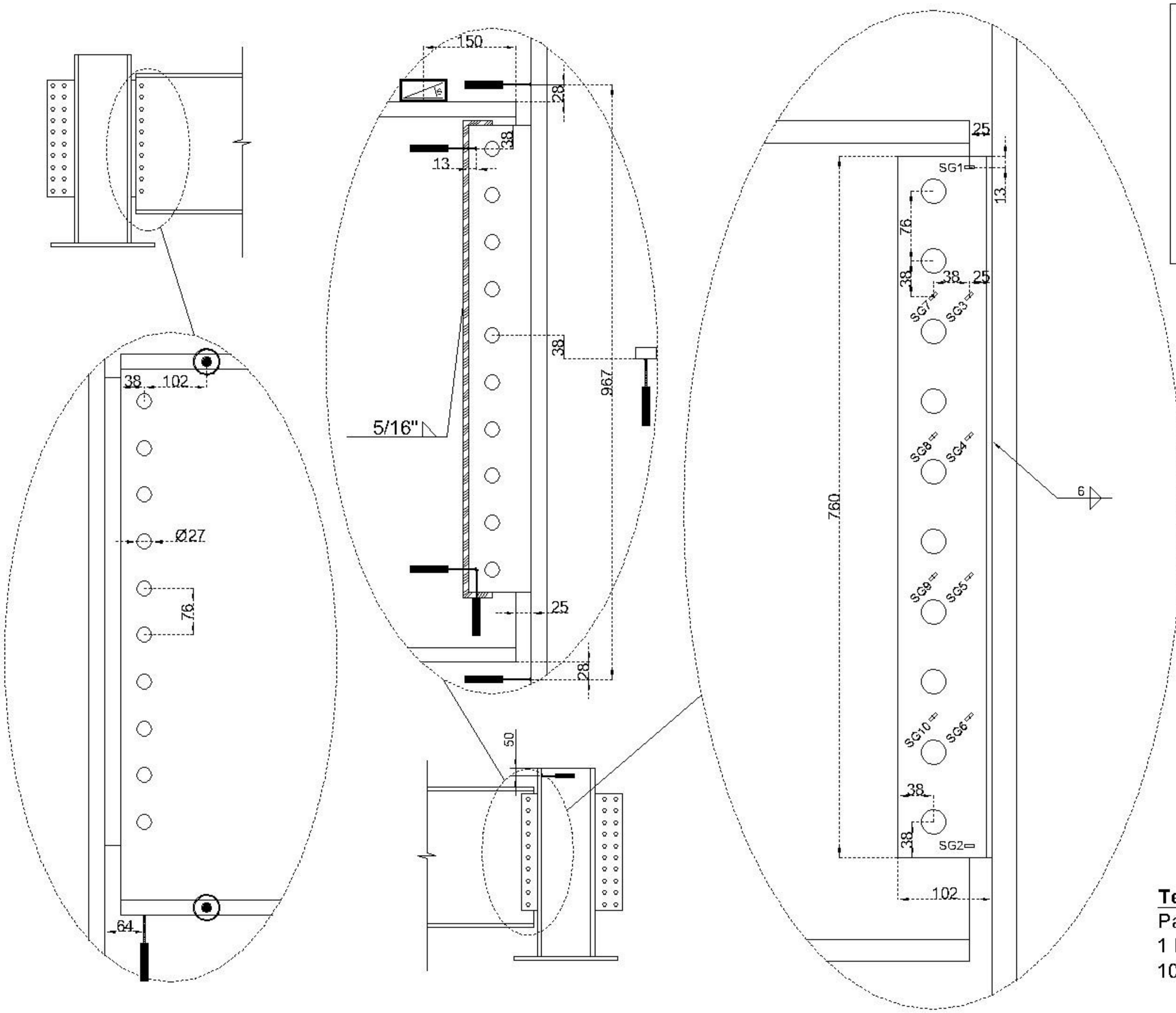

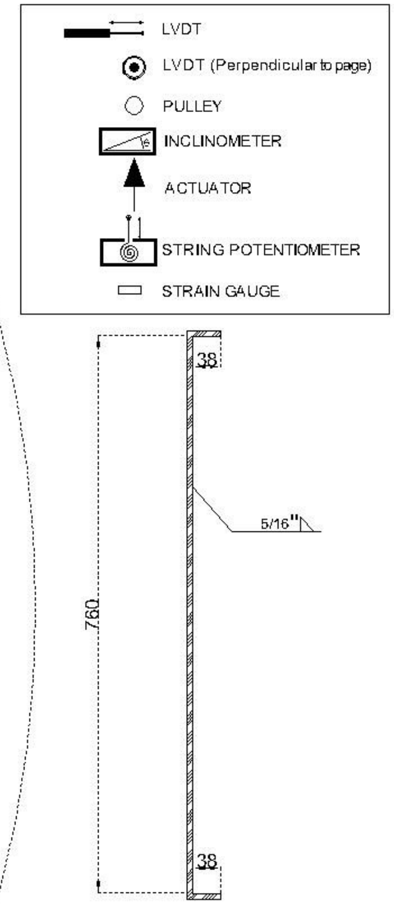

Weld Retrofit Dimensions
Around Shear Tab

Test 14: W920x223 Test Beam
Partial "C-Shape" Weld Retrofit
1 Row of Holes
10mm Plate Thickness

Test 14: Drawing 2 of 2

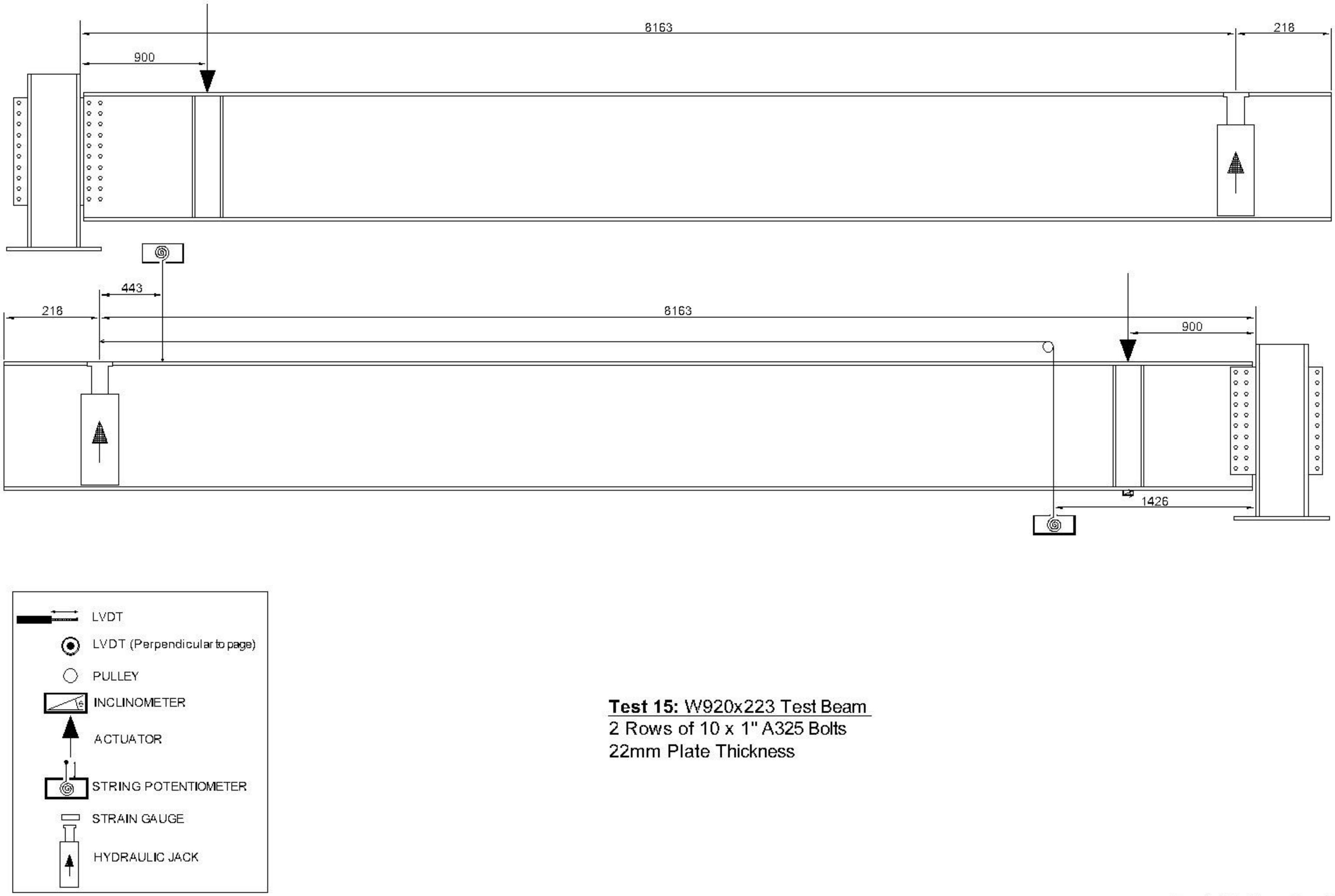

Test 15: W920x223 Test Beam
2 Rows of 10 x 1" A325 Bolts
22mm Plate Thickness

Test 15: Drawing 1 of 2

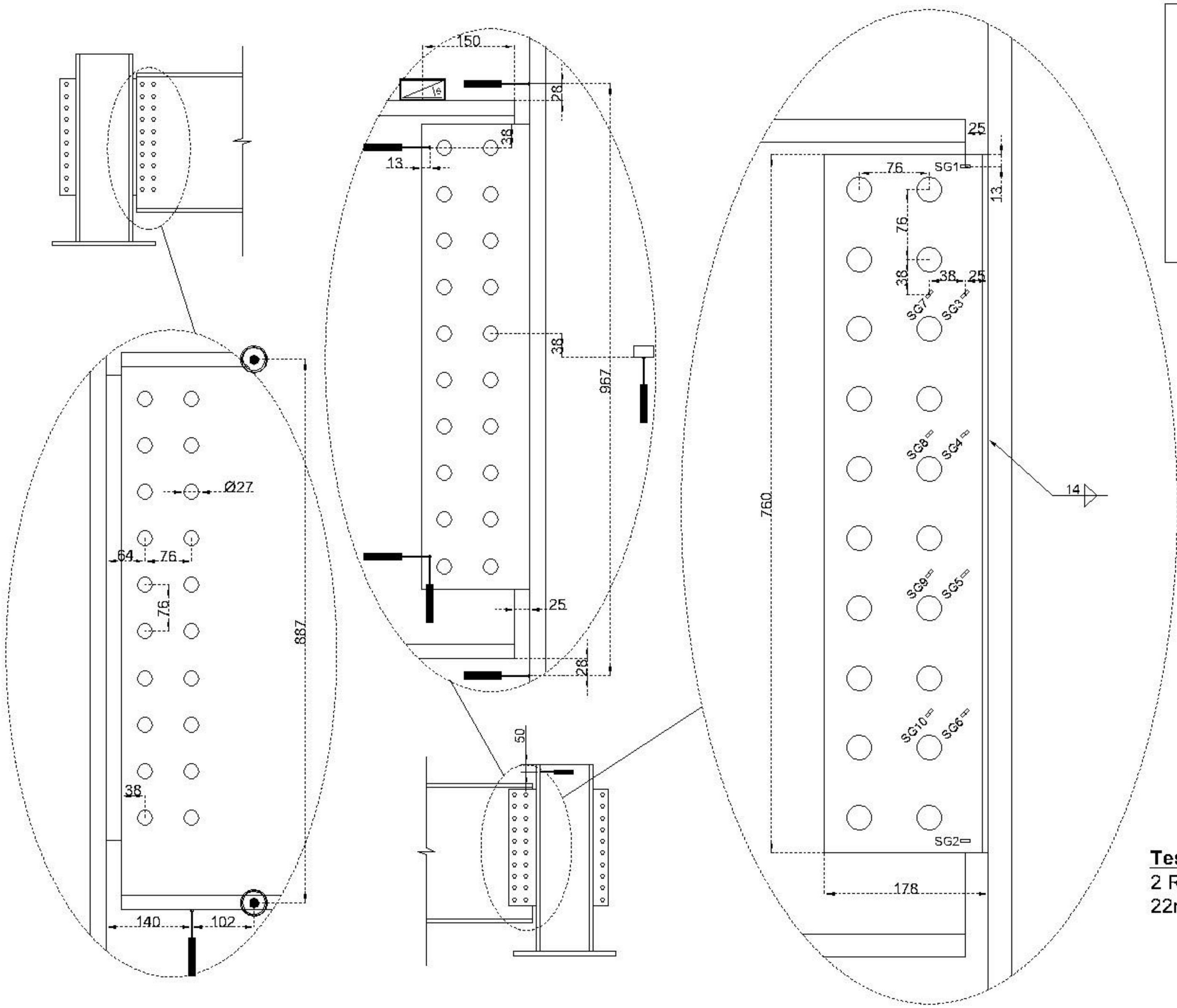

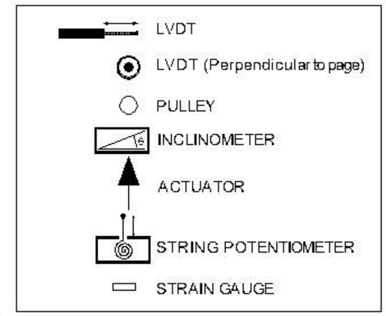

Test 15: W920x223 Test Beam
2 Rows of 10 x 1" A325 Bolts
22mm Plate Thickness

Test 15: Drawing 2 of 2

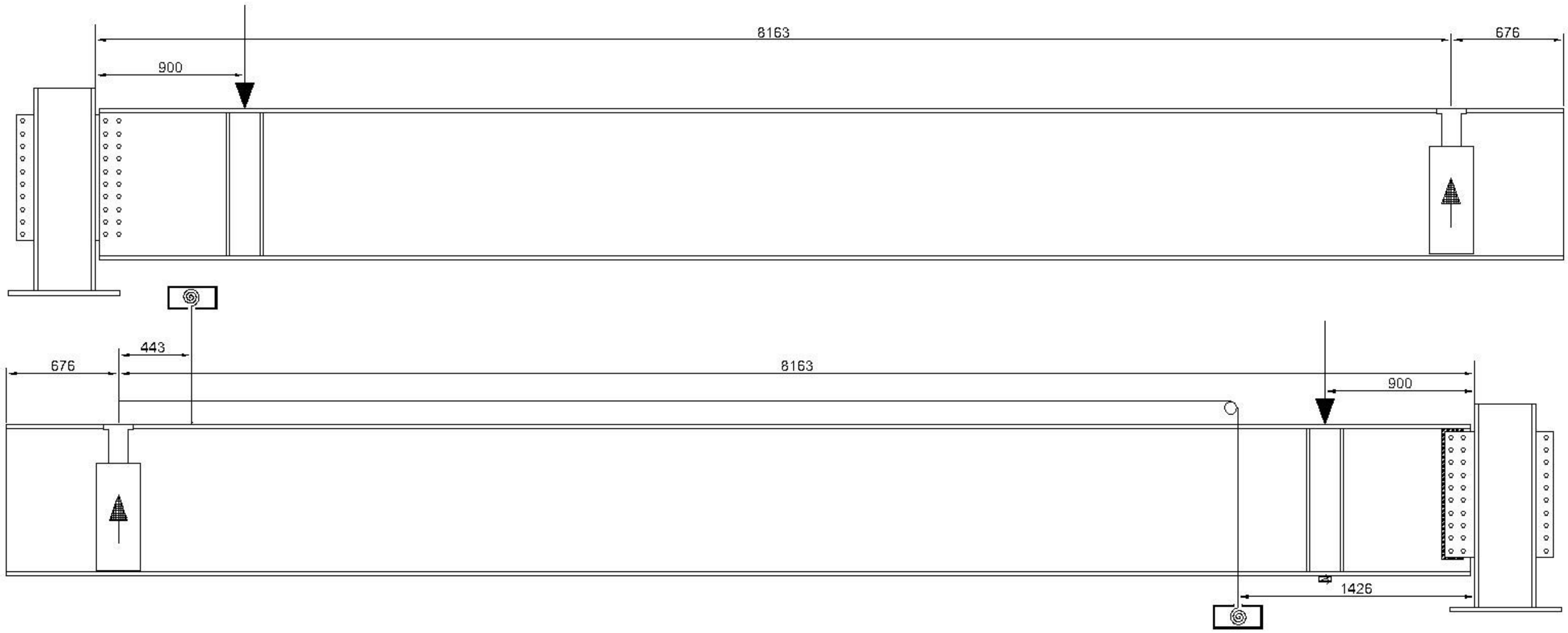

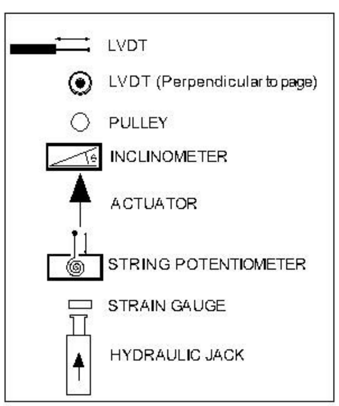

Test 16: W920x223 Test Beam
Partial "C-Shape" Weld Retrofit
2 Row of Holes
22mm Plate Thickness

Test 16: Drawing 1 of 2

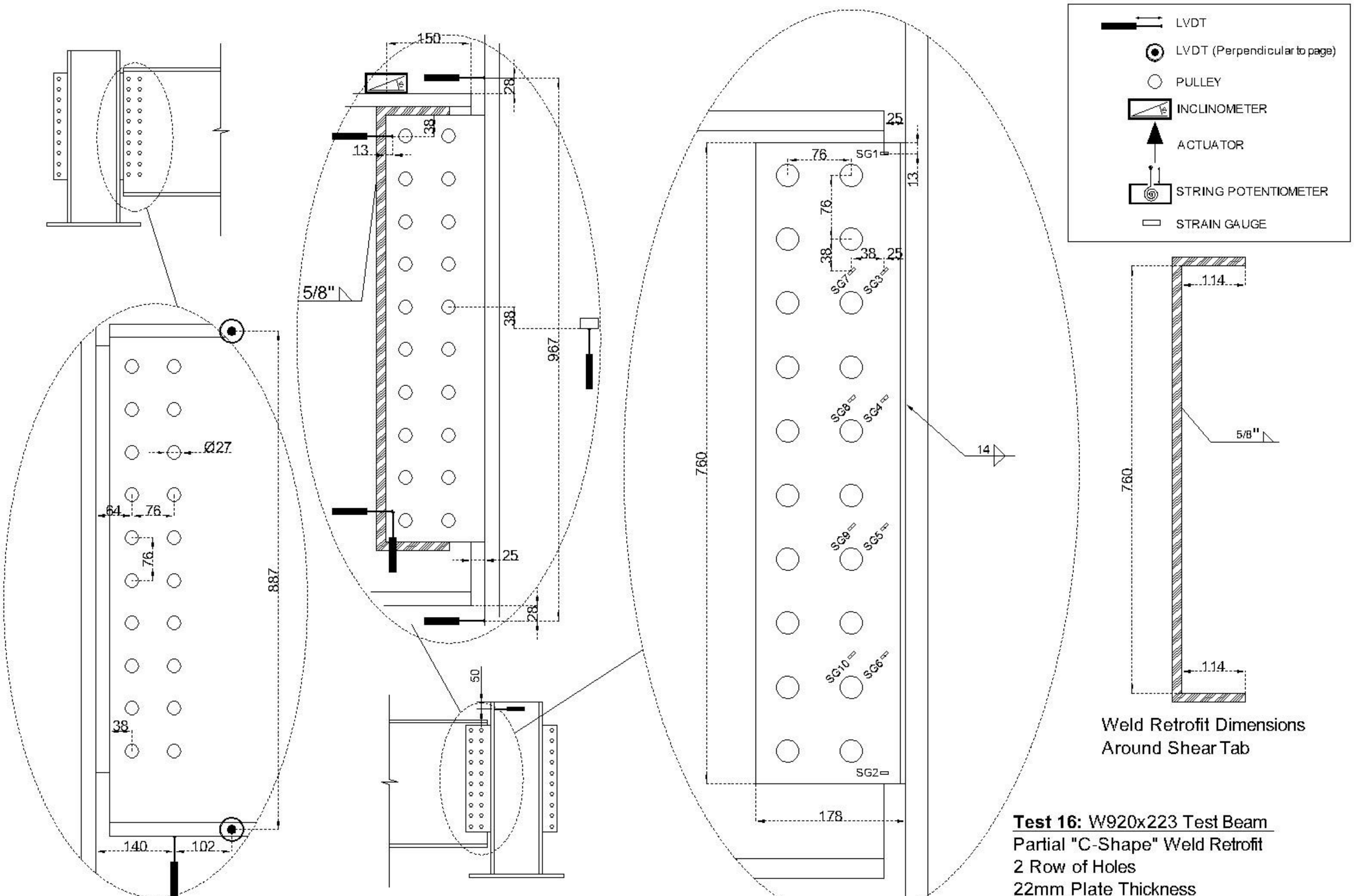

Test 16: W920x223 Test Beam
Partial "C-Shape" Weld Retrofit
2 Row of Holes
22mm Plate Thickness

Test 16: Drawing 2 of 2

APPENDIX B: Sample Calculations

13th Edition AISC Conventional Configuration Method

Sample Design Calculation for Test 1: W310x60 – 1 Row of 3 x ¾" A325 Bolts

CHECK LIMITATIONS:

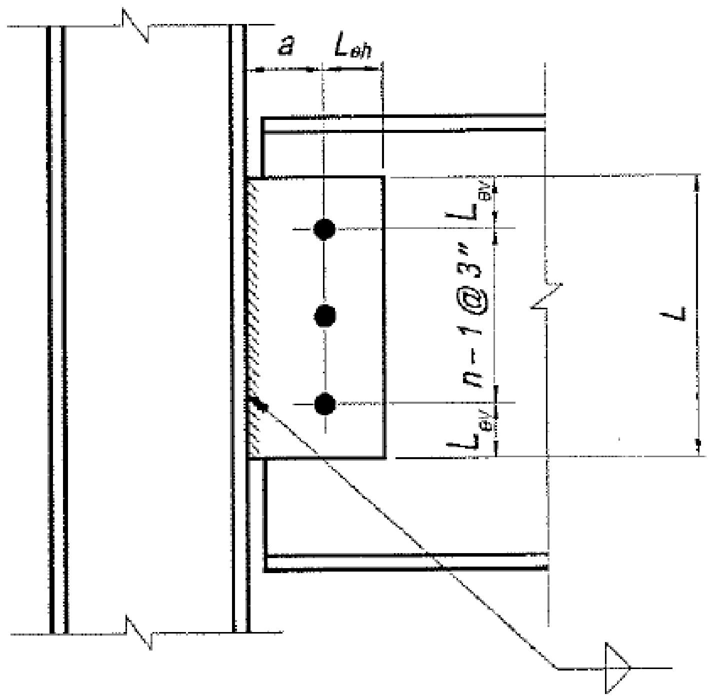

(AISC, 2005)

- ✓ Single vertical row of bolts (1 Row of 3 Bolts)
- ✓ Distance from bolt line to weld line, a, must be less than 3.5'' (a = 2'')
- ✓ STD or SSL holes are used (STD drilled holes are used)
- ✓ Horizontal edge distance, L_{eh}, must be ≥ $2d_b$, for both plate and beam web. L_{eh} is measured from the center of the hole to the edge of the plate or web.
    - L_{eh} = 1.5'' $2d_b$ = 1.5''
- ✓ Vertical edge distance, L_{ev}, must satisfy AISC Specification Table J3.4 requirements
    - L_{ev} = 1.5'' Minimum L_{ev} allowed = 1''
- ✓ Either plate or beam web must satisfy $t \leq d_b/2 + 1/16''$

$t_{plate} = 0.25''$ $d_b/2 + 1/16'' = 0.4375''$

MATERIAL PROPERTIES:

Material Parameters of the Plate			Material Parameters of the Beam		
	ksi	MPa		ksi	MPa
F_{yp} =	50.0	344.7	F_{yp} =	50.0	344.7
F_{up} =	65.0	448.2	F_{up} =	65.0	448.2
E =	29000.0	199948.0	E =	29000.0	199948.0

DESIGN CHECKS: (Note that Φ values are taken as 1.0)

Bolt Shear: Equation J3-1 of AISC Specification

	in.	mm	
d_b =	0.75	19.05	
d_h =	0.81	20.64	
Pitch =	3.00	76.20	
L_{ev} =	1.50	38.10	(Table J3.4 for $L_{ev\text{-}min}$)
L_{eh} =	1.50	38.10	($L_{eh} \geq 2d_b$)

	ksi	MPa
F_{ub} =	120.00	827.37
F_v =	60.00	413.69

Design Shear Resistance per Bolt		
	kips	kN
$\Phi F_v A_b$ =	26.51	117.91
Φ =	1.00	

Design Shear Resistance of Bolt Group		
Number of bolts in row =		3
	kips	kN
$\Phi R_n = \Phi F_v A_b n$ =	**79.52**	**353.73**

Bolt Bearing: Equation J3-6b of AISC Specification

$\Phi Rn = \Phi 1.5 L_c t F_u \leq \Phi 3.0 d_b t F_u$

Plate		
	kips	kN
$\Phi 1.5 L_c t_p F_u$ =	26.66	118.59
$\Phi 3.0 d_b t_p F_u$ =	36.56	162.64
Φ =	1.00	

Beam Web		
	kips	kN
$\Phi 3.0 d_b t_w F_u$ =	43.18	192.09
Φ =	1.00	

	kips	kN
ΦR_n =	**99.79**	**443.87**

For the edge bolt, $\Phi 1.5 L_c t F_u$ was used because there is less steel at the edge of the plate than there is between bolts. For the remaining two bolts, $\Phi 3.0 d_b t F_u$ was used. The sum of these three resistances is 99.79 kips (443.87 kN). See the diagram indicating L_c :

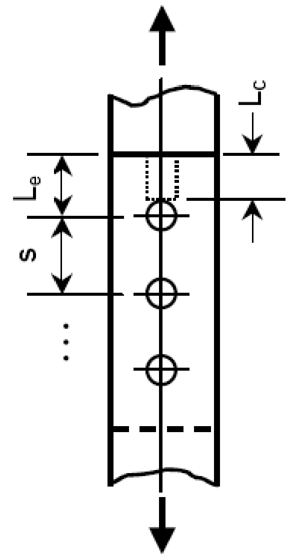

Single Plate Shear Yielding: Equation J4-3 in AISC Specification

Single Plate Block Shear Rupture: Equation J4-5 in AISC Specification

Single Plate Single Plate Shear Rupture: Equation J4-4 in AISC Specification

Plate Material Parameters	ksi	MPa
F_{yp} =	50.0	344.7
F_{up} =	65.0	448.2
E =	29000.0	199948.0

Plate Layout	in.	mm	
t_p =	0.250	6.35	($t_p \leq d_b/2$ + 1/16")
L_{total} =	9.00	228.60	
a =	2.00	50.80	(a ≤ 3½")
L_{gv} =	7.50	190.50	
L_{nv} =	5.63	142.88	
L_{nt} =	1.09	27.78	
L_n =	6.56	166.69	

Block Shear Rupture Check		
Shear Yielding Component	kips	kN
$\Phi 0.6 F_y A_{gv}$ =	56.25	250.21
Φ =	1.00	
Shear Rupture Component	kips	kN
$\Phi 0.6 F_u A_{nv}$ =	54.84	243.96
Φ =	1.00	
Tension Rupture Component	kips	kN
$\Phi F_u A_{nt}$ =	17.77	79.06
Φ =	1.00	

Block Shear Rupture = $\Phi F_u A_{nt} U_{bs}$ + min($\Phi 0.6 F_y A_{gv}$, $\Phi 0.6 F_u A_{nv}$)	kips	kN	U_{bs}
ΦR_n =	**72.62**	**323.02**	1.00

U_{bs} = 1.0 for uniform stress and 0.5 for non-uniform stress

Shear Yielding = $\Phi 0.6 F_y A_{gv}$	kips	kN	Φ
ΦR_n =	**67.50**	**300.25**	1.00

Shear Rupture = $\Phi 0.6 F_u A_n$	kips	kN	Φ
ΦR_n =	**63.98**	**284.62**	1.00

Weld Shear Rupture: Equation J2-4 in AISC Specification

$$\Phi F_w A_w = \Phi 0.6 F_{EXX} 0.707 DL(1.0+0.50\sin^{1.5}\Theta)$$

	in	mm
D =	0.24	6.00
L =	9.00	228.60
Θ (deg.) =	0.00	

	ksi	MPa
F_{EXX} =	70.00	482.63
Φ =	1.00	

	kips	kN
$\Phi R_n = \Phi F_w A_w$	**126.26**	**561.62**

NOTE: See Table J2.4 for minimum allowable weld size

Base Metal Rupture: Equation J4-4 in AISC Specification

$\Phi F_u A_{nv} = \Phi 0.6 F_u A_{nv}$

$A_{nv} = DL$

	kips	kN
ΦR_n =	**82.91**	**368.82**

SUMMARY OF DESIGN CHECKS:

Shown below is a summary of the design checks. In this case, shear rupture through the net section controls.

Summary of Limit States	kips	kN	
Shear Resistance of Bolt Group	79.52	353.73	
Block Shear Rupture	72.62	323.02	
Shear Yielding GROSS SECTION	67.50	300.25	
Shear Rupture NET SECTION	63.98	284.62	CONTROLS
Weld Capacity	126.26	561.62	
Base Metal Capacity	82.91	368.82	
Plate/Web Bearing Capacity	99.79	443.87	

13th Edition AISC Extended Configuration Method

Sample Design Calculation for Test 2: W310x60 – 2 Rows of 3 x ¾" A325 Bolts -

CHECK LIMITATIONS:

- ✓ The use of holes must satisfy AISC Specification Section J3.2 requirements.
  - The distance between the centres of holes must be ≥ 2⅔ d_b.
  - s = 3'' 2⅔ d_b = 2''
- ✓ Horizontal and vertical edge distances must satisfy AISC Specification Table J3.4.

  Minimum edge distances L_{eh} and L_{ev} must be ≥ 1'' when ¾'' bolts are used.

  $L_{eh} = L_{ev} = 1.5''$

DESIGN CHECKS:

Bolt Group Strength

	in.	mm	
d_b =	0.75	19.05	
d_h =	0.81	20.64	
Pitch =	3.00	76.20	
Gage =	3.00	76.20	
L_{ev} =	1.50	38.10	(Table J3.4 for $L_{ev\text{-}min}$)
L_{eh} =	1.50	38.10	(Table J3.4 for $L_{eh\text{-}min}$)

	ksi	MPa
F_{ub} =	120.00	827.37
F_v =	60.00	413.69

	in.	mm
Eccentricity, e_x =	3.50	88.90
Refer to AISC 13th edition:	Table 7-8	for C & C'
C =	3.37	
C' =	15.80	
Strength of the bolt group:	kips	kN
$\Phi R_n = C\Phi r_n$ =	**89.33**	**397.36**

Shear Resistance per Bolt

	kips	kN
$\Phi F_v A_b$ =	26.51	117.91
Φ =	1.00	

Bearing Strength of Bolt

	kips	kN
$\Phi 3.0 F_{up} d_b t_p$ =	57.58	256.12
$\Phi 3.0 F_u d_b t_w$ =	43.18	192.09
Φ =	1.00	

Governing Criterion

	kips	kN
Φr_n =	26.51	117.91
	BOLT SHEAR CONTROLS	

Take eccentricity, *e*, as the distance from the support to the centroid of the bolt group. For this example, e = 3.5''. The shear resistance per bolt is then determined by multiplying the area of the bolt by the allowable shear stress, F_v. Bearing strength is checked in both the shear tab and the beam web. The number of effective bolts in the group is determined from values in the AISC (2005) tables in Chapter 7, obtained via the instantaneous centre of rotation method. The effective number of bolts is then multiplied by the shear resistance of each bolt (or by the bearing capacity if this is found to control the design).

Maximum Plate Thickness:

Determine the maximum allowable plate thickness as follows:

Max t_p such that plate will yield prior to bolt shearing:

$M_{max} = \mathbf{1.25} F_{nv} A_b C'$ $\qquad t_{max} = 6M_{max}/F_y L^2$

	ksi	MPa
F_{nv} =	60.00	413.69
	kip-in	kNm
M_{max} =	523.52	59.15
	in.	mm
t_{max} =	0.78	19.70

where F_v is the shear strength of an individual bolt (Table J3.2 of the AISC Specification), A_b is the area of n individual bolt, *C'* is the coefficient for the moment-only case using the instantaneous centre of rotation at the centroid of the bolt group (Table 7-8, AISC Handbook), F_y is the specified plate yield stress and *d* is the depth of the plate.

t_p = 10 mm This is less than t_{max}, and is therefore acceptable.

Plate Yielding, Plate Shear Rupture, Plate Block Shear Rupture:

In a similar fashion as the conventional method, the designer must check for shear yielding, shear rupture and block shear rupture based on AISC Specification Equations J4-3, J4-4, and J4-5:

Plate Material Parameters	ksi	MPa
F_{yp} =	50.0	344.7
F_{up} =	65.0	448.2
E =	29000.0	199948.0

Block Shear Rupture Check		
Shear Yielding Component	kips	kN
$\Phi 0.6F_yA_{gv}$ =	88.58	394.04
Φ =	1.00	
Shear Rupture Component	kips	kN
$\Phi 0.6F_uA_{nv}$ =	83.97	373.51
Φ =	1.00	
Tension Rupture Component	kips	kN
ΦF_uA_{nt} =	27.99	124.50
Φ =	1.00	

Plate Layout	in.	mm
t_p =	0.394	10.00
L_{total} =	9.00	228.60
a =	2.00	50.80
L_{gv} =	7.50	190.50
L_{nv} =	5.47	138.91
L_{nt} =	1.09	27.78
L_n =	6.56	166.69

Block Shear Rupture = $\Phi F_uA_{nt}U_{bs}$ + min($\Phi 0.6F_yA_{gv}$, ΦF_uA_{nv})

	kips	kN	U_{bs}
ΦR_n =	**97.96**	**435.76**	0.50

U_{bs} = 1.0 for uniform stress and 0.5 for non-uniform stress

Shear Yielding = $\Phi 0.6F_yA_{gv}$

	kips	kN	Φ
ΦR_n =	**106.30**	**472.84**	1.00

Shear Rupture = $\Phi 0.6F_uA_n$

	kips	kN	Φ
ΦR_n =	**100.76**	**448.22**	1.00

Plate Flexure with von-Mises Shear Reduction

The designer must also check the available flexural yielding strength of the plate based on the critical shear stress, F_{cr} (AISC, 2005). The check is $\phi M_n = \phi F_{cr}Z$. Here, $F_{cr} = (F_y^2 - 3f_v^2)^{1/2}$ where F_y is the yield strength of the plate, f_v is the shear stress, and Z is the section modulus of the plate. This can also be seen as finding the applied shear force that renders $\phi F_{cr}Z$ equal to the shear force times the distance from the weld to the bolt line, a. Note that the section modulus $Z = t_pd^2/4$.

Plate Flexure Check = $\Phi M_n = \Phi F_{cr} Z$		
	ksi	MPa
ΦF_{cr} =	22.83	157.40
f_v =	25.68	177.08
Φ =	1.00	
	kips	kN
$V = \Phi R_n$ =	**91.00**	**404.80**
	kip-in	kN-m
$\Phi F_{cr} Z$ =	182.00	20.56
V x a = M =	182.00	20.56

Section Moduli		
	in^3	mm^3
Z_{net} =	5.99	98129
Z =	7.97	130645

Plate Buckling Check

A plate buckling check must also be carried out. This is done by applying the procedure for double-coped beams given in Chapter 9 of the AISC Handbook (2005).

The available buckling stress can be calculated as:

$$F_{cr} = F_y Q$$

where Q is a full reduction factor for slender compression elements, based on the dimensions and yield stress of the single plate. Q decreases as slenderness, λ, of the plate increases. The terms are defined as follows in the following equations:

- $\lambda = (h_o(F_y)^{1/2}) \;/\; [10t_w(475 + 280(h_o/c)^2)^{1/2}]$
- $Q = 1$ when $\lambda \leq 0.7$
- $Q = (1.34 - 0.486\lambda)$ when $0.7 < \lambda \leq 1.41$
- $Q = (1.30 / \lambda^2)$ when $\lambda > 1.41$

where c is defined as the length of plate parallel to the compressive force, h_o is the depth of the plate, t_w is the thickness of the plate, and F_y is the yield stress of the plate.

Local Plate Buckling Check = $\Phi F_{yp}Q = \Phi F_{cr}$		
-	in.	mm
h_o =	9.00	228.60
c =	2.00	50.80
λ =	0.21	
Q =	1.00	
	ksi	MPa
$\Phi F_{yp}Q$ =	50.00	344.74
(V x a)/Z =	50.00	344.72
Φ =	1.00	
	kips	kN
V = R_n =	199.30	886.53

NOTE: Change V until $\Phi F_{yp}Q$ = (V x a)/Z

Summary

Summary of Limit States		
	kips	kN
Shear Resistance of Bolt Group OR Bearing Resistance of Web	89.33	397.36
Block Shear Rupture	97.96	435.76
Shear Yielding	106.30	472.84
Shear Rupture	100.76	448.22
Plate Flexure Check	91.00	404.80
Local Plate Buckling Check	199.30	886.53

In this case, the first predicted failure mode is rupture of the bolt group, followed closely by plate flexural yielding at F_{cr}.

Modified 13th Edition AISC Extended Configuration Method

Sample Design Calculation for Test 2: W310x60 – 2 Rows of 3 x ¾" A325 Bolts

The following method differed only from the 13th Edition AISC Extended Configuration Method (2005) with respect to the strength of the bolts. Instead of taking the shear strength of the bolts to be half of the bolt tensile strength, it was taken as 62% of the bolt tensile strength. In tests published by Kulak et al. (1987), the shear strength of A325 bolts was found to be 0.619 times the tensile strength with a standard deviation of 0.03. Shown directly below is the same bolt group resistance calculation as in the extended configuration for 2 rows of 3 x ¾" A325 Bolts; this time with the modified bolt shear strengths found by Kulak et al. (1987).

	in.	mm	
d_b =	0.75	19.05	
d_h =	0.81	20.64	
Pitch =	3.00	76.20	
Gage =	3.00	76.20	
L_{ev} =	1.50	38.10	(Table J3.4 for $L_{ev\text{-}min}$)
L_{eh} =	1.50	38.10	(Table J3.4 for $L_{eh\text{-}min}$)

	ksi	MPa	
F_{ub} =	120.00	827.37	
*F_v =	74.40	512.97	(0.62 x F_{ub})

	in.	mm
Eccentricity, e_x =	3.50	88.90
Refer to AISC 13th edition:	Table 7-8	for C & C'
C =	3.37	
C' =	15.80	
Strength of the bolt group:	kips	kN
$\Phi R_n = C\Phi r_n$ =	**110.77**	**492.72**

Shear Resistance per Bolt

	kips	kN
$\Phi F_v A_b$ =	32.87	146.21
Φ =	1.00	

Bearing Strength of Bolt

	kips	kN
$\Phi 3.0 F_{up} d_b t_p$ =	57.58	256.12
$\Phi 3.0 F_u d_b t_w$ =	45.26	201.31
Φ =	1.00	

Governing Criterion

	kips	kN
Φr_n =	32.87	146.21
	BOLT SHEAR CONTROLS	

Observe the increase in the predicted strength of the bolt group. It should also be noted that when determining the maximum plate thickness with this modified extended method, the 1.25 factor used to remove the 20% reduction in shear strength of bolts to account for end-loaded bolt groups was omitted. This is done because $0.62F_u$ is already 1.24 times $0.5F_u$.

Max t_p such that plate will yield prior to bolt shearing:		
**$M_{max} = \mathbf{1.0} F_{nv} A_b C'$	$t_{max} = 6M_{max}/F_y L^2$	
	ksi	MPa
F_{nv} =	74.40	512.97
	kip-in	kNm
M_{max} =	519.33	58.67
	in.	mm
t_{max} =	0.77	19.54

Below is the summary table for the modified AISC approach:

<u>**Summary of Limit States**</u>	kips	kN	
Shear Resistance of Bolt Group OR Bearing Resistance of Web	110.77	492.72	
Block Shear Rupture	97.96	435.76	
Shear Yielding	106.30	472.84	
Shear Rupture	100.76	448.22	
Plate Flexure Check	91.00	404.80	<== CONTROLS
Local Plate Buckling Check	199.30	886.53	

In this example, plate flexural yielding is the first predicted failure mode, followed closely by block shear rupture and shear rupture.

CISC 10th Edition Design Method

Sample Design Calculation for Test 1: W310x60 – 1 Row of 3 x ¾" A325 Bolts

This sample calculation is based on the design procedure used to obtain the shear tab connection resistance values as found in Table 3-41. This procedure forces a specific failure mode by ensuring that the plate is at least a certain thickness, *t*. For comparison purposes, additional calculations are presented at the end using a specified thickness and calculating the predicted resistances based on this value of *t*.

Bolt Group Strength

# of bolts, *n**	3	*Must be 2 ≤ *n* ≤ 7
Support Condition**	RIGID	**RIGID or FLEXIBLE

	in.	mm
Bolt Size	0.75	19.05

Distance from support to bolt line, *a*	in.	mm
	2.0	50.80

	ksi	MPa
$F_{u\,BOLT}$	119.7	825.0
$F_{v\,BOLT}$	71.8	495.0
	***Φ =	1

***Φ=0.6 used in Handbook tabulated values, but Φ has since been changed to 0.8.

Eccentricity	in.	mm
e_b =	0	0

RIGID: $e_b = (n-1) - a$

FLEXIBLE: $e_b = a$

	kip	kN
$V_{r\,BOLT}$	31.7	141.1

$V_{r\,BOLT} = 0.6\Phi n m A_b F_u$

Determine bolt group coefficient C, effective number of bolts, from "Eccentric Loads on Bolt Groups" Tables 3-14 (CISC, 2010) or Table 7-7 (AISC, 2005) based on the Instantaneous Centre of Rotation method.

Effective number of bolts in group, *C* =	3

	kip	kN
$V_{r\,BOLT\,GROUP}$ =	**95.2**	**423.3**

Note: For rigid support conditions, the eccentricity, e_b, = (n – 1) – a = 3 – 1 – 2 = 0 so the effective bolt coefficient, *C*, remains 3 and there is no reduction.

Determining Plate Thickness

Use resistance of bolt groups to calculate thickness, *t*, of shear tab plate by S16.1-94, Clause 13.4.4, with $\phi = 0.90$ and L_n being the net length. Note that this Clause no longer exists in the S16 Specifications but is still used to obtain tabular results in the current (2010) CISC Handbook.

Plate Properties	ksi	MPa
F_u	65	448.16
	in.	mm
L	9.0	228.6
L_n	6.56	166.7

$t \geq (V_{r\ BOLT\ GROUP}) / (0.50\phi L_n F_u)$

	in.	mm
$t \geq$	0.496	12.59
	Φ =	1

Check plate thickness for bearing resistance:

$t \geq (V_{r\ BOLT}) / (3\phi_{br} d_b F_u)$

	in.	mm
$t \geq$	0.217	5.51
	****Φ_{br} =	1

Also, t ≥ 6mm when 2 to 5 bolts are used and t ≥ 8mm when 6 or 7 bolts are used. In this case:

t ≥	6	mm

****Φ_{br} = 0.67 is used in the tabulated Handbook values, however Φ_{br} has since been changed to 0.8.

	in.	mm
Minimum Plate thickness, t_{min} =	**0.50**	**12.6**

Weld

The design procedure suggests using a fillet weld ¾ x plate thickness.

The following recommendations are given regarding weld size.

Use weld size = 3/4 Plate Thickness
Use E48XX Fillet Welds.
Use 5 mm fillets on 6 mm (or 1/4") plates.
Use 6 mm fillets on 8 mm (or 5/16") plates.
Use 8 mm fillets on 10 mm (or 3/8") plates.
Use 10 mm fillets on 12 mm (or 1/2") plates.

For Comparison Purposes

Since the CISC Design approach picks plate thickness to force a particular failure method, the 3 limit states will be checked separately using the nominal and actual properties specified and used in the laboratory experiments.

	in.	mm		in.	mm
Nominal Plate Thickness, *t* =	0.25	6.35	Measured Plate Thickness, *t* =	0.247	6.27

Plate Fracture Along Net Area

	kip	kN		kip	kN
$V_r = 0.5\phi L_n t F_u$ =	**53.32**	**237.2**	$V_r = 0.5\phi L_n t F_u$ =	**55.48**	**246.8**
				ksi	MPa
			$F_{u\ ACTUAL}$ =	68.5	472.0

Plate Bearing Strength

	kip	kN		kip	kN
$V_r = 3\phi_{br} d_b n F_u t$ =	**109.69**	**487.9**	$V_r = 3\phi_{br} d_b n F_u t$ =	**114.14**	**507.7**

Bolt Group Strength

	kip	kN		kip	kN
$V_r = C(V_{r\ BOLT})$ =	**95.15**	**423.3**	$V_r = C(V_{r\ BOLT})$ =	**95.15**	**423.3**

APPENDIX C: Modified Method: Bolted Shear Tab Predictions

The following spreadsheets provide the predicted resistances of connections based upon actual, rather than nominal, material properties and dimensions.

Test 1: W310x60 – 1 Row of 3 x ¾'' A325 Bolts, t_p = ¼''

Bolt Parameters

Bolts / row =	3	
# of rows =	1	

Holes =	DRILLED	(Input PUNCHED or DRILLED)
Set Φ = 1.00?	yes	(Input YES or NO)
Bolt Type	A325	(Input A325 or A490)
Thread condition	excluded	(Input INCLUDED or EXCLUDED from plane)
Shear planes	1	(Input 1 or 2)

	in.	mm	
d_b =	0.75	19.05	
d_h =	0.81	20.64	
Pitch =	3.00	76.20	
Gage =	3.00	76.20	
L_{ev} =	1.50	38.10	(Table J3.4 for $L_{ev\text{-}min}$)
L_{eh} =	1.50	38.10	(Table J3.4 for $L_{eh\text{-}min}$)

	ksi	MPa
F_{ub} =	120.00	827.37
*F_v =	74.40	512.97

	in.	mm
Eccentricity, e_x =	2.00	50.80
Refer to AISC 13th edition:	Table 7-7	for C & C'
C =	2.23	
C' =	5.89	
Strength of the bolt group:	kips	kN
$\Phi R_n = C\Phi r_n$ =	**73.30**	**326.04**

Shear Resistance per Bolt

	kips	kN
$\Phi F_v A_b$ =	32.87	146.21
Φ =	1.00	

Bearing Strength of Bolt

	kips	kN
$\Phi 3.0 F_{up} d_b t_p$ =	38.08	169.40
$\Phi 3.0 F_u d_b t_w$ =	48.95	217.73
Φ =	1.00	

Governing Criterion

	kips	kN
Φr_n =	32.87	146.21
	BOLT SHEAR CONTROLS	

Beam Parameters

Material Parameters	ksi	MPa
F_{yp} =	55.1	380.0
F_{up} =	70.3	484.7
E =	29877.8	206000.0

Web Thickness	in	mm
t_w =	0.31	7.86

Plate Parameters

Material Parameters	ksi	MPa
F_{yp} =	58.8	405.7
F_{up} =	68.5	472.0
E =	28717.5	198000.0

Plate Layout	in.	mm	
t_p =	0.247	6.28	($t_p \leq d_b/2 +$ 1/16")
L_{total} =	9.00	228.60	
a =	2.00	50.80	(a ≤ 3½")
L_{gv} =	7.50	190.50	
L_{nv} =	5.47	138.91	
L_{nt} =	1.09	27.78	
L_n =	6.56	166.69	

Block Shear Rupture Check		
Shear Yielding Component	kips	kN
$\Phi 0.6F_yA_{gv}$ =	65.47	291.21
Φ =	1.00	
Shear Rupture Component	kips	kN
$\Phi 0.6F_uA_{nv}$ =	55.54	247.04
Φ =	1.00	
Tension Rupture Component	kips	kN
ΦF_uA_{nt} =	18.51	82.35
Φ =	1.00	

Block Shear Rupture = $\Phi F_uA_{nt}U_{bs}$ + min($\Phi 0.6F_yA_{gv}$, ΦF_uA_{nv})	kips	kN	U_{bs}
ΦR_n =	**74.05**	**329.39**	1.00

U_{bs} = 1.0 for uniform stress and 0.5 for non-uniform stress

Shear Yielding = $\Phi 0.6F_yA_{gv}$	kips	kN	Φ
ΦR_n =	**78.56**	**349.46**	1.00

Shear Rupture = $\Phi 0.6F_uA_n$	kips	kN	Φ
ΦR_n =	**66.65**	**296.45**	1.00

Max t_p s.t. plate will yield prior to bolt shearing:		
M_{max} = **1.0$F_{nv}A_bC'$		$t_{max} = 6M_{max}/F_yL^2$
	ksi	MPa
F_{nv} =	74.40	512.97
	kip-in	kNm
M_{max} =	193.60	21.87
	in.	mm

Section Moduli	in^3	mm^3
Z_{net} =	3.76	61625
Z =	5.01	82045

t_{max} =	0.24	6.19

Plate Flexure Check = $\Phi M_n = \Phi F_{cr} Z$

	ksi	MPa
ΦF_{cr} =	26.87	185.24
f_v =	30.22	208.39
Φ =	1.00	
	kips	kN
$V = \Phi R_n$ =	**67.26**	**299.17**
	kip-in	kN-m
$\Phi F_{cr} Z$ =	134.51	15.20
V x a = M =	134.51	15.20

Local Plate Buckling Check = $\Phi F_{yp} Q = \Phi F_{cr}$

-	in.	mm
h_o =	9.00	228.60
c =	2.00	50.80
λ =	0.36	
Q =	1.00	
	ksi	MPa
$\Phi F_{yp} Q$ =	58.84	405.70
(V x a)/Z =	58.84	405.69
Φ =	1.00	
	kips	kN
$V = R_n$ =	147.30	655.21

NOTE: Change V until $\Phi F_{yp} Q$ = (V x a)/Z = $M_{applied}$ (or use 'Goal Seek')

Summary of Limit States

	kips	kN	
Shear Resistance of Bolt Group OR Bearing Resistance of Web	73.30	326.04	
Block Shear Rupture	74.05	329.39	
Shear Yielding	78.56	349.46	
Shear Rupture	66.65	296.45	<== CONTROLS
Plate Flexure Check	67.26	299.17	
Local Plate Buckling Check	147.30	655.21	

Test 2: W310x60 – 2 Rows of 3 x ¾" A325 Bolts, t_p = 10mm

Bolt Parameters

Holes =	DRILLED	(Input PUNCHED or DRILLED)
Set Φ = 1.00?	yes	(Input YES or NO)
Bolt Type	A325	(Input A325 or A490)
Thread condition	excluded	(Input INCLUDED or EXCLUDED from plane)
Shear planes	1	(Input 1 or 2)

Bolts / row =	3
# of rows =	2

	in.	mm	
d_b =	0.75	19.05	
d_h =	0.81	20.64	
Pitch =	3.00	76.20	
Gage =	3.00	76.20	
L_{ev} =	1.50	38.10	(Table J3.4 for $L_{ev\text{-}min}$)
L_{eh} =	1.50	38.10	(Table J3.4 for $L_{eh\text{-}min}$)

	ksi	MPa
F_{ub} =	120.00	827.37
$*F_v$ =	74.40	512.97

	in.	mm
Eccentricity, e_x =	3.50	88.90
Refer to AISC 13th edition:	Table 7-8	for C & C'
C =	3.37	
C' =	15.80	
Strength of the bolt group:	kips	kN
$\Phi R_n = C\Phi r_n$ =	**110.77**	**492.72**

Shear Resistance per Bolt

	kips	kN
$\Phi F_v A_b$ =	32.87	146.21
Φ =	1.00	

Bearing Strength of Bolt

	kips	kN
$\Phi 3.0 F_{up} d_b t_p$ =	64.51	286.96
$\Phi 3.0 F_u d_b t_w$ =	48.95	217.73
Φ =	1.00	

Governing Criterion

	kips	kN
Φr_n =	32.87	146.21
	BOLT SHEAR CONTROLS	

Beam Parameters

Material Parameters

	ksi	MPa
F_{yp} =	55.1	380.0
F_{up} =	70.3	484.7
E =	29877.8	206000.0

Web Thickness

	in	mm
t_w =	0.31	7.86

Plate Parameters

Material Parameters

	ksi	MPa
F_{yp} =	52.9	365.0
F_{up} =	73.6	507.7
E =	29877.8	206000.0

Plate Layout

	in.	mm	
t_p =	0.389	9.89	
L_{total} =	9.00	228.60	
a =	2.00	50.80	(a ≤ 3½")
L_{gv} =	7.50	190.50	
L_{nv} =	5.47	138.91	
L_{nt} =	1.09	27.78	
L_n =	6.56	166.69	

Block Shear Rupture Check

Shear Yielding Component

	kips	kN
$\Phi 0.6F_yA_{gv}$ =	92.76	412.61
Φ =	1.00	

Shear Rupture Component

	kips	kN
$\Phi 0.6F_uA_{nv}$ =	94.08	418.48
Φ =	1.00	

Tension Rupture Component

	kips	kN
ΦF_uA_{nt} =	31.36	139.49
Φ =	1.00	

Block Shear Rupture = $\Phi F_uA_{nt}U_{bs}$ + min($\Phi 0.6F_yA_{gv}$, ΦF_uA_{nv})

	kips	kN	U_{bs}
ΦR_n =	**108.44**	**482.35**	0.50

U_{bs} = 1.0 for uniform stress and 0.5 for non-uniform stress

Shear Yielding = $\Phi 0.6F_yA_{gv}$

	kips	kN	Φ
ΦR_n =	**111.31**	**495.13**	1.00

Shear Rupture = $\Phi 0.6F_uA_n$

	kips	kN	Φ
ΦR_n =	**112.89**	**502.18**	1.00

Max t_p s.t. plate will yield prior to bolt shearing:

M_{max} = **1.0$F_{nv}A_bC'$ $\quad t_{max} = 6M_{max}/F_yL^2$

	ksi	MPa
F_{nv} =	74.40	512.97
	kip-in	kNm
M_{max} =	519.33	58.67
	in.	mm
t_{max} =	0.73	18.46

Section Moduli

	in^3	mm^3
Z_{net} =	5.92	97049
Z =	7.88	129208

Plate Flexure Check = $\Phi M_n = \Phi F_{cr}Z$		
	ksi	MPa
ΦF_{cr} =	24.17	166.65
f_v =	27.19	187.48
Φ =	1.00	
	kips	kN
$V = \Phi R_n$ =	**95.29**	**423.88**
	kip-in	kN-m
$\Phi F_{cr}Z$ =	190.58	21.53
V x a = M =	190.58	21.53

Local Plate Buckling Check = $\Phi F_{yp}Q = \Phi F_{cr}$		
-	in.	mm
h_o =	9.00	228.60
c =	2.00	50.80
λ =	0.21	
Q =	1.00	
	ksi	MPa
$\Phi F_{yp}Q$ =	52.94	365.00
(V x a)/Z =	52.94	365.01
Φ =	1.00	
	kips	kN
$V = R_n$ =	208.71	928.38

NOTE: Change V until $\Phi F_{yp}Q$ = (V x a)/Z = $M_{applied}$ (or use 'Goal Seek')

Summary of Limit States			
	kips	kN	
Shear Resistance of Bolt Group OR Bearing Resistance of Web	110.77	492.72	
Block Shear Rupture	108.44	482.35	
Shear Yielding	111.31	495.13	
Shear Rupture	112.89	502.18	
Plate Flexure Check	95.29	423.88	<== CONTROLS
Local Plate Buckling Check	208.71	928.38	

Test 7: W610x140 – 1 Row of 6 x 7/8'' A325 Bolts, t_p = 8mm

Bolt Parameters

Holes =	DRILLED	(Input PUNCHED or DRILLED)
Set Φ = 1.00?	yes	(Input YES or NO)
Bolt Type	A325	(Input A325 or A490)
Thread condition	excluded	(Input INCLUDED or EXCLUDED from plane)
Shear planes	1	(Input 1 or 2)

Bolts / row =	6
# of rows =	1

	in.	mm	
d_b =	0.88	22.23	
d_h =	0.94	23.81	
Pitch =	3.00	76.20	
Gage =	3.00	76.20	
L_{ev} =	1.50	38.10	(Table J3.4 for $L_{ev\text{-}min}$)
L_{eh} =	1.50	38.10	(Table J3.4 for $L_{eh\text{-}min}$)

	ksi	MPa
F_{ub} =	120.00	827.37
*F_v =	74.40	512.97

Shear Resistance per Bolt

	kips	kN
$\Phi F_v A_b$ =	44.74	199.01
Φ =	1.00	

Bearing Strength of Bolt

	kips	kN
$\Phi 3.0 F_{up} d_b t_p$ =	58.54	260.38
$\Phi 3.0 F_u d_b t_w$ =	67.19	298.87
Φ =	1.00	

Governing Criterion

	kips	kN
Φr_n =	44.74	199.01
	BOLT SHEAR CONTROLS	

	in.	mm
Eccentricity, e_x =	2.50	63.50
Refer to AISC 13th edition:	Table 7-7	for C & C'
C =	6.27	
C' =	25.10	
Strength of the bolt group:	kips	kN
$\Phi R_n = C\Phi r_n$ =	**280.51**	**1247.77**

Beam Parameters

Material Parameters

	ksi	MPa
F_{yp} =	62.9	433.5
F_{up} =	82.7	570.3
E =	29877.8	206000.0

Web Thickness

	in	mm
t_w =	0.31	7.86

Plate Parameters

Material Parameters	ksi	MPa
F_{yp} =	53.8	370.7
F_{up} =	71.6	493.7
E =	29877.8	206000.0

Plate Layout	in.	mm	
t_p =	0.311	7.91	($t_p \leq d_b/2 +$ 1/16")
L_{total} =	18.00	457.20	
a =	2.50	63.50	(a ≤ 3½")
L_{gv} =	16.50	419.10	
L_{nv} =	11.34	288.13	
L_{nt} =	1.03	26.19	
L_n =	12.38	314.33	

Block Shear Rupture Check

Shear Yielding Component	kips	kN
$\Phi 0.6F_yA_{gv}$ =	165.76	737.34
Φ =	1.00	

Shear Rupture Component	kips	kN
$\Phi 0.6F_uA_{nv}$ =	151.77	675.12
Φ =	1.00	

Tension Rupture Component	kips	kN
ΦF_uA_{nt} =	23.00	102.29
Φ =	1.00	

Block Shear Rupture = $\Phi F_uA_{nt}U_{bs}$ + min($\Phi 0.6F_yA_{gv}$, ΦF_uA_{nv})

	kips	kN	U_{bs}
ΦR_n =	**174.77**	**777.41**	1.00

U_{bs} = 1.0 for uniform stress and 0.5 for non-uniform stress

Shear Yielding = $\Phi 0.6F_yA_{gv}$

	kips	kN	Φ
ΦR_n =	**180.83**	**804.37**	1.00

Shear Rupture = $\Phi 0.6F_uA_n$

	kips	kN	Φ
ΦR_n =	**165.57**	**736.50**	1.00

Max t_p s.t. plate will yield prior to bolt shearing:

M_{max} = **1.0$F_{nv}A_bC'$ $\qquad$ $t_{max} = 6M_{max}/F_yL^2$

	ksi	MPa
F_{nv} =	74.40	512.97
	kip-in	kNm
M_{max} =	1122.93	126.87
	in.	mm
t_{max} =	0.39	9.82

Section Moduli	in^3	mm^3
Z_{net} =	17.34	284185
Z =	25.22	413360

Plate Flexure Check = $\Phi M_n = \Phi F_{cr}Z$		
	ksi	MPa
ΦF_{cr} =	16.42	113.22
f_v =	29.56	203.80
Φ =	1.00	
	kips	kN
$V = \Phi R_n$ =	**165.69**	**737.02**
	kip-in	kN-m
$\Phi F_{cr}Z$ =	414.22	46.80
V x a = M =	414.22	46.80

Local Plate Buckling Check = $\Phi F_{yp}Q = \Phi F_{cr}$		
-	in.	mm
h_o =	18.00	457.20
c =	2.50	63.50
λ =	0.35	
Q =	1.00	
	ksi	MPa
$\Phi F_{yp}Q$ =	53.77	370.70
(V x a)/Z =	53.77	370.73
Φ =	1.00	
	kips	kN
$V = R_n$ =	542.54	2413.32

NOTE: Change V until $\Phi F_{yp}Q$ = (V x a)/Z = $M_{applied}$ (or use 'Goal Seek')

Summary of Limit States	kips	kN	
Shear Resistance of Bolt Group OR Bearing Resistance of Web	280.51	1247.77	
Block Shear Rupture	174.77	777.41	
Shear Yielding	180.83	804.37	
Shear Rupture	165.57	736.50	<== CONTROLS
Plate Flexure Check	165.69	737.02	
Local Plate Buckling Check	542.54	2413.32	

Test 8: W610x140 – 2 Rows of 6 x 7/8'' A325 Bolts, t_p = 16mm

Holes =	DRILLED	(Input PUNCHED or DRILLED)
Set Φ = 1.00?	yes	(Input YES or NO)
Bolt Type	A325	(Input A325 or A490)
Thread condition	excluded	(Input INCLUDED or EXCLUDED from plane)
Shear planes	1	(Input 1 or 2)

Bolt Parameters

Bolts / row =	6
# of rows =	2

	in.	mm	
d_b =	0.88	22.23	
d_h =	0.94	23.81	
Pitch =	3.00	76.20	
Gage =	3.00	76.20	
L_{ev} =	1.50	38.10	(Table J3.4 for $L_{ev\text{-}min}$)
L_{eh} =	1.50	38.10	(Table J3.4 for $L_{eh\text{-}min}$)

Shear Resistance per Bolt

	kips	kN
$\Phi F_v A_b$ =	44.74	199.01
Φ =	1.00	

Bearing Strength of Bolt

	kips	kN
$\Phi 3.0 F_{up} d_b t_p$ =	123.62	549.88
$\Phi 3.0 F_u d_b t_w$ =	111.81	497.36
Φ =	1.00	

	ksi	MPa
F_{ub} =	120.00	827.37
$*F_v$ =	74.40	512.97

Governing Criterion

	kips	kN
Φr_n =	44.74	199.01
	BOLT SHEAR CONTROLS	

	in.	mm
Eccentricity, e_x =	4.00	101.60
Refer to AISC 13th edition:	Table 7-8	for C & C'
C =	8.93	
C' =	54.20	
Strength of the bolt group:	kips	kN
$\Phi R_n = C\Phi r_n$ =	**399.51**	**1777.12**

Beam Parameters

Material Parameters

	ksi	MPa
F_{yp} =	62.9	433.5
F_{up} =	82.7	570.3
E =	29877.8	206000.0

Web Thickness

	in	mm
t_w =	0.51	13.08

Plate Parameters

Material Parameters

	ksi	MPa
F_{yp} =	54.1	373.3
F_{up} =	76.0	524.3
E =	30022.8	207000.0

Block Shear Rupture Check

Shear Yielding Component

	kips	kN
$\Phi 0.6F_yA_{gv}$ =	331.95	1476.58
Φ =	1.00	

Shear Rupture Component

	kips	kN
$\Phi 0.6F_uA_{nv}$ =	320.53	1425.77
Φ =	1.00	

Tension Rupture Component

	kips	kN
ΦF_uA_{nt} =	48.56	216.03
Φ =	1.00	

Max t_p s.t. plate will yield prior to bolt shearing:

M_{max} = **1.0$F_{nv}A_bC'$ $t_{max} = 6M_{max}/F_yL^2$

	ksi	MPa
F_{nv} =	74.40	512.97
	kip-in	**kNm**
M_{max} =	2424.81	273.96
	in.	**mm**
t_{max} =	0.83	21.07

Plate Layout

	in.	mm	
t_p =	0.619	15.73	
L_{total} =	18.00	457.20	
a =	2.50	63.50	(a ≤ 3½")
L_{gv} =	16.50	419.10	
L_{nv} =	11.34	288.13	
L_{nt} =	1.03	26.19	
L_n =	12.38	314.33	

Block Shear Rupture = $\Phi F_uA_{nt}U_{bs}$ + min($\Phi 0.6F_yA_{gv}$, ΦF_uA_{nv})

	kips	kN	U_{bs}
ΦR_n =	**344.81**	**1533.79**	0.50

U_{bs} = 1.0 for uniform stress and 0.5 for non-uniform stress

Shear Yielding = $\Phi 0.6F_yA_{gv}$

	kips	kN	Φ
ΦR_n =	**362.12**	**1610.81**	1.00

Shear Rupture = $\Phi 0.6F_uA_n$

	kips	kN	Φ
ΦR_n =	**349.67**	**1555.39**	1.00

Section Moduli

	in^3	mm^3
Z_{net} =	34.49	565137
Z =	50.16	822018

Plate Flexure Check = $\Phi M_n = \Phi F_{cr} Z$		
	ksi	MPa
ΦF_{cr} =	16.54	114.01
f_v =	29.77	205.23
Φ =	1.00	
	kips	kN
$V = \Phi R_n$ =	**331.80**	**1475.94**
	kip-in	kN-m
$\Phi F_{cr} Z$ =	829.51	93.72
V x a = M =	829.51	93.72

Local Plate Buckling Check = $\Phi F_{yp} Q = \Phi F_{cr}$		
-	in.	mm
h_o =	18.00	457.20
c =	2.50	63.50
λ =	0.17	
Q =	1.00	
	ksi	MPa
$\Phi F_{yp} Q$ =	54.14	373.30
(V x a)/Z =	54.14	373.31
Φ =	1.00	
	kips	kN
$V = R_n$ =	1086.40	4832.55

NOTE: Change V until $\Phi F_{yp} Q$ = (V x a)/Z = $M_{applied}$ (or use 'Goal Seek')

Summary of Limit States	kips	kN	
Shear Resistance of Bolt Group OR Bearing Resistance of Web	399.51	1777.12	
Block Shear Rupture	344.81	1533.79	
Shear Yielding	362.12	1610.81	
Shear Rupture	349.67	1555.39	
Plate Flexure Check	331.80	1475.94	<== CONTROLS
Local Plate Buckling Check	1086.40	4832.55	

Test 13: W920x223 – 1 Row of 10 x 1'' A325 Bolts, t_p = 10mm

Holes =	DRILLED	(Input PUNCHED or DRILLED)
Set Φ = 1.00?	yes	(Input YES or NO)
Bolt Type	A325	(Input A325 or A490)
Thread condition	excluded	(Input INCLUDED or EXCLUDED from plane)
Shear planes	1	(Input 1 or 2)

Bolt Parameters

Bolts / row =	10
# of rows =	1

	in.	mm	
d_b =	1.00	25.40	
d_h =	1.06	26.99	
Pitch =	3.00	76.20	
Gage =	3.00	76.20	
L_{ev} =	1.50	38.10	(Table J3.4 for L_{ev-min})
L_{eh} =	1.50	38.10	(Table J3.4 for L_{eh-min})

	ksi	MPa
F_{ub} =	120.00	827.37
*F_v =	74.40	512.97

Shear Resistance per Bolt

	kips	kN
$\Phi F_v A_b$ =	58.43	259.93
Φ =	1.00	

Bearing Strength of Bolt

	kips	kN
$\Phi 3.0 F_{up} d_b t_p$ =	88.83	395.12
$\Phi 3.0 F_u d_b t_w$ =	135.05	600.71
Φ =	1.00	

Governing Criterion

	kips	kN
Φr_n =	58.43	259.93
	BOLT SHEAR CONTROLS	

	in.	mm
Eccentricity, e_x =	2.50	63.50
Refer to AISC 13th edition:	Table 7-7	for C & C'
C =	9.37	
C' =	69.20	
Strength of the bolt group:	kips	kN
$\Phi R_n = C\Phi r_n$ =	**547.52**	**2435.50**

Beam Parameters

Material Parameters

	ksi	MPa
F_{yp} =	59.1	407.7
F_{up} =	75.2	518.3
E =	29442.7	203000.0

Web Thickness

	in	mm
t_w =	0.60	15.21

Plate Parameters

Material Parameters

	ksi	MPa
F_{yp} =	54.1	373.3
F_{up} =	76.0	524.3
E =	30022.8	207000.0

Block Shear Rupture Check

Shear Yielding Component

	kips	kN
$\Phi 0.6F_yA_{gv}$ =	360.49	1603.56
Φ =	1.00	

Shear Rupture Component

	kips	kN
$\Phi 0.6F_uA_{nv}$ =	326.99	1454.54
Φ =	1.00	

Tension Rupture Component

	kips	kN
ΦF_uA_{nt} =	28.68	127.59
Φ =	1.00	

Max t_p s.t. plate will yield prior to bolt shearing:

M_{max} = **1.0$F_{nv}A_bC'$ $\quad t_{max} = 6M_{max}/F_yL^2$

	ksi	MPa
F_{nv} =	74.40	512.97
	kip-in	kNm
M_{max} =	4043.61	456.85
	in.	mm
t_{max} =	0.50	12.65

Plate Layout

	in.	mm	
t_p =	0.389	9.89	($t_p \leq d_b/2$ + 1/16")
L_{total} =	30.00	762.00	
a =	2.50	63.50	(a ≤ 3½")
L_{gv} =	28.50	723.90	
L_{nv} =	18.41	467.52	
L_{nt} =	0.97	24.61	
L_n =	19.38	492.13	

Block Shear Rupture = $\Phi F_uA_{nt}U_{bs}$ + min($\Phi 0.6F_yA_{gv}$, ΦF_uA_{nv})

	kips	kN	U_{bs}
ΦR_n =	**355.68**	**1582.13**	1.00

U_{bs} = 1.0 for uniform stress and 0.5 for non-uniform stress

Shear Yielding = $\Phi 0.6F_yA_{gv}$

	kips	kN	Φ
ΦR_n =	**379.47**	**1687.95**	1.00

Shear Rupture = $\Phi 0.6F_uA_n$

	kips	kN	Φ
ΦR_n =	**344.20**	**1531.10**	1.00

Section Moduli

	in^3	mm^3
Z_{net} =	56.58	927186
Z =	87.61	1435642

Plate Flexure Check = $\Phi M_n = \Phi F_{cr} Z$		
	ksi	MPa
ΦF_{cr} =	10.23	70.55
f_v =	30.70	211.64
Φ =	1.00	
	kips	kN
$V = \Phi R_n$ =	**358.56**	**1594.97**
	kip-in	kN-m
$\Phi F_{cr} Z$ =	896.41	101.28
V x a = M =	896.41	101.28

Local Plate Buckling Check = $\Phi F_{yp} Q = \Phi F_{cr}$		
-	in.	mm
h_o =	30.00	762.00
c =	2.50	63.50
λ =	0.28	
Q =	1.00	
	ksi	MPa
$\Phi F_{yp} Q$ =	54.14	373.30
(V x a)/Z =	54.14	373.28
Φ =	1.00	
	kips	kN
$V = R_n$ =	1897.24	8439.37

NOTE: Change V until $\Phi F_{yp} Q$ = (V x a)/Z = $M_{applied}$ (or use 'Goal Seek')

Summary of Limit States	kips	kN	
Shear Resistance of Bolt Group OR Bearing Resistance of Web	547.52	2435.50	
Block Shear Rupture	355.68	1582.13	
Shear Yielding	379.47	1687.95	
Shear Rupture	344.20	1531.10	<== CONTROLS
Plate Flexure Check	358.56	1594.97	
Local Plate Buckling Check	1897.24	8439.37	

Test 15: W920x223 – 2 Rows of 10 x 1'' A325 Bolts, t_p = 22mm

Bolt Parameters

Bolts / row =	10	
# of rows =	2	

Holes =	DRILLED	(Input PUNCHED or DRILLED)
Set Φ = 1.00?	yes	(Input YES or NO)
Bolt Type	A325	(Input A325 or A490)
Thread condition	excluded	(Input INCLUDED or EXCLUDED from plane)
Shear planes	1	(Input 1 or 2)

	in.	mm	
d_b =	1.00	25.40	
d_h =	1.06	26.99	
Pitch =	3.00	76.20	
Gage =	3.00	76.20	
L_{ev} =	1.50	38.10	(Table J3.4 for $L_{ev\text{-}min}$)
L_{eh} =	1.50	38.10	(Table J3.4 for $L_{eh\text{-}min}$)

	ksi	MPa
F_{ub} =	120.00	827.37
$^*F_v$ =	74.40	512.97

	in.	mm
Eccentricity, e_x =	4.00	101.60
Refer to AISC 13th edition:	Table 7-8	for C & C'
C =	17.50	
C' =	143.00	
Strength of the bolt group:	kips	kN
$\Phi R_n = C\Phi r_n$ =	**1022.59**	**4548.70**

Shear Resistance per Bolt

	kips	kN
$\Phi F_v A_b$ =	58.43	259.93
Φ =	1.00	

Bearing Strength of Bolt

	kips	kN
$\Phi 3.0 F_{up} d_b t_p$ =	205.66	914.83
$\Phi 3.0 F_u d_b t_w$ =	135.05	600.71
Φ =	1.00	

Governing Criterion

	kips	kN
Φr_n =	58.43	259.93
	BOLT SHEAR CONTROLS	

Beam Parameters

Material Parameters

	ksi	MPa
F_{yp} =	59.1	407.7
F_{up} =	75.2	518.3
E =	29442.7	203000.0

Web Thickness

	in	mm
t_w =	0.60	15.21

Plate Parameters

Material Parameters

	ksi	MPa
F_{yp} =	56.3	388.3
F_{up} =	79.4	547.7
E =	30022.8	207000.0

Block Shear Rupture Check

Shear Yielding Component

	kips	kN
$\Phi 0.6F_yA_{gv}$ =	831.10	3696.90
Φ =	1.00	

Shear Rupture Component

	kips	kN
$\Phi 0.6F_uA_{nv}$ =	757.09	3367.70
Φ =	1.00	

Tension Rupture Component

	kips	kN
ΦF_uA_{nt} =	66.41	295.41
Φ =	1.00	

Max t_p s.t. plate will yield prior to bolt shearing:

M_{max} = **1.0$F_{nv}A_bC'$ $\quad$ $t_{max} = 6M_{max}/F_yL^2$

	ksi	MPa
F_{nv} =	74.40	512.97
	kip-in	kNm
M_{max} =	8356.01	944.06
	in.	mm
t_{max} =	0.99	25.12

Plate Layout

	in.	mm	
t_p =	0.863	21.92	
L_{total} =	30.00	762.00	
a =	2.50	63.50	(a ≤ 3½")
L_{gv} =	28.50	723.90	
L_{nv} =	18.41	467.52	
L_{nt} =	0.97	24.61	
L_n =	19.38	492.13	

Block Shear Rupture = $\Phi F_uA_{nt}U_{bs}$ + min($\Phi 0.6F_yA_{gv}$, ΦF_uA_{nv})

	kips	kN	U_{bs}
ΦR_n =	**790.30**	**3515.41**	0.50

U_{bs} = 1.0 for uniform stress and 0.5 for non-uniform stress

Shear Yielding = $\Phi 0.6F_yA_{gv}$

	kips	kN	Φ
ΦR_n =	**874.84**	**3891.47**	1.00

Shear Rupture = $\Phi 0.6F_uA_n$

	kips	kN	Φ
ΦR_n =	**796.94**	**3544.95**	1.00

Section Moduli

	in^3	mm^3
Z_{net} =	125.40	2054996
Z =	194.17	3181929

Plate Flexure Check = $\Phi M_n = \Phi F_{cr} Z$		
	ksi	MPa
ΦF_{cr} =	10.64	73.38
f_v =	31.93	220.15
Φ =	1.00	
	kips	kN
$V = \Phi R_n$ =	**826.64**	**3677.10**
	kip-in	kN-m
$\Phi F_{cr} Z$ =	2066.61	233.49
V x a = M =	2066.61	233.49

Local Plate Buckling Check = $\Phi F_{yp} Q = \Phi F_{cr}$		
-	in.	mm
h_o =	30.00	762.00
c =	2.50	63.50
λ =	0.13	
Q =	1.00	
	ksi	MPa
$\Phi F_{yp} Q$ =	56.32	388.30
(V x a)/Z =	56.32	388.31
Φ =	1.00	
	kips	kN
$V = R_n$ =	4374.33	19458.01

NOTE: Change V until $\Phi F_{yp} Q$ = (V x a)/Z = $M_{applied}$ (or use 'Goal Seek')

Summary of Limit States			
	kips	kN	
Shear Resistance of Bolt Group OR Bearing Resistance of Web	1022.59	4548.70	
Block Shear Rupture	790.30	3515.41	<== CONTROLS
Shear Yielding	874.84	3891.47	
Shear Rupture	796.94	3544.95	
Combined Stress Check	826.64	3677.10	
Local Plate Buckling Check	4374.33	19458.01	

APPENDIX D: Test Result Photos and Selected Data

Test 1: Single Row of 3 Bolts

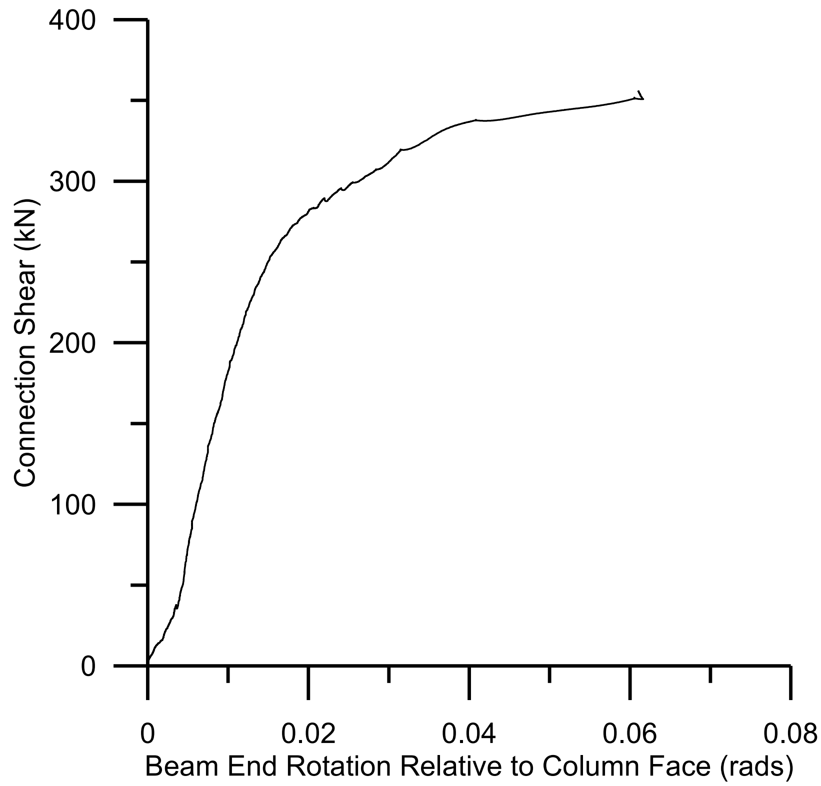

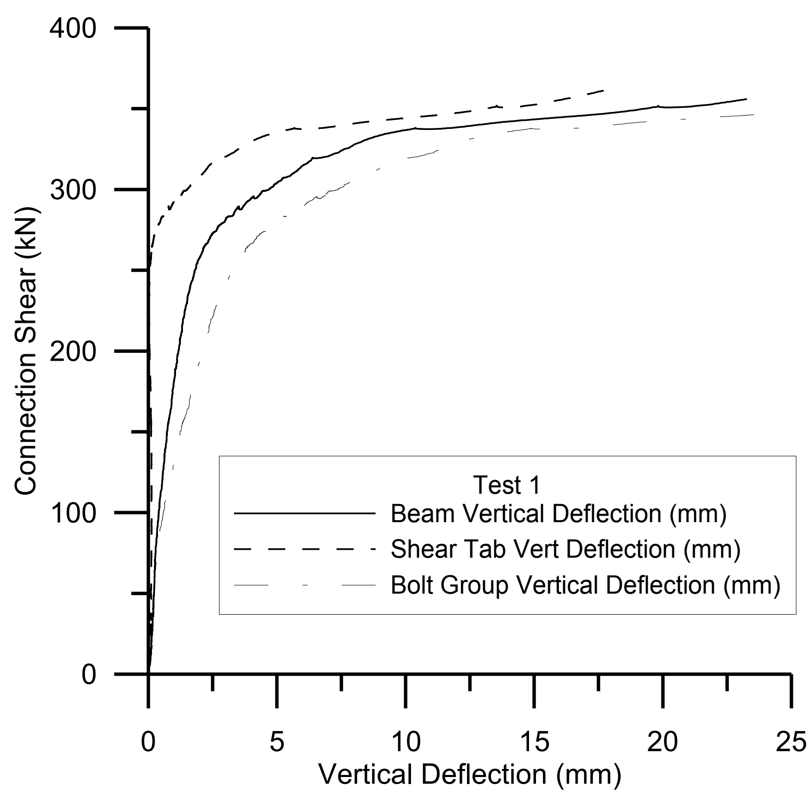

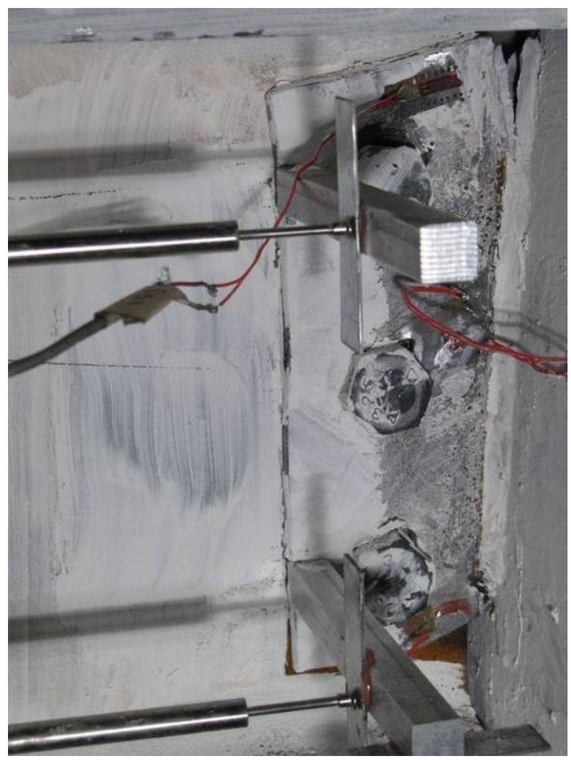

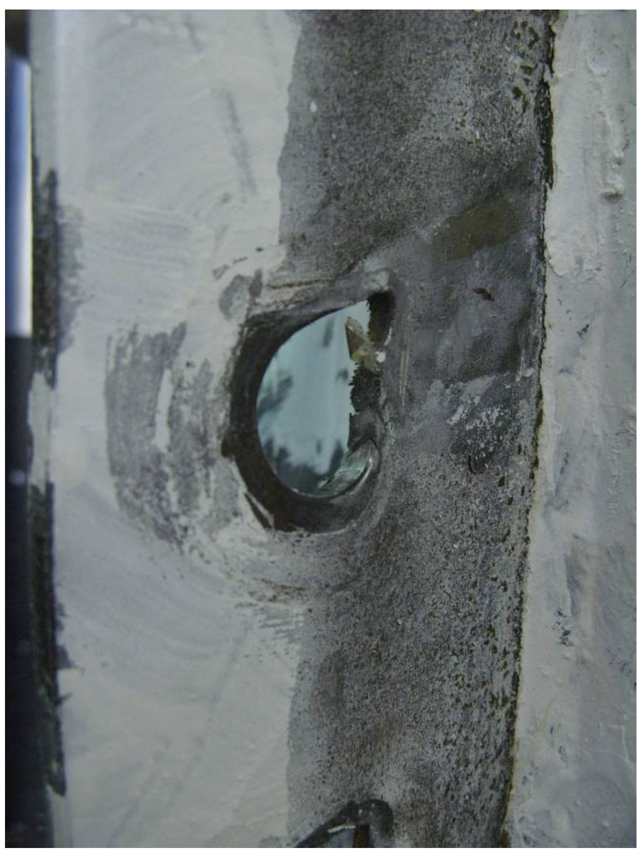

Test 2: Two Rows of 3 Bolts

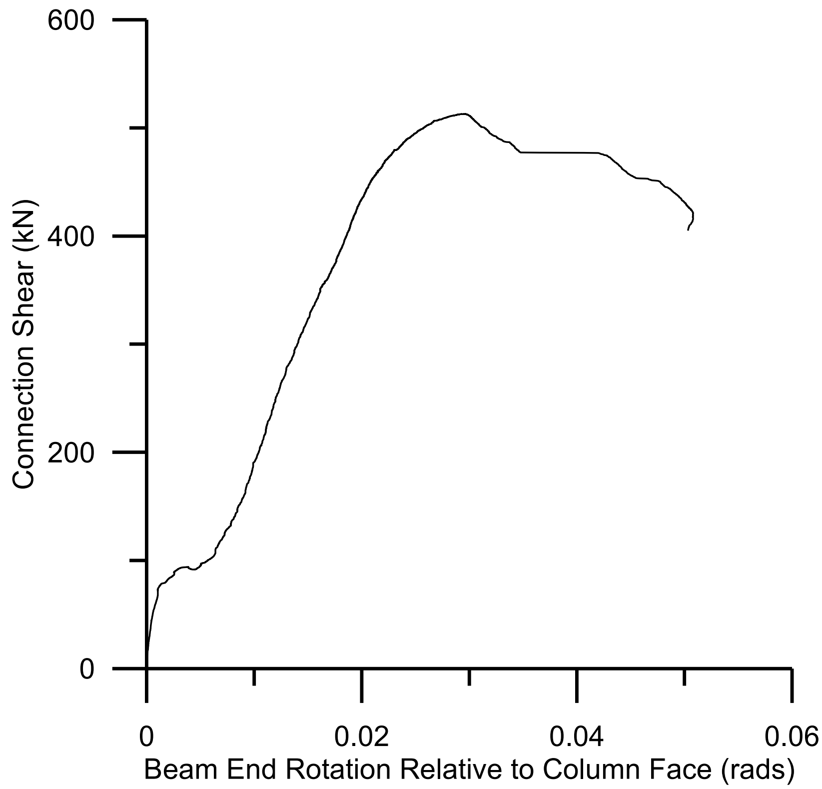

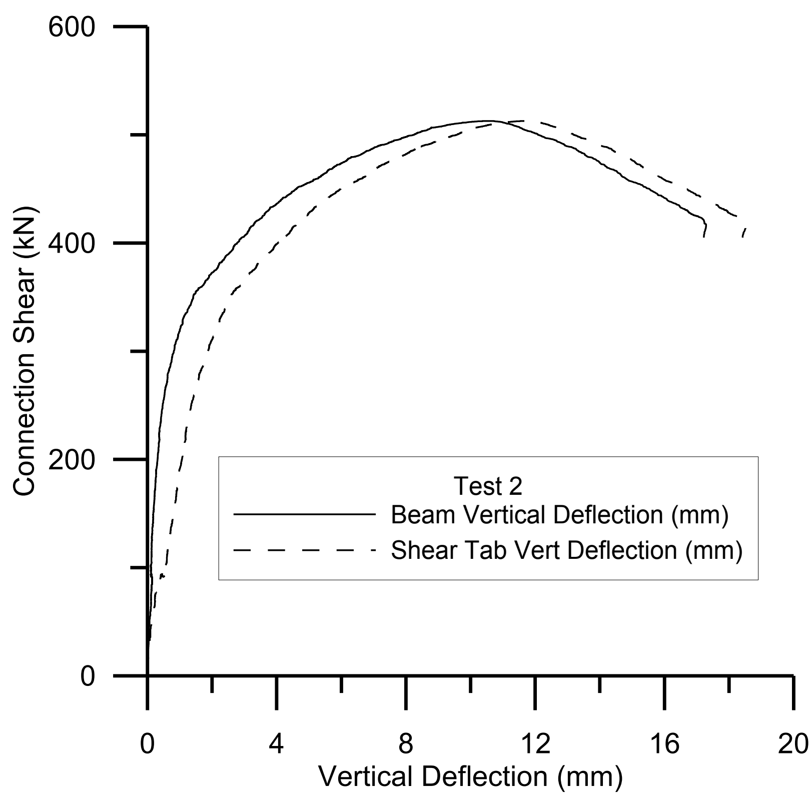


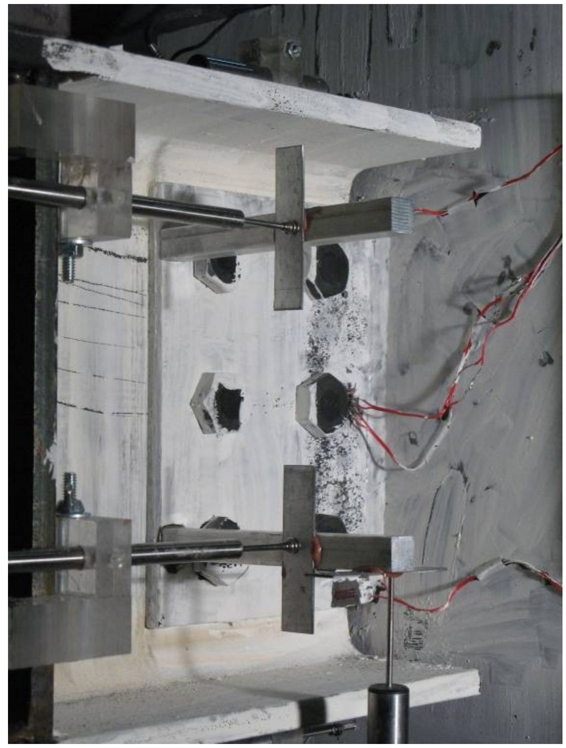
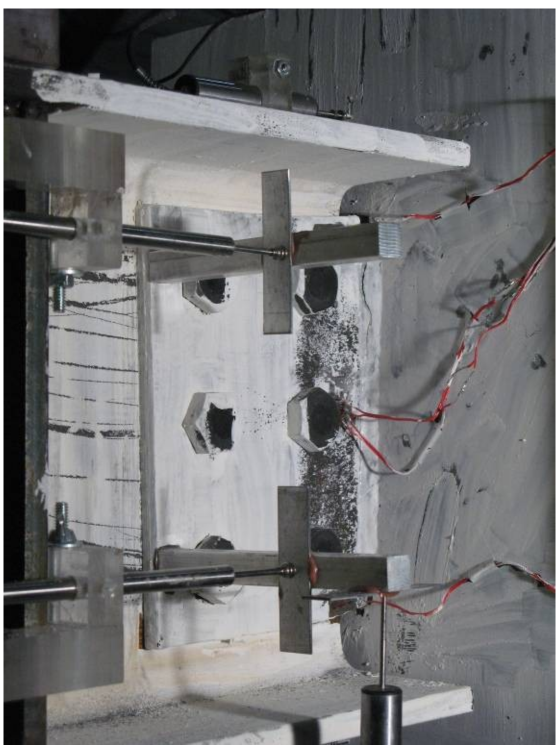


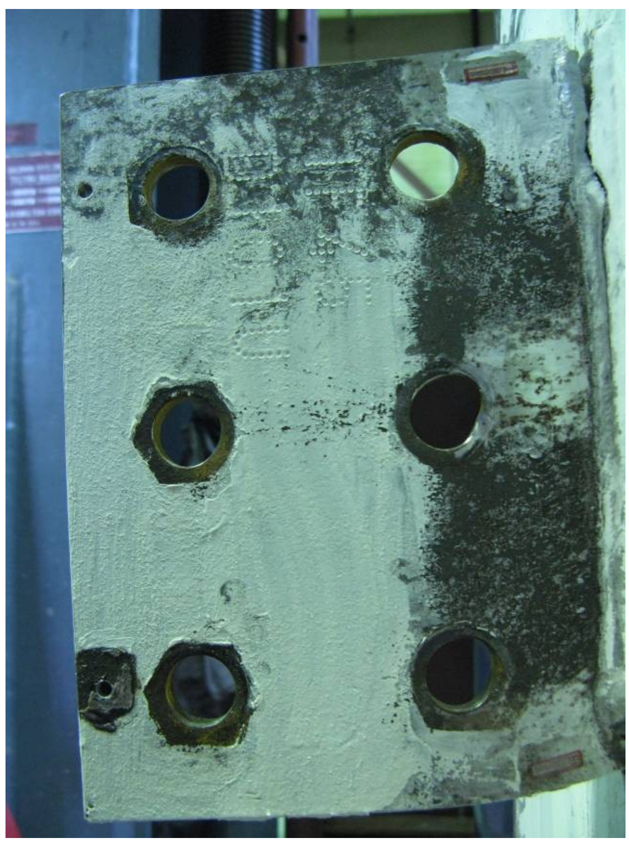

<u>Test 3: Single Row of 3 Holes – Full 'C' Weld Retrofit</u>

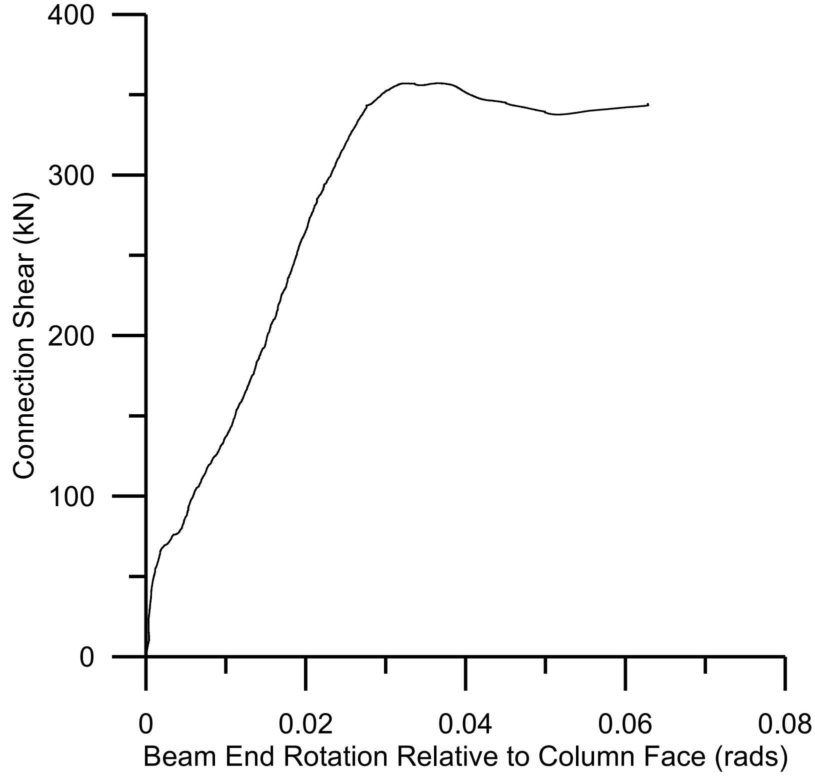

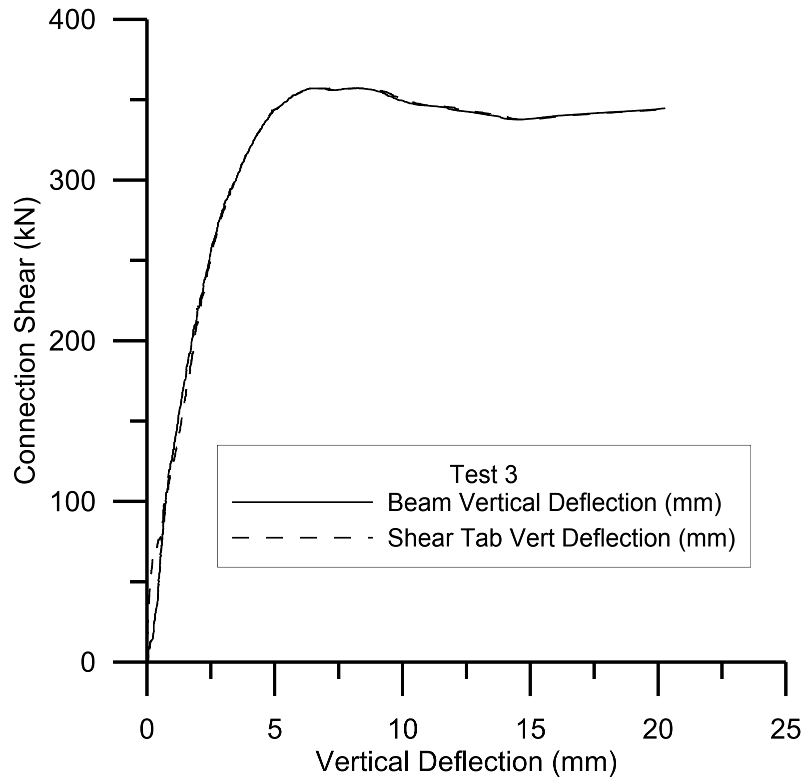

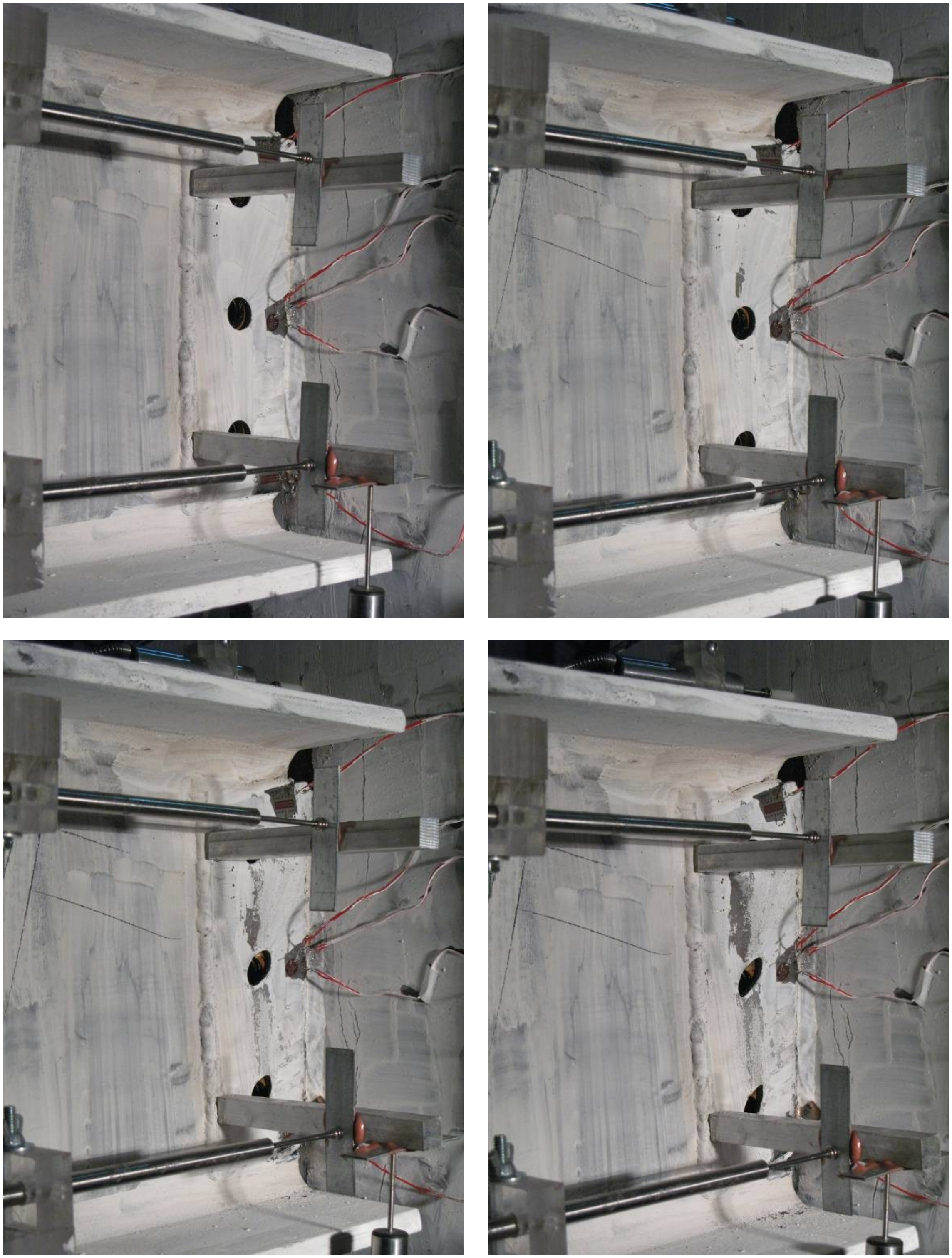

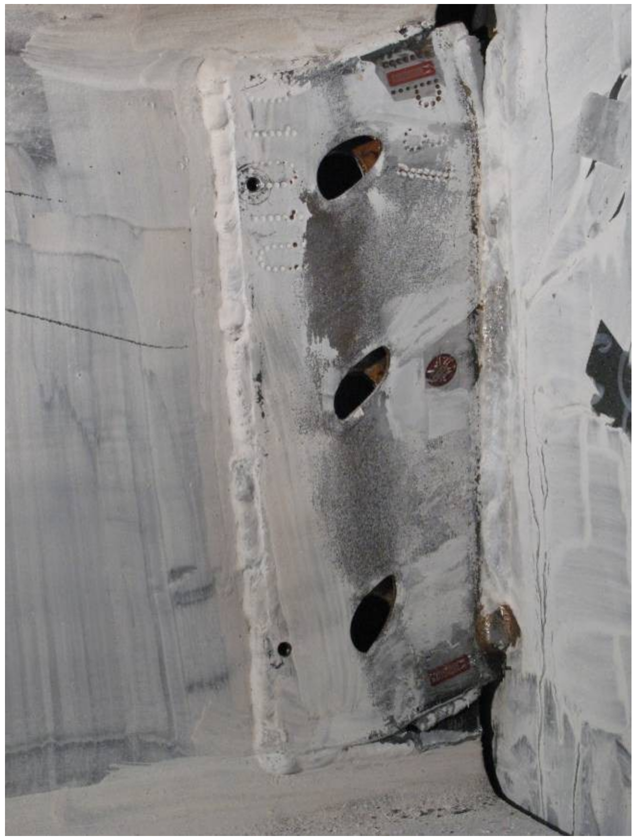

Test 4: Single Row of 3 Holes – Partial 'C' Weld Retrofit

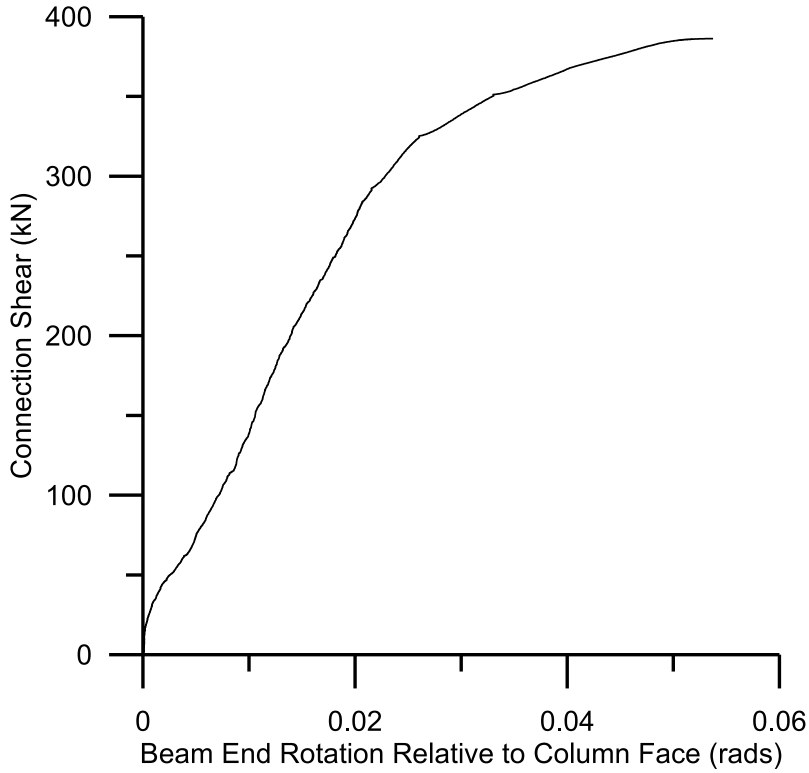

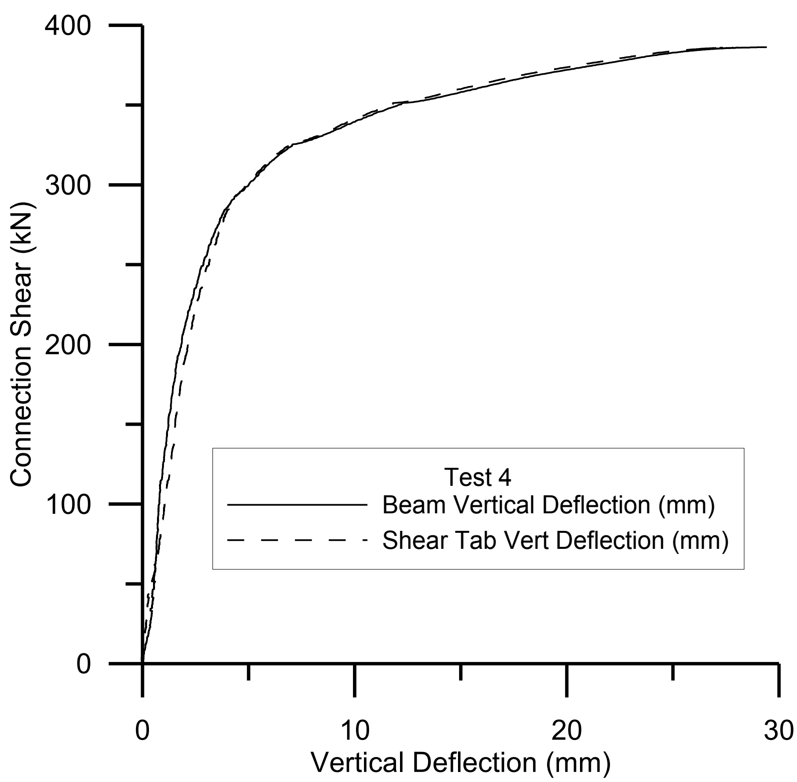




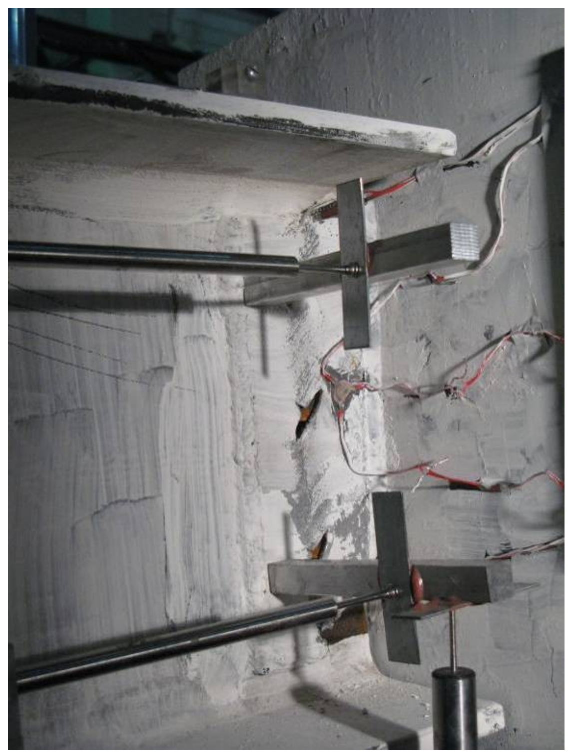

Test 5: Two Rows of 3 Holes – Full 'C' Weld Retrofit

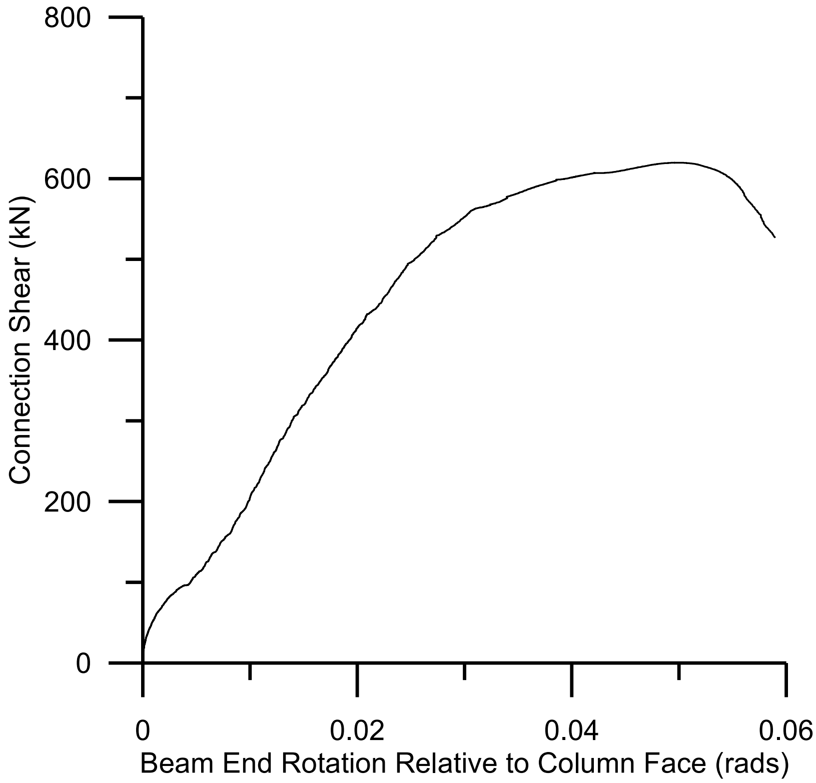

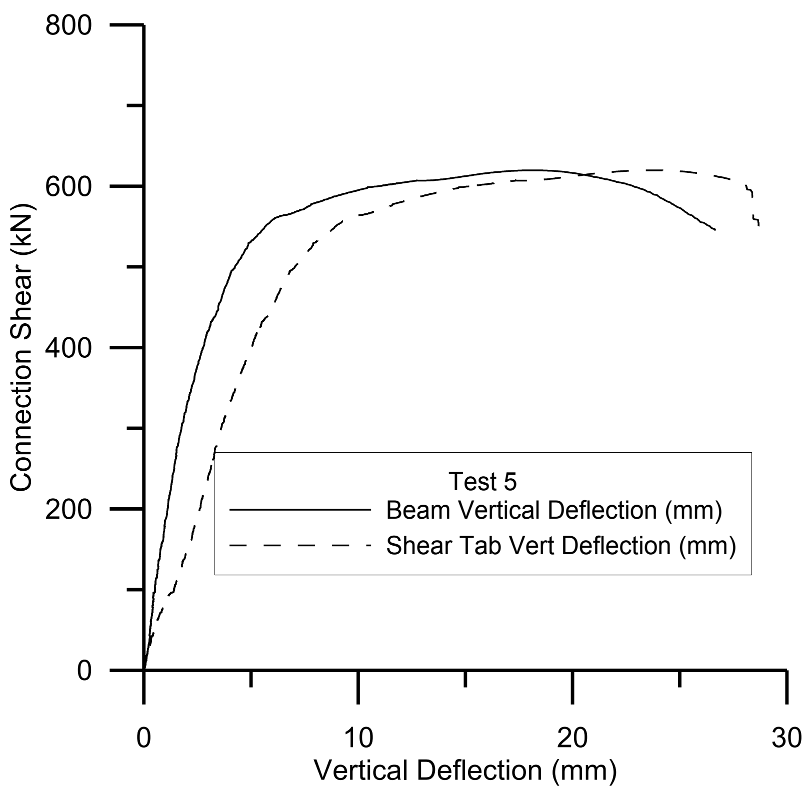

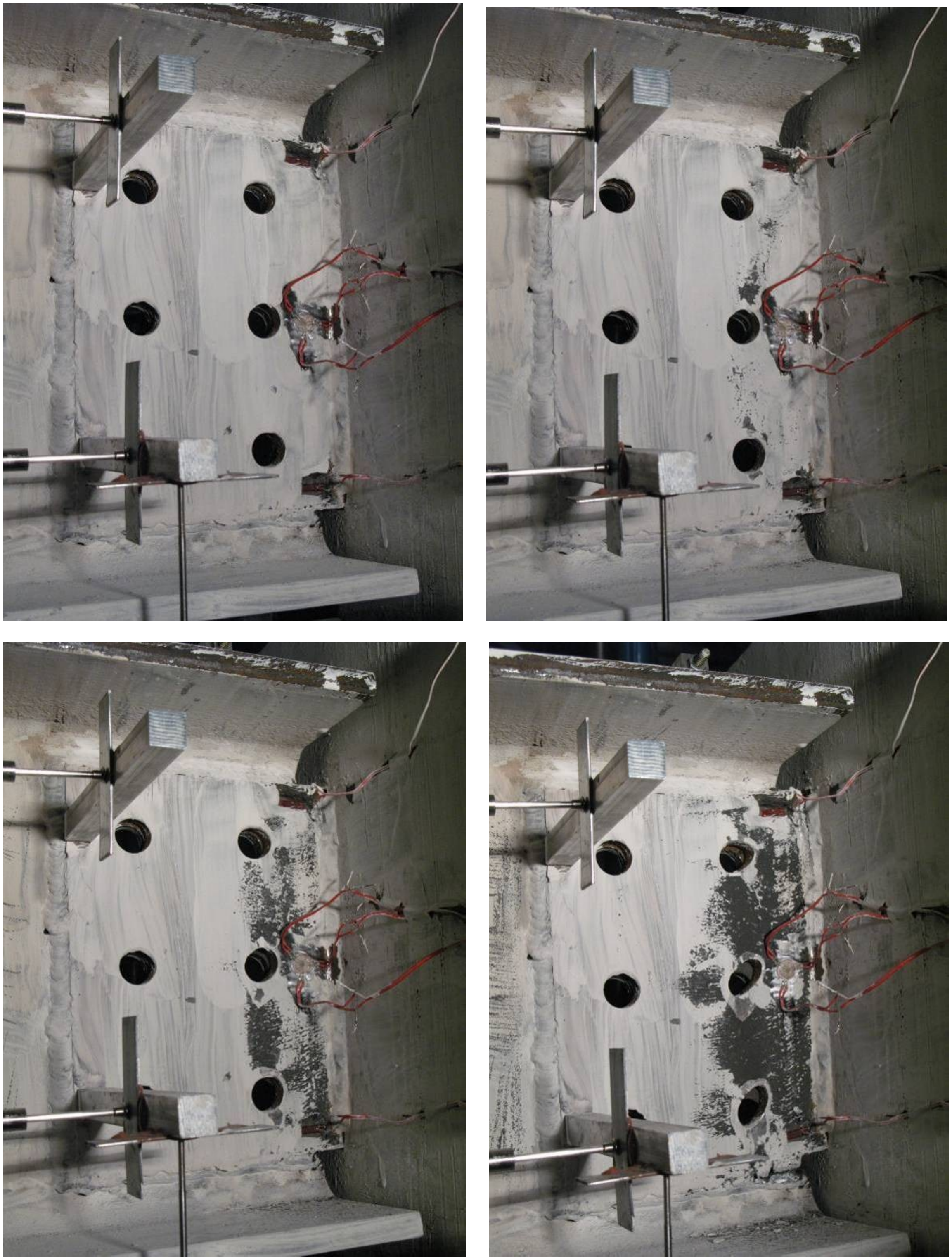

Test 6: Two Rows of 3 Holes – Partial 'C' Weld Retrofit

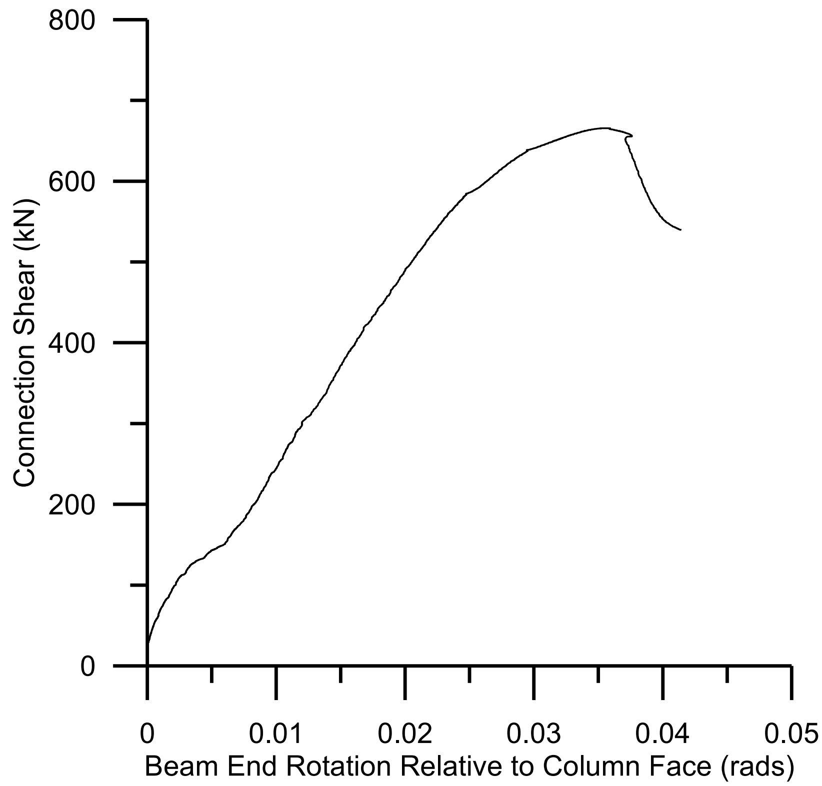

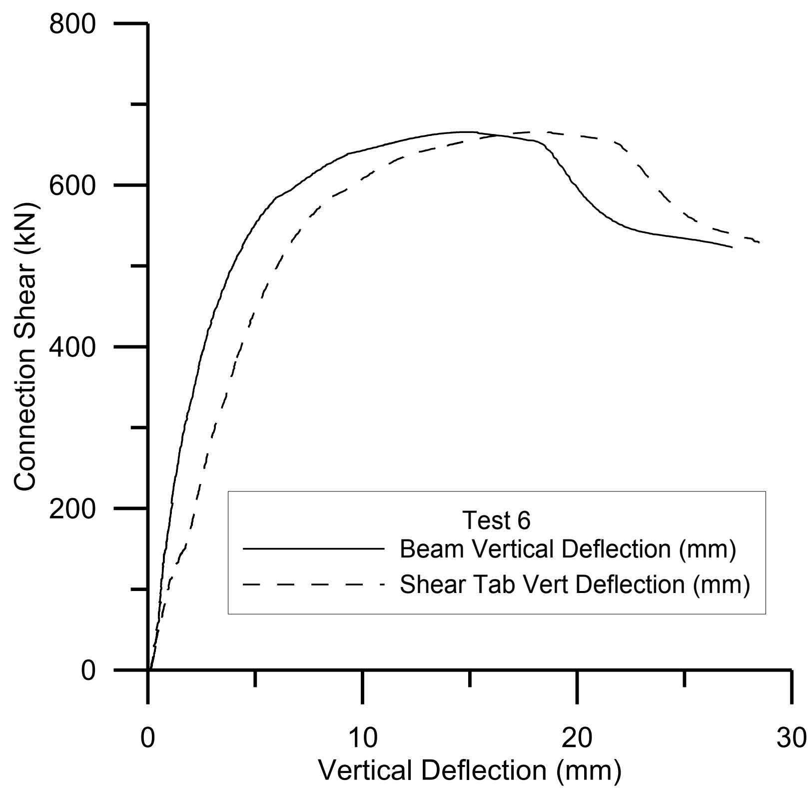

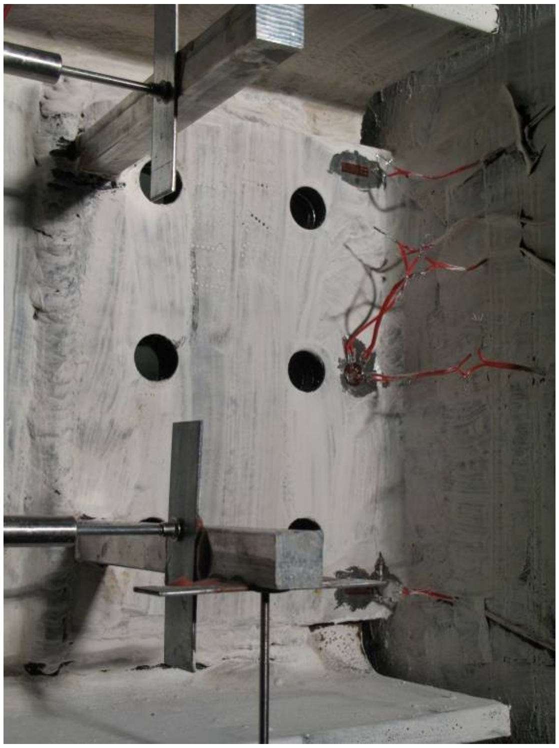


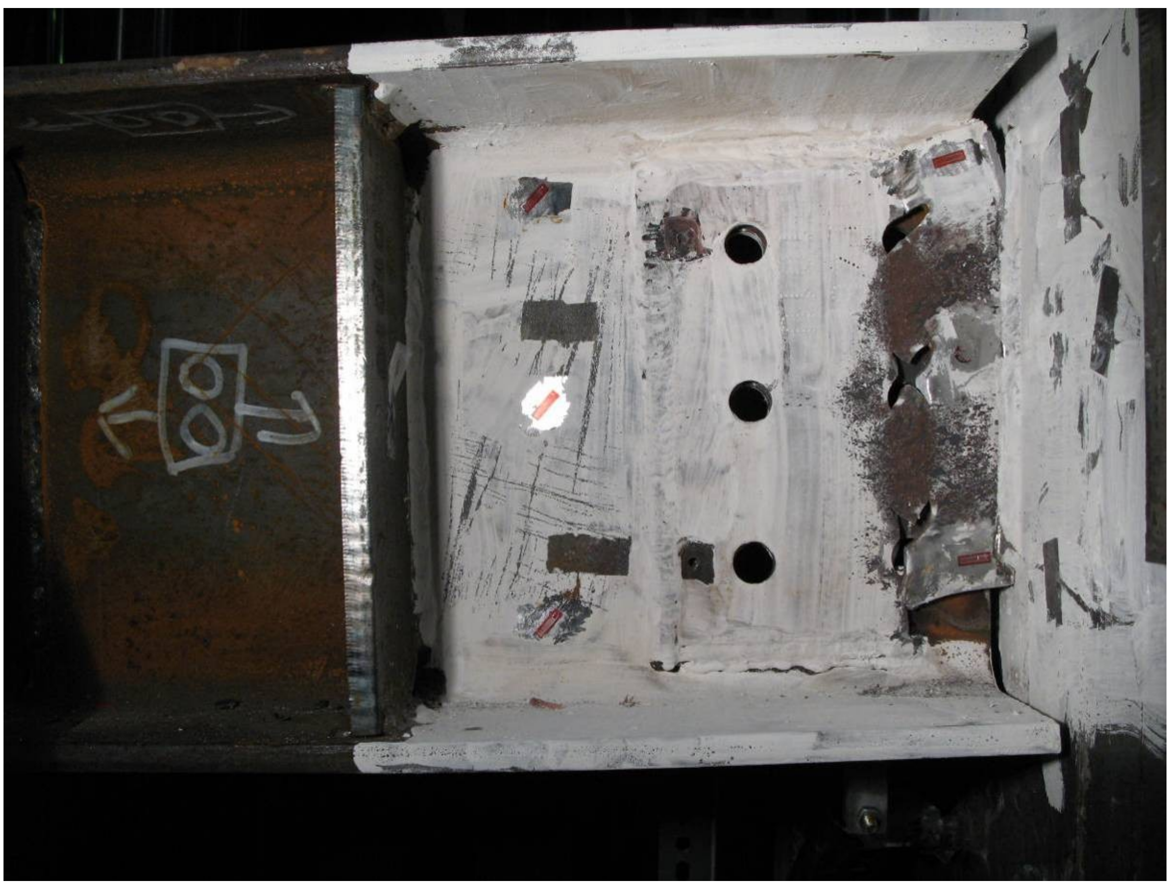

Test 7: Single Row of 6 Bolts

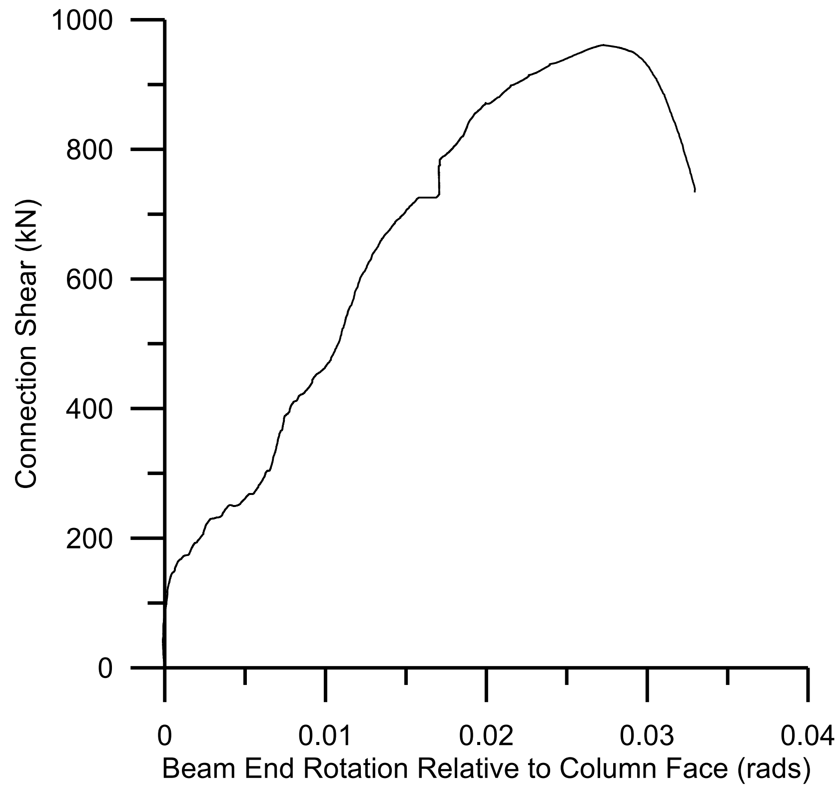

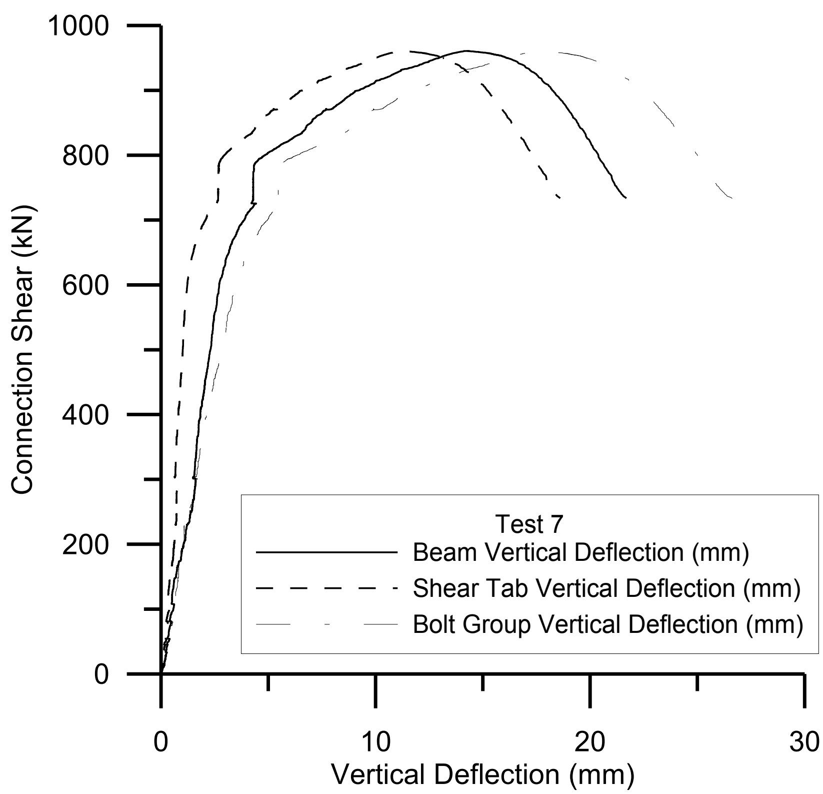

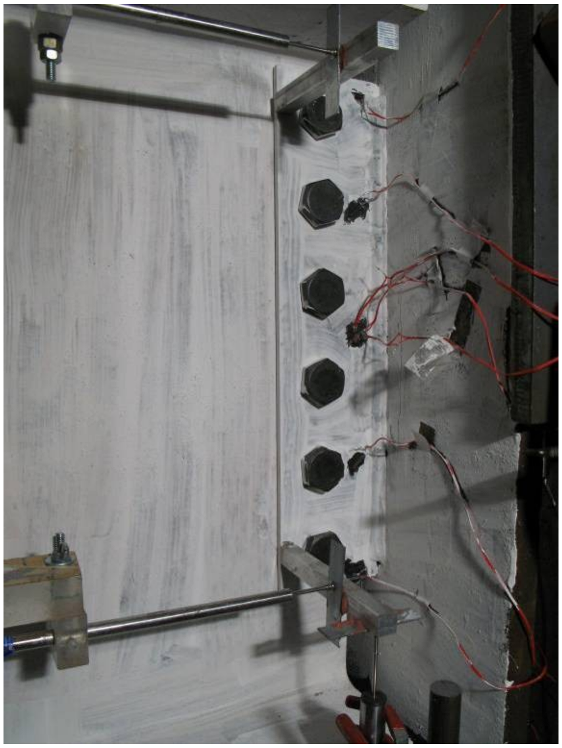
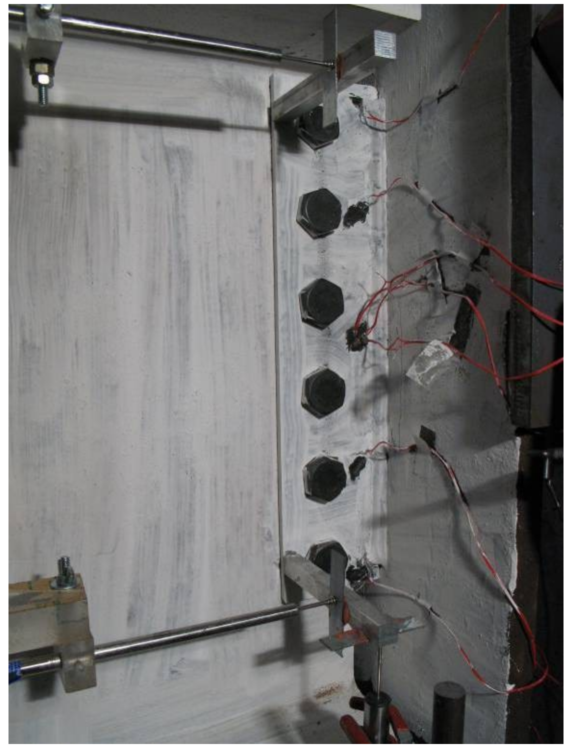
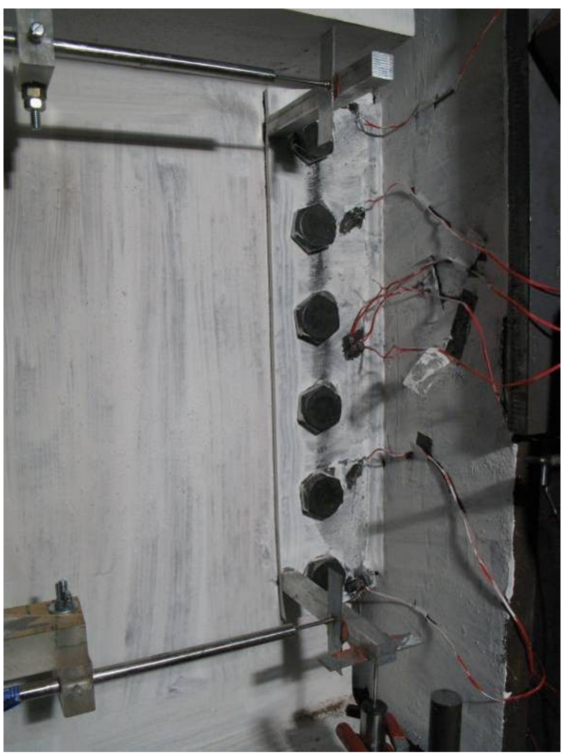
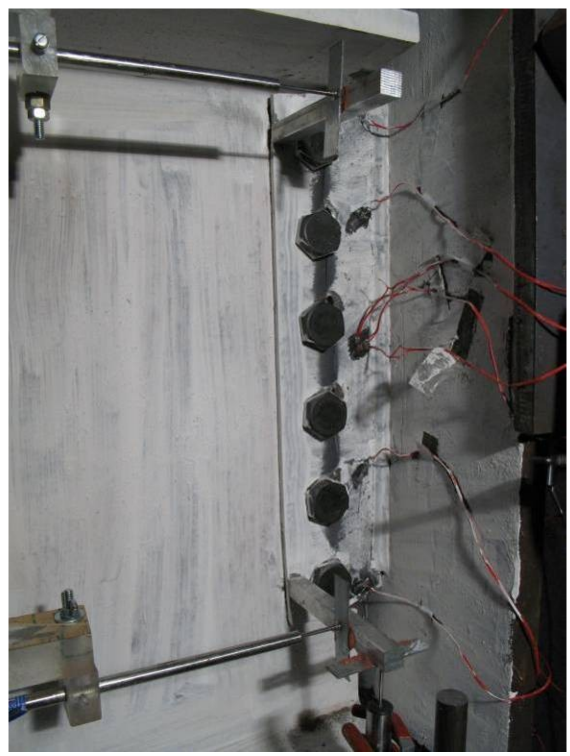

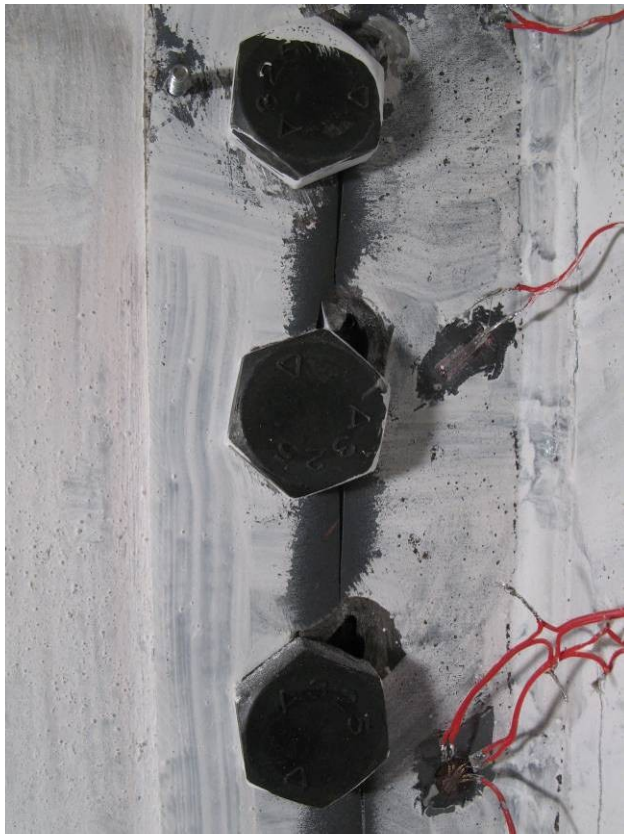

Test 8: Two Rows of 6 Bolts

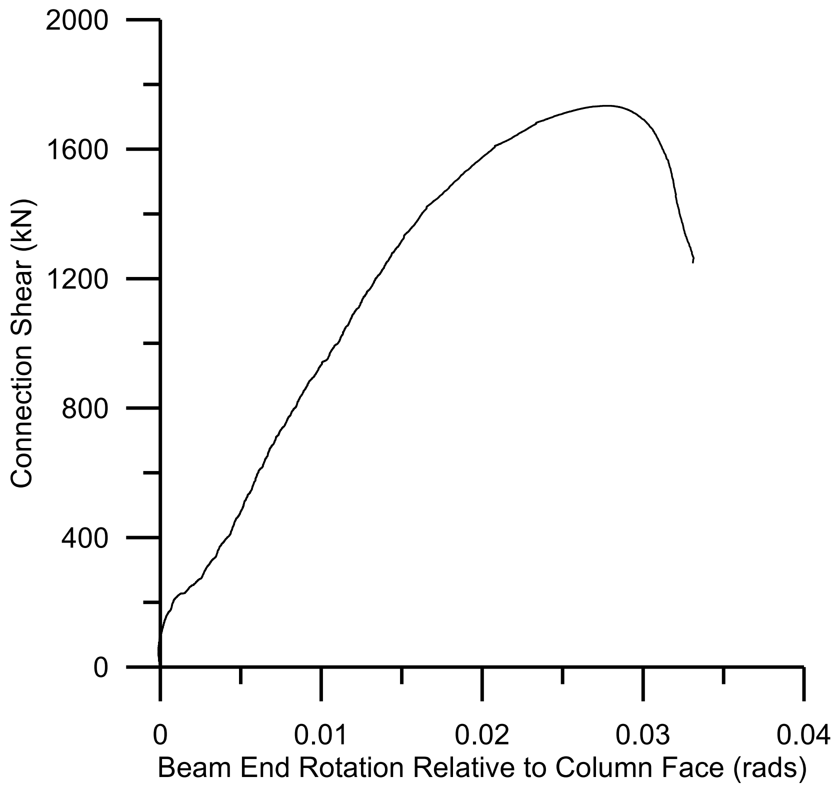

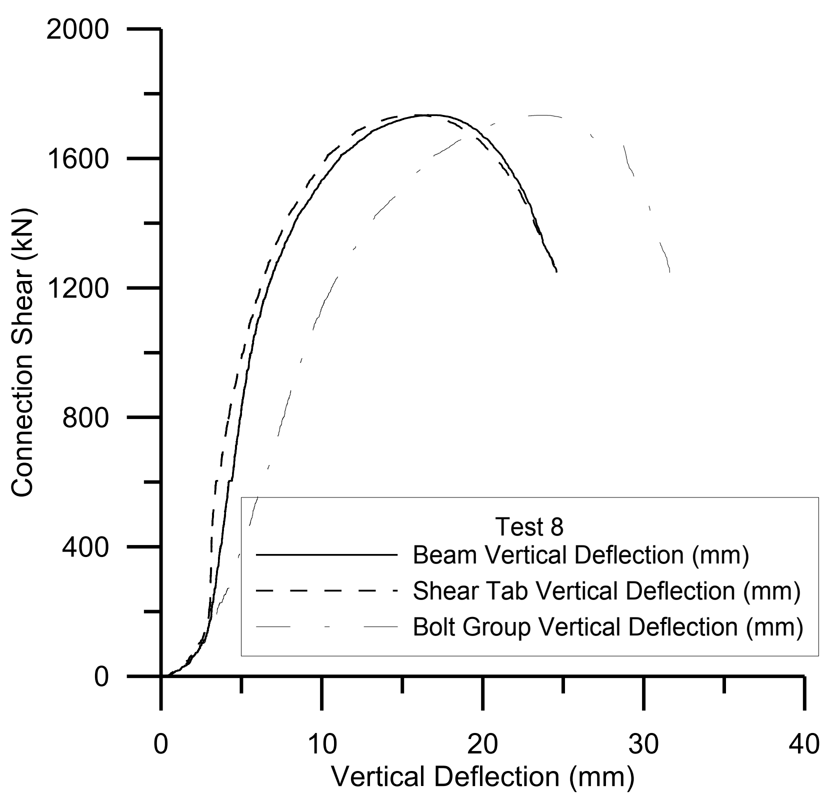

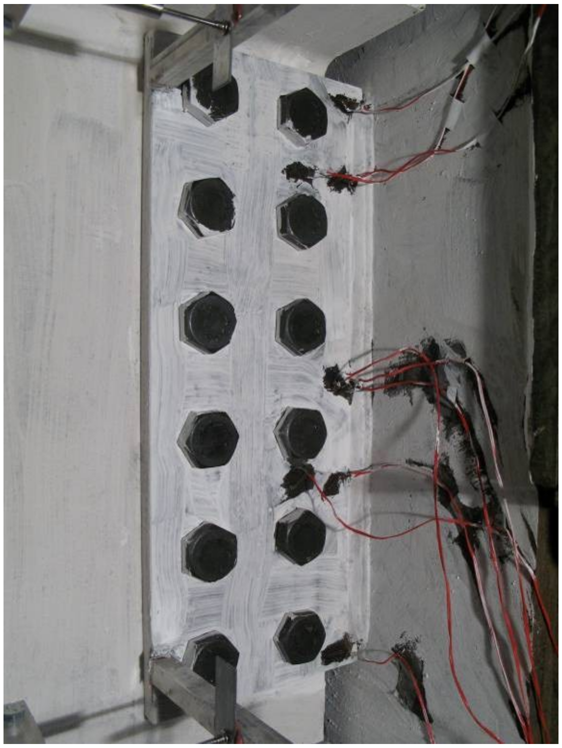
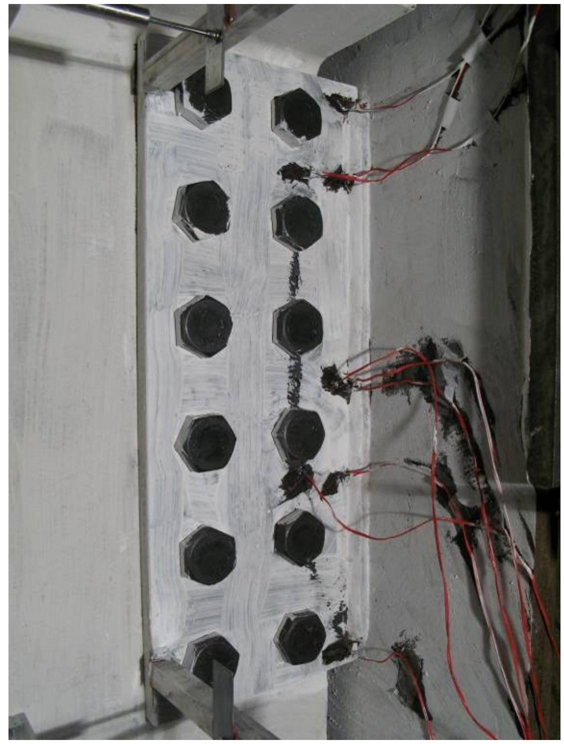
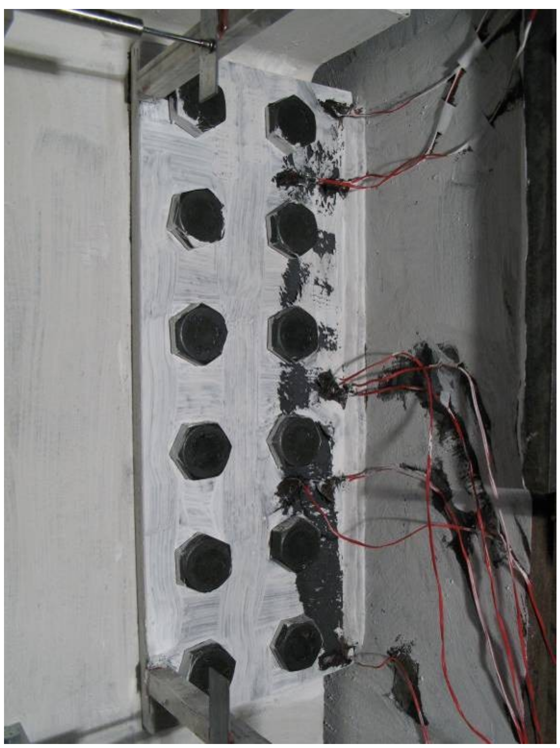
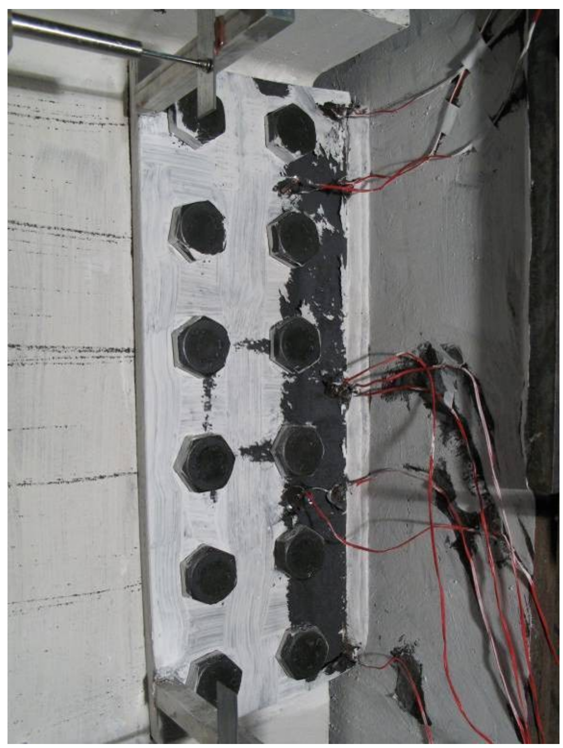

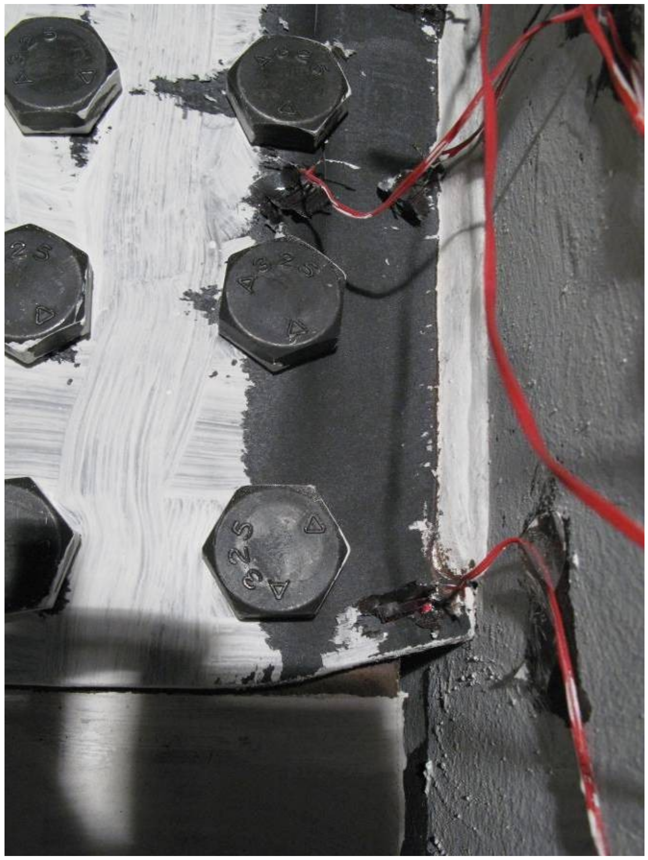
A325

Test 9: Single Row of 6 Holes – Partial `C` Weld Retrofit

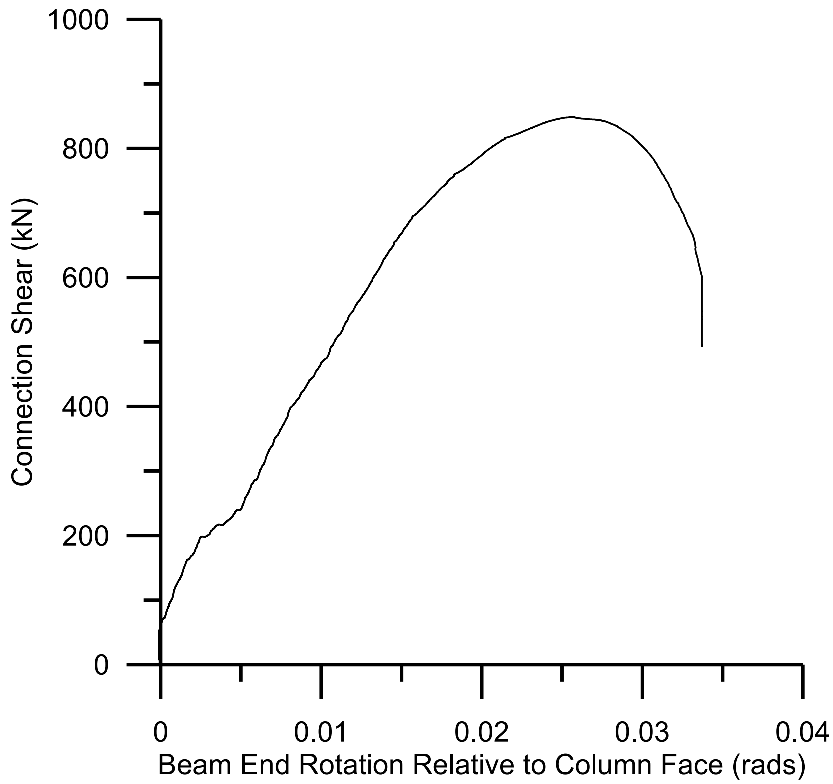

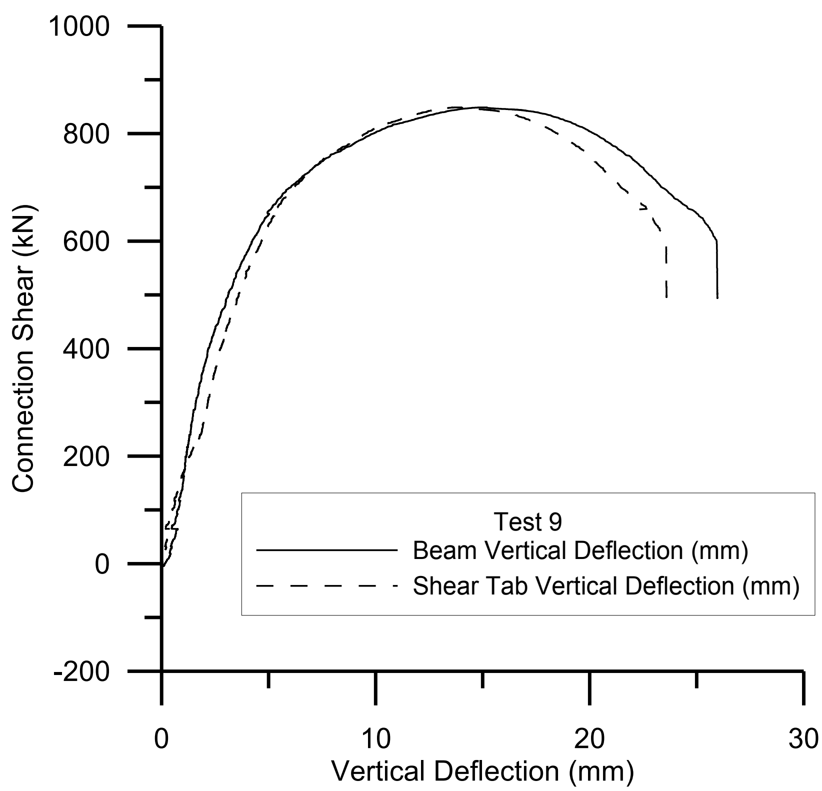

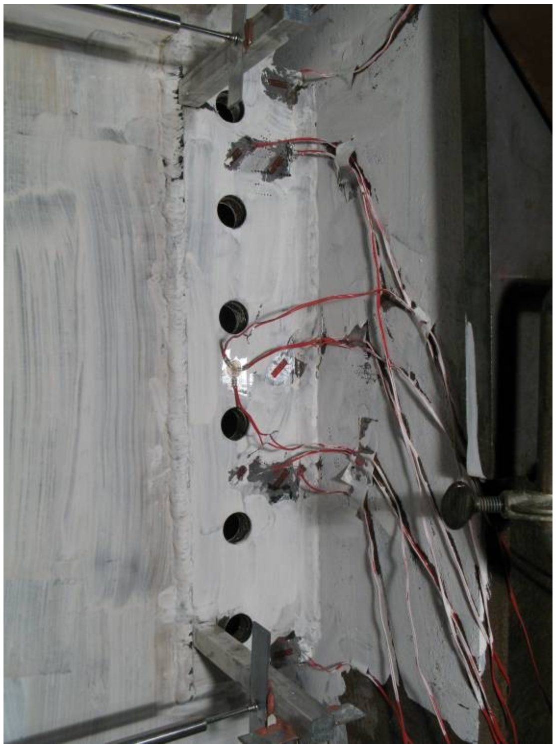
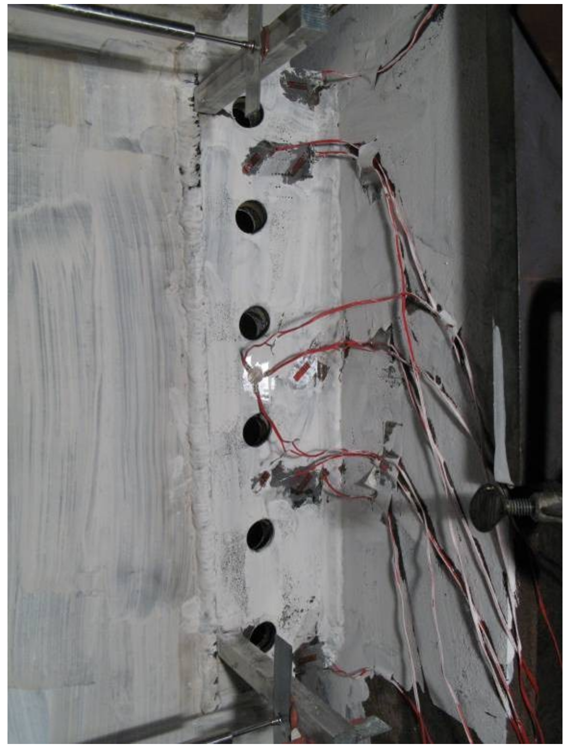

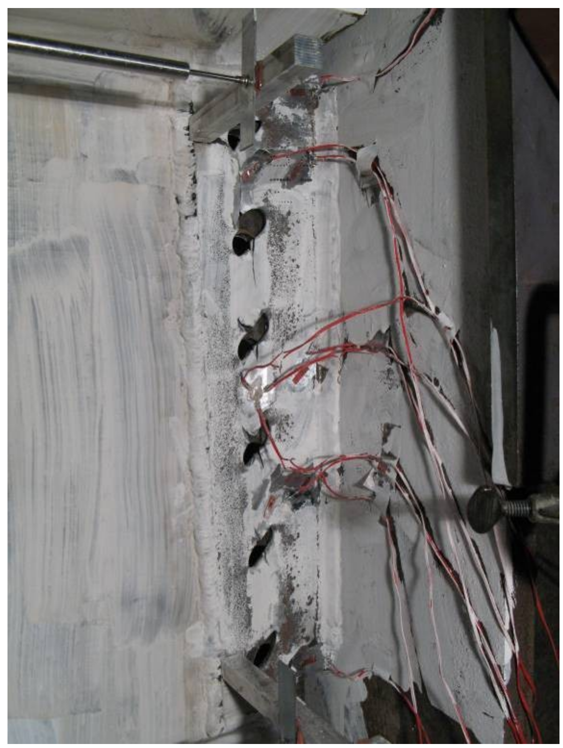

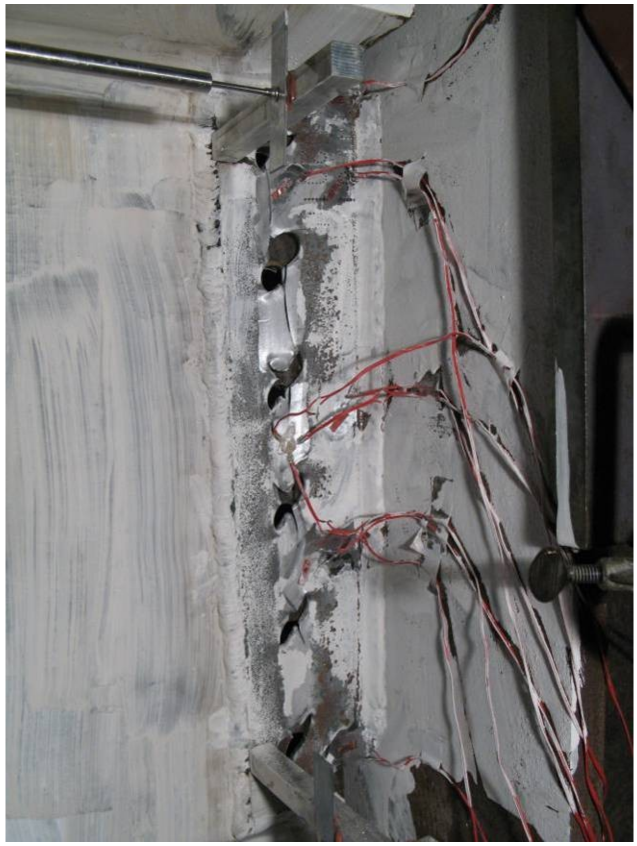

Test 10: Two Rows of 6 Holes – Partial `C` Weld Retrofit

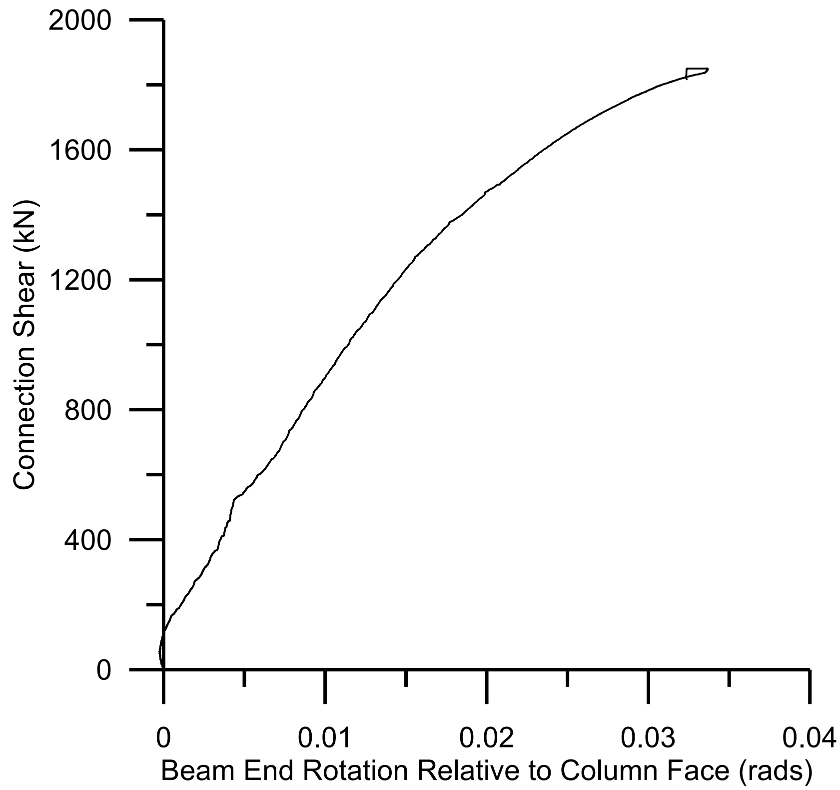

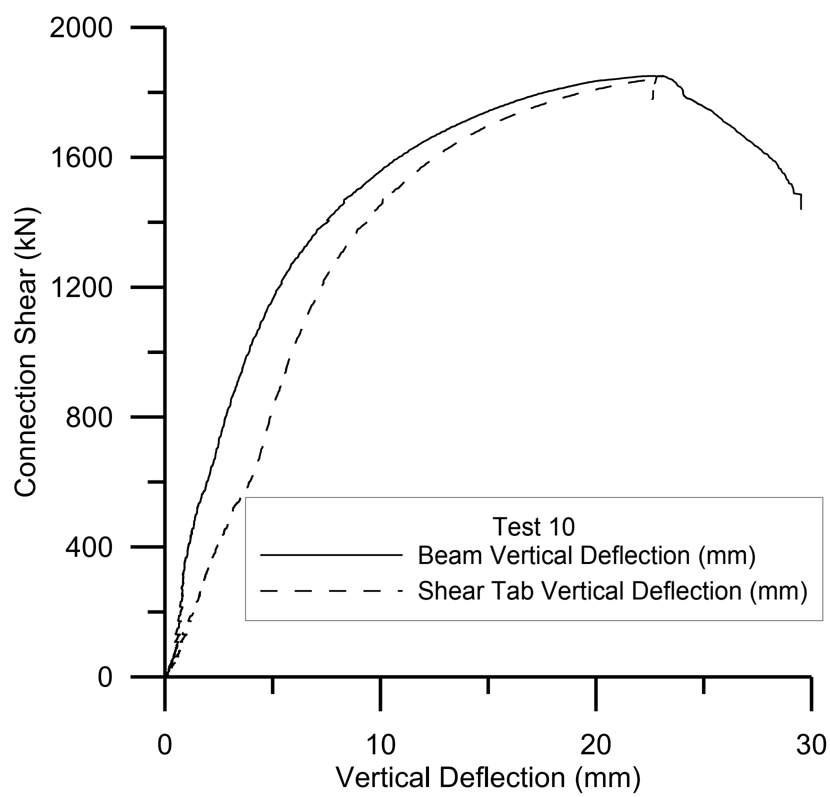

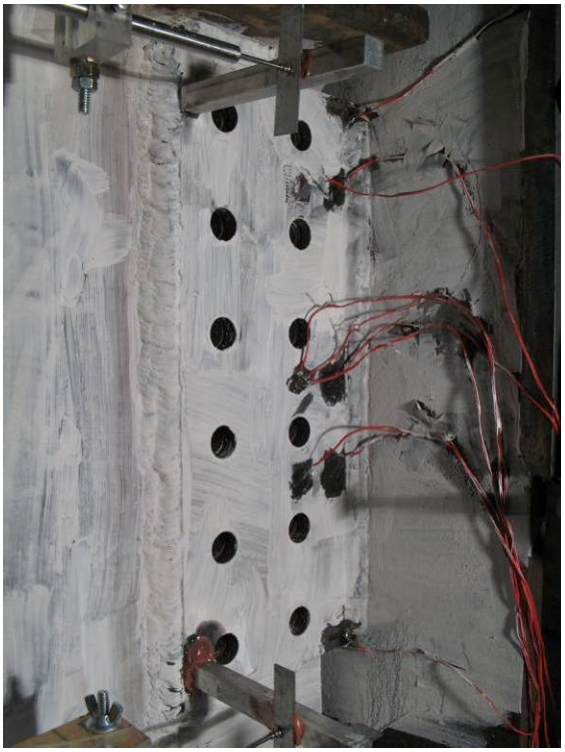
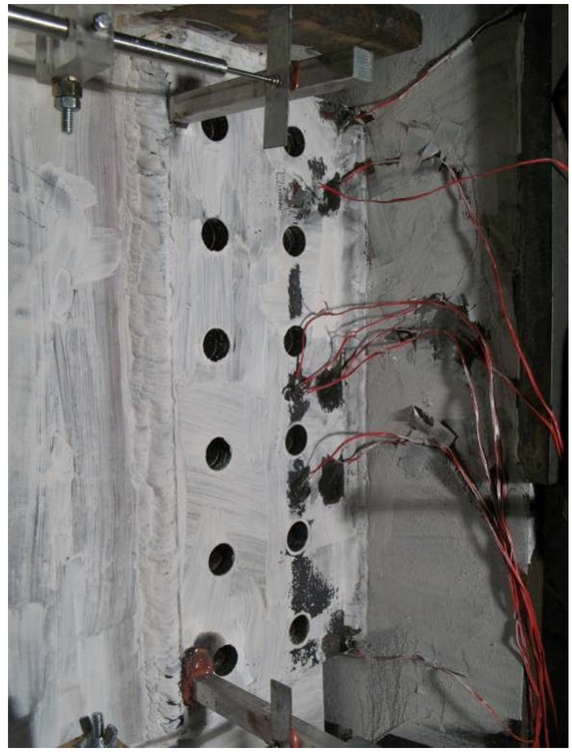
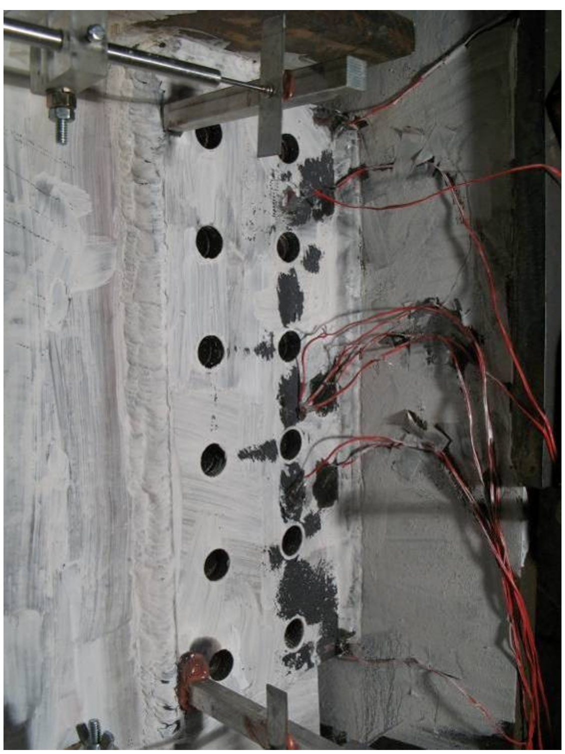
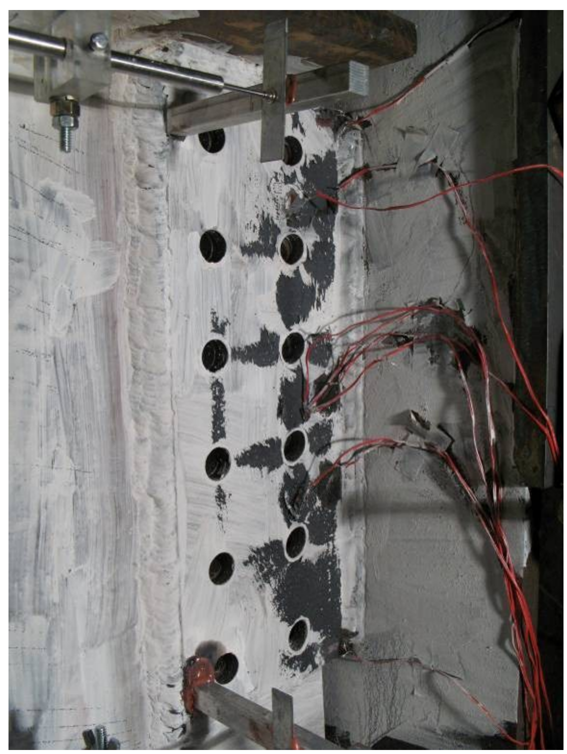

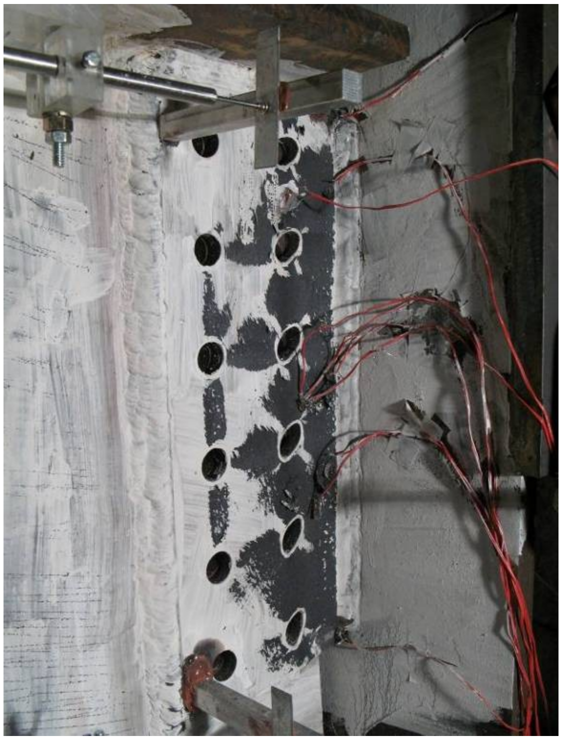

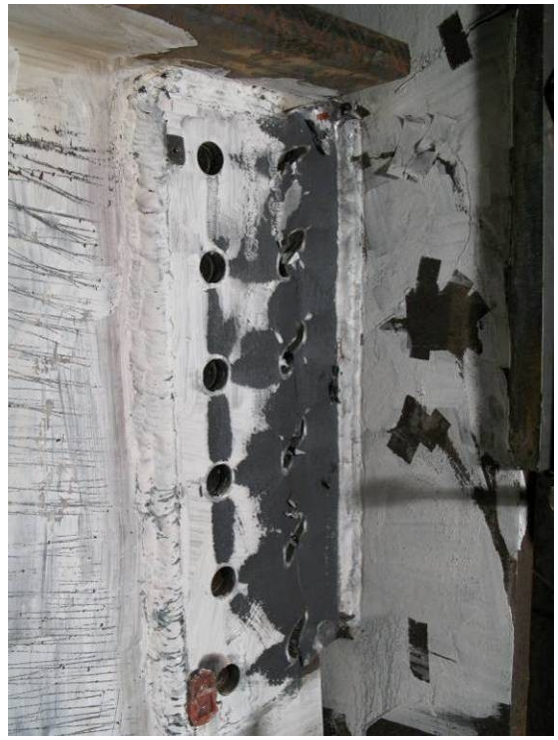

Test 11: Single Row of 6 Holes – `L`-shape Weld Retrofit

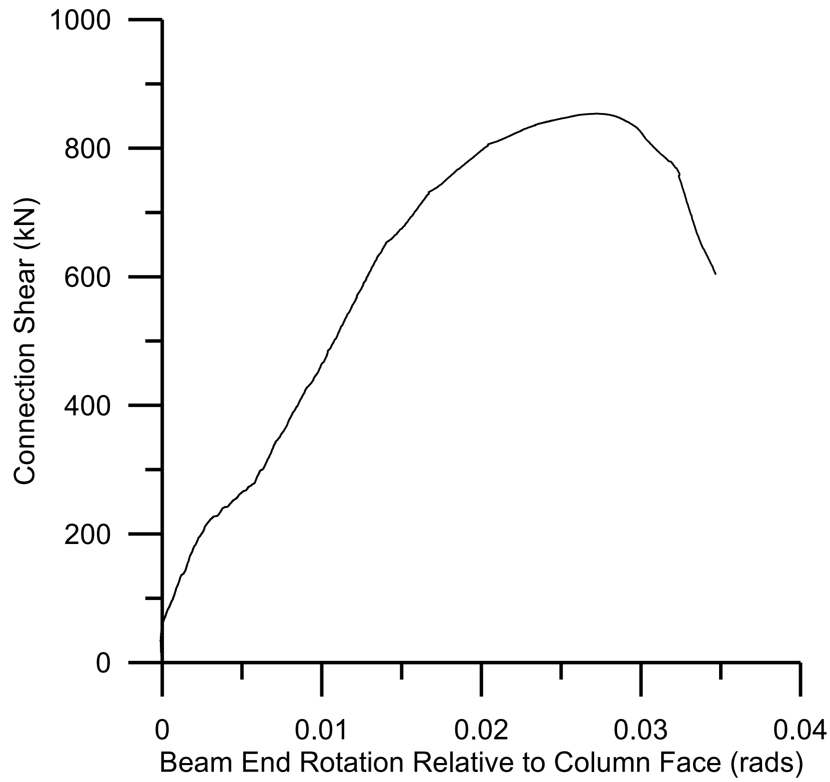

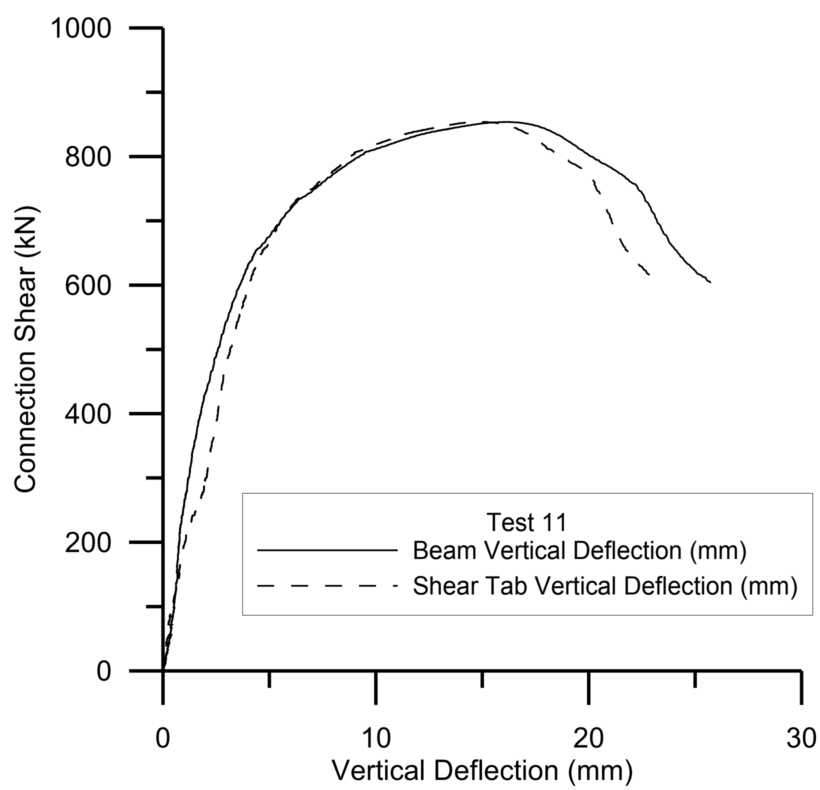

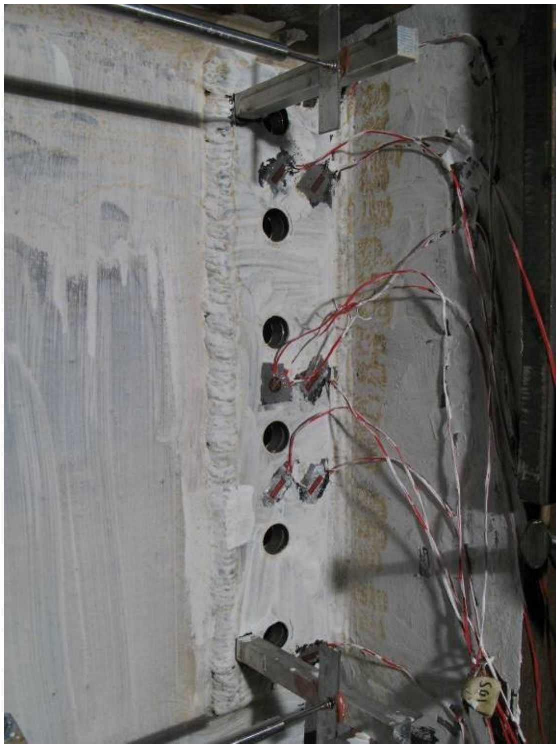
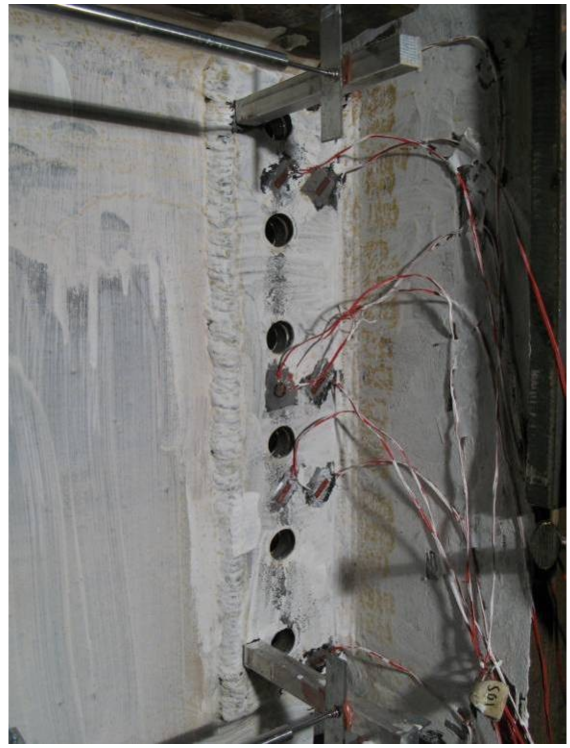
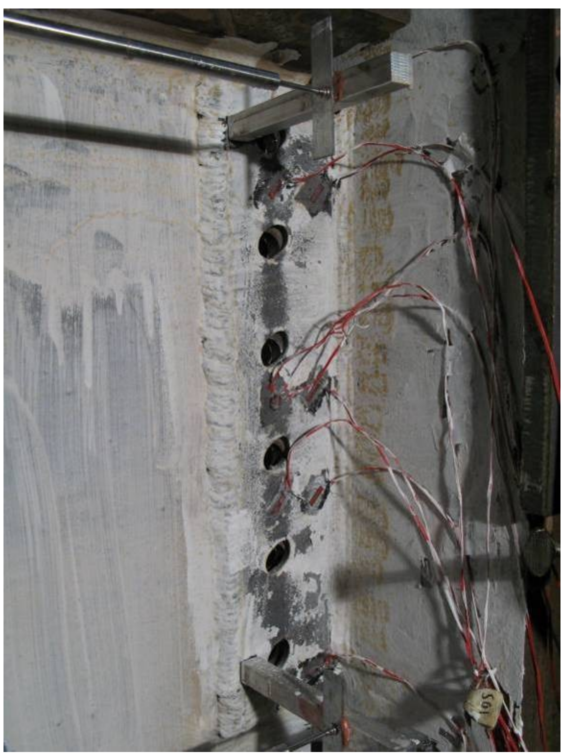
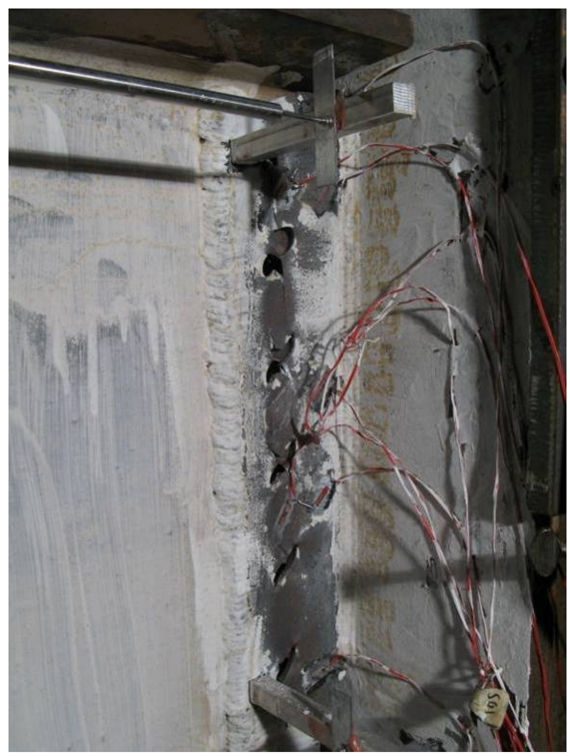

Test 12: Two Rows of 6 Holes – `L`-shaped Weld Retrofit

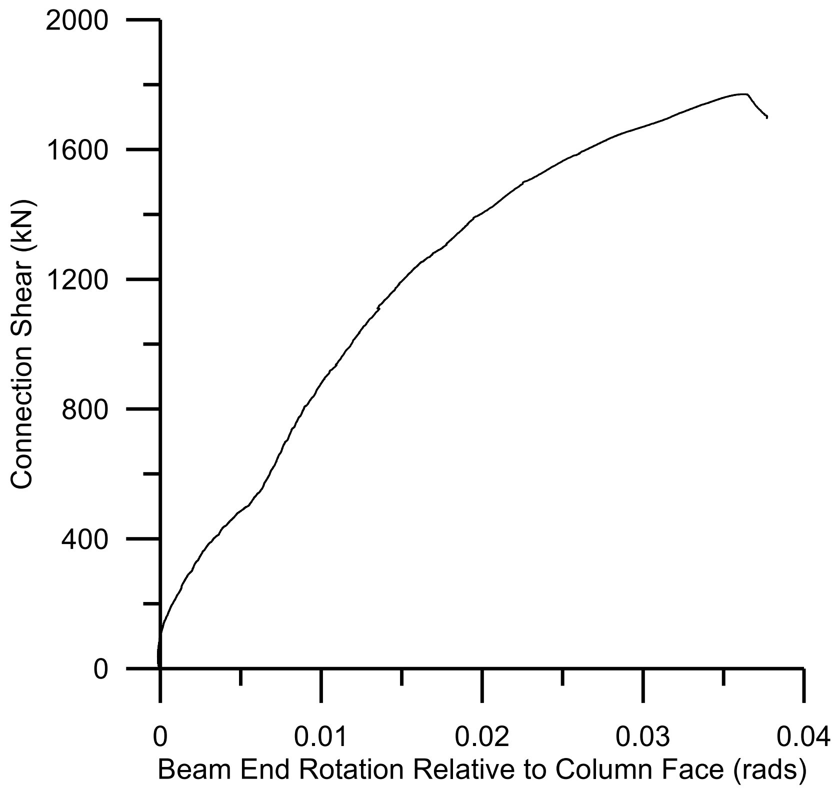

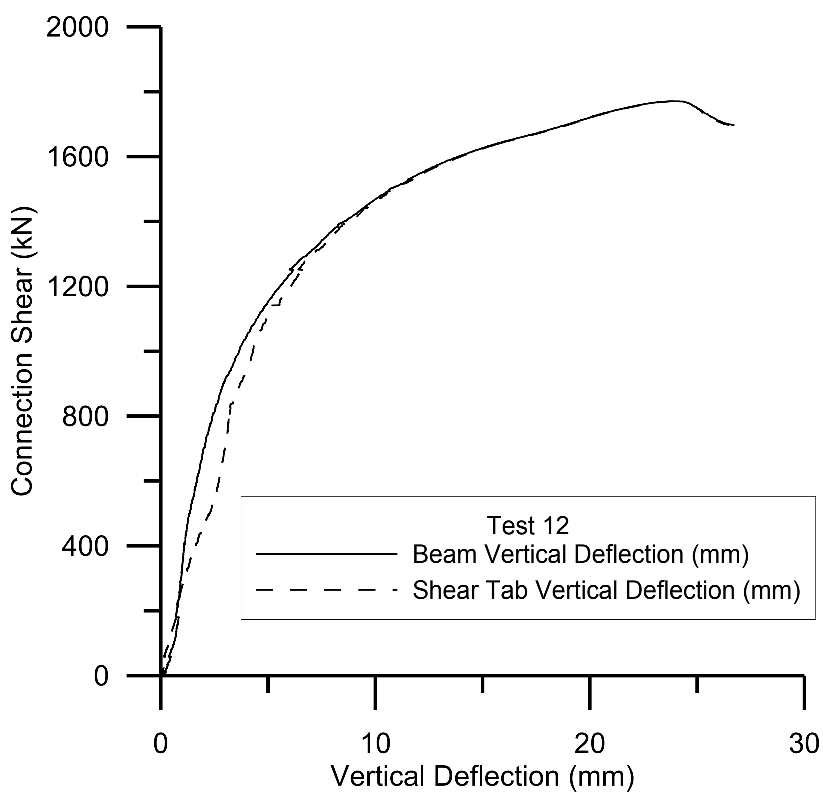

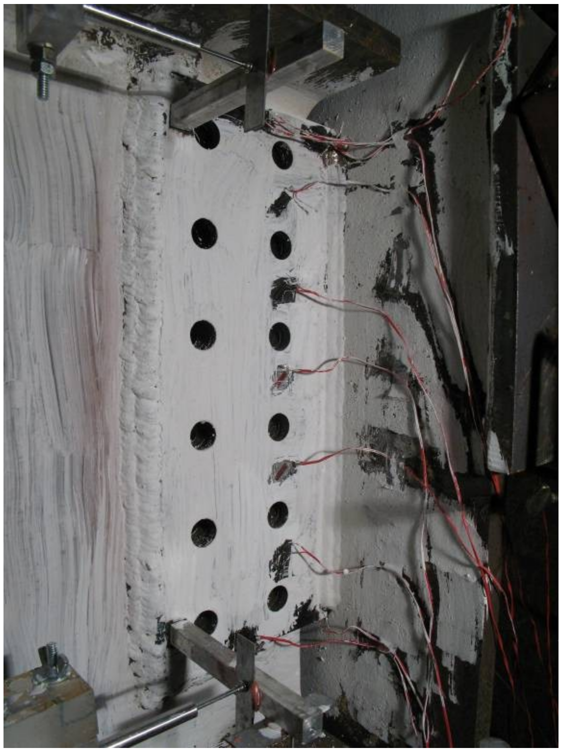
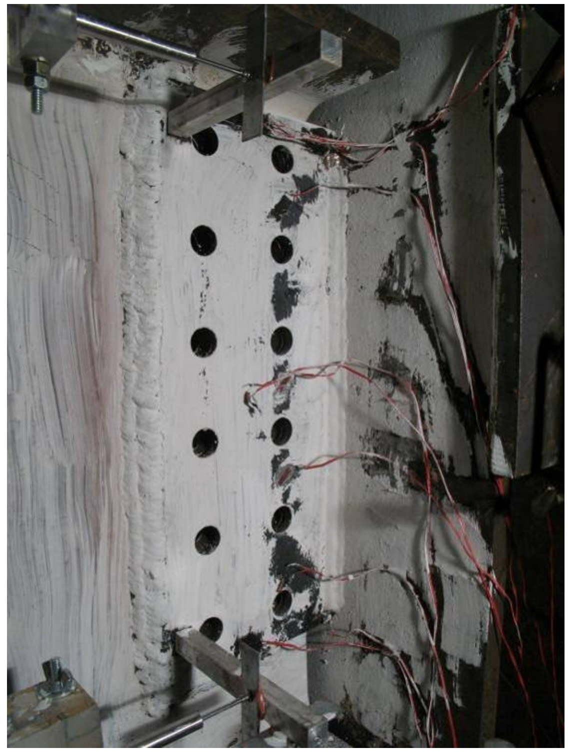
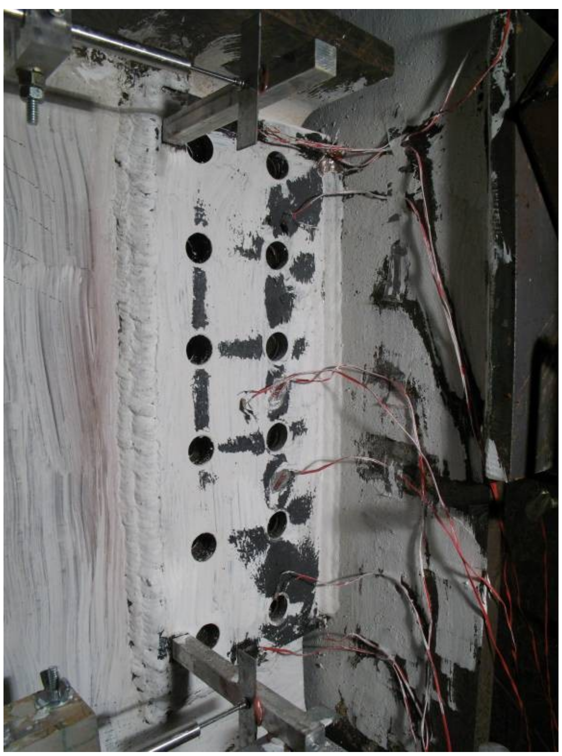
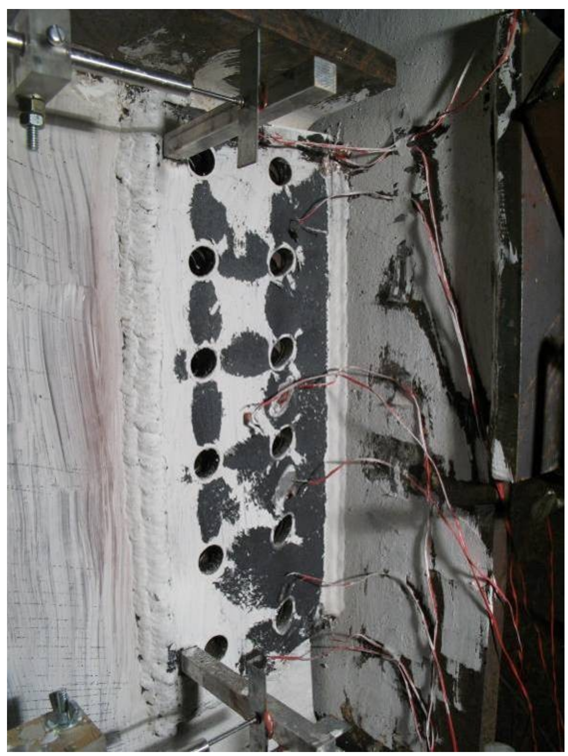

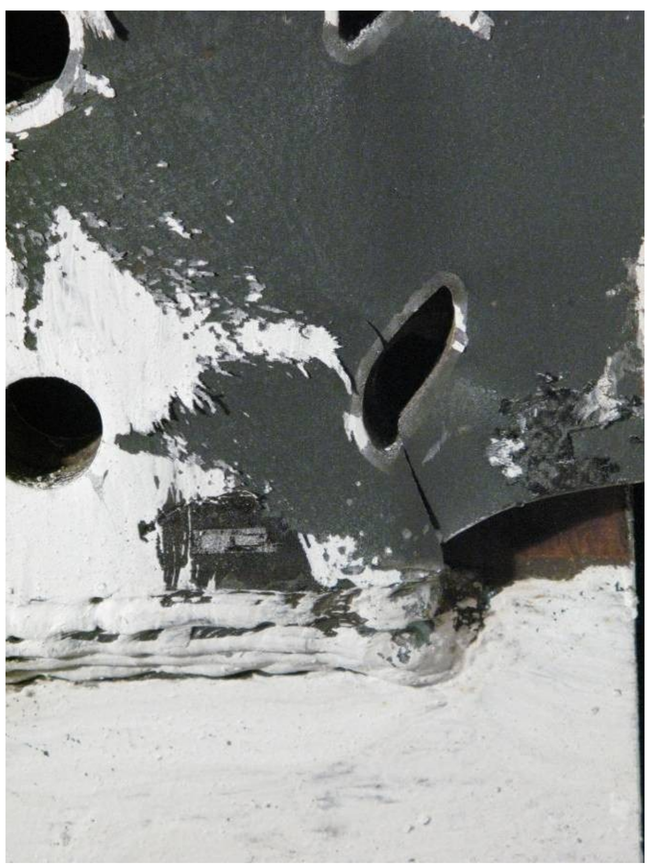

Test 13: Single Row of 10 Bolts

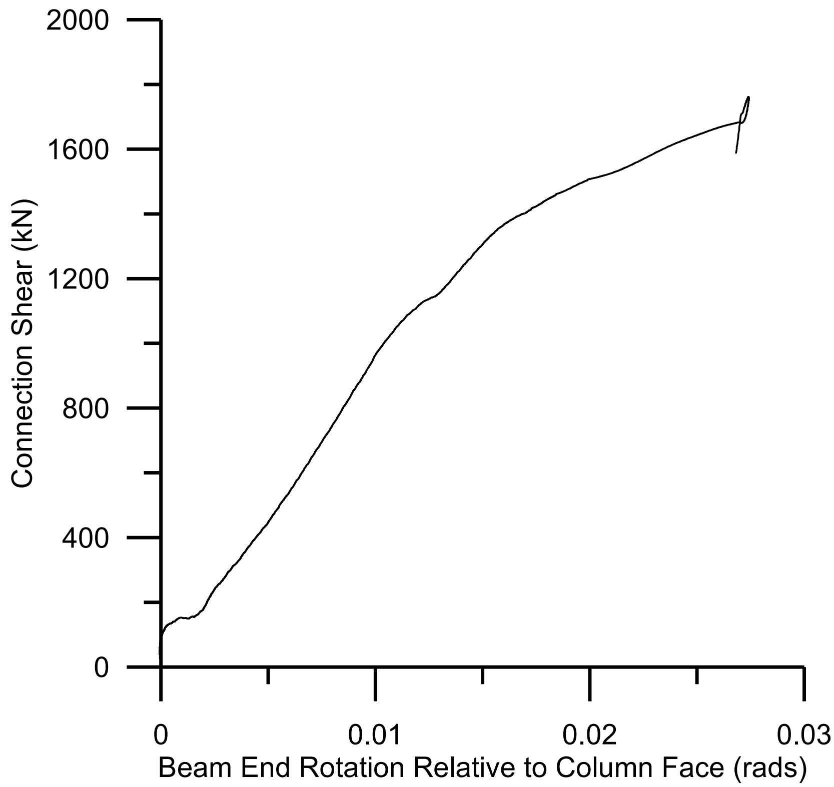

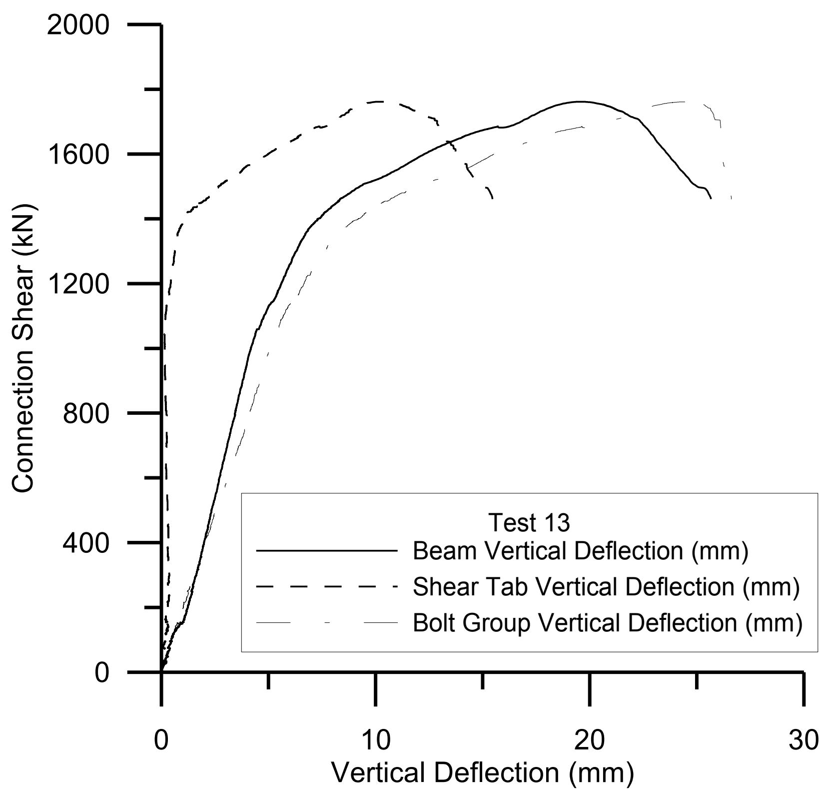


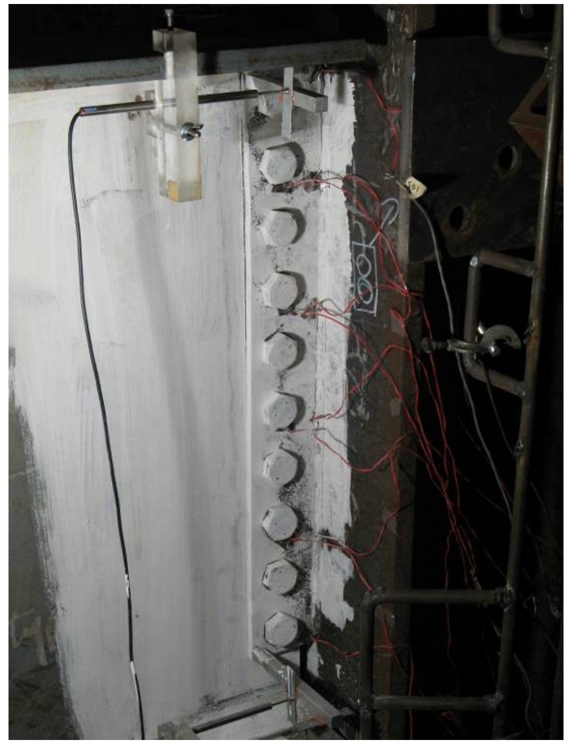

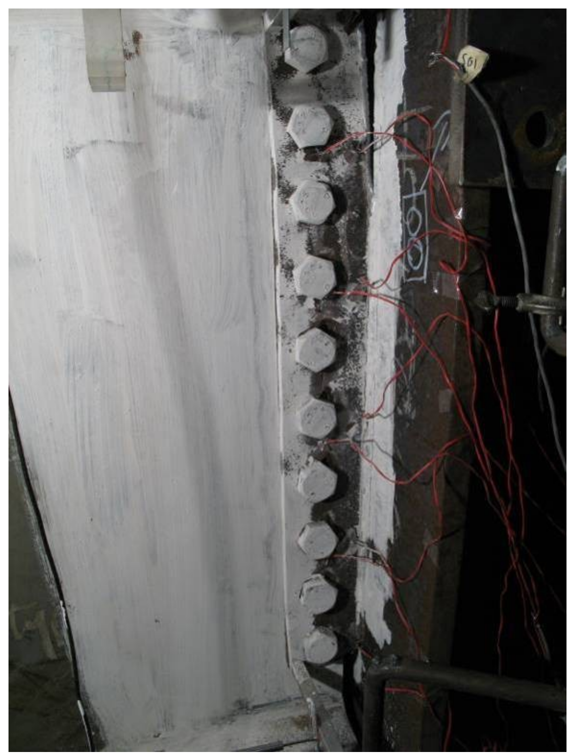

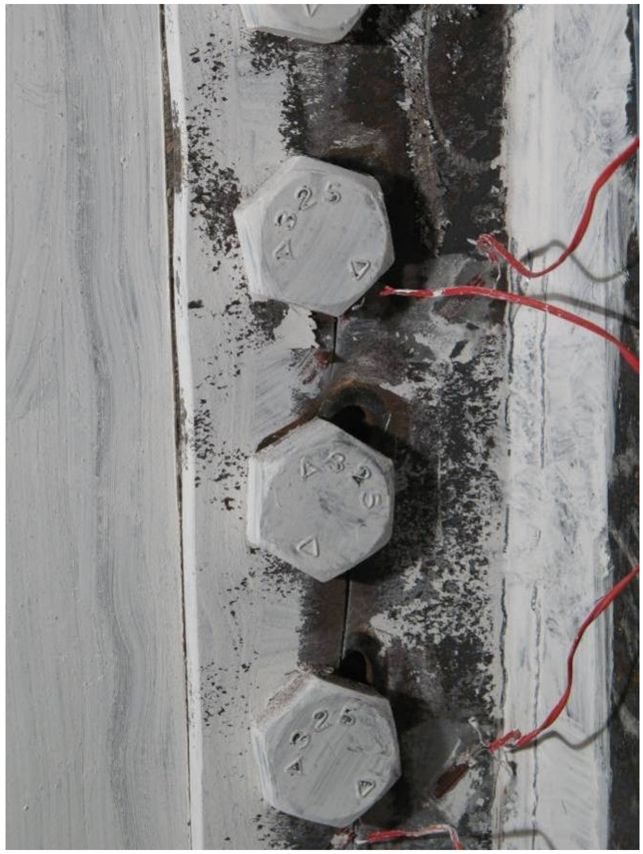

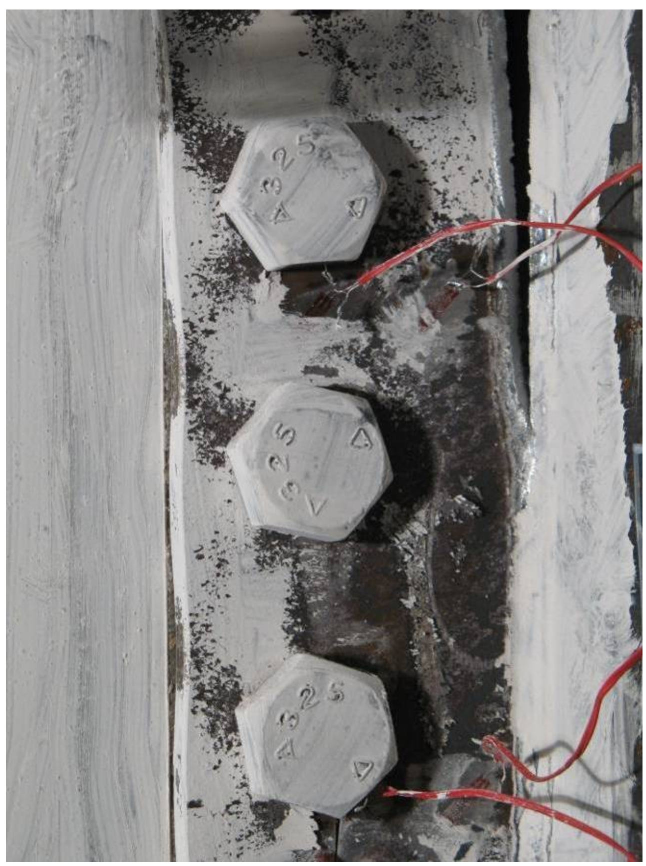

Test 14: Single Row of 10 Holes – Partial `C` Weld Retrofit

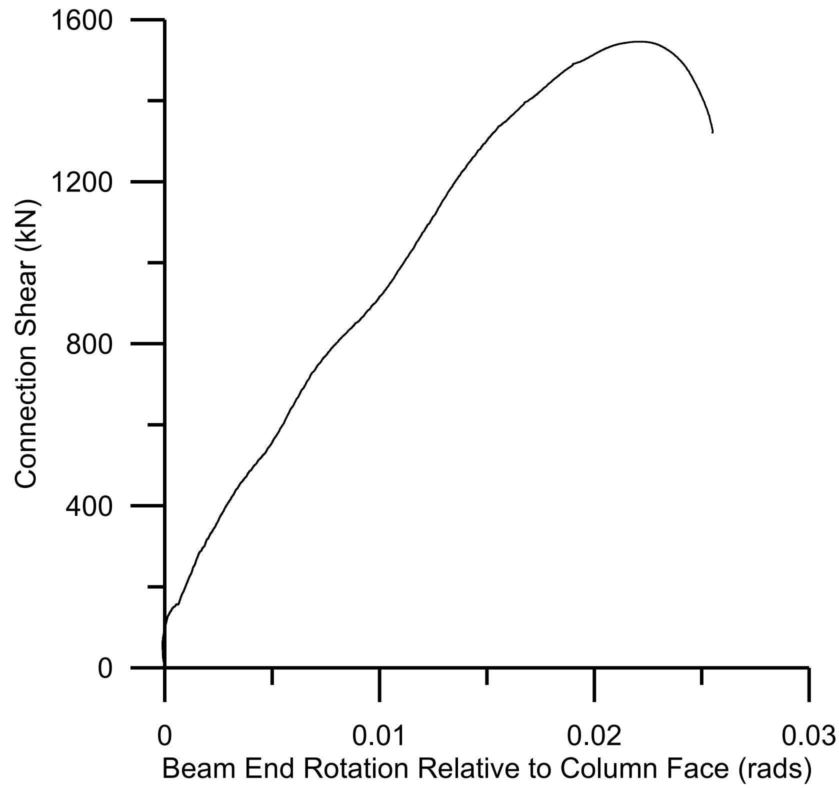

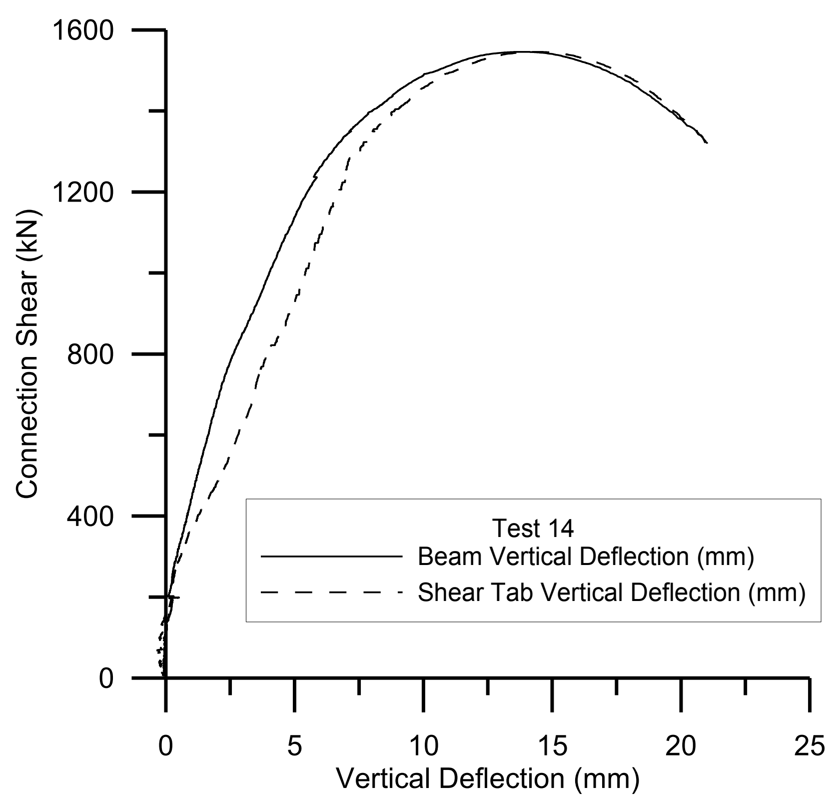

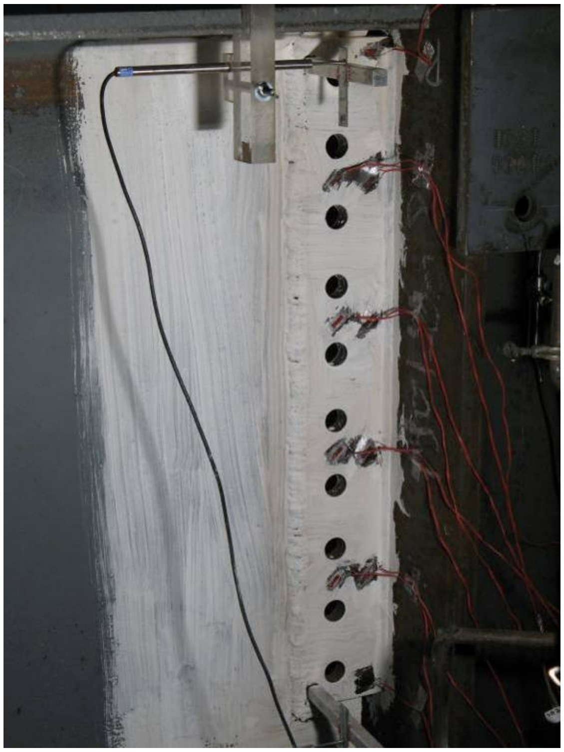
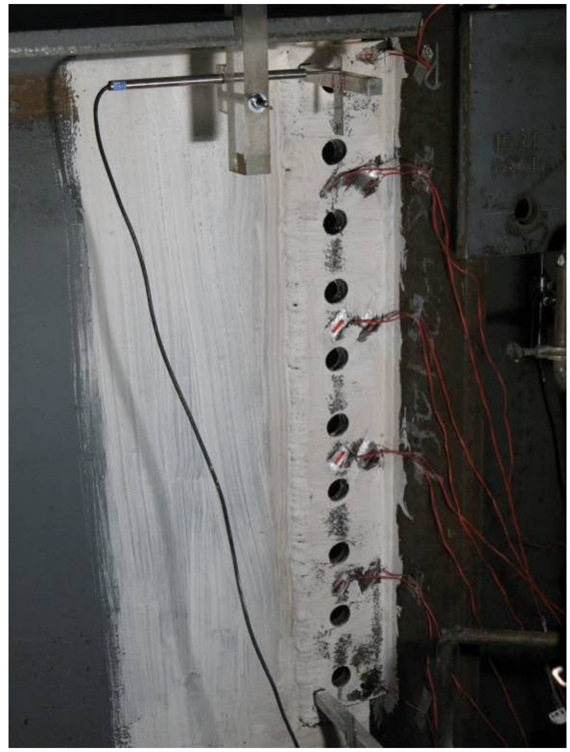
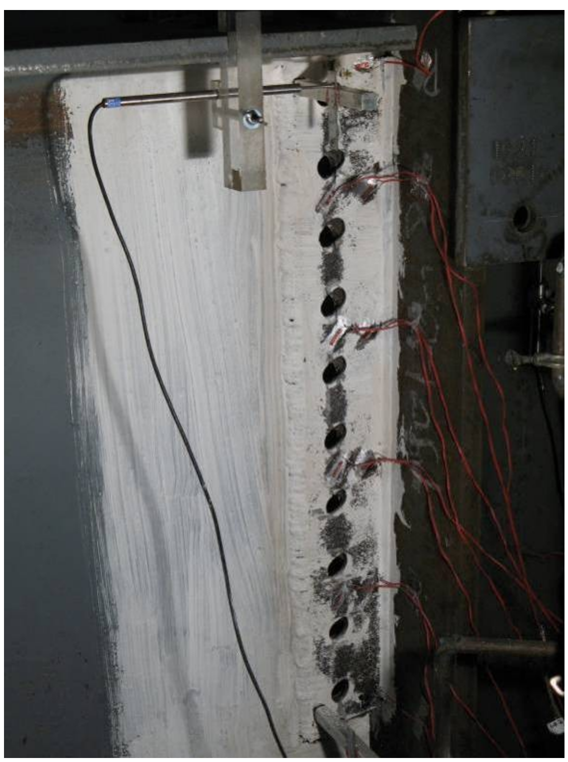


Test 15: Two Rows of 10 Bolts

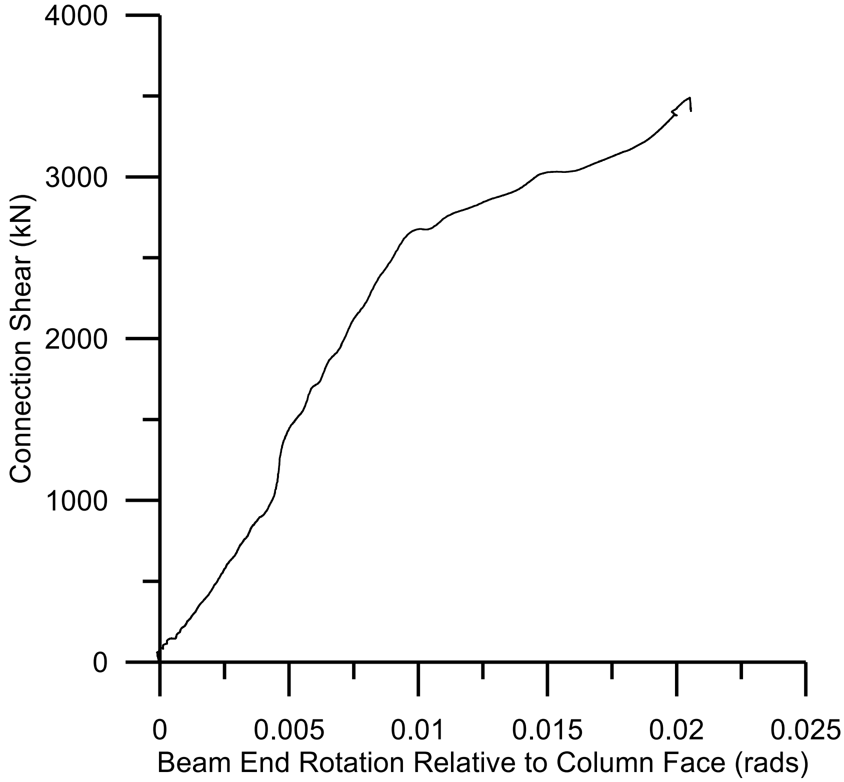

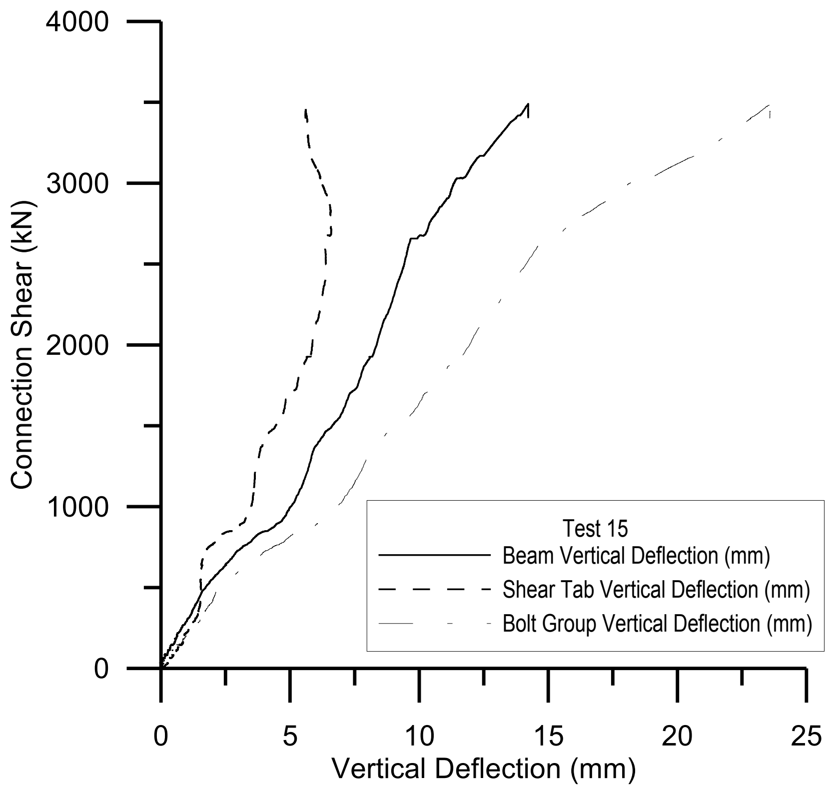

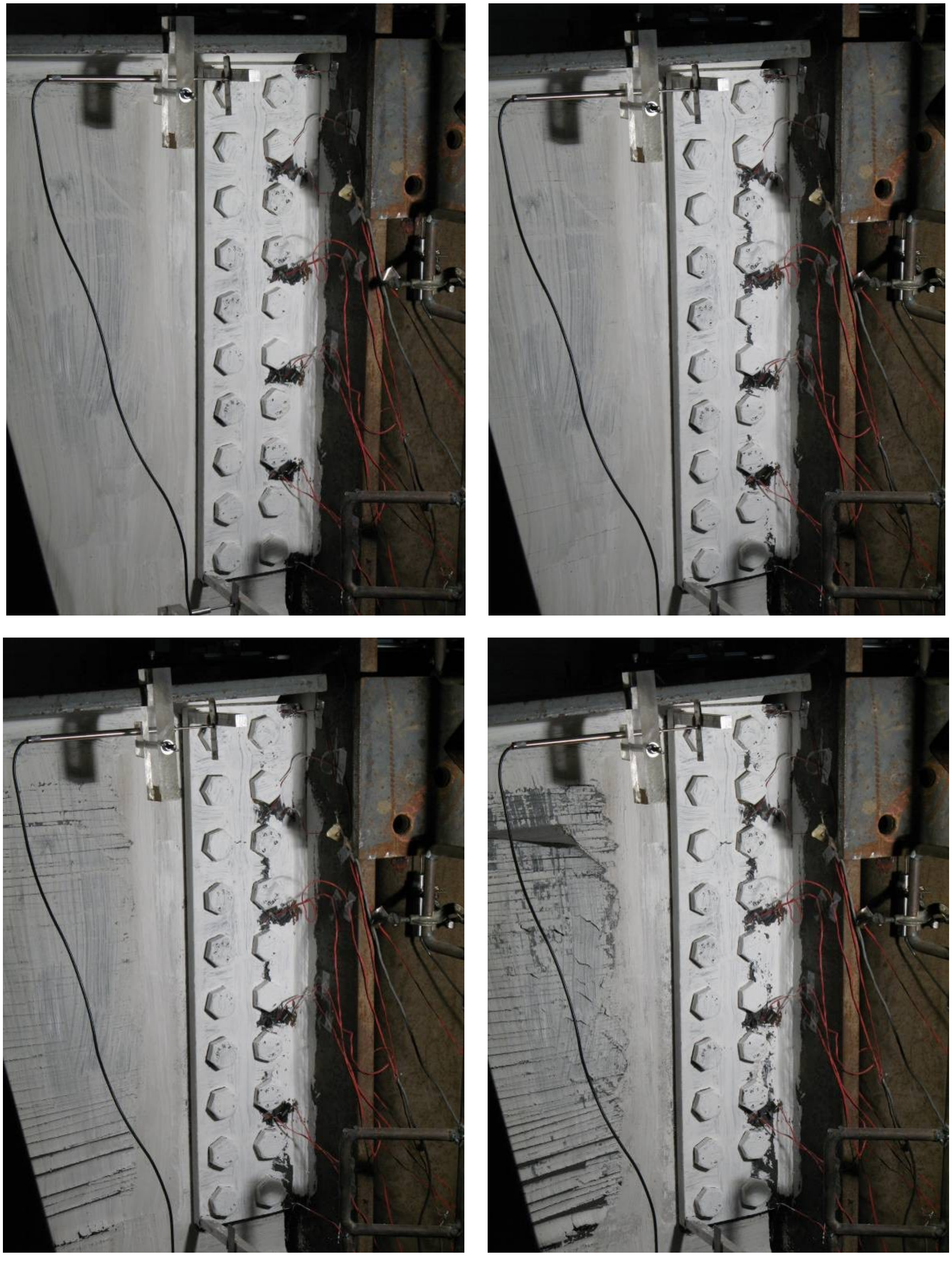

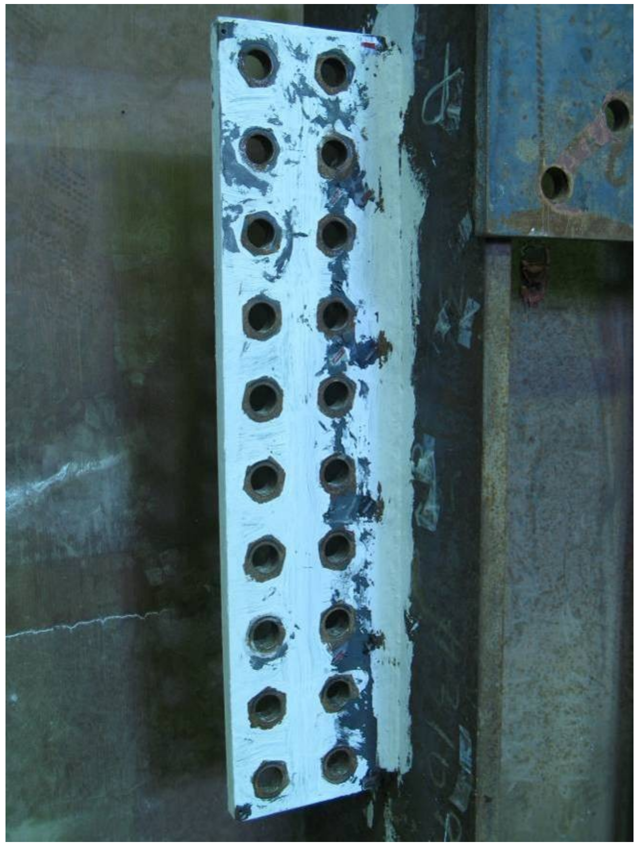

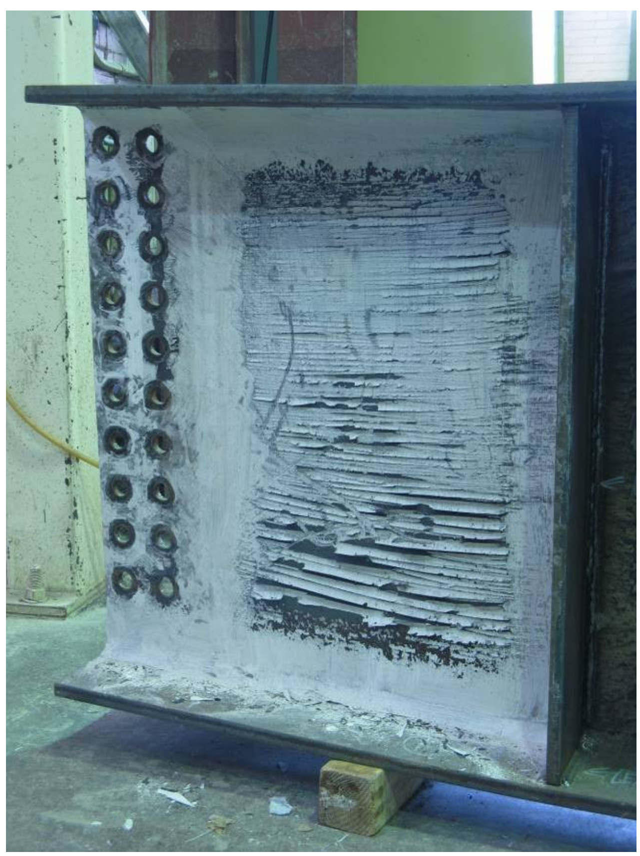

Test 16: Two Rows of 10 Holes – Partial `C` Weld Retrofit